Asset Price Dynamics with Heterogeneous Beliefs and Time Delays

Kai Li
Finance Discipline Group, UTS Business School
University of Technology, Sydney
PO Box 123 Broadway
NSW 2007, Australia

Principal Supervisor: Prof Xue-Zhong He

Co Supervisor: Prof Carl Chiarella

Co Supervisor: Dr Lei Shi

Thesis submitted for Doctor of Philosophy at the University of Technology, Sydney ·

April 2014 ·

Certificate

I certify that this thesis has not previously been submitted for a degree nor has it been submitted as part of requirement for a degree except as fully acknowledged within the text.

I also certify that the thesis has been written by me. Any help that I have received in my research work and the preparation of the thesis itself has been acknowledged. In addition, I certify that all information sources and literature used are indicated in the thesis.

Signed .....

Date .....

Acknowledgments

The completion of this thesis would not be possible without the encouragement, guidance and support from my principal supervisor Prof Xue-Zhong (Tony) He. The discussions we had throughout my PhD candidature have proven to be most helpful. His positive attitude towards research and work will continue to be a motivation for my future professional career. I would also like to thank my co supervisors Prof Carl Chiarella and Dr Lei Shi for their continuous support and the staff and fellow PhD students in the Finance Discipline Group for providing such a wonderful environment. I appreciate the financial support from the University of Technology, Sydney (UTS), UTS Business School, Quantitative Finance Research Centre (QFRC), American Finance Association (AFA) and Financial Integrity Research Network (FIRN) in contributing to cost of attending numerous national and international conferences and workshops which provided constant and timely feedback for my research. Last but not least, I am grateful to the University of Technology, Sydney for the UTS President's Scholarship and the UTS International Research Scholarship, which are of great financial assistance.

Contents

Abstract

With growing populations, the size of economies, and technological innovations, financial markets are increasingly becoming larger, more diverse, complicated, and volatile. Shocks from one market can propagate very quickly to other markets, as we saw with the global financial crisis (GFC) and the ongoing spill-over effects of the European sovereign debt crisis. These changes have had a profound impact on investor behavior and financial market and pose a great challenge to traditional asset pricing theory based on rational expectations and the representative agent paradigm. Over the last three decades, empirical evidence, unconvincing justification of the assumption of unbounded rationality, and investor psychology have led to the incorporation of heterogeneity and bounded rationality into asset pricing and financial market modelling.

This thesis contributes to the development of this literature by modelling boundedly rational behaviors, including trend chasing, herding, and adaptive switching, and examining their impact on various types of market behaviors such as price deviations from the fundamental values, excess volatility, and spill-over effect, which are then explored to explain momentum and reversal effects, two of the most challenging anomalies to finance theory in financial markets. This thesis has four main contributions.

(i) Different from the discrete-time heterogeneous agent models developed in the literature, the thesis provides a unified approach in a continuous-time framework to study the effect of trend chasing based on historical price information and explore different mechanisms and impact of trend chasing, herding and switching on various market behaviors (such as market booms and crashes, long deviations of the market price from the fundamental price), the stylized facts (such as skewness, kurtosis, excess volatility, volatility clustering and fat tails of returns), and the long range dependence in return volatility, which are widely observed in financial markets. This is the focus of Chapters 2 and 3.

(ii) It provides market conditions on the momentum profitability, which underlies the time series and cross-sectional momentum effects well documented in empirical lit-

erature. This is the focus of Chapter 4.

(iii) By applying the latest mathematical theory on the maximum principle for control problem of stochastic delay differential equations (SDDEs) to a geometrical Brownian motion of asset pricing with momentum and mean-reverting effects, Chapter 5 provides an optimal investment strategy that can outperform not only the pure momentum strategy and pure mean reversion strategy, but also the stock market index.

(iv) It develops an evolutionary CAPM and shows that rational switching behavior can destabilize the market and generate a spill-over effect, which is associated with high trading volumes characterized by significantly decaying autocorrelations of, and positive correlation between, price volatility and trading volume. This is the focus of Chapter 6.

Overall, this thesis shows that asset pricing models with heterogeneous beliefs and boundedly rational behaviors can better explain the mechanisms which generate various financial market behaviors and market anomalies.

Chapter 1

Introduction

1.1 Literature Review and Motivation

1.1.1 Heterogeneous Agent Models

Over the last two decades, there is a growing dissatisfaction with models of asset price dynamics based on the representative agent paradigm (see, for example, Kirman 1993) and the extreme informational assumptions of rational expectations. As a result, there is another growing body of literature on heterogeneous agent models (HAMs) in economics and finance, which considers the financial market as a nonlinear expectation-feedback system. In such models, traders are boundedly rational (defined in Simon, 1956) in the sense they are rational with the information they have and use certain heuristics to make decisions rather than a strict rigid rule of optimization. They do this because of the complexity of the situation, and their inability to process and compute the expected utility of every alternative action (see Keynes 1936). HAMs have successfully explained many types of features (such as market booms and crashes, multiple market equilibria, long deviations of the market price from the fundamental price), stylized facts (such as non-normality in return distributions, excess volatility, volatility clustering, fat tails), and various power laws (such as the long memory in return volatility) observed in financial markets, see recent survey papers by Hommes (2006), LeBaron (2006) and Chiarella, Dieci and He (2009).

HAMs date back to Zeeman (1974) who describes the rise and fall of bull and bear markets by considering the co-existence of two types of agents: fundamentalists and chartists. Beja and Goldman (1980), Day and Huang (1990) and Chiarella (1992) are among the first to consider dynamic HAMs. Beja and Goldman (1980) attempt to characterize how a market maker adjusts prices according to aggregate excess demand. Day and Huang

(1990) introduce a stylized market maker framework in discrete-time and their model exhibits complicated, chaotic price fluctuations around a fundamental price with random switching bear and bull market episodes. The continuous-time model introduced by Chiarella (1992) shows interaction of agents with heterogeneous expectations may lead to market instability. Lux (1995) models the herding behavior through the master equation and shows that herding can give rise to realistic time series. The seminal papers of Brock and Hommes (1997, 1998) develop an asset pricing model of heterogeneous beliefs, bounded rationality and adaptiveness. It is a simple and standard discounted asset pricing model derived from a mean-variance framework and is extended from a homogenous-belief case to the heterogeneous one where traders are boundedly rational and update strategies based upon past performance (such as realized profits). They show that such boundedly rational behavior of agents can lead to market instability, and the resulting nonlinear dynamical system is capable of generating complex behavior from local stability to high order cycles and chaos as the intensity of choice to switch predictors increases. Along this line, Boswijk, Hommes and Manzan (2007) study the behavior of price to earnings ratio and offer an explanation for the recent stock prices run-up. Brock, Hommes and Wagener (2009) incorporate derivatives and investigate the impact of hedging instruments on the market stability. In another direction, Chiarella and He (2002, 2003*b*) and Chiarella, He and Hommes (2006) extend Brock and Hommes models to study the impact of different time horizons on the price dynamics in discrete-time. Recently, Diks and van der Weide (2003) introduce the concept of a continuous beliefs system (CBS). This framework is built around a continuous beliefs space representing the possible point predictors agents can choose from. On this space a time-dependent beliefs distribution is defined, which is updated according to a continuous choice model. Based on the CBS, Diks and van der Weide (2005) examine the effects on price dynamics of a number of behavioral assumptions, including herd behavior, a-synchronous updating of beliefs and heterogeneity in the memory of agents.

The above models with one risky asset and one riskless asset make the first step to understand price dynamics under the interaction of heterogeneous agents. Within a multiple risky assets framework, the way agents form and update their beliefs about the covariance structure of asset returns also becomes an important factor in determining the dynamics of prices. A number of recent papers deal with the multiple risky assets decision problem within the HAM paradigm. Westerhoff (2004) considers a multi-asset model with fundamentalists who concentrate on only one market and chartists who invest in all markets, and offers reasons for the high degree of co-movements in stock prices observed empirically. Dieci and Westerhoff (2010, 2012) develop deterministic models to

study two stock markets denominated in different currencies, which are linked via and with the related foreign exchange market, and explore potential spill-over effects between foreign exchange and stock markets. We refer readers to Chiarella, Dieci and Gardini (2005), Westerhoff and Dieci (2006) and Chiarella, Dieci and He (2007) for the recent developments in multi-asset market dynamics in the literature of HAMs.

The econometric analysis, especially estimation and calibration, of HAMs is a difficult and challenging task due to the complexity of the HAMs, together with many parameters, which makes verification of identification rather difficult, and thus proving the consistency of the estimation is troublesome. Recently, a growing part of the literature conducts the task and provides a support to the explanatory power of HAMs. He and Li (2007) study the source of power-law distributed fluctuations in volatility. Amilon (2008) and Franke (2010) investigate the sources of different stylized facts. Franke and Westerhoff (2011, 2012) characterize the structural stochastic volatility and estimate the models on daily returns by the method of simulated moments (MSMs). Chen, Chang and Du (2012) summarize the ability of HAMs to generate stylized facts in econometrics approach.

Most of the HAMs in the literature are in discrete-time rather than a continuous-time setup. The discrete-time setup facilitates the economic understanding and mathematical analysis, it however faces some limitations when dealing with expectations formed over different time horizons. In discrete-time HAMs, different time horizons used to form the expectation or trading strategy lead to different dimensions of the system which need to be analyzed separately (see Chiarella, He and Hommes 2006). In particular, when the time horizon of historical information used is long, the resulting models are high dimensional. Very often, a theoretical analysis of the impact of lagged prices over different time horizon is difficult when the dimension of the system is high. However, the continuous-time HAMs can overcome the limitation easily.[1] Recently, He, Li, Wei and Zheng (2009) and He and Zheng (2010) extend Brock and Hommes model to a continuous-time framework characterized by a stochastic delay differential system. They consider financial markets in which the price trend of the trend followers is formed as a weighted moving average of historical prices. The model exhibits a powerful advantage to accommodate different time horizons used by chartists and excavates a double-edged role of momentum traders. In fact, the continuous-time framework is more realistic since in reality agents can submit their market orders in practically continuous-time. Another advantage of the continuous-time framework is the fact that it is hard to specify the natural time scale of a single time step for the discrete-time models. When comparing

[1] Early continuous-time HAMs do not consider the time horizons, see, for example, Chiarella (1992), which is further extended by Chiarella, He, Wang and Zheng (2008) to show that speculative behavior of chartists can cause the market price to display different forms of equilibrium distributions by applying the theory of random dynamical systems.

the discrete-time models with real data, this faces people with the choice of whether the models are suitable for daily, weekly, or monthly data, for instance. Such a choice on the time-scale is usually rather arbitrary, and often driven by availability of data. The continuous-time framework, on the other hand, does not necessarily force the researcher to decide upon the natural time scale up front. These models typically have parameters that can be interpreted as adjustment speeds and/or memory parameters, allowing the natural time scale to be estimated from data at any basic frequency in principle.[2] Along this line, this thesis extends the continuous-time HAM in He et al. (2009) to study the impacts of adaptive switching and herding behavior on the financial market, and to provide further understanding of the profitability mechanism of momentum and reversal.

1.1.2 The Momentum and Reversal Effects

Two of the most prominent financial market anomalies are momentum and reversal. Momentum, on the one hand, is the tendency of assets with good (bad) recent performance to continue outperforming (underperforming) in short-run. Reversal, on the other hand, concerns predictability of assets that performed well (poorly) over a long period tend to subsequently underperform (outperform). Momentum and reversal have been documented extensively for a wide variety of assets. Jegadeesh and Titman (1993) document momentum for individual U.S. stocks, predicting returns over horizons of 3-12 months by returns over the past 3-12 months. De Bondt and Thaler (1985) document the reversal, predicting returns over horizons of up to five years by returns over the past 3-5 years. Fama and French (1992) document the value effect, which is closely related to reversal, whereby the ratio of an assets price relative to book value is negatively related to subsequent performance. Mean reversion in equity returns has been shown to induce significant market timing opportunities, see Campbell and Viceira (1999), Wachter (2002) and Koijen, Rodríguez and Sbuelz (2009). The evidence has been extended to stocks in other countries (Fama and French 1998), stocks within industries (Cohen and Lou 2012), across industries (Cohen and Frazzini 2008), and the global market with different asset classes (Asness, Moskowitz and Pedersen 2013). More recently, Moskowitz, Ooi and Pedersen (2012) investigate time series momentum that characterizes the strong positive predictability of a security's own past returns. For a large set of futures and forward contracts, Moskowitz et al. (2012) find time series momentum based on the past 12 month excess returns persists for 1 to 12 months that partially reverses over longer horizons. They provide strong evidence on the time series momentum based on the moving aver-

[2] I would like to thank Cees G.H. Diks (an examiner) for providing the argument.

age of "look-back" returns. This effect based purely on a security's own past returns is related to, but different from, the cross-sectional momentum phenomenon studied extensively in the literature. Through return decomposition, Moskowitz et al. (2012) argue that positive auto-covariance is the main driving force for time series momentum and cross-sectional momentum effects, while the contribution of serial cross-correlations and variation in mean returns is small.

The size and apparent persistence of momentum and reversal profits have attracted considerable attention, and many theoretical studies have tried to explain the phenomena. Among which, the three-factor model of Fama and French (1996) can explain long-run reversal but not short-run momentum. Barberis, Shleifer and Vishny (1998) argue that these phenomena are the result of systematic errors that investors make when they use public information to form expectations of future cash flows. Daniel, Hirshleifer and Subrahmanyam (1998)'s model with a representative agent and Hong and Stein (1999)'s model with different trader types attribute the under- and overreaction to overconfidence and biased self-attribution. Barberis and Shleifer (2003) show that style investing can explain momentum and value effects. Sagi and Seasholes (2007) present a growth options model to identify observable firm-specific attributes that drive momentum. Vayanos and Woolley (2013) show the slow-moving capital can also generate momentum. However, the mechanism which generates momentum and reversal profitability is still not clear.

1.1.3 The Capital Asset Pricing Model

Within the rational expectations and representative agent paradigm, the Sharpe-Lintner-Mossin (Sharpe 1964, Lintner 1965 and Mossin 1966) Capital Asset Pricing Model (CAPM) is the most widely-used tool to price risky assets. However, there is considerable empirical evidence documenting cyclical behavior of market characteristics, including risk premium, volatility, trading volume, price to dividend ratio, and in particular, market betas. The conditional CAPM was developed to provide a convenient way to incorporate a time-varying beta and it exhibits empirical superiority in explaining the cross-section of returns and anomalies.[3] There exists a large literature on time-varying beta models, but most of it is motivated by econometric estimation. It is often assumed that there are discrete changes in betas across subsamples but constant betas within subsamples.[4] It has been shown that when betas vary over time, the standard OLS inference is misspecified and cannot be used to assess the fitness of a conditional CAPM. In addition, most of

[3] See, for example, Engle (1982), Bollerslev (1986), Bollerslev et al (1988), Dybvig and Ross (1985), Hansen and Richard (1987), Hamilton (1989, 1990), Braun et al (1990), and Jagannathan and Wang (1996).

[4] See Campbell and Vuolteenaho (2004), Fama and French (2006), and Lewellen and Nagel (2006)). We point out that Ang and Chen (2007) treat betas as endogenous variables that vary slowly and continuously over time.

the econometric models of time-varying beta lack an economic explanation and intuition. Recently, Chiarella, Dieci and He (2010, 2011) introduce a multi-asset CAPM framework for analyzing the impact of heterogeneous beliefs on asset prices via the construction of a consensus belief and find that heterogeneity becomes part of an asset's systematic risk. Chiarella, Dieci and He (2013) use this framework in a dynamic setting and demonstrate the stochastic behavior of time-varying betas and show that there is an inconsistency between ex-ante and ex-post estimates of asset betas when beliefs are heterogeneous. This suggests that the methods for estimating asset betas currently used in the literature can be inappropriate.

1.1.4 Motivation

Although the efficient market hypothesis (EMH) of financial markets (see Fama, 1970) has been taken as support for the random walk model and financial economists are contented with this view as the explanation of the time series behavior of observed asset prices for a long time, a range of empirical studies lead to some questioning of the basic tenets of the EMH. They include various anomalies of equity markets (see Thaler 1987*a*, 1987*b* and Keim 1988) and stylized facts in asset returns (see Pagan 1996 and Lux 2009). The dependence of stock prices on past returns (Akgiray 1989 and Pesaran and Timmermann 1995) is also unexplained by the random walk models. The short run price momentum (Jegadeesh and Titman 1993) and long run reversal (DeBondt and Thaler 1989), two of the most studied phenomena in financial market, have become central to the market efficiency debate. The above literature has suggested asset prices can be affected by historical information, however, this fact has not otherwise been considered by the standard asset pricing theory. Although the recent heterogeneous agent models (HAMs) literature has started to consider the impact of lagged prices (used by chartists to form their expectations), the roles of the lagged prices, especially the corresponding time horizons have not been well understood due to the problem of high dimensional systems. This thesis is largely motivated by the above literature and proposes dynamic asset price models with heterogeneous beliefs and time delays. It extends the HAMs literature in a discrete-time framework to a continuous-time framework to provide a unified approach in modelling different boundedly rational behavior, including trend chasing, adaptive switching and herding behavior, and to examine their impacts on various market behavior, which are then explored to explain momentum and reversal effects, two of the most challenging anomalies to asset pricing theory.

1.2 Structure of the Thesis

The thesis consists of three main components. The first part, consisting of Chapters 2 and 3, is devoted to examining the impact of historical information, especially the time horizons on various market behavior, stylized facts and power laws behavior in a continuous-time framework. Chapters 2 considers the switching mechanism of the adaptive behavior of heterogeneous agents based on certain fitness measure (such as cumulated profits) whereas the herding behavior is incorporated into Chapter 3. The results of Chapter 2 have been published in He and Li (2012). The second part, consisting of Chapters 4 and 5, focuses on the momentum and reversal effects. Chapter 4 extends the models in the first part to provide market conditions on the momentum profitability with respect to time horizons and market dominance. By taking advantage of the continuous-time framework in modelling the time horizons, Chapter 5 explores the optimality of momentum and reversal effects. Chapter 6, the third part of the thesis, extends the models to a multi-asset case to study the spill-over effect. The results of Chapter 6 have been published in Chiarella, Dieci, He and Li (2013). Chapter 7 summarizes the main results of the thesis and related future research is discussed. All proofs and some model extensions are collected in the Appendices (unless specified otherwise).

Chapters 2 and 3 show that the continuous-time HAMs can provide a better way to characterize and examine the impact of the time horizons used by agents to form their expectations. Chapter 2 introduces adaptive behavior of agents who switch their strategies in a boundedly rational way according to certain fitness measures such as cumulated profits of strategies. The analysis of the model provides not only some consistent results to the discrete-time HAMs, such as stabilizing effect of fundamentalists, destabilizing effect of chartists, and rational routes to market instability, but also a double edged effect of an increase in lagged prices on market stability. An increase in the using of lagged prices can not only destabilize, but also stabilize the market price. By including noise traders and imposing a stochastic process on the fundamental price, we demonstrate that the model is able to generate various market phenomena and stylized facts. In particular, we show that switching can generate more realistic long range dependence in volatility. Based on the model in Chapter 2, Chapter 3 also considers herding behavior and shows adaptive switching and herding behavior of agents can increase market price fluctuations. In this chapter, we extensively examine how the market volatility can be affected by trend chasing, adaptive switching, and herding, which are among the most important factors affecting market volatility well documented and studied in the empirical literature. We show that, both herding and trend chasing based on a long time horizon increase the

fluctuations of market price deviation from the fundamental price and volatility of market return. With respect to the switching, it reduces the volatility in returns but leads to a "U"-shaped price volatility as the switching intensity increases. Therefore herding and switching have an opposite effect on the return volatility. We also show that, although the trend chasing, switching and herding all contribute to the power-law behavior, the significant levels for the ACs increase in the time horizon and herding, but an initial increase and then decrease when the switching intensity increases. In addition, with the herding, the market noise characterizing noise traders or liquidity trading plays an essential role in generating the power-law behavior.

According to the time horizons and the states of the market dominance, the thesis further provides market conditions on momentum profitability, which underlies the momentum effects well documented in empirical literature. Chapter 4 extends the models in Chapters 2 and 3 and proposes a continuous-time heterogeneous agent model of investor behavior consisting of fundamental, contrarian, and momentum strategies. By examining their impact on market stability explicitly and analyzing the profitability numerically, we show that the profitability of time series momentum is closely related to the market states defined by the stability of the underlying deterministic model. In particular, we show that when the momentum traders dominate the market, the momentum strategy is profitable when the time horizon is short and unprofitable when the time horizon is long. Otherwise, the momentum strategy is not profitable for any time horizon. We also provide some explanation to the profitability mechanism through autocorrelation patterns and the classical underreaction and overreaction hypotheses.

Chapter 4 shows the profitability of the momentum and contrarian strategies is conditional. In order to achieve an unconditional profitability, Chapter 5 provides an optimal investment strategy to explore the momentum and reversal effects by applying the latest mathematical theory on the maximum principle for control problem of stochastic delay differential equations (SDDEs). In the standard asset price model based on geometric Brownian motion, the drift is modelled as a weighted average of mean reversion and moving average. We find that pure momentum and pure mean reversion strategies cannot outperform the market, however, a combination of them can outperform the market by taking the timing opportunity with respect to the trend in return and the market volatility. We show that the optimal strategy can achieve an unconditional profitability in the sense that the strategy is immune to the market states, investor sentiment and market volatility. We also show that the profitability pattern reflected by the average return in most empirical studies can be affected by the wealth effect.

The models introduced in the previous chapters only consider the price dynamics of

one risky asset. Chapter 6 extends the models to a multi-asset framework of an evolutionary CAPM with heterogeneous beliefs. By analyzing the stability of the underlying deterministic model, we show that the evolutionary CAPM is capable of characterizing the spill-over effects, the persistence in price volatility and trading volume, and realistic correlations between price volatility and trading volume. We show that the spill-over effect is associated with high trading volumes and persistent volatility characterized by significantly decaying autocorrelations of, and positive correlation between, price volatility and trading volume. Also, the stochastic nature of time-varying betas implied by the equilibrium model may not be consistent with the rolling window estimate of betas used in the empirical literature. The model provides further explanatory power of the recently developed HAMs.

Chapter 2

Heterogeneous Beliefs and Adaptive Behavior in a Continuous-time Asset Price Model

2.1 Introduction

It is well recognized that the traditional view of homogeneity and perfect rationality in financial markets faces a number of theoretical limitations and empirical challenges. Over the last two decades, there is a growing research on heterogeneity and bounded rationality in financial markets. With different groups of traders having different expectations about future prices, asset price fluctuations can be caused by an endogenous mechanism. For instance, the seminal papers of Brock and Hommes (1997, 1998) introduce the concept of an adaptively rational equilibrium. A key aspect of their models is that they exhibit expectations feedback. Agents adapt their beliefs over time by choosing from different predictors or expectation functions based upon their past performance (such as realized profits). They show that such boundedly rational behavior of agents can lead to market instability and the resulting nonlinear dynamical system is capable of generating complex behavior from local stability to high order cycles and chaos as the intensity of choice to switch predictors increases.

The framework of Brock and Hommes and its various extensions are in a discrete-time setup. The setup facilitates economic understanding of the role of heterogeneous expectations and mathematical analysis, it however faces a limitation when dealing with expectations formed from the lagged prices over different time horizons and a challenge to characterize the adaptive behavior in a continuous-time. In discrete-time models,

different time horizons used to form the expectations or trading strategies lead to different dimensions of the systems which need to be analyzed individually. In particular, when the time horizon of historical information used is long, the resulting models are high dimensional systems. Very often, a theoretical analysis of the impact of lagged prices over different time horizons is difficult when the dimension of the system is high[1]. The recent development of HAMs in continuous-time in He et al. (2009) and He and Zheng (2010) overcomes this limitation in discrete-time. In the continuous-time HAM, the time horizon of historical price information used by chartists is simply presented by a time delay. The resulting model is characterized mathematically by a system of delay differential equations[2]. It provides a uniform treatment on various time horizons used in the discrete-time models.

Motivated by the continuous-time HAMs developed in He et al. (2009) and He and Zheng (2010), this chapter intends to characterize the switching mechanism of the adaptive behavior of heterogeneous agents in a continuous-time asset pricing model under a market maker scenario, instead of the Walrasian scenario used in Brock and Hommes (1998). Within the proposed model, this chapter has three aims. The first is to examine if the result of Brock and Hommes (1998) on rational routes to market instability still holds in a continuous-time setup. The second is to study the joint impact of the adaptive switching mechanism and the increase in time horizon on market stability. The third is to explore potential of the model to replicate various market behavior, stylized facts and long range dependence observed in financial markets. In order to focus the analysis on the roles of time horizons, both He et al. (2009) and He and Zheng (2010) do not consider adaptive behavior of agents. In this chapter, we follow Brock and Hommes (1998) to introduce adaptive behavior of agents who switch their strategies in a boundedly rational way according to some 'performance' or 'fitness' measure such as cumulated profits of strategies over past time horizons. For the corresponding deterministic model, we first show that the result of Brock and Hommes on rational routes to market instability in discrete-time holds in continuous-time. That is, the adaptive switching behavior of agents can lead to market instability as the switching intensity increases, generating excess volatility. We then show a double edged effect of an increase in the lagged price information used by the chartists on market stability, meaning that an increase in time

[1]For example, to examine the role of different moving average rules used by chartists on market stability, Chiarella et al. (2006) propose a discrete-time HAM whose dimension depends on the time horizon of chartists used in moving average.

[2]Although the applications of delay differential equation models to asset pricing and financial market modelling are relatively new, their applications to characterize fluctuation of commodity prices and cyclic economic behavior have a long history, see, for example, Haldane (1932), Kalecki (1935), Goodwin (1951), Larson (1964), Howroyd and Russell (1984) and Mackey (1989). The development further leads to the studies on the effect of policy lag on macroeconomic stability, see, for example, Phillips (1954, 1957), Yoshida and Asada (2007), and on neoclassical growth model in Matsumoto and Szidarovszky (2011).

delay not only can destabilize the market but also can stabilize the market, a very different feature in the continuous-time HAM which is not presented in the discrete-time HAMs. This phenomenon is also observed in the continuous-time model in He et al. (2009) and He and Zheng (2010) without switching, implying that this phenomenon is not due to the switching mechanism. However, the switching affects the price dynamics significantly when market becomes unstable. By including noise traders and imposing a stochastic process on fundamental price, we demonstrate that the model is able to generate various market phenomena, such as long-term deviations of the market price from the fundamental price, bubbles, crashes, and stylized facts, including non-normality in asset returns, volatility clustering, and long-range dependence of high-frequency returns, observed in financial markets. In particular, we show that the switching can generate more realistic long range dependence in volatility.

The chapter is based on He and Li (2012) and organized as follows. We first introduce a stochastic HAM of asset pricing in continuous-time with heterogeneous agents who are allowed to switch among two types of strategies, fundamentalists and chartists, based on accumulated profits of the strategies in Section 2.2. In Section 2.3, we apply stability and bifurcation theory of delay differential equations, together with numerical analysis of the nonlinear system, to examine the impact of switching and time horizon used by the chartists on the market stability. Section 2.4 provides some numerical simulation results of the stochastic model in exploring the impact of switching and the potential of the model to generate various market behavior and the stylized facts. Section 2.5 concludes.

2.2 The Model

Consider a financial market with a risky asset (such as stock market index) and let $P(t)$ be the (cum dividend) price of the risky asset at time t. The modelling of the dynamics of the risky asset follows closely to the current HAMs. However, instead of using a discrete-time setup and Walrasian scenario, we consider a continuous-time setup and a market maker scenario (as in Beja and Goldman 1980, Chiarella and He 2003*b*, Hommes et al 2005 and Chiarella et al. 2006).[3] The market consists of fundamentalists who trade according to fundamental analysis, chartists who trade based on price trend calculated from weighted moving averages of historical prices over a time horizon, and a market maker who clears the market by providing liquidity. To focus on price dynamics, we motivate the excess demand functions of the two types of traders directly, rather than

[3]As presented in Chiarella et al. (2009), the Walrasian scenario, even though widely used in economic analysis, only plays a part in one real market (the market for silver in London).

deriving them from utility maximization of their portfolio investments. The behavior of the traders is modelled as in He et al. (2009) and He and Zheng (2010). For completeness, we introduce the demand functions of the fundamentalists and the chartists briefly and refer readers to He et al. (2009) and He and Zheng (2010) for details.

The fundamentalists believe that the market price $P(t)$ is mean-reverting to the fundamental price $F(t)$ that can be estimated based on various types of fundamental information. They buy (sell) the stock when the current price $P(t)$ is below (above) the fundamental price $F(t)$. For simplicity, the demand of the fundamentalists, $Z_f(t)$ at time t, is assumed to be proportional to the price deviation from the fundamental price, namely,

$$Z_f(t) = \beta_f[F(t) - P(t)], \tag{2.1}$$

where $\beta_f > 0$ is a constant parameter, measuring the speed of mean-reversion of the market price to the fundamental price, which may be weighted by a risk aversion coefficient of the fundamentalists, and $F(t)$ is the fundamental price of an exogenous random process to be specified in Section 2.4.

The chartists are modelled as trend followers. They believe that the future market price follows a price trend $u(t)$. When the current price is above the trend, the trend followers believe the price will rise and they like to hold a long position of the risky asset; otherwise, the trend followers take a short position. We assume that the demand of the chartists is given by

$$Z_c(t) = \tanh\big(\beta_c[P(t) - u(t)]\big). \tag{2.2}$$

The S-shaped demand function capturing the trend following behavior is well documented in the HAM literature (see, for example, Chiarella et al. 2009), where the parameter β_c represents the extrapolation rate of the trend followers on the future price trend when the price deviation from the trend is small. However, they limit their positions when the deviation is large. Among various price trends used in practice, we assume that the price trend $u(t)$ at time t is calculated by an exponentially decaying weighted average of historical prices over a time interval $[t - \tau, t]$,

$$u(t) = \frac{k}{1 - e^{-k\tau}} \int_{t-\tau}^{t} e^{-k(t-s)} P(s) ds, \tag{2.3}$$

where time delay $\tau \in (0, \infty)$ represents a price history used to calculate the price trend, and $k > 0$ is a decay rate. Equation (2.3) implies that, when forming the price trend, the trend followers believe the more recent prices contain more information about the future price movement so that the weights associated to the historical prices decay exponentially

with a decay rate k. In particular, when $k \to 0$, the price trend $u(t)$ in equation (2.3) is simply given by the standard moving average with equal weights,

$$u(t) = \frac{1}{\tau}\int_{t-\tau}^{t} P(s)ds. \tag{2.4}$$

When $k \to \infty$, all the weights go to the current price so that $u(t) \to P(t)$. For the time delay, when $\tau \to 0$, the trend followers regard the current price as the price trend. When $\tau \to \infty$, they use all the historical prices to form the price trend

$$u(t) = \frac{1}{k}\int_{-\infty}^{t} e^{-k(t-s)}P(s)ds. \tag{2.5}$$

In general, for $0 < k < \infty$, equation (2.3) can be expressed as a delay differential equation with time delay τ

$$du(t) = \frac{k}{1-e^{-k\tau}}\big[P(t) - e^{-k\tau}P(t-\tau) - (1-e^{-k\tau})u(t)\big]dt. \tag{2.6}$$

In the spirit of Brock and Hommes (1997, 1998) and Chiarella et al. (2006), we now introduce the evolution of market population of agents. Let $N_f(t)$ and $N_c(t)$ be the numbers of agents who use the fundamental and chartist strategies, respectively, at time t. Assume that market population of agents $N_f(t) + N_c(t) = N$ is a constant. Denote by $n_f(t) = N_f(t)/N$ and $n_c(t) = N_c(t)/N$ the market fractions of agents who use the fundamental and trend following strategies, respectively. The net profits of the fundamental and trend following strategies over a short time interval $[t-dt, t]$ are measured by, respectively,

$$\pi_f(t)dt = Z_f(t)dP(t) - C_f dt, \qquad \pi_c(t)dt = Z_c(t)dP(t) - C_c dt, \tag{2.7}$$

where $C_f,\ C_c \geq 0$ are constant costs of the strategies per unit time. The performances of the strategies are measured by cumulated and weighted net profits over time intervals $[t-\tau_i, t]$[4],

$$U_i(t) = \frac{\eta_i}{1-e^{-\eta_i\tau_i}}\int_{t-\tau_i}^{t} e^{-\eta_i(t-s)}\pi_i(s)ds, \qquad i = f, c, \tag{2.8}$$

where $\eta_i > 0$ and $\tau_i > 0$ for $i = f, c$ represent the decay parameter and time horizon respectively used to measure the performance of the fundamentalists and trend followers.

[4]The time delays used to measure the performances can be different from the delay used by the chartists to calculate the price trend in general. In addition, comparing to the trend followers, the fundamentalists use historical prices over a longer time horizon τ_f with lower decaying rate η_f. The impact of different time horizons and decay rates in the performance is discussed in footnote 11.

Consequently,

$$dU_i(t) = \eta_i \left[\frac{\pi_i(t) - e^{-\eta_i \tau_i} \pi_i(t - \tau_i)}{1 - e^{-\eta_i \tau_i}} - U_i(t) \right] dt, \qquad i = f, c. \tag{2.9}$$

By using the replicator dynamics (see, for example, Chapter 7 in Hofbauer and Sigmund, 1998), the evolution dynamics of the market populations are governed by

$$dn_i(t) = \beta n_i(t)[dU_i(t) - d\bar{U}(t)], \qquad i = f, c, \tag{2.10}$$

where $d\bar{U}(t) = n_f(t)dU_f(t) + n_c(t)dU_c(t)$ is the change of the average performance (over a time interval $[t, t + dt]$) of the two strategies and $\beta > 0$ is a constant, measuring the switching intensity of agents who change their strategy to a better performing strategy. In particular, if $\beta = 0$, there is no switching among agents, while for $\beta \to \infty$ all agents immediately switch to the better strategy.

It can be verified that the above switching mechanism in continuous-time setup is consistent with the one used in discrete-time HAMs. In fact, the dynamics of the market fraction $n_f(t)$ satisfies

$$dn_f(t) = \beta n_f(t)(1 - n_f(t))[dU_f(t) - dU_c(t)], \tag{2.11}$$

leading to

$$n_f(t) = \frac{e^{\beta U_f(t)}}{e^{\beta U_f(t)} + e^{\beta U_c(t)}}, \tag{2.12}$$

which is the discrete choice model used in Brock and Hommes (1997, 1998).[5] In addition, when $\tau_i \to 0$, $U_i(t) \approx \pi_i(t)$, defining the performance by the current profit. When $\tau_i \to \infty$, $U_i(t+dt) \approx U_i(t)+\delta_i \pi_i(t)$ with $\delta_i = \eta_i dt$, defining the performance as cumulated historical profits that decay geometrically at a rate of δ_i.

Finally, the price $P(t)$ at time t is adjusted by the market maker according to the aggregate market excess demand, that is,

$$dP(t) = \mu \big[n_f(t) Z_f(t) + n_c(t) Z_c(t) \big] dt + \sigma_M dW_M(t),$$

where $\mu > 0$ represents the speed of the price adjustment by the market maker, $W_M(t)$ is a standard Wiener process capturing the random excess demand process either driven by unexpected market news or noise traders, and $\sigma_M > 0$ is a constant.

To sum up, the market price of the risky asset is determined according to the following stochastic delay differential system with three different time delays and two noise

[5] The equivalence of (2.11) and (2.12) is demonstrated in Appendix A.1.

processes[6]

$$\begin{cases} dP(t) = \mu\Big[n_f(t)Z_f(t) + \big(1-n_f(t)\big)Z_c(t)\Big]dt + \sigma_M dW_M(t), \\ du(t) = \dfrac{k}{1-e^{-k\tau}}\Big[P(t) - e^{-k\tau}P(t-\tau) - (1-e^{-k\tau})u(t)\Big]dt, \\ dU_f(t) = \dfrac{\eta_f}{1-e^{-\eta_f\tau_f}}\Big[\pi_f(t) - e^{-\eta_f\tau_f}\pi_f(t-\tau_f) - (1-e^{-\eta_f\tau_f})U_f(t)\Big]dt, \\ dU_c(t) = \dfrac{\eta_c}{1-e^{-\eta_c\tau_c}}\Big[\pi_c(t) - e^{-\eta_c\tau_c}\pi_c(t-\tau_c) - (1-e^{-\eta_c\tau_c})U_c(t)\Big]dt, \end{cases} \tag{2.13}$$

where $n_f(t)$ is defined by (2.12), $Z_f(t)$ and $Z_c(t)$ are defined by (2.1) and (2.2), respectively, and $\pi_i(t)$ is defined by (2.7) for $i = f, c$.

In summary, we have established an adaptively heterogeneous belief model of asset price in a continuous-time. The resulting model is characterized by a five-dimensional system of nonlinear stochastic delay differential equations, which can be difficult to analyze directly. To understand the interaction of the deterministic dynamics and noisy processes, we first study the dynamics of the corresponding deterministic model in Section 2.3. The stochastic model (2.13) is then analyzed in Section 2.4.

2.3 Dynamics of the Deterministic Delay Model

By assuming that the fundamental price is a constant $F(t) \equiv \bar{F}$ and there is no market noise $\sigma_M = 0$, the system (2.13) becomes a deterministic differential system with three time delays

$$\begin{cases} \dfrac{dP(t)}{dt} = \mu\Big[n_f(t)\beta_f(\bar{F} - P(t)) + \big(1-n_f(t)\big)\tanh\Big(\beta_c\big(P(t)-u(t)\big)\Big)\Big], \\ \dfrac{du(t)}{dt} = \dfrac{k}{1-e^{-k\tau}}\Big[P(t) - e^{-k\tau}P(t-\tau) - (1-e^{-k\tau})u(t)\Big], \\ \dfrac{dU_f(t)}{dt} = \dfrac{\eta_f}{1-e^{-\eta_f\tau_f}}\Big[\pi_f(t) - e^{-\eta_f\tau_f}\pi_f(t-\tau_f) - (1-e^{-\eta_f\tau_f})U_f(t)\Big], \\ \dfrac{dU_c(t)}{dt} = \dfrac{\eta_c}{1-e^{-\eta_c\tau_c}}\Big[\pi_c(t) - e^{-\eta_c\tau_c}\pi_c(t-\tau_c) - (1-e^{-\eta_c\tau_c})U_c(t)\Big], \end{cases} \tag{2.14}$$

where

$$\pi_i(t) = \mu Z_i(t)\Big[n_f(t)Z_f(t) + \big(1-n_f(t)\big)Z_c(t)\Big] - C_i, \qquad i = f, c.$$

[6]Note that $Z_f(t)$ is a stochastic process depending on the stochastic fundamental process $F(t)$ specified later in Eq. (2.17).

It is easy to see that $(P, u, U_f, U_c) = (\bar{F}, \bar{F}, -C_f, -C_c)$ is a unique steady state of the system (2.14), which consists of the constant fundamental price and the costs of the strategies per unit time. We therefore call $(P, u, U_f, U_c) = (\bar{F}, \bar{F}, -C_f, -C_c)$ the *fundamental steady state*. We now study the dynamics of the deterministic model (2.14), including the stability and bifurcation of the fundamental steady state.

At the fundamental steady state, the market fractions of the fundamentalists and the chartists become $n_f^* := 1/(1+e^{\beta C})$ and $n_c^* := 1/(1+e^{-\beta C})$ respectively, where $C = C_f - C_c$ measures the disparity of the strategy cost rates. Obviously, when $C = 0$, $n_f^* = n_c^* = 0.5$, meaning that the market fractions at the fundamental steady state is independent of the switching intensity parameter β. However, if it costs agents more to use the fundamental strategy, that is $C > 0$, then there are more chartists than the fundamentalists at the fundamental steady state, that is $n_c^* > n_f^*$. Furthermore, when $C > 0$, an increase in β decreases the steady state market fraction n_f^* of the fundamentalists.

It is known (see Gopalsamy 1992) that[7] the stability is characterized by the eigenvalues of the characteristic equation of the system at the steady state. Denote $\gamma_f = \mu n_f^* \beta_f$ and $\gamma_c = \mu(1-n_f^*)\beta_c$. Then the characteristic equation of the system (2.14) at the fundamental steady state $(P, u, U_f, U_c) = (\bar{F}, \bar{F}, -C_f, -C_c)$ is given by[8]

$$\Delta(\lambda) := (\lambda + \eta_f)(\lambda + \eta_c)\widetilde{\Delta}(\lambda) = 0, \tag{2.15}$$

where

$$\widetilde{\Delta}(\lambda) = \lambda^2 + (k + \gamma_f - \gamma_c)\lambda + k\gamma_f - k\gamma_c + \frac{k\gamma_c}{1 - e^{-k\tau}} - \frac{k\gamma_c e^{-(\lambda+k)\tau}}{1 - e^{-k\tau}}. \tag{2.16}$$

Note that equation (2.16) has the same form as the characteristic equation of the model studied in He *et al* (2009) and He and Zheng (2010) except that γ_f and γ_c are defined differently. Hence we can apply Theorems 3.2, 3.3 and 3.4 in He et al. (2009) and Proposition 3.5 in He and Zheng (2010) to system (2.14). For completeness, we summarize the results as follows and refer the details to He et al. (2009) and He and Zheng (2010).

Firstly, the stability of the steady state do not change for time delay $\tau > \tilde{\tau}$, where

$$\widetilde{\tau} = \frac{1}{k} \ln \left[1 + \frac{2k\gamma_c}{(k + \gamma_f - \gamma_c)^2 + 2 \mid k + \gamma_f - \gamma_c \mid \sqrt{k\gamma_f}} \right].$$

That is, there is an upper bound on the time delay for stability change. Secondly, the

[7] For a general theory of functional differential equations, we refer readers to Hale (1997).

[8] Interestingly, the time delays τ_f, τ_c and decaying rates η_f, η_c introduced in the performance measures in (2.8) do not appear in the characteristic equation, hence they do not affect the local stability and bifurcation analysis. This is due to the fact that they are in higher order terms and they affect the nonlinear dynamics, rather than the dynamics of the linearized system. Their impact on the nonlinear dynamics is addressed there in footnote 11.

change in stability happens only when there is a $\tau \in (0, \widetilde{\tau}]$ and a non-negative integer n such that $S_n^+(\tau) = 0$ or $S_n^-(\tau) = 0$ defined by[9]

$$S_n^{\pm}(\tau) = \tau - \frac{\theta_{\pm}(\tau) + 2n\pi}{\omega_{\pm}(\tau)}, \qquad \tau \in (0, \widetilde{\tau}], \qquad n = 0, 1, 2, \cdots,$$

where

$$\omega_{\pm} = \left(\frac{-a_1 \pm \sqrt{a_1^2 - 4a_2}}{2} \right)^{\frac{1}{2}}, \quad \theta_{\pm}(\tau) = \begin{cases} \arccos(a_{4\pm}), & \text{for } a_{3\pm} \geq 0; \\ 2\pi + \arcsin(a_{3\pm}), & \text{for } a_{3\pm} < 0,\ a_{4\pm} \geq 0; \\ 2\pi - \arccos(a_{4\pm}), & \text{for } a_{3\pm} < 0,\ a_{4\pm} < 0 \end{cases}$$

and

$$a_1 = k^2 + \gamma_f^2 + \gamma_c^2 - 2\gamma_f\gamma_c - \frac{2k\gamma_c}{1 - e^{-k\tau}}, \qquad a_2 = k^2\gamma_f^2 + \frac{2k^2\gamma_f\gamma_c e^{-k\tau}}{1 - e^{-k\tau}},$$
$$a_{3\pm} = \frac{-\omega_{\pm}(\tau)(1 - e^{-k\tau})(k + \gamma_f - \gamma_c)}{k\gamma_c e^{-k\tau}}, \qquad a_{4\pm} = 1 - \frac{(1 - e^{-k\tau})(\omega_{\pm}^2(\tau) - k\gamma_f)}{k\gamma_c e^{-k\tau}}.$$

Denote

$$\tau_0 = \inf \left\{ \{\widetilde{\tau}\} \bigcup \{\tau \in (0, \widetilde{\tau}] \mid \exists n \in \{0, 1, 2, \cdots\},\ \ S_n^+(\tau) = 0 \ \text{ or } \ S_n^-(\tau) = 0 \} \right\}.$$

Then the local stability and bifurcation of the fundamental steady state with respect to the time delay of system (2.14) are summarized in the following proposition.

Proposition 2.1 *The fundamental steady state of system* (2.14) *is*

(i) asymptotically stable for $\tau \in [0, \tau_0)$*;*

(ii) asymptotically stable for $\tau > \widetilde{\tau}$ *when* $\gamma_f > \gamma_c - k$*;*

(iii) unstable for $\tau > \widetilde{\tau}$ *when* $\gamma_f < \gamma_c - k$*.*

In addition, the system (2.14) *undergoes Hopf bifurcations at the zero solutions of functions* $S_n^{\pm}(\tau)$*.*

Proposition 2.1 implies that the fundamental steady state is stable for either small or large time delay when the market is dominated by the fundamentalists (in the sense of $\gamma_f + k > \gamma_c$). Otherwise, when the trend followers become more active comparing with the fundamentalists (in the sense of $\gamma_c > \gamma_f + k$), the fundamental steady state becomes unstable through Hopf bifurcations when time delay increases. Meanwhile, when the

[9] We refer to Theorem 3.3 in He et al. (2009) for the properties of functions $S_n^{\pm}(\tau)$.

trend followers put more weights to the most recent historical prices (so that k is large), the fundamental price is stabilized. This result is in line with the results obtained in discrete-time HAMs. In fact, when the time horizon is small, the insignificant price trend, resulting in weak trading signals, limits the destabilizing activity of the chartists. Consequently, the fundamentalists dominate the market and the market becomes stable. However, Proposition 2.1 also indicates a very interesting phenomenon of the continuous-

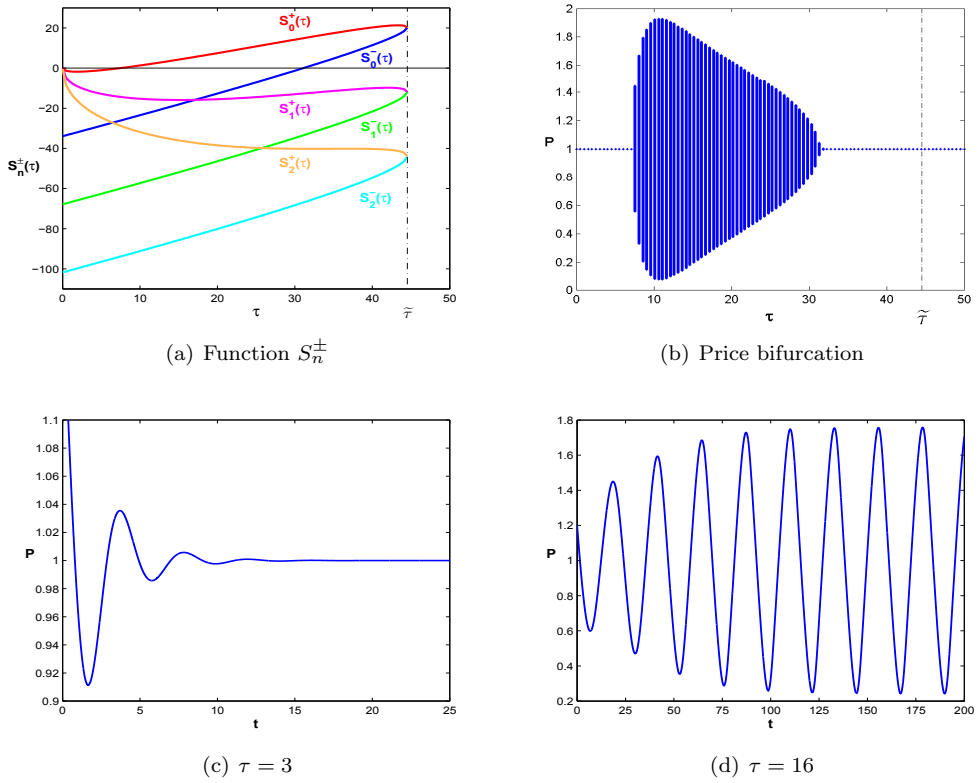

(a) Function $S_n^{\pm}$ (b) Price bifurcation

(c) $\tau = 3$ (d) $\tau = 16$

Figure 2.1: (a) The plots of $S_n^{\pm}$ as functions of τ; (b) the corresponding bifurcation diagram of the market prices with respect to τ; and the market price for (c) $\tau = 3$ and (d) $\tau = 16$. Here $k = 0.05$, $\mu = 1$, $\beta_f = 1.4$, $\beta_c = 1.4$, $\beta = 2$, $C_f = 0.05$, $C_c = 0.03$, $\eta_f = 0.5$, $\eta_c = 0.6$, $\tau_f = 17$, $\tau_c = 16$, and $\bar{F} = 1$.

time model, which is not easy to obtain in a discrete-time model, that is the stability switching[10]. That is, the system becomes unstable as time delay increases initially, but the stability can be recovered when the time delay becomes large enough. Intuitively, when time horizon is large, the price trend becomes significant, resulting in strong trading signals. However, the activity of the trend followers, measured by γ_c and k, is limited by

[10]This phenomenon is also observed in the continuous-time model in He et al. (2009) and He and Zheng (2010) without switching, implying that this is not crucially due to the switching mechanism introduced in this chapter. However, the switching affects the price dynamics significantly when the steady state becomes unstable and/or when the stochastic model is considered. This is demonstrated by Figs 2.3, 4.1 and 4.3 and the related discussions there.

the activity of the fundamentalists, measured by γ_f. Therefore, the market is dominated by the fundamentalists, leading to a stable market. Fig. 2.1 illustrates such interesting stability switching phenomenon[11]. Fig. 2.1 (a) indicates two Hopf bifurcation values in τ, say $\tau_0 < \tau_1$, determined by two zero solutions of $S_0^{\pm}(\tau)$. The first one occurs when $S_0^{+}(\tau)$ crosses 0 at $\tau = \tau_0 \approx 7.45$ and the second one occurs when $S_0^{-}(\tau)$ crosses 0 at $\tau = \tau_1 \approx 31.09$. Fig. 2.1 (b) plots the corresponding bifurcation diagram of the market price with respect to τ showing that the fundamental steady state is stable for $\tau \in [0, \tau_0) \cup (\tau_1, \infty)$ and Hopf bifurcations occur at $\tau = \tau_0$ and $\tau = \tau_1$. Figs 2.1 (c) and (d) illustrate that the fundamental steady state is asymptotically stable for $\tau = 3\,(< \tau_0)$ and unstable for $\tau = 16\,(\in (\tau_0, \tau_1))$. Numerical simulations for $\tau > \tau_1$ (not reported here) verify the stability of the fundamental steady state. The difference of the stability between small τ ($\tau < \tau_0$) and large τ ($\tau > \tau_1$) is that the speed of the convergence is high for small delays and low for large delays. We can see that it is the continuous-time model that facilitates such analysis on the stability effect of lagged price information and stability switching, an advantage of the continuous-time model over the discrete-time model.

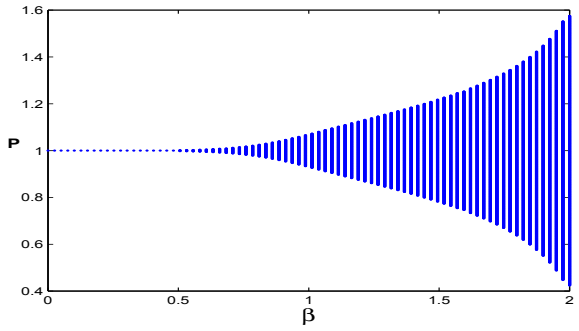

Figure 2.2: The bifurcation of price with respect to β, here $\tau = 8$.

In the discrete-time Brock and Hommes framework, the rational routes to complicated price dynamics are characterized as the switching intensity β increases. For the continuous-time model developed in this chapter, this result also holds. Fig. 2.2 plots the price bifurcation diagram with respect to the switching intensity parameter β. It shows that the steady state is stable when the switching intensity β is low, but becomes unstable as the switching intensity increases, bifurcating to stable periodic price with increasing fluctuations. The periodic fluctuations of the market prices are associated with periodic

[11] All the numerical results in this chapter are based on $k = 0.05$, $\mu = 1$, $\beta_f = 1.4$, $\beta_c = 1.4$, $\beta = 2$, $C_f = 0.05$, $C_c = 0.03$, $\eta_f = 0.5$, $\eta_c = 0.6$, $\tau_f = 17$, $\tau_c = 16$ and $\bar{F} = 1$, unless specified otherwise. In particular, we choose $\eta_f = 0.5$, $\eta_c = 0.6$, $\tau_f = 17$ and $\tau_c = 16$ to take into account that the fundamentalists calculate the weighted cumulated profit over longer time horizons with small decaying rate in weights comparing to the trend followers. As we indicated earlier, they do not affect the local stability and bifurcations. However, simulations (not reported here) show that an increase in η_f (or a decrease in η_c) can increase the fluctuations in price and population switching, but τ_f and τ_c appear to have marginal effect on the fluctuations.

fluctuations of the market fractions. To illustrate this feature, Fig. 2.3 plots the time

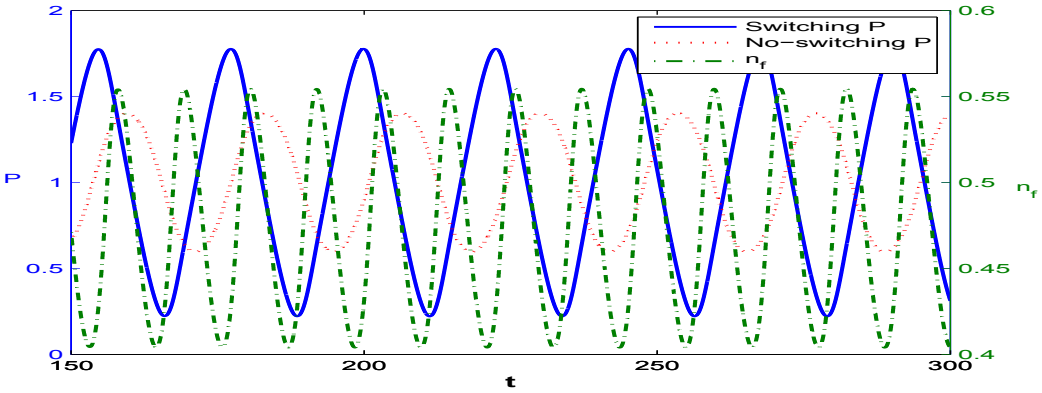

(a) Time series of the prices P with and without switching and market fraction n_f

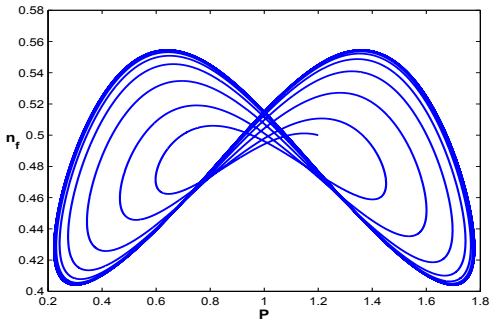

(b) Phase plot of (P, n_f)

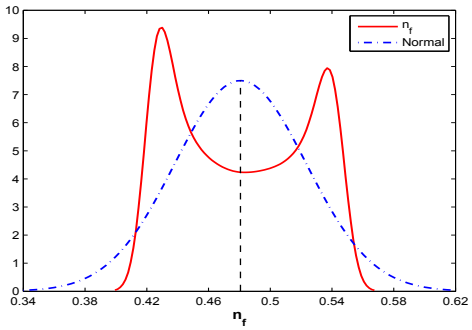

(c) The density of n_f

Figure 2.3: (a) The time series of the market prices $P(t)$ with switching (the blue solid line with high volatility) and without switching (the red dotted line with low volatility) and the market fraction $n_f(t)$ of fundamentalists (the green dash dot line); (b) the phase plot of $(P(t), n_f(t))$; (c) the density distribution of the market fraction $n_f(t)$ of the fundamentalists.

series of prices $P(t)$ and the market fraction of the fundamentalists $n_f(t)$, a phase plot of the price, and the distribution of the market fraction $n_f(t)$ of the fundamentalists for time delay $\tau = 16$. Based on the bifurcation diagram in Fig. 2.1 (b), the steady state is unstable for $\tau = 16$. Fig 2.3 (a) shows the periodic fluctuations in both the market fraction and the market price of the switching model (2.14). To better understand the impact of agents' adaptive switching behavior when the fundamental steady state becomes unstable, we also plot in Fig. 2.3 (a) the market price of the no-switching model in He et al. (2009)[12]. One can see that the switching increases the price fluctuations. The phase plot in Fig. 2.3 (b) shows that price and fraction converge to a *figure-eight shaped*

[12]The parameters in model (2.14) are chosen in such a way so that the steady state population fractions n_f^* and n_c^* are the same in the two models. Previous stability analysis demonstrates that when the market price of the switching model is unstable, so is the no-switching model.

attractor, a phenomenon which is also observed in the discrete-time model in Chiarella et al. (2006). More interestingly, the period of the fluctuation of the market price is twice as much as that of the market fraction and the market prices are close to the fundamental prices whenever the market fractions of the fundamentalists are high. The corresponding distribution of the market fraction $n_f(t)$ of the fundamentalists illustrated in Fig. 2.3 (c) shows clearly the switching of agents' trading strategies over the time. Further simulations (not reported here) show that the fluctuations in both price and population fraction increase as the switching intensity increases.

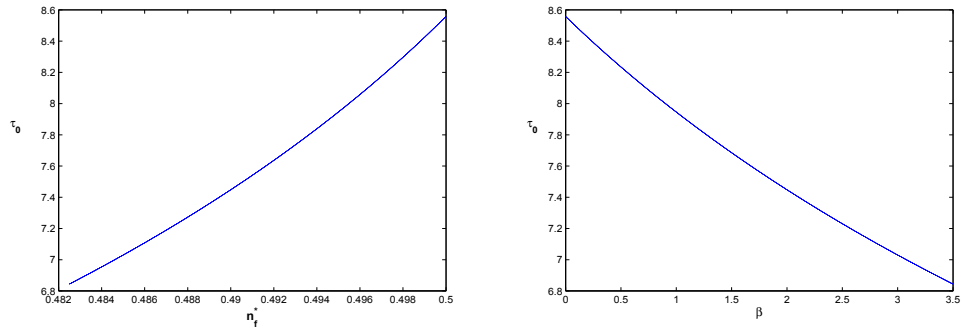

(a) The bifurcation value τ_0 as a function of n_f^* (b) The bifurcation value τ_0 as a function of β

Figure 2.4: The relationships of the first bifurcation value τ_0 with n_f^* and β.

Regarding the joint impact of the time delay, the switching, and the steady state market fractions on market stability, we have shown that an initial increase in time delay destabilizes the fundamental price, however a high steady state market fraction of the fundamentalists stabilizes the price. Also, an increase in switching intensity destabilizes the fundamental price. Hence, with respect to the stability of the steady state, a positive relation between the market fraction of the fundamentalists and the time delay and a negative relation between the switching intensity and the time delay are expected. The above intuition is verified in Fig. 2.4 which plots the first bifurcation value τ_0 with respect to the market fraction of the fundamentalists at the fundamental steady state n_f^* in Fig. 2.4 (a) and the intensity β in Fig. 2.4 (b).

We complete this section with an observation. The *twin-peak-shaped* density distribution in Fig. 2.3 (c) imply that, when the fundamental price is unstable, the market fractions tend to stay away from the steady state market fraction level most of the time and a mean of $n_f(t)$ below 0.5 clearly indicates the dominance of the chartist strategy. In summary, the analysis shows that the continuous-time HAM provides a better understanding of the market dynamics. Apart from providing some consistent results to

the discrete-time HAMs on rational routes to market instability, we are able to study the impact of lagged prices used by the chartists on market stability. Also, the adaptive switching behavior of agents can increase the price fluctuations.

2.4 Price Behavior of the Stochastic Model

In this section, through numerical simulations, we focus on the interaction between the dynamics of the deterministic model and noise processes and explore the potential power of the model to generate various market behavior and the stylized facts observed in financial markets. To complete the stochastic model (3.7), we introduce the stochastic fundamental price process,

$$dF(t) = \frac{1}{2}\sigma_F^2 F(t)dt + \sigma_F F(t)dW_F(t), \qquad F(0) = \bar{F}, \tag{2.17}$$

where $\sigma_F > 0$ represents the volatility of the fundamental return and $W_F(t)$ is a standard Wiener process. The market noise $W_M(t)$ and fundamental price noise $W_F(t)$ can be correlated and let ρ be their correlation. It follows from (2.17) that the fundamental return defined by $d\big(\ln(F(t))\big)$ is a pure white noise process following the normal distribution with mean of 0 and standard deviation of $\sigma_F\sqrt{dt}$. This ensures that any non-normality and volatility clustering of market returns that the model could generate are not carried from the fundamental returns.

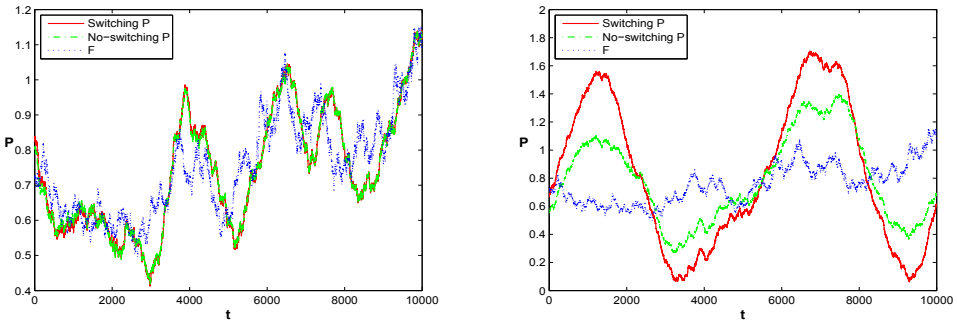

(a) $\tau = 3$ (b) $\tau = 16$

Figure 2.5: The time series of the fundamental price (the blue dotted line) and the market prices of the switching model (the red solid line) and the no-switching model (the green dash dot line) for two delays (a) $\tau = 3$ and (b) $\tau = 16$. Here $\sigma_F = 0.12$, $\sigma_M = 0.05$ and $\rho = 0$.

Firstly, we explore the joint impact of the time horizon τ of the chartists and the two noise processes on the market price dynamics. For the corresponding deterministic model (2.14), Figs 2.1 (c) and (d) show that the fundamental steady state is stable for $\tau = 3$ and unstable for $\tau = 16$, leading to periodic fluctuations of the market price.

For the stochastic model, with the same random draws of the fundamental price and the market noise processes, we plot the fundamental price (the blue dotted line) and the market prices of both the switching model (2.13) (the red solid line) and the no-switching model with population fractions being n_f^* and n_c^* (the green dash dot line) in Fig. 2.5 for two different values of τ. For $\tau = 3$, Fig. 2.5 (a) demonstrates that the market price[13] follows the fundamental price closely and there is no significant difference for the market prices with and without switching. For $\tau = 16$, Fig. 2.5 (b) indicates that the market price fluctuates around the fundamental price in cyclic way, which is underlined by the bifurcated periodic oscillation of the corresponding deterministic model. In addition, similar to the deterministic model, the price fluctuations of the stochastic model are high with switching.

Secondly, we explore the potential of the stochastic model in generating the stylized facts for daily data observed in financial markets. We choose $\tau = 3$ so that the steady state is stable[14], as illustrated in Fig. 2.1 (c). We study at first the case when the two stochastic processes are independent, that is $\rho = 0$. For the stochastic model with both noisy processes, Fig. 2.6 represents the results of a typical simulation. Fig. 2.6 (a) shows that the market price (the red solid line) follows the fundamental price (the blue dotted line) in general, but accompanied with large deviations from time to time. The returns of the market prices in Fig. 2.6 (b) show significant volatility clustering. Comparing to the corresponding normal distribution, the return distribution in Fig. 2.6 (c) displays high kurtosis. The returns show almost insignificant autocorrelations (ACs) in Fig. 2.6 (d), but the ACs for the absolute returns and the squared returns in Figs. 2.6 (e) and (f) are significant with strong decaying patterns as time lag increases, implying a long range dependence. These results demonstrate that the stochastic model established in this chapter has a great potential to generate most of the stylized facts observed in financial markets.

We may argue that the above features of the stochastic model is a joint outcome of the interaction of the nonlinear HAM and the two stochastic processes similar to He and Zheng (2010). With the same random seeds, we report the simulation results in Figs. 2.7 and 2.8 when there is only one stochastic process involved. In Fig. 2.7, there is no market noise and the fundamental price is the only stochastic process. The time series, return density distribution, and the ACs of the returns, the absolute returns and the squared returns do not replicate these stylized facts demonstrated in Fig. 2.6. Alterna-

[13] In the simulations in this section, time unit is a year, an annual volatility is given by $\sigma_F = 0.12$, and the time step of numerical simulations is 0.004, corresponding to one day.

[14] It appears that the stylized facts can also be obtained by choosing τ from its unstable interval. The implications of different choice of delays on the stylized facts would be interesting.

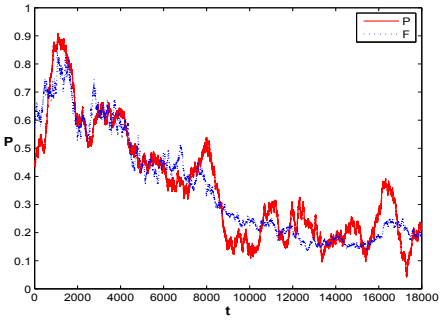

(a) The market price and the fundamental price

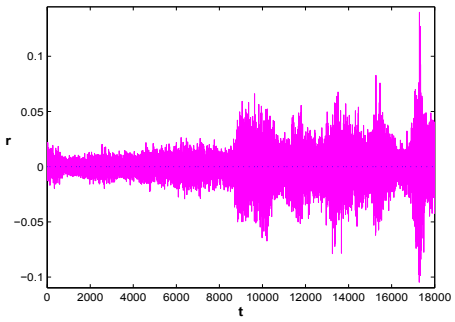

(b) The market returns (r)

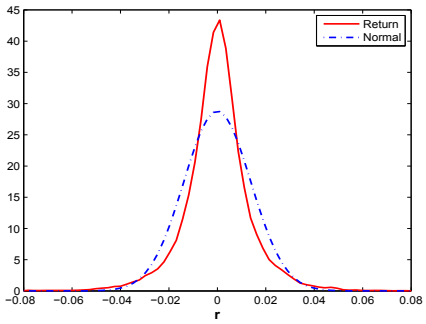

(c) The density of the market returns

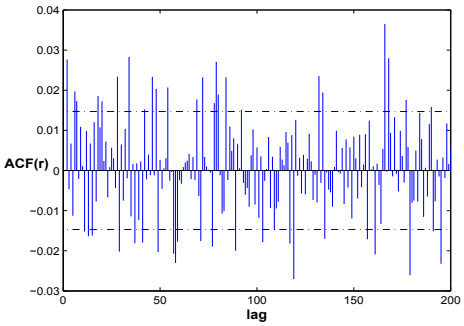

(d) The ACs of the market returns

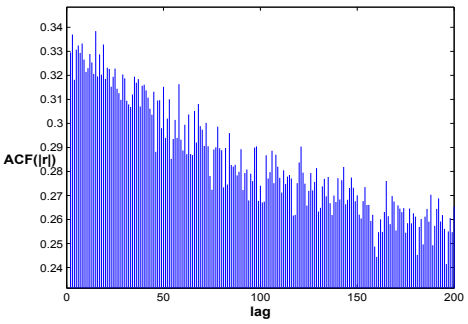

(e) The ACs of the absolute returns

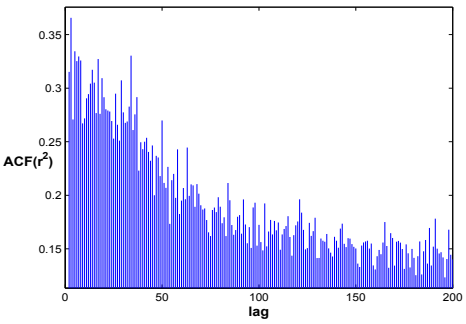

(f) The ACs of the squared returns

Figure 2.6: The time series of (a) the market price (red solid line) and the fundamental price (blue dotted line) and (b) the market returns; (c) the return distribution; the ACs of (d) the returns; (e) the absolute returns, and (f) the squared returns. Here $\sigma_F = 0.12$, $\sigma_M = 0.05$ and $\rho = 0$.

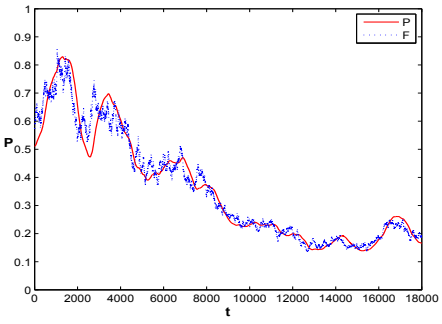

(a) The market price and the fundamental price

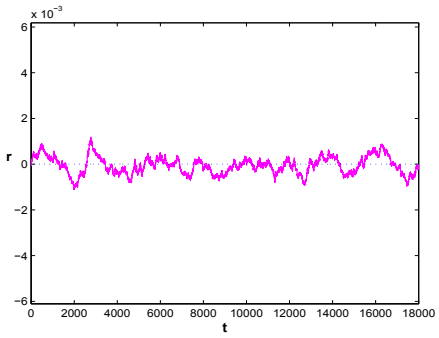

(b) The market returns (r)

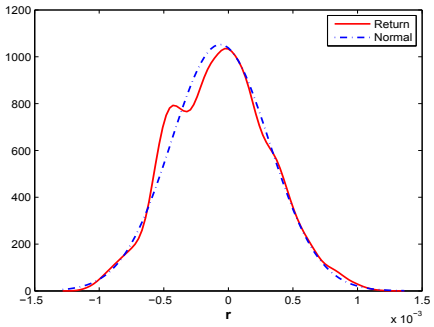

(c) The density of the market returns

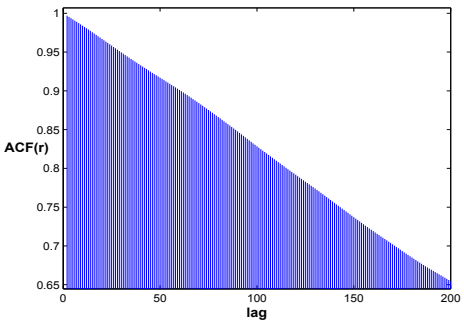

(d) The ACs of the market returns

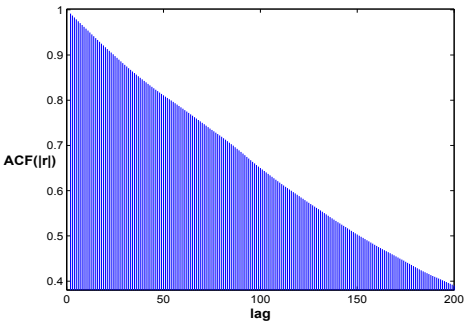

(e) The ACs of the absolute returns

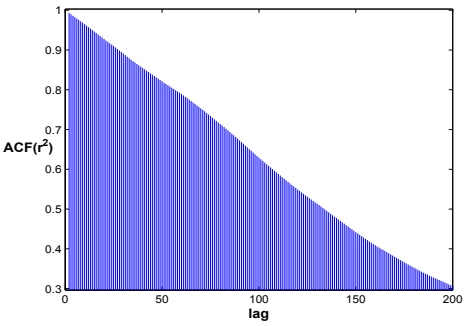

(f) The ACs of the squared returns

Figure 2.7: The time series of (a) the market price (red solid line) and the fundamental price (blue dotted line) and (b) the returns; (c) the return distribution; the ACs of (d) the returns; (e) the absolute returns, and (f) the squared returns. Here $\sigma_F = 0.12$, $\sigma_M = 0$ and $\rho = 0$.

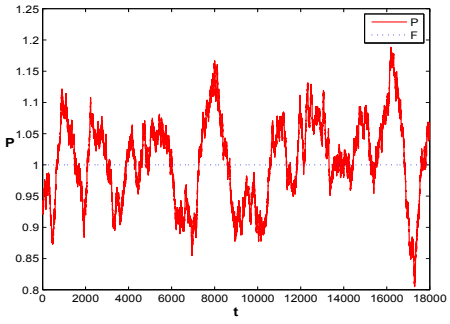

(a) The market price and the fundamental price

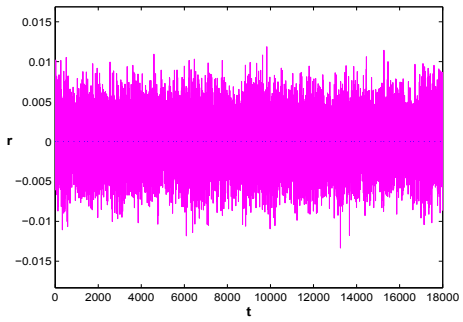

(b) The market returns (r)

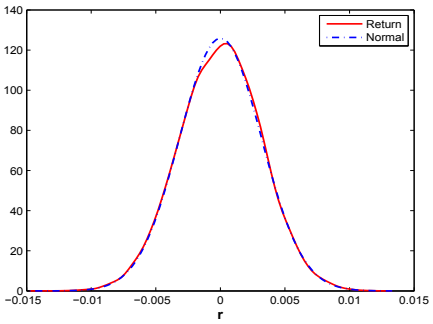

(c) The density of the market returns

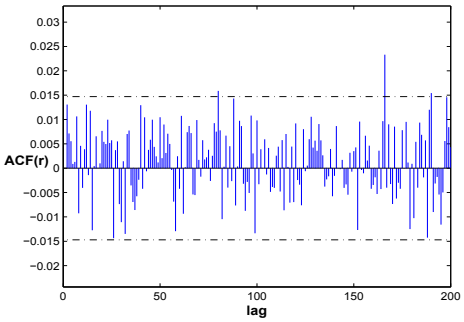

(d) The ACs of the market returns

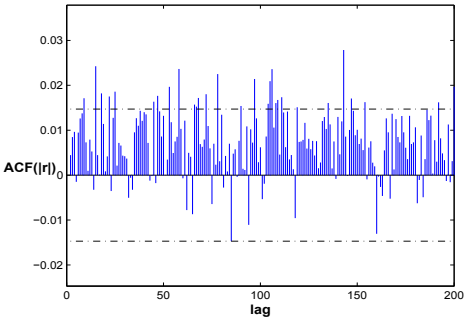

(e) The ACs of the absolute returns

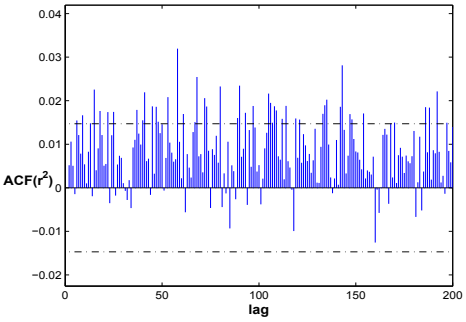

(f) The ACs of the squared returns

Figure 2.8: The time series of (a) the market price (red solid line) and the fundamental price (blue dotted line) and (b) the returns; (c) the return distribution; the ACs of (d) the returns; (e) the absolute returns, and (f) the squared returns. Here $\sigma_F = 0$, $\sigma_M = 0.05$ and $\rho = 0$.

tively, in Fig. 2.8 the market noise process is the only stochastic process. It shows that the return is basically described by a white noise process. Both Figs 2.7 and 2.8 indicate that the potential of the model in generating the stylized facts is not due to either one of the two stochastic processes, rather than to both processes. The underlying mechanism in generating the stylized facts, long range dependence, and the interplay between the nonlinear deterministic dynamics and noises are very similar to the one explored in He and Li (2007) for a discrete-time HAM. Economically, the fundamental noise can be very different from the market noise and consequently they affect the market price differently. Without the market noise, the market price is driven by the mean-reverting of the fundamentalists (to the fundamental price) and the trend chasing of the chartists; both contribute to building up market price trend. Due to the randomness of the fundamental price, there are persistent mean-reverting activities from the fundamentalists that provide the chartists opportunities to explore the price trend. Therefore, the significant ACs of the market returns, absolute returns and squared returns in Fig. 2.7 reflect the interaction of the fundamentalists and the chartists. However, with the market noise and a constant fundamental price, the price trend is less likely formed and explored by the chartists. This limits the impact of the speculative behavior of the chartists, which explains the insignificant ACs of the market returns, absolute returns and squared returns in Fig. 2.8. With both noise processes, the price trend is difficult to explore (due to the market noise) and consequently the returns become less predictable. However, the interaction of the fundamentalists and the chartists becomes intensive due to some large changes in the fundamental price from time to time, implying the significant ACs in return volatility, shown in Fig. 2.6 (d)-(f).

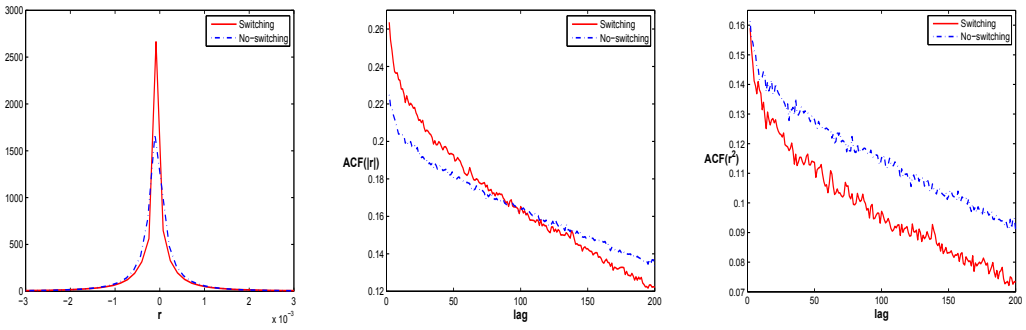

(a) The return distributions (b) The ACs of the absolute returns (c) The ACs of the squared returns

Figure 2.9: (a) The return distributions; the average ACs of (b) the absolute returns and (c) the squared returns based on 200 simulations for both the switching (the red solid line) and no-switching (the dash-dotted blue line) models . Here $\sigma_F = 0.12$, $\sigma_M = 0.05$ and $\rho = 0$.

To understand the impact of the adaptive switching behavior of agents on the stylized facts and the AC patterns, based on 200 simulations with different random seeds, Fig. 2.9 reports the return distributions and the average ACs of the absolute returns and the squared returns of the switching model (2.13) (the red solid line) and the no-switching model (the blue dash-dotted line). Fig. 2.9 (a) shows that the switching model displays higher kurtosis than the no-switching model. In addition, Figs. 2.9 (b) and (c) show that the ACs of both the absolute returns and the squared returns are significantly. However, the ACs for the switching model decay quickly, which are more close to the AC patterns observed in financial time series[15].

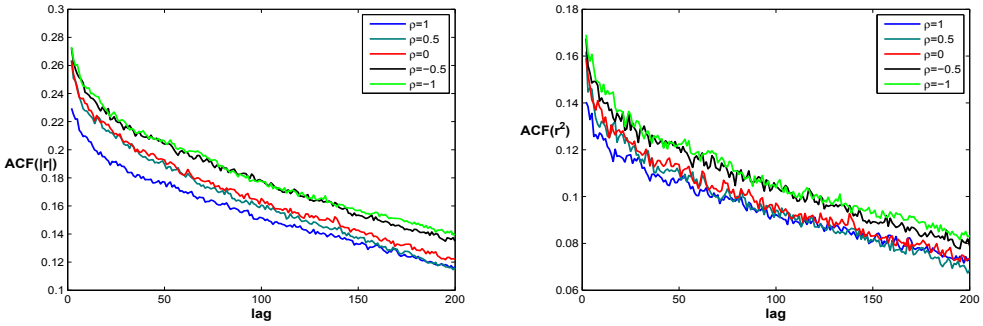

(a) The ACs of the absolute returns (b) The ACs of the squared returns

Figure 2.10: The average ACs of (a) the absolute returns and (b) the squared returns based on 200 simulations for $\rho = 0, \pm 0.5, \pm 1$. Here $\sigma_F = 0.12$ and $\sigma_M = 0.05$.

Given that the market noise may be correlated with the fundamental price noise, we now examine the impact of the correlated noises on the AC patterns. Based on 200 simulations for different ρ $(0, \pm 0.5, \pm 1)$, Fig. 2.10 compares the ACs of the absolute and squared returns, from which we have a number of interesting observations. Firstly, the ACs are significant and decaying for all correlations, implying that the mechanism in generating the long range dependence can be independent of the correlation of the two noise processes. Secondly, the ACs become more significant when the noise processes are negatively correlated, in particular, when $\rho = -1$; while they become less significant when they are positively correlated, in particular, when $\rho = 1$. Thirdly, not perfectly positively correlated noises lead to more realistic AC decaying patterns.

We conclude this section with a remark on the predictability of asset returns over different trading frequency. As one of the stylized facts, the insignificant ACs of daily returns imply that daily returns are not predictable. However, it is well documented

[15] In a discrete-time model, He and Li (2007) show that the no-switching model is able to replicate the significant decaying AC patterns in the absolute and squared returns, but the speed of the decaying is low comparing to the AC patterns observed in financial time series. Further statistic test would be useful to clarify such difference and we leave this to the future research.

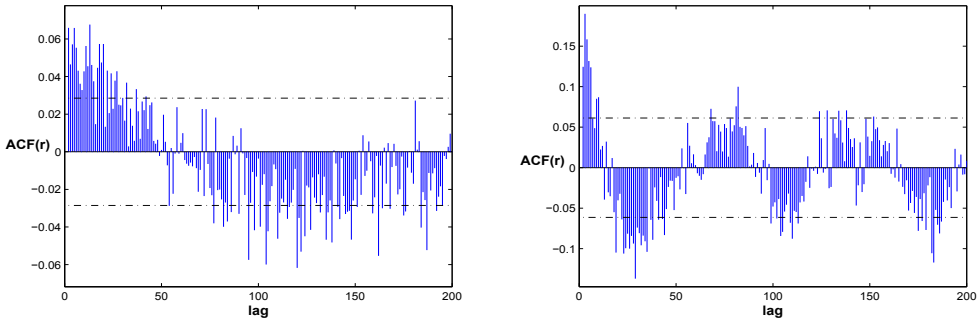

(a) The ACs of the weekly market return (b) The ACs of the monthly market return

Figure 2.11: The ACs of the weekly and monthly market returns. Here $\tau_c = 16$, $\sigma_F = 0.12$, $\sigma_M = 0.05$ and $\rho = 0$.

(see for example Pesaran and Timmermann 1994, 1995) that weekly and monthly returns are predictable. Fig. 2.11 illustrates the ACs of (a) weekly and (b) monthly returns. The significant ACs indicate that weekly and monthly returns are predictable, showing that the model has potential to replicate the return predictability for different trading frequency. It would be interesting to explore this potential further.

2.5 Conclusion

This chapter contributes to the development of financial market modelling and asset price dynamics with bounded rationality and heterogeneous agents. Most of the heterogeneous agent models developed in the literature are in the discrete-time setup. Among various issues in this literature, the impact of adaptive behavior on market stability has been well studied, while the impact of lagged prices (used by chartists to form their expectations) on market stability has not been well understood due to the problem of high dimensional systems. This chapter develops a continuous-time framework to study the joint impact of lagged prices and adaptive behavior of heterogeneous agents. By using the replicator dynamics in population evolution literature, we extend the discrete choice model used in discrete-time HAMs to a continuous-time model. The delay differential equations provide a uniform approach to study the impact of the lagged prices through a time delay parameter.

The continuous-time model developed in this chapter studies a financial market consisting of adaptive and heterogeneous agents using fundamental and technical strategies. Agents change their strategies in a boundedly rational way according to a performance measure of the accumulated profits. The analysis of the model provides not only some

consistent results to the discrete-time HAMs, such as stabilizing effect of fundamentalists, destabilizing effect of chartists, and the rational routes to market instability, but also a double edged effect of an increase in lagged prices on market stability. An increase in the using of lagged prices can not only destabilize, but also stabilize the market price. More importantly, the adaptive switching behavior of agents can increase market price fluctuations. By introducing a market noise characterizing noise traders or liquidity trading and imposing a stochastic process on fundamental price, we demonstrate that the model is able to generate long deviations of the market price from the fundamental price, bubbles, crashes, and most of the stylized facts, including non-normality in return, volatility clustering, and long range dependence of high-frequency returns, observed in financial markets. In addition, comparing to the no-switching model, the adaptive behavior of agents can generate more realistic AC patterns in the absolute and squared returns.

The continuous-time framework developed in this chapter has shown some advantages comparing to the discrete-time framework, in particular when dealing with the impact of lagged prices. The framework can be used to study the joint impact on the markets of the irrational herding behavior and the more rational switching. This is the focus of Chapter 3. Also, the profitability of different trading strategies, including momentum and contrarian strategies, are well documented in empirical literature and it would be interesting to explore these empirical features within the continuous-time framework developed in this chapter. We leave these studies to Chapter 4.

Chapter 3

Herding, Trend Chasing and Market Volatility

3.1 Introduction

Trend chasing, switching among different trading strategies and herding behavior are the most commonly observed boundedly rational behaviors of investors in financial markets. In Chapter 2, we focus on trend chasing and switching, and show that the proposed model is able to generate various market phenomena and stylized facts. Herding refers broadly to the tendency of many different agents to take similar actions at roughly the same time.[1] Based on the model in Chapter 2, this chapter also incorporates herding behavior and studies their joint impact on market volatility.

Large fluctuations in market price, excess volatility in return, and volatility clustering are the most common stylized facts in financial markets. The question is how these boundedly rational behaviors of investors contribute to market volatility differently. This chapter introduces a heterogeneous agent asset pricing model in a continuous-time framework to address this question. We show that herding and trend chasing based on long time horizon increase market volatility in price and return. However, the effect of switching is different for price volatility and opposite for return volatility. We also show that these boundedly rational behavior of investors contribute to the power-law behavior, characterized by insignificant autocorrelations (ACs) in the returns and significant and decaying ACs in the absolute and squared returns; however, their effects are different. More precisely, the level of the significant ACs increases with the herding and trend chasing based on long time horizon, but increases initially and then decreases as the switching intensity

[1] Scharfstein and Stein (1990) attribute it to the reputational concerns and the unpredictable components to investment outcomes. Banerjee (1992) shows that herd behavior is rational in term of obtaining others' information.

increases. In general, it is the interaction of nonlinear dynamics and noises that generates realistic market price dynamics. We show that the market noise characterizing noise trading or liquidity trading plays more important role than the fundamental noise in generating the power-law behavior. To our knowledge, this chapter is the first showing that the herding and switching have opposite effect on the return volatility and different impact on the power-law behavior.

This chapter is closely related to the recent development of heterogeneous agent models (HAMs) considering financial markets as expectation feedback systems and hence asset price fluctuations can be caused by an endogenous mechanism with heterogeneity and bounded rationality. Various agent-based financial market models have been developed to incorporate trend chasing, switching and herding. For instance, both Brock and Hommes (1998) in discrete-time and Chapter 2 in continuous-time show that switching can generate complex behavior from local stability to high order cycles and chaos. Within a continuous-time framework, Lux (1995) and Alfarano, Lux and Wagner (2008) model the herding behavior through the master equation and show that herding can give rise to realistic time series. Within a discrete-time framework, Hohnisch and Westerhoff (2008) show how herding behavior at the level of individual economic sentiment may lead to enduring business cycles, and Franke and Westerhoff (2012) show a strong role for a herding component when generating realistic moments in financial time series.

This chapter provides a unified framework in a continuous-time model to examine the joint impact of trend chasing, switching, and herding on market price dynamics and compare different roles they play in generating market volatility in price and return and the power-law behavior of stock return volatility. Following Chapter 2, we introduce a continuous-time financial market with two types of agents, the fundamentalists who trade on the fundamental value and the trend followers who extrapolate the market price trend based on weighted moving average price over a finite time horizon. The herding behavior among the agents is characterized by the master equation. The market price is determined by a market maker who adjusts the market price to the excess demand from the fundamentalists and trend followers, together with a noisy demand. The continuous-time setup chosen in the chapter not only mathematically facilitates the modelling of the time horizon of the historical price information used by the trend followers, but also easily accommodates the herding behavior through the master equation with endogenously determined volatility.

We first examine the dynamics of the underlying deterministic model. Differently from the adaptive switching model in Chapter 2, we find that the herding mechanism does not affect the local stability of the steady state fundamental price, although it does affect the

nonlinear behavior. Based on the analysis of the deterministic dynamics, we then study the joint impact of trend chasing, herding, and switching on the volatility of market price and return of the stochastic model. We find that the trend chasing based on historical prices over a long time horizon always leads to high volatility in both market prices and stock returns, which is underlined by the destabilizing effect of the trend chasing. Also, herding and switching have very different effect on the market volatility. A strong herding contributes to high fluctuation in market fractions and market price and hence generates high volatilities in prices and returns, while a more intense switching reduces the return volatility and has a non-monotonic effect on the volatilities of market fractions and prices. More interestingly, we observe a "hump" shaped volatility in the market fraction and a "U"-shaped price volatility as the switching intensity increases.

We explore further the potential of the model to generate the power-law behavior in volatility. Following the HAMs literature, we find that it is the interaction of the nonlinear dynamics of the underlying deterministic model and the noises that generates the power-law behavior. We examine the impact of different noises (including fundamental noise, market noise and market fraction noise), time horizon, switching and herding on the ACs of the returns, absolute returns, and squared returns. We find that market noise is the main driving force in generating the power-law behavior. The AC patterns become more significant as the time horizon and herding increase, but non-monotonic with the switching. Specifically, an initial increase in the switching intensity leads to an increase in the significant levels of ACs but a decrease as the switching increases further. In general, it is the combination of switching and herding, together with the market noise, that generates realistic power-law behavior.

The chapter is based on Di Guilmi, He and Li (2013) and organized as follows. We first introduce a stochastic HAM of asset pricing in continuous-time with trend chasing, herding, switching and heterogeneous beliefs in Section 3.2. In Section 3.3, we apply stability and bifurcation theory of delay differential equations, together with numerical analysis of the nonlinear system, to examine the impact of herding, switching and time horizon used by the trend followers on market stability. The effect of and different role played by trend chasing, herding and switching on market volatility and power-law behavior are then discussed in Sections 3.4 and 3.5, respectively. Section 3.6 concludes. All proofs and some additional results are given in Appendix B.

3.2 The Model

Consider a financial market with a risky asset (such as stock market index) and let $P(t)$ be the (cum dividend) price of the risky asset at time t. Following the standard approach of HAMs, see, for example, Brock and Hommes (1998), we assume that the market consists of fundamentalists who trade according to the fundamental value of the risky asset, trend followers who trade based on price trend of a weighted moving averages of historical prices over a time horizon, and a market maker who clears the market by providing liquidity. The behavior of the fundamentalists and trend followers is modelled as usual. Different from the discrete-time HAMs in the literature (for example, Chiarella and He, 2002 and 2003a), we consider a continuous-time setup to accommodate different time horizon used by the trend followers and the stochastic master equation characterizing the herding behavior of agents. The demand functions of the fundamentalists and the trend followers $Z_i(t)$, the net profits $\pi_i(t)$ and the performances of the strategies $U_i(t)$, $i = f, c$ are of the same forms given by Chapter 2. Instead of studying switching effect in Chapter 2, we characterize the market fraction dynamics of the fundamentalists and the trend followers $n_i(t), i = f, c$ with herding effect in current chapter.

Denote by $a(t)$ the transition probability of an agent switching from being trend follower to fundamentalist and by $b(t)$ the probability of the inverse transition. Following Lux (1995), the probabilities can be quantified by

$$a(t) = ve^{\beta(U_f(t)-U_c(t))}, \qquad b(t) = ve^{\beta(U_c(t)-U_f(t))}, \tag{3.1}$$

where $U_i(t), i = f, c$ is given by (2.8) in Chapter 2, β measures the switching intensity and $v > 0$ captures the intensity of herding explained in the following. Let $\zeta(t)$ denote the probability of observing a change of an agent from the trend follower to the fundamentalist and $\xi(t)$ denote the probability of recording the opposite transition. Both $\zeta(t)$ and $\xi(t)$ are assumed to be proportional to the transition probability of the switching and the corresponding market fractions to capture the herding behavior. Then the transition rates can be expressed as

$$\zeta(t) = (1 - n_f(t))a(t) = v(1 - n_f(t))e^{\beta(U_f(t)-U_c(t))}, \tag{3.2}$$

$$\xi(t) = n_f(t)b(t) = vn_f(t)e^{\beta(U_c(t)-U_f(t))}. \tag{3.3}$$

Note that, when $\beta = 0$, a large v means a strong herding among the agents. Hereafter, we use β and v to measure the (performance based) switching and herding, respectively, among the agents. Following Lux (1995), the master equation measuring the variation of

probability in a unit of time by taking the number of fundamentalists as a state variable is given by

$$\frac{dp(N_f,t)}{dt} = \zeta(t)p(N_f-1,t) + \xi(t)p(N_f+1,t) - [\zeta(t)+\xi(t)]p(N_f,t), \tag{3.4}$$

where $p(N_f,t)$ is the probability of recording a number of N_f fundamentalists at time t. Following Chiarella and Di Guilmi (2011*b*), the dynamics of population evolution can be characterized by[2]

$$dn_f(t) = n_f(t)[-(\zeta(t)+\xi(t))n_f(t) + \zeta(t)]dt + \sigma_{n_f}dW_{n_f}(t), \tag{3.5}$$

where

$$\sigma_{n_f}(t) = \frac{\sqrt{\zeta(t)\xi(t)}}{\zeta(t)+\xi(t)}, \tag{3.6}$$

and $W_{n_f}(t)$ is the stochastic fluctuation component in the market population fraction of fundamentalists, which is assumed to be independent from the fundamental noises $W_F(t)$.

Finally, the price $P(t)$ at time t is adjusted by the market maker according to the aggregate market excess demand, that is,

$$dP(t) = \mu\big[n_f(t)Z_f(t) + n_c(t)Z_c(t)\big]dt + \sigma_M dW_M(t),$$

where $Z_f(t)$ and $Z_c(t)$ are given by (2.1) and (2.2) respectively, $\mu > 0$ represents the speed of the price adjustment by the market maker, $\sigma_M > 0$ is a constant and $W_M(t)$ is a standard Wiener process capturing the random excess demand process either driven by unexpected market news or noise traders,[3] which is independent of $W_F(t)$ and $W_{n_f}(t)$.

To sum up, the market price of the risky asset is determined according to the following stochastic delay differential system with three different time delays and three noise

[2]The derivation is given in Appendix B.1.

[3]The additive noise comes naturally when a demand from noise traders is introduced into the aggregated excess demand function.

processes

$$\begin{cases} dP(t) = \mu\Big[n_f(t)Z_f(t) + \big(1-n_f(t)\big)Z_c(t)\Big]dt + \sigma_M dW_M(t), \\ du(t) = \dfrac{k}{1-e^{-k\tau}}\Big[P(t) - e^{-k\tau}P(t-\tau) - (1-e^{-k\tau})u(t)\Big]dt, \\ dn_f(t) = vn_f(t)\Big[\big(1-n_f(t)\big)^2 e^{\beta(U_f(t)-U_c(t))} - n_f^2(t)e^{\beta(U_c(t)-U_f(t))}\Big]dt \\ \qquad\qquad + \sigma_{n_f} dW_{n_f}(t), \\ dU_f(t) = \dfrac{\eta_f}{1-e^{-\eta_f\tau_f}}\Big[\pi_f(t) - e^{-\eta_f\tau_f}\pi_f(t-\tau_f) - (1-e^{-\eta_f\tau_f})U_f(t)\Big]dt, \\ dU_c(t) = \dfrac{\eta_c}{1-e^{-\eta_c\tau_c}}\Big[\pi_c(t) - e^{-\eta_c\tau_c}\pi_c(t-\tau_c) - (1-e^{-\eta_c\tau_c})U_c(t)\Big]dt, \\ dF(t) = \dfrac{1}{2}\sigma_F^2 F(t)dt + \sigma_F F(t)dW_F(t), \end{cases} \tag{3.7}$$

where $Z_f(t)$ and $Z_c(t)$ are defined by (2.1) and (2.2), respectively, and $\pi_i(t)$ is defined by (2.7) for $i = f, c$ in Chapter 2. The stochastic differential system (3.7) characterizes the market price dynamics with heterogeneity in trading strategies, trend chasing, switching, and herding.

In the following sections, we first conduct a stability analysis of the underlying deterministic model. Then we examine the impact of the interaction of the deterministic dynamics with the noises on the fluctuations of the market population fractions (of using different strategies) and market volatility in both prices and return. Furthermore, we explore the power-law behavior in volatility.

3.3 The Stability Analysis of the Deterministic Model

To understand the interaction of the nonlinear deterministic dynamics and the noise processes, we first study the local stability of the corresponding deterministic system. By assuming $F(t) = \bar{F}$, $\sigma_M = 0$ and considering the mean process of the market fraction of

the fundamentalists, system (3.7) reduces to

$$\begin{cases} \dfrac{dP(t)}{dt} = \mu\Big[n_f(t)\beta_f[F(t)-P(t)] + \big(1-n_f(t)\big)\tanh\big[\beta_c(P(t)-u(t))\big]\Big], \\ \dfrac{du(t)}{dt} = \dfrac{k}{1-e^{-k\tau}}\Big[P(t) - e^{-k\tau}P(t-\tau) - (1-e^{-k\tau})u(t)\Big], \\ \dfrac{dn_f(t)}{dt} = vn_f(t)\Big[\big(1-n_f(t)\big)^2 e^{\beta(U_f(t)-U_c(t))} - n_f^2(t)e^{\beta(U_c(t)-U_f(t))}\Big], \\ \dfrac{dU_f(t)}{dt} = \dfrac{\eta_f}{1-e^{-\eta_f\tau_f}}\Big[\pi_f(t) - e^{-\eta_f\tau_f}\pi_f(t-\tau_f) - (1-e^{-\eta_f\tau_f})U_f(t)\Big], \\ \dfrac{dU_c(t)}{dt} = \dfrac{\eta_c}{1-e^{-\eta_c\tau_c}}\Big[\pi_c(t) - e^{-\eta_c\tau_c}\pi_c(t-\tau_c) - (1-e^{-\eta_c\tau_c})U_c(t)\Big], \end{cases} \tag{3.8}$$

where

$$\pi_i(t) = \mu Z_i(t)\Big[n_f(t)Z_f(t) + \big(1-n_f(t)\big)Z_c(t)\Big] - C_i, \qquad i = f, c.$$

The system has a steady state[4]

$$Q := (P, u, n_f, U_f, U_c) = (\bar{F}, \bar{F}, \frac{1}{1+e^{\beta(C_f-C_c)}}, -C_f, -C_c),$$

in which the market price is given by the fundamental value. We call Q the fundamental steady state of the system (3.8). At the fundamental steady state, the market fraction of fundamentalists becomes $n_f^* = \frac{1}{1+e^{\beta(C_f-C_c)}}$. When $C_f = C_c$, $n_f^* = n_c^* = 0.5$, meaning that the market fractions at the fundamental steady state is independent of the switching intensity β and the herding parameter v. However, when the fundamental strategy costs more, that is $C_f > C_c$, then $n_c^* > n_f^*$, meaning that there are more trend followers than fundamentalists at the fundamental steady state.

Denote $\gamma_f = \mu n_f^* \beta_f$ and $\gamma_c = \mu(1-n_f^*)\beta_c$. The characteristic equation of the system (3.8) at the fundamental steady state is given by $\Delta(\lambda) := (\lambda + 2vn_f^*)\widetilde{\Delta}(\lambda) = 0$, where

$$\widetilde{\Delta}(\lambda) = (\lambda+\eta_f)(\lambda+\eta_c)\Big[\lambda^2 + (k+\gamma_f-\gamma_c)\lambda + k\gamma_f - k\gamma_c + \frac{k\gamma_c}{1-e^{-k\tau}} - \frac{k\gamma_c e^{-(\lambda+k)\tau}}{1-e^{-k\tau}}\Big]. \tag{3.9}$$

Note that equation (3.9) has the same form as the characteristic equation of the model studied in Chapter 2. Hence we can apply Proposition 2.1 in Chapter 2 and its corresponding discussions to system (3.8) and the local stability and bifurcation of the fundamental steady state with respect to the time delay of system (3.8) are summarized in the following

[4]In addition, the line $P = u$, $n_f = 0$, $U_f = -C_f$, $U_c = -C_c$ is a steady state line of the system. This means that the system has infinite many steady states. Near the line, the solution with different initial values converge to different steady states on the line. Hence the line is locally attractive. A similar result is found in He et al. (2009) and He and Zheng (2010).

proposition.

Proposition 3.1 *The fundamental steady state Q of system* (3.8) *is*

(i) asymptotically stable for $\tau \in [0, \tau_0)$;

(ii) asymptotically stable for $\tau > \widetilde{\tau}$ when $\gamma_f + k > \gamma_c$;

(iii) unstable for $\tau > \widetilde{\tau}$ when $\gamma_f + k < \gamma_c$.

In addition, system (3.8) *undergoes Hopf bifurcations at the zero solutions of functions $S_n^{\pm}(\tau)$.*

Proposition 3.1 implies that the fundamental steady state is stable for either small or large time delay when the market is dominated by the fundamentalists (in the sense of $\gamma_f + k > \gamma_c$). Otherwise, when the trend followers become more active comparing to the fundamentalists (in the sense of $\gamma_c > \gamma_f + k$), the fundamental steady state becomes unstable through Hopf bifurcations when time delay increases. Same as the model in Chapter 2, Proposition 3.1 indicates the interesting phenomenon of continuous-time HAM again: the stability switching when the fundamentalists dominate the market. That is, the system becomes unstable as the time delay increases initially, but the stability can be recovered when the time delay becomes large enough. Intuitively, when time horizon is small, the price trend becomes less significant, which limits the activity of the trend followers. As the time horizon increases, the price trend becomes more sensitive to market price change and hence the trend followers become more active, which destabilizes the market. However, as the time horizon becomes very large, the price trend becomes smooth and less sensitive to price changes. Therefore the trend followers become less active and then, because of the dominance of the fundamentalists, the market becomes stable. We refer readers to the discussions following Proposition 2.1 in Chapter 2 for more details on the dynamical properties of system (3.8).

By simulating the nonlinear model (3.8),[5] Fig. 3.1 verifies the stability results in Proposition 3.1. Fig. 3.1 (a) plots the bifurcation diagram of the market price of model (3.8) with respect to τ, showing that the fundamental steady state is stable for $\tau \in [0, \tau_0) \cup (\tau_1, \infty)$ and Hopf bifurcations occur at $\tau = \tau_0 \approx 8.5$ and $\tau = \tau_1 \approx 27$. Fig. 3.1 (b) plots the price bifurcation diagram with respect to the switching intensity parameter β. It shows that the steady state is stable when the switching intensity β is low, but becomes unstable as the switching intensity increases, bifurcating to stable periodic price with increasing fluctuations. This result shares the same spirit of rational routes to complicated

[5] Unless specified otherwise, the following set of parameters are used in all the simulations in this chapter: $k = 0.05, \mu = 1, \beta_f = 1.4, \beta_c = 1.4, \beta = 1, C_f = 0.05, C_c = 0.03, \eta_f = 0.5, \eta_c = 0.6, \tau = 16, \tau_f = 10, \tau_c = 5, v = 0.5$ and $\bar{F} = 1$.

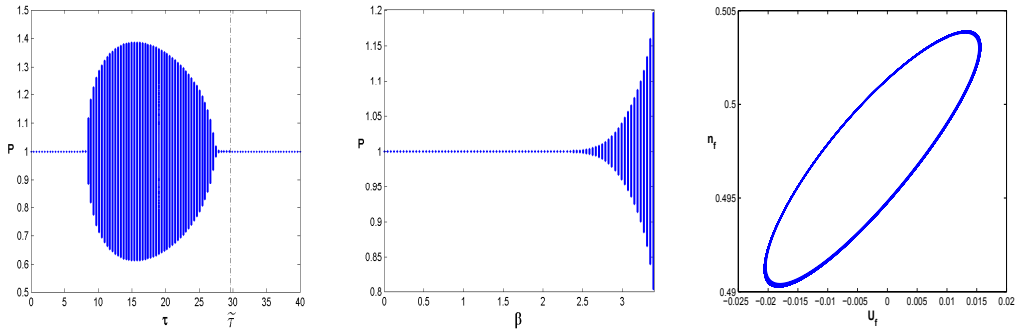

(a) Price bifurcation in τ (b) Price bifurcation in β (c) Phase plot of U_f and n_f

Figure 3.1: (a) The bifurcation of the market prices with respect to τ with $\beta = 1$; (b) The bifurcation of market price with respect to β with $\tau = 8.3$; (c) The phase plot of the relationship between the fitness U_f and the market fraction n_f with $\tau = 16$ and $\beta = 1$.

price dynamics in the discrete-time Brock and Hommes (1997, 1998) framework. Fig. 3.1 (c) illustrates the phase plot of (U_f, n_f), showing the positive relation between the fitness U_f and the market fraction n_f.

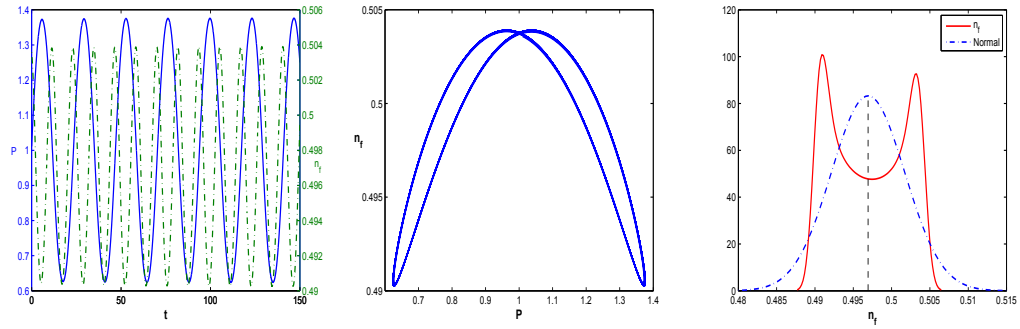

(a) Time series of P and n_f (b) Phase plot of (P, n_f) (c) The density of n_f

Figure 3.2: (a) The time series of the market prices $P(t)$ (the blue solid line) and the market fraction $n_f(t)$ of fundamentalists (the green dash dot line); (b) the phase plot of $(P(t), n_f(t))$; and (c) the density distribution of the market fraction $n_f(t)$. Here $\tau = 16$.

Fig. 3.2 provides further insights into the nonlinear dynamics of the market price and market fraction of the fundamentalists for $\tau = 16$ when the fundamental steady state is unstable. Fig. 3.2 (a) illustrates the time series of the market prices $P(t)$ and the market fraction $n_f(t)$ of fundamentalists. It shows that the market fractions fluctuate with the market price. Fig. 3.2 (b) presents the phase plot of $(P(t), n_f(t))$ showing that the price and fraction converge to a *figure-eight shaped* attractor, a phenomenon also observed in the discrete-time model in Chiarella et al. (2006). Fig. 3.2 (c) plots the

corresponding density distribution of the market fraction $n_f(t)$ of the fundamentalists. The *twin-peak-shaped* density distribution implies that, when the fundamental price is unstable, the market fractions tend to stay away from the steady state market fraction level most of the time and a mean of $n_f(t)$ below 0.5 clearly indicates the dominance of the trend chasing strategy.

Interestingly, the herding parameter v does not affect the local stability of the fundamental price and the deterministic price dynamics are very similar to the results in Chapter 2 without herding. To illustrate the herding effect, we compare this model with the model in Chapter 2. In Appendix B.2, corresponding to Figs. 3.1 and 3.2, we present Figs. B.1 and B.2, respectively, for the model in Chapter 2. It is observed that both models exhibit similar deterministic dynamics in price and market fraction. However, the nonlinear dynamics can be affected by the herding parameter v. Comparing Fig. 3.2 with $v = 0.5$ and Fig. B.3 with $v = 0.1$ in Appendix B.2, we observe that, when herding among agents are not very strong indicating by a decrease in the parameter v, the fluctuations of market price and, in particular, the market fractions of the fundamentalists are reduced. In other words, a strong herding among agents contributes to high fluctuations in market fractions, which then results in high volatility in market prices. This effect is further examined for the stochastic model in the following section.

3.4 Price Behavior of the Stochastic Model

In this section, through numerical simulations, we examine the price dynamics of the stochastic model by focusing on the impact of the three parameters, the time horizon τ, herding v, and switching intensity β, and the two noisy processes characterized by σ_F and σ_M, on market volatility in both price and return. The analysis provides further insights into the different roles played by herding and switching in financial markets.

We first explore the interaction between the underlying deterministic dynamics and the two noisy processes by choosing two different values of time horizons. For the deterministic model (3.8), Fig. 3.1 (a) shows that the time horizon can affect the stability of the fundamental price. In particular, the fundamental steady state is stable for $\tau = 3$ and unstable for $\tau = 16$, leading to periodic fluctuations of the market price. For the stochastic model, we choose the volatility of the fundamental price $\sigma_F = 0.12$ and the volatility of the market noise $\sigma_M = 0.15$.[6] With the same random draws of the fundamental price and market noise processes, we plot the fundamental price (the blue dotted line) and the

[6]The constraint $n_f(t) \in [0, 1]$ is imposed when simulating the stochastic system. In all the simulations, time unit is a year, and the time step corresponds to one day. Unless specified otherwise, an annual volatility of $\sigma_F = 0.12$ and a market noise volatility of $\sigma_M = 0.15$ are used in the chapter.

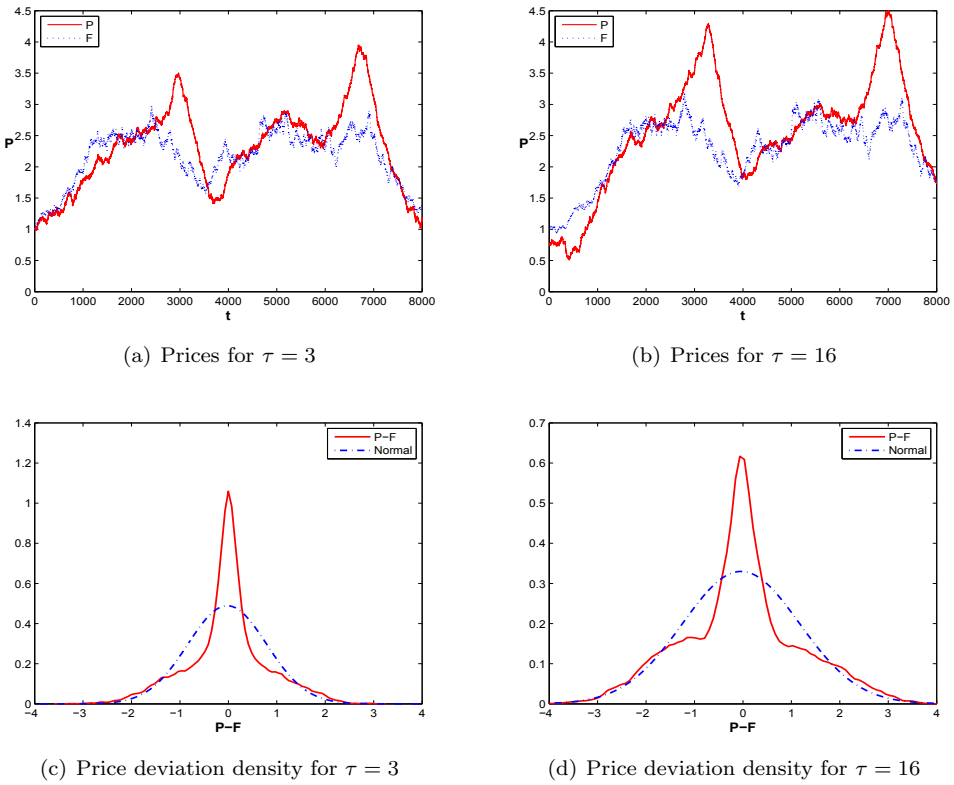

(a) Prices for $\tau = 3$

(b) Prices for $\tau = 16$

(c) Price deviation density for $\tau = 3$

(d) Price deviation density for $\tau = 16$

Figure 3.3: The time series of the fundamental price $F(t)$ (the blue dotted line) and the market prices $P(t)$ (the red solid line) with (a) $\tau = 3$ and (b) $\tau = 16$, and the distributions of the deviations of the market prices from the fundamental prices $P(t) - F(t)$ with (c) $\tau = 3$ and (d) $\tau = 16$. Here $\sigma_F = 0.12$ and $\sigma_M = 0.15$.

market prices (the red solid line) in Fig. 3.3 for the two different values of τ under the same set of parameters for Fig. 3.1 (a).[7] For $\tau = 3$ and $\tau = 16$, Figs. 3.3 (a) and (b) show that the market prices fluctuate around the fundamental prices and the fluctuations for $\tau = 16$ are significantly larger than that for $\tau = 3$. This observation is further supported by the distribution plots of the deviations of the market prices from the fundamental prices $P(t) - F(t)$ in Fig. 3.3 (c) for $\tau = 3$ and in Fig. 3.3 (d) for $\tau = 16$. With the standard deviations of 0.8158 for $\tau = 3$ and 1.2091 for $\tau = 16$, the deviations are more spread for $\tau = 16$. This is partially underlined by the change in the stability of the underlying deterministic dynamics. Further simulations (not reported here) show that when the time horizon increases further to the stabilizing range indicated by Fig. 3.1 (a), the fluctuations of the market price deviations from the fundamental price become even more significant. This result illustrates that, when the underlying deterministic dynamics are stable, the

[7] Because we consider the cum dividend price, there should be an increasing trend in the fundamental price.

stochastic dynamics can become very *unstable* with large fluctuations in price deviations. This is mainly due to the slow convergence of the market price to the fundamental price of the underlying deterministic model and its interaction with the fundamental and market noises. Therefore, an increase in time horizon increases the deviations of the market price from the fundamental price and the fluctuations of the market price.

To examine the effect of herding, with the same parameters and random draws, Fig. B.4 in Appendix B.3 illustrates the corresponding results of the model in Chapter 2 without herding. It displays similar price patterns but with less significant deviations in prices (with the standard deviations of 0.2477 for $\tau = 3$ and 0.4703 for $\tau = 16$). The comparison implies that the herding behavior contributes to the excess volatility of the market price, a higher acceleration to market highs and lows, and a quicker mean reversion to the fundamental price.

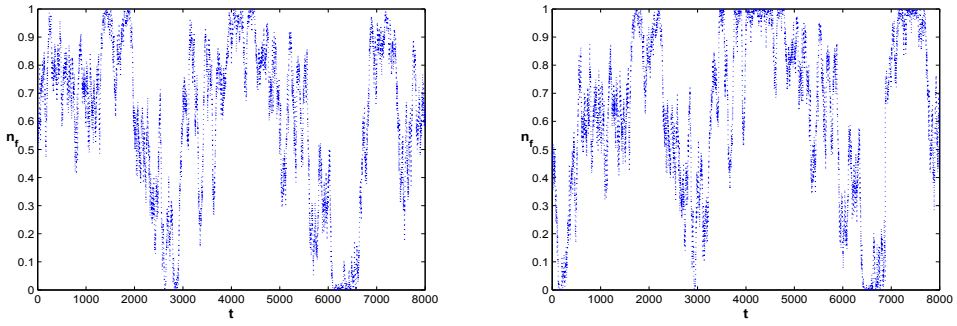

(a) Market fraction for $\tau = 3$

(b) Market fraction for $\tau = 16$

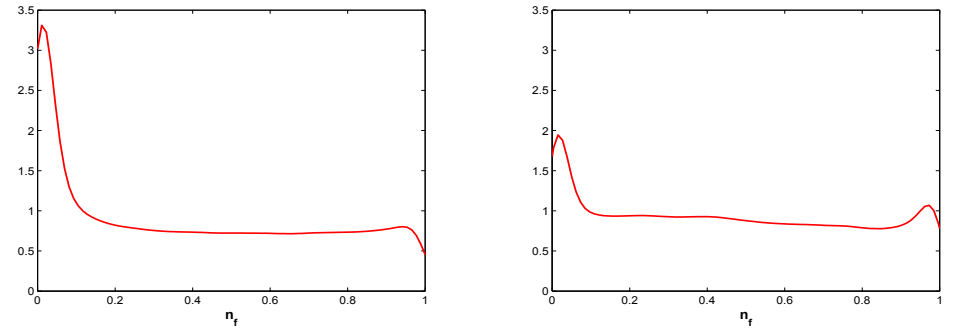

(c) Market fraction density for $\tau = 3$

(d) Market fraction density for $\tau = 16$

Figure 3.4: The time series of the fractions of the fundamentalists with (a) $\tau = 3$ and (b) $\tau = 16$ and the corresponding distributions with (c) $\tau = 3$ and (d) $\tau = 16$. Here $\sigma_F = 0.12$ and $\sigma_M = 0.15$.

We also plot the corresponding time series and distributions of the market fractions of the fundamentalists in Fig. 3.4 for both $\tau = 3$ (the left panel) and $\tau = 16$ (the right panel). Comparing to Fig. B.5 in Appendix B.3 for the model in Chapter 2 (with switching but

without herding), we obtain two observations. (i) With herding, the market fractions fluctuate wildly between 0 and 1, are almost uniformly distributed except for the spike near 0, as shown in Fig. 3.4. However, without herding, the market fractions fluctuate around the steady state ($n_f = 0.495$) in a small range (from 35% to 75%), illustrated by both the time series and distribution plots in Fig. B.5. This implies that the herding effect dominates the switching effect in generating high fluctuations in the market fractions. (ii) For the market fraction, by comparing the time series and distributions of the market fractions in Fig. 3.4 for $\tau = 3$ (the left panel) and $\tau = 16$ (the right panel), the effect of the time horizon is not highly significant. However, note the small peak near 1 for $\tau = 16$ in Fig. 3.4 (d), the time horizon does affect the market fractions. In general we observe that herding leads to the dominance of the trend followers in the market, while an increase in time horizon reduces the dominance of the trend followers and increases the dominance of the fundamentalists.

One of the innovative features of the model is that the market fraction is determined by the stochastic master equation (3.5) with endogenously determined volatility (3.6). Because of the dependence of the transition rates on the time horizon τ, the switching β and herding v, the volatility also depends on τ, β and v. Therefore the variations in the market fractions can affect the deviation of the market price from the fundamental price and return volatility. In general, the impact on market volatility can be different for price and return. To provide further insights into the different roles of the herding, switching and time horizon on fluctuations of market fractions and market volatility, we consider three cases focusing each of the three parameters of τ, v and β with some typical choices of the other two parameters. In each case, we examine the impact on the endogenously determined volatility of the market fractions (of the fundamentalists), σ_{n_f}, the volatility of the price deviations, $\sigma(P-F)$, and the volatility of the market returns, $\sigma(r)$. Based on the common set of the parameters, we run 100 simulations for each parameter combination and plot the averages of $\sigma_{n_f}, \sigma(P-F)$ and $\sigma(r)$ and denote by $\bar{\sigma}_{n_f}$, $\bar{\sigma}(P-F)$ and $\bar{\sigma}(r)$, respectively.

3.4.1 The Effect of the Time Horizon

For $\tau \in [0, 20]$, we conduct Monte Carlo simulations and plot $\bar{\sigma}_{n_f}, \bar{\sigma}(P-F)$ and $\bar{\sigma}(r)$ in the upper panel for $\beta = 0.1, 1, 2$ and the lower panel for $v = 0.01, 0.1, 0.5$ in Fig. 3.5, from which we can draw two observations about the volatility.

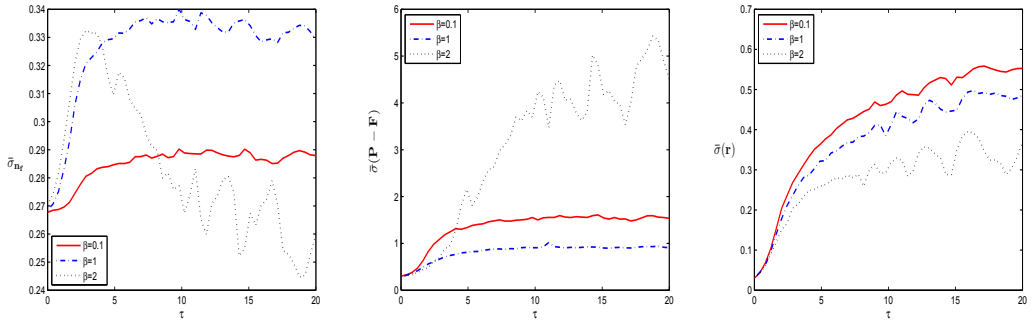

(a) $\bar{\sigma}_{n_f}$ in τ and β (b) $\bar{\sigma}(P-F)$ in τ and β (c) $\bar{\sigma}(r)$ in τ and β

(d) $\bar{\sigma}_{n_f}$ in τ and v (e) $\bar{\sigma}(P-F)$ in τ and v (f) $\bar{\sigma}(r)$ in τ and v

Figure 3.5: The average variations of market fraction volatility $\bar{\sigma}_{n_f}$ (a) and (d), price deviation volatility $\bar{\sigma}(P-F)$ (b) and (e), and return volatility $\bar{\sigma}(r)$ (c) and (f) with $\beta = 0.1, 1, 2$ (and $v = 0.5$) in the upper panel and $v = 0.01, 0.1, 0.5$ (and $\beta = 1$) in the lower panel, respectively, with respect to time horizon $\tau \in [0, 20]$.

(i) All the volatilities, in terms of $\bar{\sigma}_{n_f}, \bar{\sigma}(P-F)$ and $\bar{\sigma}(r)$, increase as the time horizon and herding increase.[8] For $\tau = 0$, the trend followers are not participating in the market and the lower volatilities simply reflect the resulting volatilities of the market noise and fundamental noise. In this case, herding plays no role in market volatility in both the price and return (as indicated by the constant volatility for various β and v when $\tau = 0$ in the middle and right panels). As τ increases, all the volatilities increase significantly. This effect becomes less significant for the market fraction volatility $\bar{\sigma}_{n_f}$ after an initial increase in τ (from 0 to about 5). The increase in the price deviation volatility in the time horizon is underlined by the destabilizing effect of τ on the underlying deterministic dynamics. Because of the fluctuations in the market fractions, we observe an increase in the return volatility as well. We also observe the same effect as the herding parameter v increases in the low panel of Fig. 3.5. Due to the independence of the local stability to the herding, this result reflects more on the interaction of nonlinearity and noises.

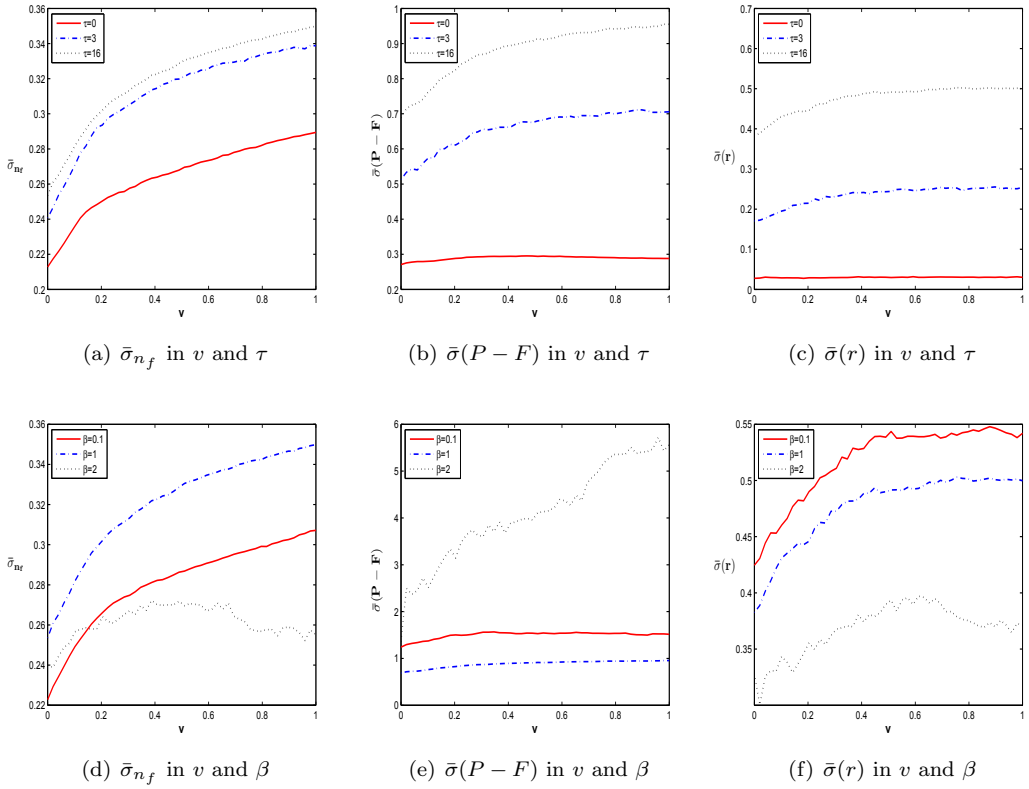

(a) $\bar{\sigma}_{n_f}$ in v and τ (b) $\bar{\sigma}(P-F)$ in v and τ (c) $\bar{\sigma}(r)$ in v and τ

(d) $\bar{\sigma}_{n_f}$ in v and β (e) $\bar{\sigma}(P-F)$ in v and β (f) $\bar{\sigma}(r)$ in v and β

Figure 3.6: The average variations of market fraction volatility $\bar{\sigma}_{n_f}$ (a) and (d), price deviation volatility $\bar{\sigma}(P-F)$ (b) and (e), and return volatility $\bar{\sigma}(r)$ (c) and (f) with $\tau = 0, 3, 16$ (and $\beta = 1$) in the upper panel and $\beta = 0.1, 1, 2$ (and $\tau = 16$) in the lower panel, respectively, with respect to $v \in [0, 1]$.

[8] Except $\bar{\sigma}_{n_f}$ for time horizon and large β that the volatility seems to decrease as time horizon increases further. This is related to the non-monotonic impact of β on the volatilities illustrated in Fig. 3.7.

(ii) Switching has a non-monotonic impact on the volatilities of market fraction and market price, but reduces the return volatility as the switching intensity increases. Figs. 3.5 (a) and (b) show that the volatilities of market fraction and market price deviations are non-monotonic as β increases. An initial increase in β leads to an increase in the volatility of market fraction but the effect reverses as β increases further, implying a "hump" shaped effect on the volatilities of market fraction. However, we also observe a "U"-shaped effect on the volatility of price deviation. This non-monotonic feature is explored further in the following discussion. Furthermore, Fig. 3.5 (c) shows that the volatilities of market return decrease in β, an opposite effect to the herding. Such different impact of the switching and herding on volatility of price and return has not been explored in the literature. This provides some insights into the distinct role played by switching and herding in market volatility. If one argues that switching is a more rational behavior than herding, the result indicates that herding can increase the return volatility, while switching can reduce the return volatility.

3.4.2 The Effect of the Herding

For $v \in [0, 1]$, we plot $\bar{\sigma}_{n_f}, \bar{\sigma}(P - F)$ and $\bar{\sigma}(r)$ for $\tau = 0, 3, 16$ in the upper panel and for $\beta = 0.1, 1, 2$ in the lower panel in Fig. 3.6 based on Monte Carlo simulations. It provides consistent observations as in the previous case. When the herding parameter v and the time horizon τ increase, all the volatilities increase. However an increase in the switching parameter reduces the average volatility of return, as illustrated in Fig. 3.6 (f). Also Figs. 3.6 (d) and (e) show that the switching has a non-monotonic impact on the volatilities of market fraction and price. Consistently with the previous observations, the herding increases the fluctuations of the market price from the fundamental price and return fluctuations.

3.4.3 The Effect of Switching

For $\beta \in [0, 2]$, we plot $\bar{\sigma}_{n_f}, \bar{\sigma}(P - F)$ and $\bar{\sigma}(r)$ for $\tau = 0, 3, 8, 16$ in the upper panel and for $v = 0.01, 0.1, 0.5$ in the lower panel in Fig. 3.7 based on Monte Carlo simulations. When $\beta = 0$, the market fractions are driven purely by the herding behavior. In general, we observe consistent results in terms of the impact of time horizon and herding obtained in the previous two cases. However, there is a significantly non-monotonic relationship between the volatilities and the switching intensity β. We observe a "hump" shaped volatility in the market fraction (in Figs. 3.7 (a) and (d)), a "U"-shaped price volatility (in Figs. 3.7 (b) and (e)), and a decreasing volatility in returns (in Figs. 3.7 (c) and (f))

as the switching parameter β increases. Interestingly, an initial increase in the switching leads to higher market fraction volatility and lower market price volatility, following by the decreasing volatility in fractions and the increasing volatility in price deviations when β increases beyond certain threshold value. This result explains the phenomenon in Fig. 3.5 (a) that for large β, an increase in the time horizon τ leads to an initial increase in the market fraction volatility, but a dramatic decline when τ increases further. It also implies that large fluctuations in the market fractions reduce the market price deviation from the fundamental price when the switching intensity is low, but the effect becomes opposite when the switching intensity is high. However, a strong switching always reduces return volatility. Therefore, we can have a market with high fluctuations in market price and low volatility in returns at the same time.

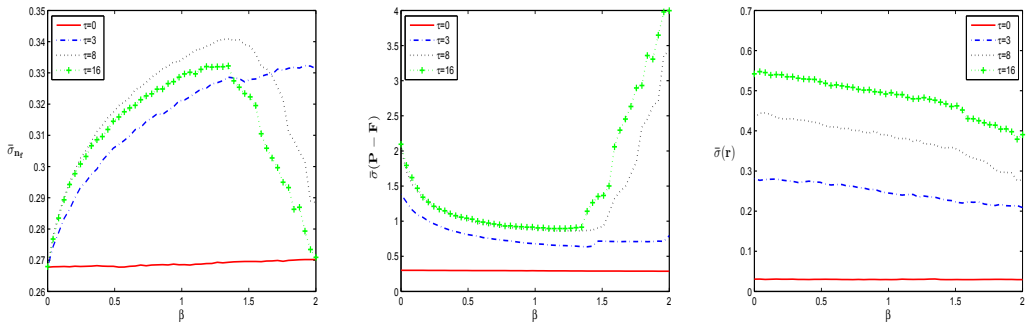

(a) $\bar{\sigma}_{n_f}$ in β and τ (b) $\bar{\sigma}(P-F)$ in β and τ (c) $\bar{\sigma}(r)$ in β and τ

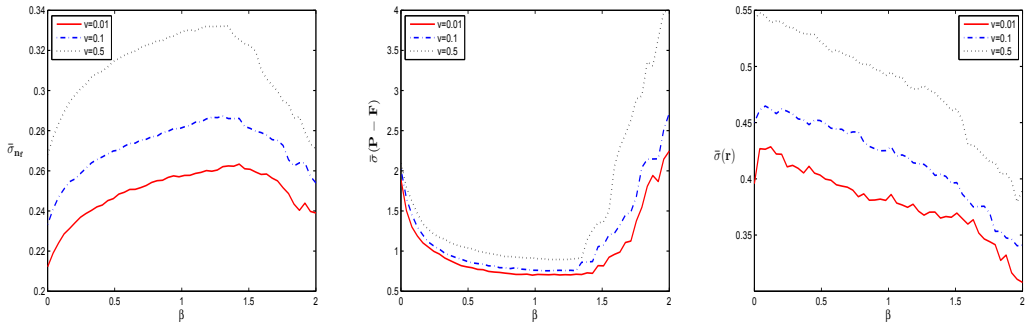

(d) $\bar{\sigma}_{n_f}$ in β and v (e) $\bar{\sigma}(P-F)$ in β and v (f) $\bar{\sigma}(r)$ in β and v

Figure 3.7: The average variations of market fraction volatility $\bar{\sigma}_{n_f}$ (a) and (d), price deviation volatility $\bar{\sigma}(P-F)$ (b) and (e), and return volatility $\bar{\sigma}(r)$ (c) and (f) with $\tau = 0, 3, 16$ (and $v = 0.5$) in the upper panel and $v = 0.01, 0.1, 0.5$ (and $\tau = 16$) in the lower panel, respectively, with respect to $\beta \in [0, 1]$.

In summary, the impact on the volatility can be very different for price and return. The trend chasing over a long time horizon and herding always lead to high volatility. However the switching and herding have an opposite effect on the market return volatility.

Although the switching has significant and non-monotonic impact on the market volatility, it can actually reduce return volatility. The analysis demonstrates different mechanisms of herding and switching in explaining volatilities in price and return.

3.5 Power-law Behavior in Volatility

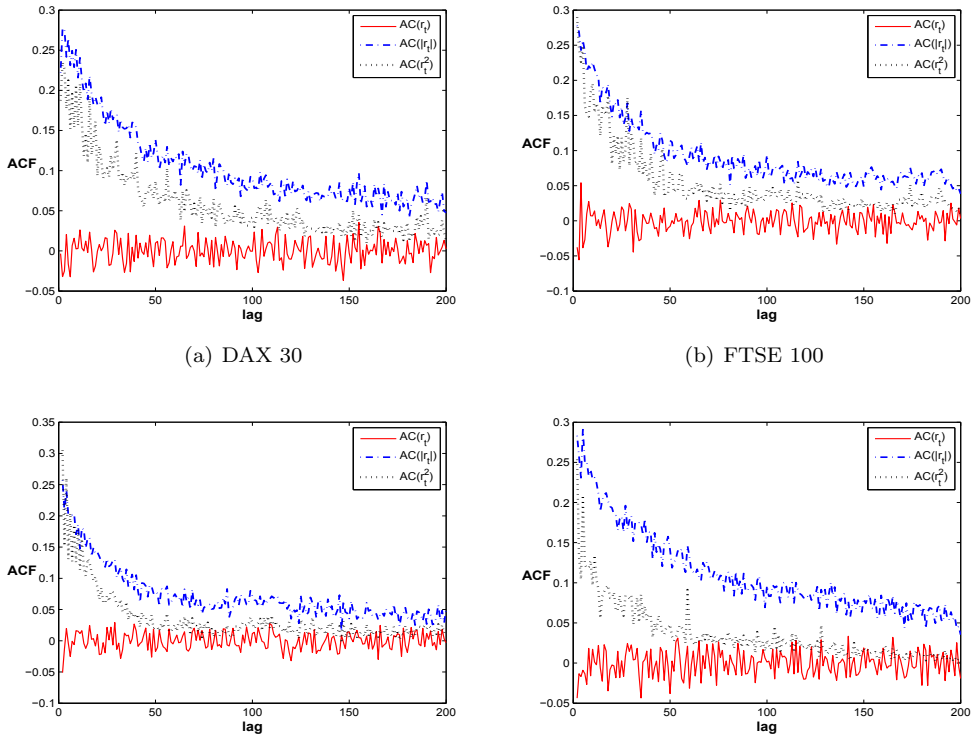

(a) DAX 30 (b) FTSE 100

(c) NIKKEI 225 (d) S&P 500

Figure 3.8: The ACs of the returns (the bottom lines), the squared returns (the middle lines) and the absolute returns (the upper lines) for (a) the DAX 30, (b) the FTSE 100, (c) the NIKKEI 225, and (d) the S&P 500.

After exploring the impact of the time horizon, herding, and switching on market volatility in the previous section, we are now interested in their impact on the power-law behavior in volatility. It has been well explored in the HAM literature that it is the interaction of the nonlinear dynamics of the underlying deterministic model and the noises that generate the power-law behavior. Both switching and herding mechanisms have been explored, but a comparison of different mechanism is missing in the literature. This section is devoted to such a comparison. We first examine the impact of the noises and then of the time horizon, switching and herding on the ACs of the returns, absolute

returns, and squared returns with the two noises.

To motivate the analysis, we first present the ACs of the returns, absolute returns, and squared returns for market daily closing price indices of the DAX 30, the FTSE 100, the NIKKEI 225, and the S&P 500 from 01/02/1984 to 31/07/2013 from Datastream in Fig. 3.8. Note that all the ACs for the returns are not significant, but they are significant and decaying for the absolute and squared returns. This phenomenon is referred as the power-law behavior or long memory in market volatility in empirical literature, see He and Li (2007) and references cited there.

3.5.1 The Effect of the Noises

For the two exogenously given fundamental and market noises, we examine the impact of the noises by considering three combinations of (i) both the fundamental and market noises; (ii) the market noise only; and (iii) the fundamental noise only.

We first consider the effect of the fundamental and market noises with $\sigma_F = 0.12$ and $\sigma_M = 0.15$. Fig. 3.9 represents the results of a typical simulation based on the same set of parameters in Fig. 3.3 with $\tau = 16$. The results demonstrate that the stochastic model established in this chapter is able to generate market price deviations from the fundamental value (in Fig. 3.9 (a)), most of the stylized facts (including volatility clustering in Fig. 3.9 (b), high kurtosis in in Fig. 3.9 (c)), and the power-law behavior in volatility (insignificant autocorrelations (ACs) for returns in Fig. 3.9 (d), but significant decaying ACs for the absolute returns and the squared returns in Figs. 3.9 (e) and (f)) observed in financial markets.

Next we consider the effect of the market noise. With the same parameters and random seeds, Fig. 3.10 shows that the model is able to generate a similar result to the previous case with the two noises, although the level of the significant ACs is lower. This implies that, even with a constant fundamental value, the model has a great potential in generating the power-law behavior. This result is significantly different from the switching model in Chapter 2, in which the model is not able to generate the power-law behavior without fundamental noise.

Finally, we consider the effect of the fundamental noise. Fig. 3.11 shows that the model is not able to generate the volatility clustering and the power-law behavior, which is consistent with the model in Chapter 2. Meanwhile the market returns, absolute returns and squared returns exhibit highly significant ACs with strong decaying patterns, which is mainly due to the strong effect of the deterministic dynamics of the price process.

To further investigate the effect of the fundamental noise on the AC patterns, Fig. 3.12

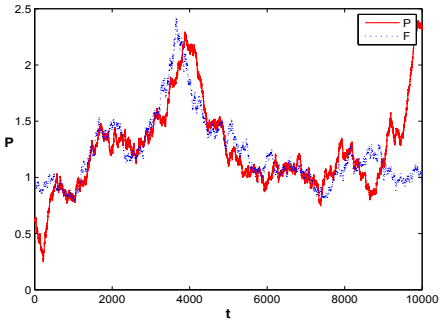

(a) The market price and the fundamental price

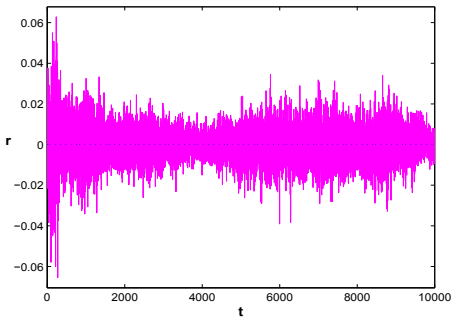

(b) The market returns (r)

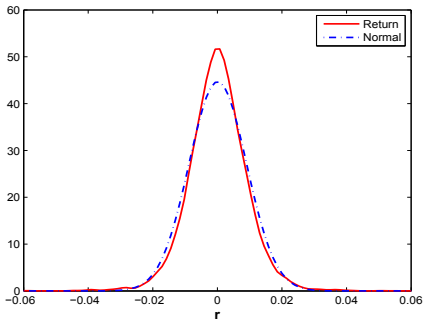

(c) The density of the market returns

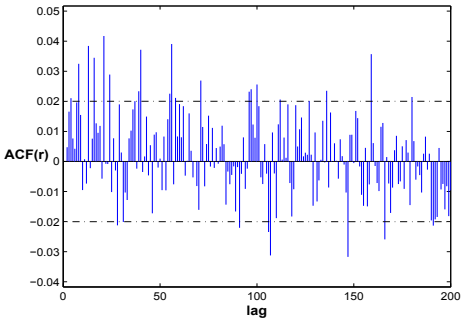

(d) The ACs of the market returns

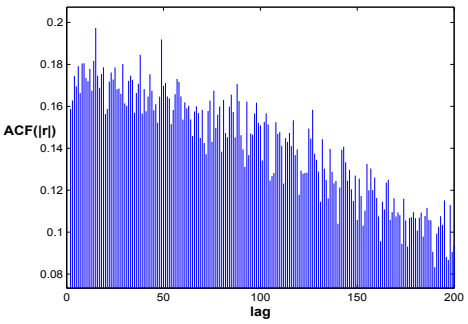

(e) The ACs of the absolute returns

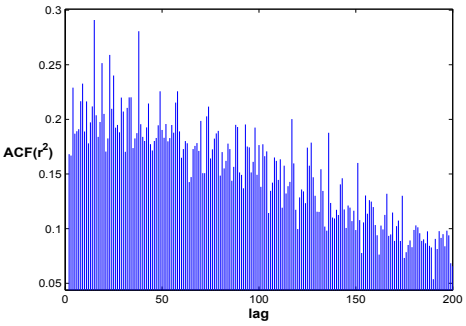

(f) The ACs of the squared returns

Figure 3.9: The effect of the two noises: the time series of (a) the market price (red solid line) and the fundamental price (blue dotted line) and (b) the market returns; (c) the return distribution; the ACs of (d) the returns; (e) the absolute returns, and (f) the squared returns. Here $\sigma_F = 0.12$ and $\sigma_M = 0.15$.

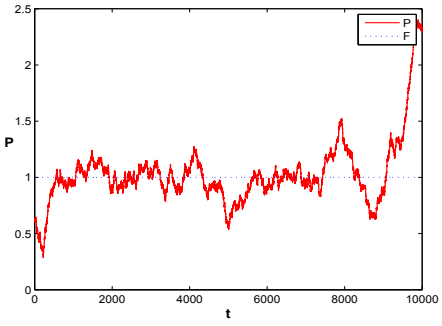

(a) The market price and the fundamental price

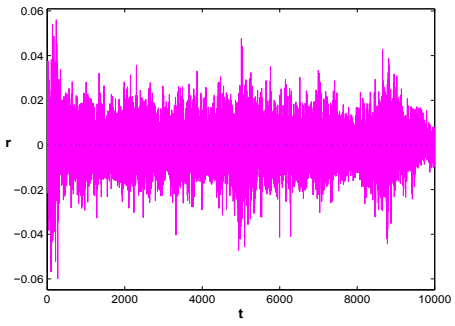

(b) The market returns (r)

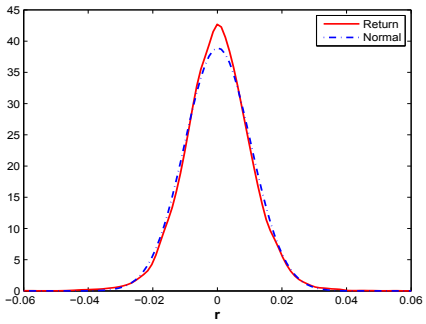

(c) The density of the market returns

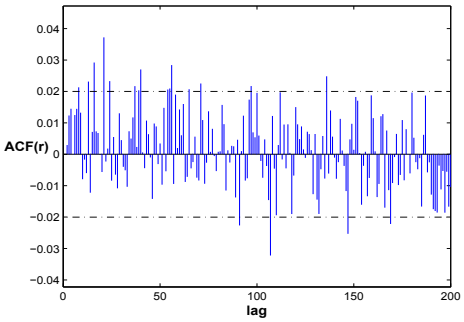

(d) The ACs of the market returns

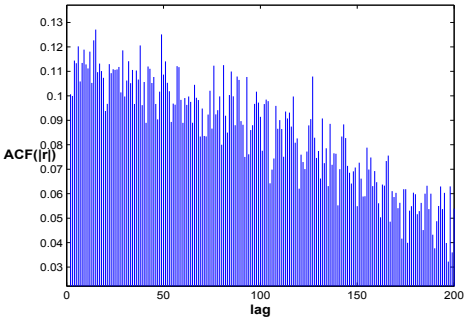

(e) The ACs of the absolute returns

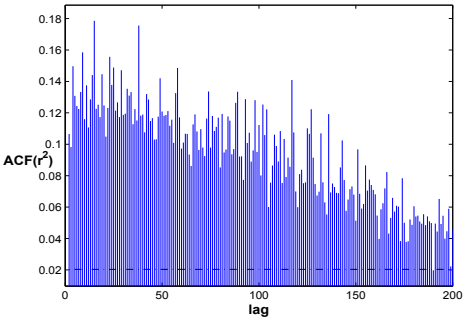

(f) The ACs of the squared returns

Figure 3.10: The effect of the market noise only: the time series of (a) the market price (red solid line) and the fundamental price (blue dotted line) and (b) the market returns; (c) the return distribution; the ACs of (d) the returns; (e) the absolute returns, and (f) the squared returns. Here $\sigma_F = 0$ and $\sigma_M = 0.15$.

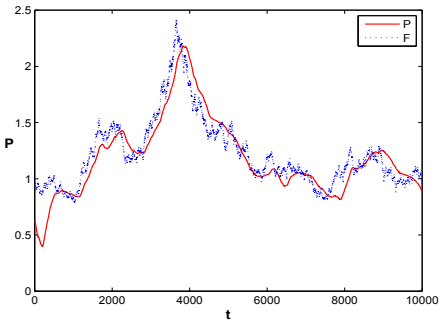

(a) The market price and the fundamental price

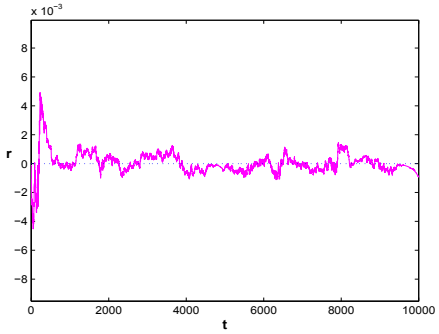

(b) The market returns (r)

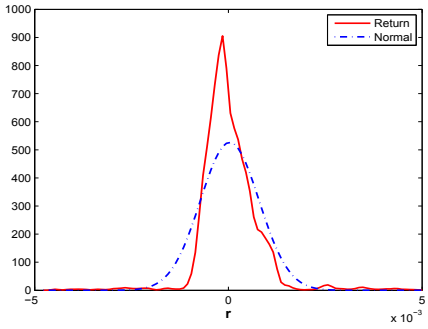

(c) The density of the market returns

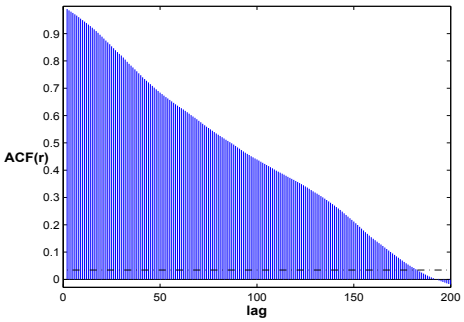

(d) The ACs of the market returns

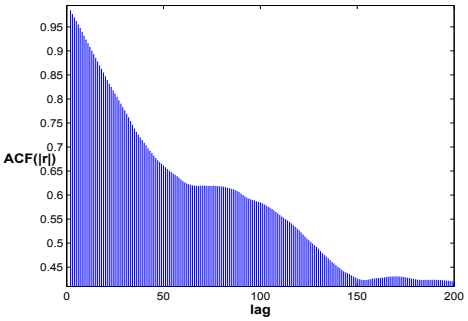

(e) The ACs of the absolute returns

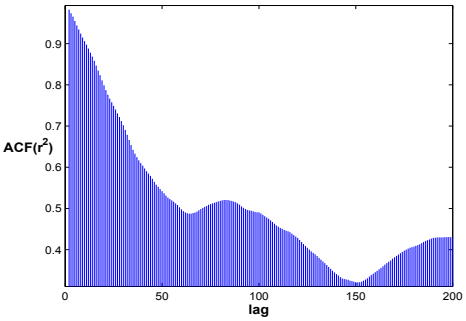

(f) The ACs of the squared returns

Figure 3.11: The effect of the fundamental noise only: the time series of (a) the market price (red solid line) and the fundamental price (blue dotted line) and (b) the market returns; (c) the return distribution; the ACs of (d) the returns; (e) the absolute returns, and (f) the squared returns. Here $\sigma_F = 0.12$ and $\sigma_M = 0$.

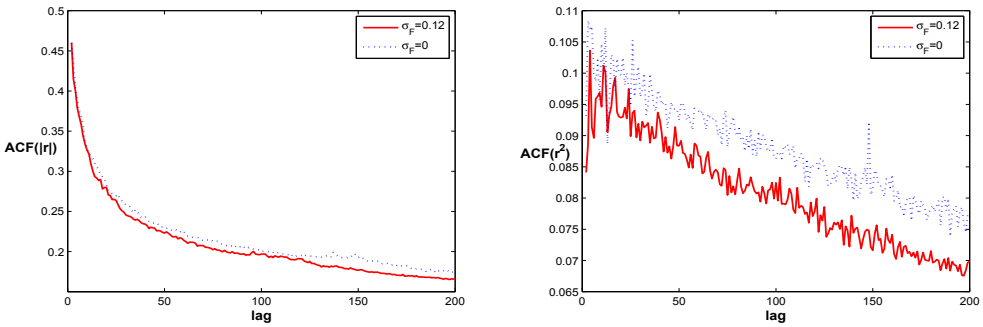

(a) The ACs of the absolute returns (b) The ACs of the squared returns

Figure 3.12: The effect of the fundamental noise: the ACs of (a) the absolute returns and (b) the squared returns based on 100 simulations with $\tau = 16$, $v = 0.5$ for $\sigma_F = 0.12$ (the red solid line) and $\sigma_F = 0$ (the blue dash-dotted line).

compares the ACs of the absolute returns and the squared returns for $\sigma_F = 0.12$ (the red solid line) and $\sigma_F = 0$ (the blue dash-dotted line) based on 100 simulations. The ACs of the absolute returns and squared returns are significant and decaying. However, with the market noise $\sigma_F = 0.12$, the ACs decay quickly than those for $\sigma_F = 0$. This indicates that the market noise plays a key role in generating the power-law behavior, though it is not the only factor, as argued in He and Li (2007).

The previous analysis on the effect of the time horizon, switching, and herding shows that they play different roles in generating volatility in market price and return. We now further investigate their effect on the the power-law behavior. Similarly, we consider three cases focusing on each of the three parameters of τ, v and β. For each case, we examine the impact on the AC patterns of the absolute and squared returns. Based on the common set of the parameters, we run 100 simulations for each parameter combination and plot the average ACs for the absolute and squared returns.[9]

3.5.2 The Effect of the Time Horizon

First, we present in Fig. 3.13 the effect of the time horizon on the AC patterns for the absolute returns (the left panel) and the squared returns (the right panel). We observe that the trend chasing based on different time horizons contributes to the significant decaying AC patterns for both the absolute and squared returns. Also the significant levels of the ACs increase as the time horizon increases, in particular, when the time horizon is large. This suggests that a commonly observed slow decaying AC patterns in the discrete-time HAM literature (see for example He and Li (2007)) might be due to the

[9]The average ACs for the returns are insignificant in all three cases reported.

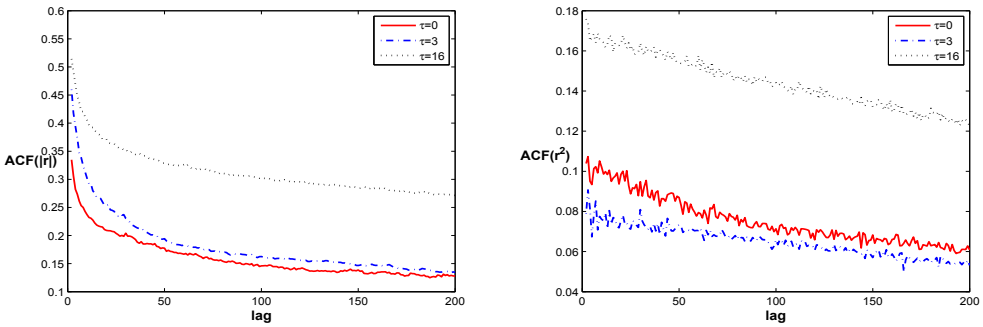

(a) The ACs of the absolute returns (b) The ACs of the squared returns

Figure 3.13: The effect of the time horizon: the ACs of (a) the absolute returns and (b) the squared returns based on 100 simulations with $v = 0.5$, $\beta = 1$, $\sigma_F = 0.12$, $\sigma_M = 0.15$ for $\tau = 0$, $\tau = 3$ and $\tau = 16$.

long time horizons used for modeling the trend chasing. In other words, trend chasing based on short time horizons contributes to more realistic power-law behavior in volatility. Intuitively, technical analysis such as trend following strategy is mainly used for short-term investment comparing to the fundamental analysis for long-term investment. Therefore the trend chasing based on short-time horizon contributes to volatility in financial markets.

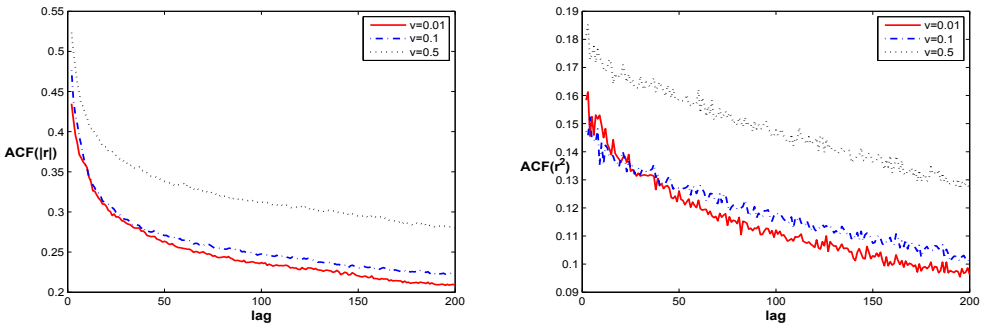

(a) The ACs of the absolute returns (b) The ACs of the squared returns

Figure 3.14: The effect of the herding: the ACs of (a) the absolute returns and (b) the squared returns based on 100 simulations with $\tau = 16$, $\beta = 1$, $\sigma_F = 0.12$, $\sigma_M = 0.15$ for $v = 0.01$, $v = 0.1$ and $v = 0.5$.

3.5.3 The Effect of the Herding

Second, we present in Fig. 3.14 the effect of the herding on the AC patterns for the absolute returns (the left panel) and the squared returns (the right panel), showing the contribution of the herding to the power-law behavior in volatility. Similar to the effect of the time horizon, an increase in the herding increases the level of the significant ACs for

both the absolute and squared returns. However, differently from the effect of the time horizon, the ACs decay quickly under the herding.

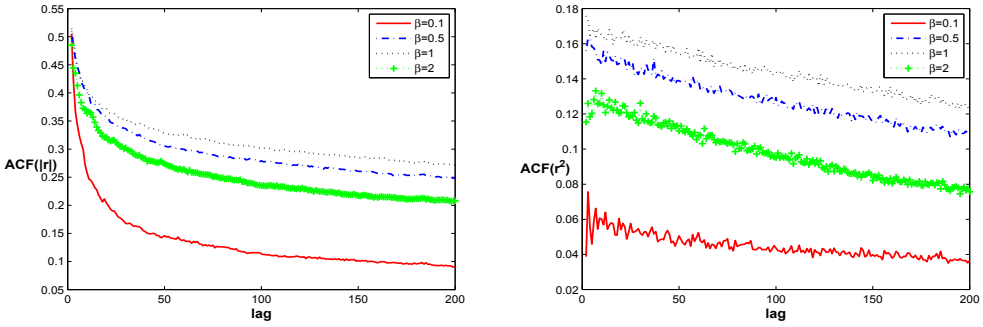

(a) The ACs of the absolute returns

(b) The ACs of the squared returns

Figure 3.15: The effect of the switching: the ACs of (a) the absolute returns and (b) the squared returns based on 100 simulations with $v = 0.5$, $\tau = 16$, $\sigma_F = 0.12$, $\sigma_M = 0.15$ for $\beta = 0.1$, $\beta = 0.5$, $\beta = 1$ and $\beta = 2$.

3.5.4 The Effect of the Switching

Third, we present in Fig. 3.15 the effect of the switching on the AC patterns for the absolute and squared returns. It shows that the switching contributes to the power-law behavior. Interestingly, different from the effect of the time horizon and herding, the level of the significant ACs for both the absolute and squared returns is not monotonic with respect to the switching intensity β. The level increases significantly when β increases from 0.1 to 0.5, and then less significantly when β increases to 1, but decreases when β increases further to 2. In particular, the ACs for the absolute returns decay very quickly, comparing to the effect of the herding. This observation, together with the discussion in Subsection 3.4.3, suggests that an increase in the switching can reduce the return volatility and generate the power-law behavior at the same time. This provides further support on the explanatory power of the adaptive switching in financial markets initiated in Brock and Hommes (1998).

In summary, we have explored different mechanisms of the switching and herding on the market volatility and power-law behavior in particular. We show that both contribute to the power-law behavior, however the effect is monotonically increasing with the herding, but not monotonic for the switching.

Finally, we investigate the question if pure herding is enough to explain the power-law behavior by considering the case with $\sigma_F = 0$ and $\tau = 0$. In this case, the fundamental value becomes constant and the trend followers become naive traders who take the current

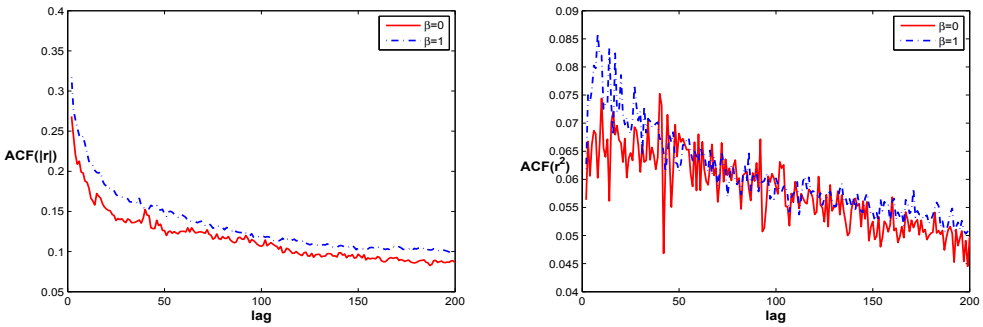

(a) The ACs of the absolute returns (b) The ACs of the squared returns

Figure 3.16: The ACs of (a) the absolute returns and (b) the squared returns based on 100 simulations with $v = 0.5$, $\tau = 0$, $\sigma_F = 0$, $\sigma_M = 0.15$ for $\beta = 0$ and $\beta = 1$.

price as the expected future market price and hence do not trade in the market anymore. Thus the market is driven by pure herding mechanism. Fig. 3.16 illustrates the significant and decaying AC patterns in both the absolute and squared returns, although the AC level for the squared returns is significantly lower comparing to the cases discussed previously. Interestingly, there is no significant difference in the AC patterns of the absolute return between no switching ($\beta = 0$) and the switching ($\beta = 1$). This result is consistent with Alfarano et al. (2005) who show that a pure herding model with fundamentalists and noise traders can generate power-law behavior. As a robustness check, we present Fig. 3.17 with three different values of v. Similar to Fig. 3.14, we observe more significant AC patterns as the herding parameter v increases.

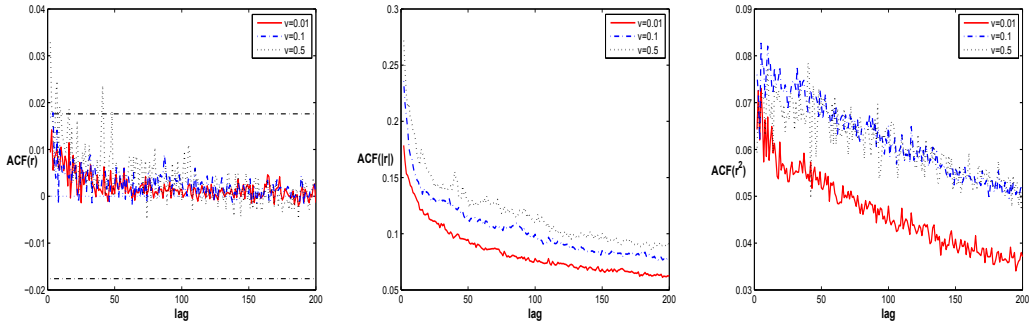

(a) $AC(r_t)$ (b) $AC(|r_t|)$ (c) $AC(r_t^2)$

Figure 3.17: The ACs of (a) the market returns; (b) the absolute returns and (c) the squared returns based on 100 simulations with $\tau = 0$, $\beta = 0$, $\sigma_F = 0$, $\sigma_M = 0.15$ for $v = 0.01$, $v = 0.1$ and $v = 0.5$.

Comparing to the AC patterns of the market indices in Fig. 3.8, we may argue that the switching generates similar AC patterns to the NIKKEI 225 and the S&P 500 with quickly

decaying AC patterns, while the herding generates similar AC patterns to the DAX 30 and FTSE 300 with relatively slow decaying AC patterns. Whether this observation suggests different market behavior in different markets is an empirical and challenging question. Our analysis explores different mechanism in explaining volatility in different markets.

To complete this chapter, I want to compare the mechanisms of the model introduced in Chapters 2 and 3 leading to the stylized facts. First, we have examined the impacts on stylized facts of the main components of the models in Chapters 2 and 3, including different noise processes, time horizons, switching and herding behaviors, and their different roles in generating stylized facts. Second, the model in Chapter 2 can be regarded as a continuous-time version of Brock and Hommes (1998)'s model and the mechanisms have been studied in detail in various extensions of Brock and Hommes (1998), see, for example, He and Li (2007). Third, the model in Chapter 3 examines the joint impact of switching and herding. The herding behavior has been demonstrated to contribute various stylized facts in the literature, see, for example, Lux (1995) and Alfarano et al. (2008). In all, we find that it is the interaction of the nonlinear deterministic dynamics and the noises that generates stylized facts. In order to generate the stylized facts, we need two noise processes for the model in Chapter 2 but only one noise process for the model in Chapter 3 when herding is considered. Therefore, we conclude that the market noise plays a more important role than the fundamental noise in contributing to the stylized facts.

3.6 Conclusion

Market volatility is one of the most important features in financial markets and the question is what drives it. To answer this question, one way is to consider how agents behave in financial markets. This chapter incorporates trend chasing, adaptive switching, and herding, three well documented and studied behavioral elements in the empirical literature, into an asset pricing model in a continuous-time framework and shows that they all contribute to market volatility in a different manner.

Most of the asset pricing models with heterogeneous agents are in discrete-time focusing on trend chasing over short time horizon and adaptive switching. Herding is commonly modelled by the master equation in a continuous-time setting. Therefore the roles of trend chasing, switching and herding in market volatility have been studied in separate frameworks. Within a continuous-time framework, this chapter is the first, to our knowledge, to combine trend chasing based on different time horizon, switching and herding together to examine their roles on market volatility in price and return. We show that, both the herding and trend chasing based on long time horizon increase the fluctuations of

market price deviation from the fundamental price and volatility of market return. With respect to the switching, it reduces the volatility in returns but leads to a "U"-shaped price volatility as the switching intensity increases. Therefore herding and switching have an opposite effect on return volatility. We also examine the explanatory power of the model in generating the power-law behavior in return volatility. We show that, although the trend chasing, switching and herding all contribute to the power-law behavior, the significant levels for the ACs increase in the time horizon and herding, but an initial increase and then decrease when the switching intensity increases. In addition, with herding, the market noise plays an essential role in generating the power-law behavior.

The model proposed in this chapter provides a unified framework to deal with trend chasing, switching and herding in financial markets. The results provide some further insights into different mechanism of generating bubbles and crashes, excess volatility, and power-law behavior in volatility. Whether a particular market is dominated by herding or switching is an empirical question which is left for future research.

Chapter 4

Time Series Momentum and Market Stability

4.1 Introduction

This chapter extends the model in Chapter 2 by incorporating many heterogeneous strategies based on different lagged prices and studies the mechanism which generates the profitability of time series momentum. Time series momentum investigated recently in Moskowitz et al. (2012) characterizes the strong positive predictability of a security's own past returns. For a large set of futures and forward contracts, Moskowitz et al. (2012) find a time series momentum or "trend" effect based on the past 12 month excess returns persists for 1 to 12 months that partially reverses over longer horizons. This effect based purely on a security's own past returns is related to, but different from, the cross-sectional momentum phenomenon studied extensively in the literature. Through return decomposition, Moskowitz et al. (2012) argue that positive auto-covariance is the main driving force for time series momentum and cross-sectional momentum effects, while the contribution of serial cross-correlations and variation in mean returns is small. This chapter provides an explanation on the profitability of time series momentum over short horizons and reversal over longer horizons.

To explain the time series momentum, we introduce a simple continuous-time asset pricing model of financial market consisting of three types of agents based on typical fundamental, momentum, and contrarian trading strategies. Fundamental agents trade based on the expectation of mean-reversion of market price to the fundamental price; while momentum and contrarian agents trade respectively based on the continuation and reverse of the past prices trends over different time horizons. The market price is deter-

mined via a market maker mechanism. The model, characterized by a stochastic delay integro-differential system, provides a unified approach to examine the impact of different time horizons of momentum and contrarian strategies on market stability and profitability of these strategies. We show that profitability is closely related to market dominance and stability. In particular, we show that: (i) momentum trading destabilizes the market, while contrarian trading stabilizes the market; (ii) the profitability of momentum strategies is related positively to the dominance of momentum traders and negatively to the time horizon used for estimating the price trend and, when the market is dominated by momentum traders, short horizon momentum strategies stabilize the market, but longer horizon momentum strategies destabilize the market; (iii) the market under-reacts in short-run and over-reacts in long-run, leading to profitability of momentum strategy with short horizons and loss with longer horizons. Therefore the analysis provides some insights into the profitability of time series momentum documented in Moskowitz et al. (2012).

The size and apparent persistence of momentum profits have attracted considerable attention. De Bondt and Thaler (1985) and Lakonishok, Shleifer and Vishny (1994) find supporting evidence on the profitability of contrarian strategies for a holding period of 3-5 years based on the past 3 to 5 year returns. In contrast, Jegadeesh and Titman (1993, 2001) among many others, find supporting evidence on the profitability of momentum strategies for a holding period of 3-12 months based on the returns over past 3-12 months.[1] It is clearly that the time horizons and holding periods play crucial roles in the performance of contrarian and momentum strategies. Many theoretical studies have tried to explain the momentum,[2] however, as argued in Griffin, Ji and Martin (2003), "*the comparison is in some sense unfair since no time horizon is specified in most behavioral models*". This chapter provides a uniform treatment on various time horizons used in momentum and contrarian trading strategies and develops a simple financial market model of heterogeneous agents in a continuous-time framework to study the impact of different time horizons on the market. To our knowledge, this chapter is the first to analyze a financial market model with all three types of fundamental, momentum, and contrarian strategies in a continuous-time framework.

[1] In addition to individual stock momentum, Moskowitz and Grinblatt (1999) show industry momentum for a holding period of 1-12 months based on the past 1-12 months and long-run reversals. George and Hwang (2004) find the momentum in price levels by investigating 52-week high. Recently, Novy-Marx (2012) find the term-structure momentum that is primarily driven by firm's performance 12 to 7 months prior to portfolio formation.

[2] Among which, the three-factor model of Fama and French (1996) can explain long-run reversal but not short-run momentum. Daniel et al. (1998) model with single representative agent and Hong and Stein (1999) model with different trader types attribute the under and overreaction to overconfidence and biased self-attribution. Sagi and Seasholes (2007) present a growth option model to identify observable firm-specific attributes that drive momentum. Recently, Vayanos and Woolley (2013) show the slow-moving capital can also generate momentum.

The state of the market is also a critically important factor that affects the profitability as shown in Griffin et al. (2003) and Lou and Polk (2013).[3] Different investment strategies play different roles in market stability and have different implications on the market states. Intuitively, momentum strategies are based on the hypothesis of underreaction with the expectation that the future price will follow the price trend. Consequently the strategies tend to destabilize the market price when momentum traders dominate the market. While contrarian strategies are based on the hypothesis of overreaction with the expectation that the future price will go against the price trend. Therefore the strategies can stabilize the market when contrarian traders dominate the market. However, the joint impact of both strategies on market stability can be complicated, depending on the states of the market dominance. We show that (i) when the market is dominated by fundamental and contrarian traders, the market is stabilizing and the momentum strategies do not generate profit; (ii) when the activity of the momentum traders is balanced by the activities of the fundamental and contrarian traders, there is a significant overreaction in short horizon and hence the momentum trading becomes not profitable; (iii) when the market is dominated by the momentum traders, the market is destabilized and can under-react in short-run but over-react in long-run. The results are consistent with the "crowded trading" proposed by Lou and Polk (2013) that "*the underreaction or overreaction characteristic of momentum is time-varying, crucially depending on the size of the momentum crowd*". In addition, we find that, with momentum crowd, the momentum trading leads to gain for the strategies with short horizons and loss for the strategies with longer horizons.

This chapter is closely related to the literature on the use of technical trading rules. Despite the efficient market hypothesis of financial markets in the academic finance literature (Fama 1970), the use of technical trading rules based on past returns, in particular momentum and contrarian strategies, still seems to be widespread amongst financial market practitioners (Allen and Taylor 1990). The profitability of these strategies and their consistency with the efficient market hypothesis have been investigated extensively in the literature, see for example, Frankel and Froot (1986) and Brock, Lakonishok and LeBaron (1992). This chapter also extends the deterministic delay differential equation models in economics and contributes to the recent development in heterogeneous agent models (HAMs) of financial markets.

This chapter is based on He and Li (2014) and organized as follows. We first present

[3]Cooper, Gutierrez and Hameed (2004) find that short-run (6 months) momentum strategies make profits in the up market and lose in the down market, but the up-market momentum profits reverse in the long-run (13-60 months). Hou, Peng and Xiong (2009) find momentum strategies with short time horizon (1 year) are not profitable in "down" market, but return significant profits in "up" market. Similar results of profitability are also reported in Chordia and Shivakumar (2002) that commonly using macroeconomic instruments related to the business cycle can generate positive returns to momentum strategies during expansionary periods and negative returns during recessions.

some empirical evidence on the time series momentum in financial market index in Section 4.2. Section 4.3 proposes a stochastic HAM in continuous time with time delays to incorporate fundamental, momentum and contrarian traders. To better understand the model, Section 4.4 follows the standard approach in HAMs and focuses on the dynamics of the underlying deterministic model to examine the impact of these strategies, in particular the different time horizons, on market stability. Section 4.5 examines the stochastic model numerically and investigates the connection between market stability and profitability. Section 4.6 concludes. All the proofs and model extensions are included in Appendix C.

4.2 Time Series Momentum of the S&P 500

This section provides some evidence on time series momentum in the S&P500. Most momentum literature is cross-sectional. The time series momentum is explored recently in Moskowitz et al. (2012) who show that a security's own past returns have strong positive predictability for its future return among almost five dozen diverse futures and forward contracts. Similar to Moskowitz et al. (2012), we apply the momentum strategy based on the standard moving average rules (MA) to the monthly data of the total return index of the S&P 500 from Jan. 1988 to Dec. 2012 obtained from *Datastream*.

We first define the trading signal for momentum trading. Let $P(t)$ be the log (cum dividend) price of a stock index at time t. The trading signal can be defined by

$$\begin{aligned} S_t^{(1)} :=& sign\Big(P_t - \frac{P_{t-1} + \cdots + P_{t-m}}{m}\Big) \\ =& sign\Big(\frac{1}{m}\big[m\Delta P_{t-1} + (m-1)\Delta P_{t-2} + \cdots + \Delta P_{t-m}\big]\Big), \end{aligned} \tag{4.1}$$

which is a decaying weighted average of past return over a horizon of m-month. Alternatively, motivated by Moskowitz et al. (2012), we also consider the trading signal defined by

$$S_t^{(2)} := sign\Big(\frac{1}{m}\big[(\Delta P_{t-1} - r_{f,t-1}) + (\Delta P_{t-2} - r_{f,t-2}) + \cdots + (\Delta P_{t-m} - r_{f,t-m}\big]\Big), \tag{4.2}$$

which is an equally weighted average excess return over the past m periods.

The mean profit of a momentum strategy with m-month horizon and n-month holding period ($m, n = 1, 2, \cdots, 60$) is calculated as follows. The strategy is to long (short) one unit of index for n months when the trading signal is positive (negative). Hence, at each time t, we have n long/short positions in the index (except for $t < n - 1$). The average (log) excess return of the momentum strategy at time t is calculated by the average

monthly returns of n positions in the index,

$$\left[\frac{1}{n}\sum_{k=1}^{n} S_{t-k}^{(i)}\right] \times \left(\Delta P_t - r_{f,t}\right), \quad i = 1, 2, \tag{4.3}$$

where $r_{f,t}$ is the 1 month Treasury bill rate.

$(m \setminus n)$	1	3	6	12	24	36	48	60
1	2.63	3.77**	1.99	3.43***	2.28**	1.96**	1.68*	1.34
3	1.38	2.91	3.36*	3.80**	3.40**	2.92**	2.50*	2.29*
6	6.03**	5.01*	4.62**	4.39**	3.25*	2.45	2.21	2.02
12	7.52**	6.54**	5.93**	5.00**	2.95	2.23	2.18	2.25
24	6.57**	7.87***	6.16**	5.03*	3.08	2.37	2.30	2.55
36	6.72**	6.76**	5.55*	3.47	2.38	2.08	2.21	2.76
48	4.34	2.07	1.52	1.22	0.67	1.15	1.47	2.30
60	1.05	0.66	-0.56	-0.44	0.06	0.72	1.17	2.27

Table 4.1: The annualized percentage (log) excess returns of the momentum strategies (4.1) for the S&P 500 with the horizon (m) and holding (n) from 1 to 60 months period. Note: *, **, *** denote the significance at 10%, 5% and 1% levels, respectively.

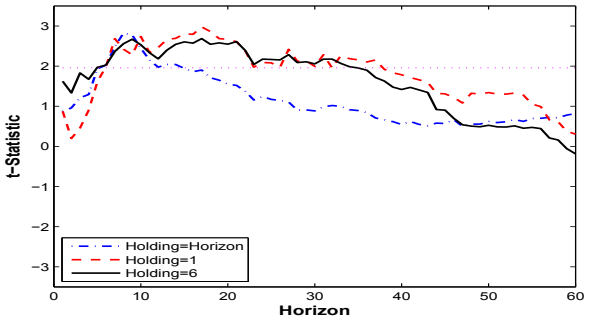

Figure 4.1: The t-statistic of the average excess return of the momentum strategies the S&P 500 based on (4.1) for time horizon from 1 to 60 months periods and holding periods equal to horizon ($n = m$), 1 month ($n = 1$) and 6 month periods ($n = 6$).

With the trading signal defined by (4.1),[4] Table 4.1 reports the annualized (log) excess returns of the momentum strategies for the S&P 500 with the horizon (m) and holding (n) from 1 to 60 months. It shows that the momentum strategies are profitable for time horizons and holding periods up to 3 years. In particular, the profits become significant (up to about 7% p.a.) for time horizons from 6 month to 3 years and holding periods from 1 to 12 months. Fig. 4.1 reports the t-statistic of the excess return of the momentum strategies investing in the S&P 500 for time horizon from 1 to 60 months periods and

[4] With the trading signal defined by (4.2), similar results are obtained and reported in Table C.1 and Fig. C.1 in Appendix C.1.

holding period equals to the time horizon ($n = m$), 1 month ($n = 1$) and 6 month periods ($n = 6$). It shows that the momentum strategies are significantly profitable for short holding periods from 1 to 6 months with time horizons from 6 to 30 months with the corresponding t-statistics being above 1.96, the critical value at 95% confidence level.

$(m \setminus n)$	1	3	6	12	24	36	48	60
1	0.050	0.128	0.093	0.187	0.134	0.114	0.099	0.078
3	0.026	0.070	0.106	0.137	0.138	0.122	0.105	0.095
6	0.116	0.109	0.118	0.123	0.105	0.083	0.075	0.068
12	0.145	0.135	0.129	0.116	0.077	0.062	0.060	0.061
24	0.126	0.159	0.131	0.114	0.074	0.061	0.058	0.064
36	0.129	0.135	0.117	0.076	0.056	0.051	0.054	0.068
48	0.083	0.042	0.032	0.026	0.016	0.027	0.035	0.055
60	0.020	0.014	-0.012	-0.010	0.001	0.017	0.027	0.000

Table 4.2: The Sharpe ratio of the momentum strategies (4.1) for the S&P 500 with the horizon (m) and holding (n) from 1 to 60 months period.

We also report the Sharpe ratio of the strategies to adjust for risk, which is defined as the ratio of the mean excess return on the (managed) portfolio and the standard deviation of the portfolio return. If a strategy's Sharpe ratio exceeds the market Sharpe ratio, the active portfolio dominates the market portfolio (in an unconditional mean-variance sense). For empirical applications, the (ex post) Sharpe ratio is usually estimated as the ratio of the sample mean of the excess return on the portfolio and the sample standard deviation of the portfolio return. The average monthly return on the total return index of the S&P 500 over the period January 1988–December 2012 is 0.76% with an estimated (unconditional) standard deviation of 4.30%. The Sharpe ratio of the market index is 0.108. The Sharpe ratio of the strategy based on (4.1) and (4.3) is documented in Table 4.2. Tables 4.1 and 4.2 are perfectly consistent. Specifically, when Table 4.1 shows a momentum strategy with certain time horizon and holding period generates significantly positive excess return, Table 4.2 also shows this strategy can outperform the market correspondingly according to the Sharpe criteria.

4.3 The Model

In this section, we establish an asset pricing model of single risky asset to characterize the time series momentum.

4.3.1 Fundamental Traders

Let $P(t)$ and $F(t)$ denote the log (cum dividend) price and (log) fundamental value $F(t)$, respectively of a risky asset at time t.[5] The fundamental traders believe that the market price[6] $P(t)$ is mean-reverting to the fundamental price $F(t)$, which can be estimated based on some fundamentals. They buy (sell) the stock when the current price $P(t)$ is below (above) the fundamental price $F(t)$ of the stock. For simplicity, we follow Chapter 2 and assume that the excess demand of the fundamental traders, $D_f(t)$ at time t, is proportional to the deviation of the market price $P(t)$ from the fundamental value $F(t)$, namely,

$$D_f(t) = \beta_f\big(F(t) - P(t)\big), \tag{4.4}$$

where $\beta_f > 0$ is constant, measuring the speed of mean-reversion of $P(t)$ to $F(t)$, which may be weighted by the risk aversion coefficient of the traders. For simplicity, we assume that the fundamental return follows a pure white noise process:

$$dF(t) = \sigma_F dW_F(t), \qquad F(0) = \bar{F}, \tag{4.5}$$

where $\sigma_F > 0$ represents the volatility of the fundamental return and $W_F(t)$ is a standard Wiener process.

4.3.2 Momentum and Contrarian Traders

Both momentum and contrarian traders trade based on their estimated market price trends, although they behave differently. Momentum traders believe that future market price follows a price trend $u_m(t)$. When the current market price is above the trend, they expect future market price to rise and therefore they take a long position of the risky asset; otherwise, they take a short position. Different from the momentum traders, contrarians believe that future market price goes opposite to a price trend $u_c(t)$. When the current market price is above the trend, they expect future market price to decline and therefore they take a short position of the risky asset; otherwise, they take a long position.

The price trend used for the momentum traders and contrarians can be different in general. Among various price trends used in practice, the standard moving average (MA) rules with different time horizons are the most popular ones,

$$u_i(t) = \frac{1}{\tau_i}\int_{t-\tau_i}^{t} P(s)ds, \qquad i = m, c, \tag{4.6}$$

[5] Notice that different from Chapters 2 and 3, we model log prices in this chapter rather than prices.
[6] For convenience, the price is referred to the log price in this chapter, unless specified otherwise.

where the time delay $\tau_i \geq 0$ represents the time horizon of the MA.[7] We therefore assume that the excess demand of the momentum traders and contrarians are given, respectively, by

$$D_m(t) = g_m\big(P(t) - u_m(t)\big), \qquad D_c(t) = g_c\big(u_c(t) - P(t)\big), \tag{4.7}$$

where the S-shaped demand function $g_i(x)$ for $i = m, c$ satisfies

$$g_i(0) = 0, \qquad g_i'(x) > 0, \qquad g_i'(0) = \beta_i > 0, \qquad x g_i''(x) < 0, \quad \text{for } x \neq 0, \tag{4.8}$$

and parameter β_i represents the extrapolation rate of the price trend when the market price deviation from the trend is small. Notice the trading signal of the strategy (4.7) is consistent with (4.1). In the following discussion, we take $g_i(x) = \tanh(\beta_i x)$, which satisfies condition (4.8).[8]

4.3.3 Market Price via a Market Maker

Assume net zero supply in the risky asset and let α_f, α_m and α_c be the market population fractions of the fundamental, momentum, and contrarian traders, respectively, with $\alpha_f + \alpha_m + \alpha_c = 1$ and $\alpha_i > 0$ for $i = f, m, c$.[9] Then the aggregate market excess demand for the risky asset, weighted by the population weights, is given by $\alpha_f D_f(t) + \alpha_m D_m(t) + \alpha_c D_c(t)$. Following Beja and Goldman (1980) and Farmer and Joshi (2002), we assume that the price $P(t)$ at time t is set via a market maker mechanism and adjusted according to the aggregate excess demand, that is,

$$dP(t) = \mu[\alpha_f D_f(t) + \alpha_m D_m(t) + \alpha_c D_c(t)]dt + \sigma_M dW_M(t), \tag{4.9}$$

where $\mu > 0$ represents the speed of the price adjustment by the market maker, $W_M(t)$ is a standard Wiener process capturing the random excess demand process driven by either unexpected market news or noise traders, and $\sigma_M \geq 0$ is constant. $W_M(t)$ is assumed to be independent of the Wiener process for the fundamental price $W_F(t)$.[10] Based on Eqs.

[7] The price trend $u_i(t)$ can be regarded as the logarithm of the geometric mean of market price over the past τ_i periods. In particular, $u_i(t) \to P(t)$ as $\tau_i \to 0$, implying that the price trend is given by the current price.

[8] Chiarella (1992) provides an explanation for the increasing and bounded S-shaped excess demand function. For example, traders may seek to allocate a fixed amount of wealth between the risky asset and a bond so as to maximize their expected utility of consumption. The demand becomes bounded due to wealth constraints. From behaviorial point of view, traders may become cautious when the deviation is large. This together leads approximately to an S-shaped increasing excess demand function.

[9] To simplify the analysis, we first assume that the market fractions are constant. When agents are allowed to switch among different strategies based on some fitness measure (see Chapter 2), the market fractions become time-varying. An analysis of this extension is given in Appendices C.4 and C.5.

[10] The two Wiener processes can be correlated. We refer readers to Chapter 2 for the impact of the correlation on the price behavior and the stylized facts in financial market.

(4.4)-(4.9), the market price of the risky asset is determined by

$$\begin{aligned} dP(t) =&\mu\Big[\alpha_f\beta_f\big(F(t)-P(t)\big)+\alpha_m\tanh\Big(\beta_m\big(P(t)-\frac{1}{\tau_m}\int_{t-\tau_m}^{t}P(s)ds\big)\Big) \\ &+\alpha_c\tanh\Big(-\beta_c\big(P(t)-\frac{1}{\tau_c}\int_{t-\tau_c}^{t}P(s)ds\big)\Big)\Big]dt+\sigma_M dW_M(t), \end{aligned} \tag{4.10}$$

where the fundamental price $F(t)$ is defined by (4.5). Therefore, the asset price dynamics is determined by the stochastic delay integro-differential equation (4.10).

We are interested in the connection between market stability and profitability of the trading strategies. Given the complex structure of the nonlinear model, we follow the standard approach in the HAM literature and combine the stability analysis of the underlying deterministic model with numerical simulation of the stochastic model. The stability analysis provides some insight into the effect of the interaction and dominance of different types of traders on market stability. It helps us to understand the relation between different states of market stability and profitability of trading strategies. Note that it is the interaction of deterministic dynamics and noise processes that provides a complete picture of the price dynamics of the stochastic model. In the following section, we first examine the stability of the corresponding deterministic delay integro-differential equation model.

4.4 Market Stability

By assuming a constant fundamental price $F(t)\equiv\bar{F}$ and no market noise $\sigma_M=0$, system (4.10) becomes a deterministic delay integro-differential equation, which represents the process of the mean value of the market return

$$\begin{aligned} \frac{dP(t)}{dt} =&\mu\Big[\alpha_f\beta_f\big(\bar{F}-P(t)\big)+\alpha_m\tanh\Big(\beta_m\big(P(t)-\frac{1}{\tau_m}\int_{t-\tau_m}^{t}P(s)ds\big)\Big) \\ &+\alpha_c\tanh\Big(-\beta_c\big(P(t)-\frac{1}{\tau_c}\int_{t-\tau_c}^{t}P(s)ds\big)\Big)\Big]. \end{aligned} \tag{4.11}$$

It is easy to see that $P(t)=\bar{F}$ is the unique steady state price of the system (4.11). We therefore call $P=\bar{F}$ the *fundamental steady state*.

In this section, we study the dynamics of the deterministic model (4.11) by focusing on the local stability of the fundamental steady state. Denote $\gamma_i=\mu\alpha_i\beta_i$ $(i=f,m,c)$, which characterize the activity of type-i traders.[11] In general, the dynamics depend on

[11] Intuitively, the speed of the price adjustment μ of the market maker measures the activity across the market. Both

the behavior of fundamental, momentum, contrarian traders, market maker, and time horizons. To understand the different impact of fundamental, momentum and contrarian traders, we first consider two special cases where only momentum traders or contrarians are involved.

4.4.1 The Stabilizing Role of the Contrarians

Contrarian trading strategies are based on the hypothesis of market overreaction. Intuitively, contrarians can induce market stability. To support the intuition, we consider a market with the fundamental and contrarian traders only, that is, $\alpha_m = 0$. In this case the system (4.11) reduces to

$$\frac{dP(t)}{dt} = \mu\Big[\alpha_f\beta_f\big(\bar{F} - P(t)\big) + \alpha_c \tanh\Big(- \beta_c\big(P(t) - \frac{1}{\tau_c}\int_{t-\tau_c}^{t} P(s)ds\big)\Big)\Big]. \tag{4.12}$$

The following proposition confirms the stabilizing role of the contrarians.[12]

Proposition 4.1 *The fundamental steady state price $P = \bar{F}$ of the system* (4.12) *is asymptotically stable for all $\tau_c \geq 0$.*

Proposition 4.1 shows that the market consisting of fundamental and contrarian investors is always stable, and the result is independent of the time horizon and extrapolation of the contrarians.[13]

4.4.2 The Destabilizing Role of the Momentum Traders

Momentum trading strategies based on the hypothesis of market underreaction are aimed to explore the opportunities of market price continuity. Intuitively, when the market is dominated by fundamental traders, the market is expected to reflect the fundamental price and then the impact of the momentum traders on market stability can be very limited. However, when the market is dominated by the momentum traders, the extrapolation of the market price continuity can have significant impact on market stability. To explore the impact, we now consider a market consisting of the fundamentalists and momentum

the population size α_i and behavior activity β_i qualify the trading behavior of type-i traders. Therefore, γ_i measures the activity or dominance of type i traders.

[12] All the proofs can be found in Appendix C.2.

[13] Note that this result is different from that in discrete-time HAMs, in which market can become unstable when activity of contrarians is strong, see for example, Chiarella and He (2002). This difference is due to the continuous adjustment of the market price. The impact of any strong activity from the contrarians becomes insignificant over a small time increment. Hence the time horizon used to form the MA becomes more irrelative in this case.

traders only, that is $\alpha_c = 0$. In this case, system (4.11) reduces to

$$\frac{dP(t)}{dt} = \mu\left[\alpha_f\beta_f\big(\bar{F} - P(t)\big) + \alpha_m \tanh\Big(\beta_m\big(P(t) - \frac{1}{\tau_m}\int_{t-\tau_m}^{t} P(s)ds\big)\Big)\right], \tag{4.13}$$

and the price dynamics can be described by the following proposition.

Proposition 4.2 *The fundamental steady state price $P = \bar{F}$ of the system* (4.13) *is*

(i) asymptotically stable for all $\tau_m \geq 0$ when $\gamma_m < \frac{\gamma_f}{1+a}$;

(ii) asymptotically stable for either $0 \leq \tau_m < \tau^*_{m,l}$ or $\tau_m > \tau^*_{m,h}$ and unstable for $\tau^*_{m,l} < \tau_m < \tau^*_{m,h}$ when $\frac{\gamma_f}{1+a} \leq \gamma_m \leq \gamma_f$; and

(iii) asymptotically stable for $\tau_m < \tau^*_{m,l}$ and unstable for $\tau_m > \tau^*_{m,l}$ when $\gamma_m > \gamma_f$.

Here $a = \max\{-\sin x/x; x > 0\}(\approx 0.2172)$, $\tau^*_{m,1} = 2\gamma_m/(\gamma_f - \gamma_m)^2$, $\tau^*_{m,l}(< \tau^*_{m,1})$ is the minimum positive root of equation

$$f(\tau_m) := \frac{\tau_m}{\gamma_m}(\gamma_f - \gamma_m)^2 - \cos\left[\sqrt{2\gamma_m\tau_m - (\gamma_f - \gamma_m)^2\tau_m^2}\right] - 1 = 0, \tag{4.14}$$

and $\tau^*_{m,h}(\in (\tau^*_{m,l}, \tau^*_{m,1}))$ is the maximum one among all the roots of (4.14) *which are less than $\tau^*_{m,1}$.*

Proposition 4.2 shows that the impact of the time horizon used in forming the MA for the momentum traders depends on γ_m and γ_f, which measure the dominance of the momentum and fundamental traders, respectively, with respect to their extrapolation and market fraction. On the one hand, when the fundamental traders dominate momentum traders (so that $\gamma_m < \gamma_f/(1+a)$), the market is always stable and time horizon plays no role in market stability. On the other hand, when momentum traders dominate fundamental traders (so that $\gamma_m > \gamma_f$), the market is stable when time horizon is small (so that $\tau_m < \tau^*_{m,l}$), but becomes unstable when the time horizon is large (so that $\tau_m > \tau^*_{m,l}$). In fact, the difference between price and the price trend based on the MA becomes insignificant when the time horizon is small and strong activity from the momentum traders has very limited impact on market stability, yielding the stability for small horizon. However, due to the smoothness of the MA when the time horizon is longer, the difference can become significant, which, together with strong activity from the momentum traders, makes the market become unstable. When the activity of the trend followers is balanced by that of the fundamental traders (so that $\gamma_f/(1+a) \leq \gamma_m \leq \gamma_f$), the market is stable when the time horizon is either short (so that $\tau_m < \tau^*_{m,l}$) or longer (so that $\tau_m > \tau^*_{m,h}$),

but becomes unstable with medium time horizon (so that $\tau^*_{m,l} < \tau_m < \tau^*_{m,h}$). This is an unexpected result. Intuitively, when time horizon is short, the price trend follows the price closely, which limits the trading opportunity for the momentum traders. When horizon is longer, the price trend becomes insensitive to the price changes. However, due to the balanced activity from the fundamental traders, the extrapolation activity of the momentum traders is limited. Therefore, in both cases, the market becomes stable.

4.4.3 The Joint Impact of Momentum and Contrarian Trading

The previous analysis shows the different role of the time horizon used in the MA by either the contrarians or momentum traders. We analyze the market stability when both strategies are employed in the market. For simplicity, we consider $\tau_m \equiv \tau_c := \tau$ in the rest of the chapter and leave the general case with different τ_m and τ_c in Appendix C.3. It is found that this special case can well reflect the impact of different types of traders' activities on the stability and further on their profitability. Let $\tau^*_1 = 2(\gamma_m - \gamma_c)/(\gamma_f - \gamma_m + \gamma_c)^2$, and $\tau^*_l (< \tau^*_1)$ and $\tau^*_h (\in (\tau^*_l, \tau^*_1))$ be the minimum and maximum positive roots which are less than τ^*_1, respectively, of the equation

$$h(\tau) := \frac{\tau}{\gamma_m - \gamma_c}(\gamma_f - \gamma_m + \gamma_c)^2 - \cos\left[\sqrt{2(\gamma_m - \gamma_c)\tau - (\gamma_f - \gamma_m + \gamma_c)^2\tau^2}\right] - 1 = 0.$$

In this case, the market stability of the system (4.11) can be characterized by the following proposition.

Proposition 4.3 *If $\tau_m \equiv \tau_c := \tau$, then the fundamental steady state price $P = \bar{F}$ of the system* (4.11) *is*

(1) asymptotically stable for all $\tau \geq 0$ when $\gamma_m < \gamma_c + \frac{\gamma_f}{1+a}$;

(2) asymptotically stable for either $0 \leq \tau < \tau^*_l$ or $\tau > \tau^*_h$ and unstable for $\tau^*_l < \tau < \tau^*_h$ when $\gamma_c + \frac{\gamma_f}{1+a} \leq \gamma_m \leq \gamma_c + \gamma_f$; and

(3) asymptotically stable for $\tau < \tau^*_l$ and unstable for $\tau > \tau^*_l$ when $\gamma_m > \gamma_c + \gamma_f$.

Despite the activity of both momentum and contrarian traders, Proposition 4.3 shares the same message to Proposition 4.2 with respect to the joint impact of the time horizons and the activity of the momentum traders on market stability, except that the activity of the fundamental traders in Proposition 4.2 is measured jointly by the activities of the fundamental and contrarian traders in Proposition 4.3. Given the stabilizing nature of the contrarian strategy indicated in Proposition 4.1, this is not unexpected. The three

conditions:

$$(1): \gamma_m < \gamma_c + \frac{\gamma_f}{1+a}, \qquad (2): \gamma_c + \frac{\gamma_f}{1+a} \leq \gamma_m \leq \gamma_c + \gamma_f, \qquad (3): \gamma_m > \gamma_c + \gamma_f$$

in Proposition 4.3 characterize three different states of market stability, which have different implications to the profitability of momentum trading strategy. For convenience, market state k is referred to condition (k) for $k = 1, 2, 3$ in the following analysis.

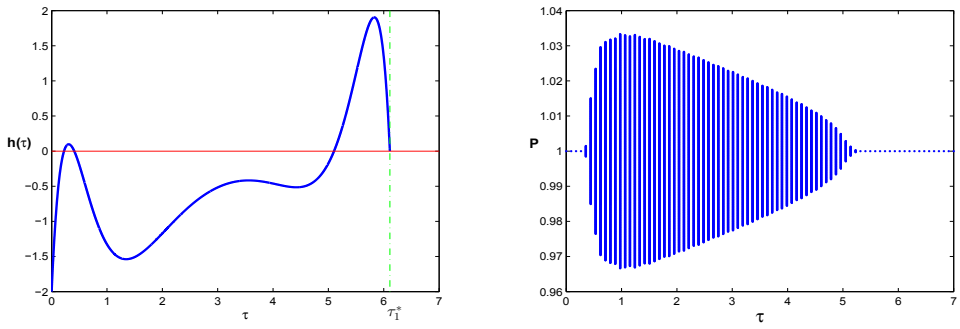

(a) The function $h(\tau)$ (b) Price bifurcation

Figure 4.2: (a) The function $h(\tau)$; (b) the corresponding bifurcation diagram for market state 2. Here $\gamma_f = 20$, $\gamma_m = 22.6$ and $\gamma_c = 5$.

To illustrate the price dynamics in different market state, we now conduct numerical analysis.[14] For market state 1, the fundamental price is stable, independent of the time horizon. For market state 2, Fig. 4.2 (a) illustrates the three Hopf bifurcation values $\tau_l^* \approx 0.23$, $\tau_3^* \approx 0.41$, and $\tau_h^* \approx 5.10$. Correspondingly, Fig. 4.2 (b) shows that the fundamental steady state price $P = \bar{F}$ is stable when $\tau \in [0, \tau_l^*) \cup (\tau_h^*, \infty)$ and unstable when $\tau \in (\tau_l^*, \tau_h^*)$. The stability switches twice.[15] For market state 3, Fig. 4.3 (a) illustrates the first (Hopf bifurcation) value $\tau_l^* \approx 0.22$, which leads to stable limit cycles for $\tau > \tau_l^*$, as shown in Fig. 4.3 (b). The stability switches only once at τ_l^*.

The above numerical analysis clearly illustrates that dependence of the market price dynamics on the time horizon is different in different market states. We show in the following section that the market states also have different implications on the underreaction/overreaction and momentum profitability. We complete the discussion of this section by considering a very special case when $\alpha_m = \alpha_c$, $\beta_m = \beta_c$ and $\tau_m = \tau_c$, that is

[14] The numerical results in this chapter (except for the Appendices C.4 and C.5) are based on $\alpha_f = 0.3$, $\alpha_m = 0.4$, $\alpha_c = 0.3$, $\mu = 5$ and $\bar{F} = 1$, unless specified otherwise.

[15] Simulations (not reported here) show that the speed of the convergence when the fundamental steady state becomes stable after switching from instability as τ increases is very slow, although F is stable. The properties on the number of bifurcations and the stability switching are further illustrated in Fig. C.3 in Appendix C.2. There are some interesting properties on the nature of bifurcations related to Proposition 4.3, including the number of bifurcations, stability switching and the dependence of the bifurcation values on the parameters. We provide the detailed analysis in Appendix C.2.

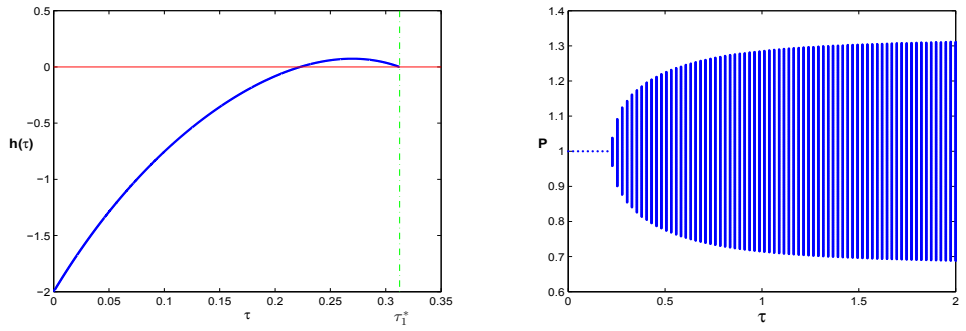

(a) The function $h(\tau)$ (b) Price bifurcation

Figure 4.3: (a) The function $h(\tau)$; (b) the bifurcation diagram of the market price for market state 3. Here $\gamma_f = 2$, $\gamma_m = 20$ and $\gamma_c = 10$.

the momentum and the contrarian traders have the same population, extrapolation rate and time horizon. In this case, system (4.11) reduces to $dP(t)/dt = \gamma_f(\bar{F} - P(t))$. The destabilizing effect of momentum traders is completely offset by contrarians, which leads to the global stability of the fundamental price.

4.5 Momentum Profitability

This section numerically examines the profitability of the time series momentum trading strategies. We show that the profitability is closely related to the market states defined according to the stability analysis in the previous section. In particular, we show that, in market state 3, the momentum strategy is profitable when the time horizon is short and unprofitable when the time horizon is long. In other market states, the strategy is not profitable for any time horizon. We also provide some explanation to the profitability mechanism through autocorrelation and time series analysis.

As in the previous section, we focus on the special case when momentum and contrarian traders use the same time horizon and holding period. The profit is calculated using a buy-and-hold strategy on the number and position determined by the demand function of the trading strategy.[16] It follows from Eq. (4.7) that the excess demands of momentum

[16] Alternatively, the profit can be calculated based on buy-and-hold strategy on one unit of position taking, as in Section 4.2. However, we find that this does not affect the profitability results obtained in this section.

and contrarian traders with time horizon τ are given, respectively, by

$$\begin{aligned} D_m(t) &= \tanh\Big(\beta_m\big(P(t) - \frac{1}{\tau}\int_{t-\tau}^{t} P(s)ds\big)\Big), \\ D_c(t) &= \tanh\Big(-\beta_c\big(P(t) - \frac{1}{\tau}\int_{t-\tau}^{t} P(s)ds\big)\Big). \end{aligned} \tag{4.15}$$

Based on buy and hold strategy, the spot profits yielded by using the fundamental, momentum, contrarian trading strategies, and the market maker at time t can be calculated by

$$U_i(t) = D_i(t)\big(P(t+\tau) - P(t)\big), \qquad i = f, m, c, M, \tag{4.16}$$

where the excess demand of the fundamental strategy $D_f(t)$ is defined by Eq. (4.4) and the excess demand of the market maker is given by $D_M(t) = -\big(\alpha_f D_f(t) + \alpha_m D_m(t) + \alpha_c D_c(t)\big)$, which is based on the liquidity provided to clean the market. In addition, we also calculate the average accumulated profit yielded over a time interval $[t_0, t]$ by

$$\bar{U}_i(t) = \frac{1}{t - t_0}\int_{t_0}^{t} D_i(s)\big(P(s+\tau) - P(s)\big)ds, \qquad i = f, m, c, M. \tag{4.17}$$

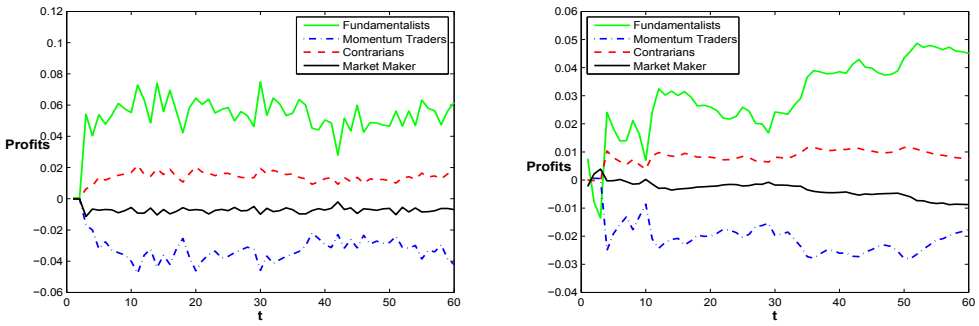

(a) Average spot profits (b) Average accumulated profits

Figure 4.4: (a) The average spot profits of trading strategies based on 1000 simulations; (b) the average accumulated profits based on a typical simulation for market state 1. Here $\gamma_f = 15$, $\gamma_m = 15$ and $\gamma_c = 3$ and $\tau = 0.5$.

We now examine the profitability in different market states. In the rest of the chapter, the time unit is one year and the time step Δt is one month. Given 14.9% annually standard deviation of the log return for the S&P 500 index used in Section 4.2, we choose $\sigma_M = 0.15$ for the annual market volatility and $\sigma_F = 0.1$ for the annual volatility of the fundamental price.

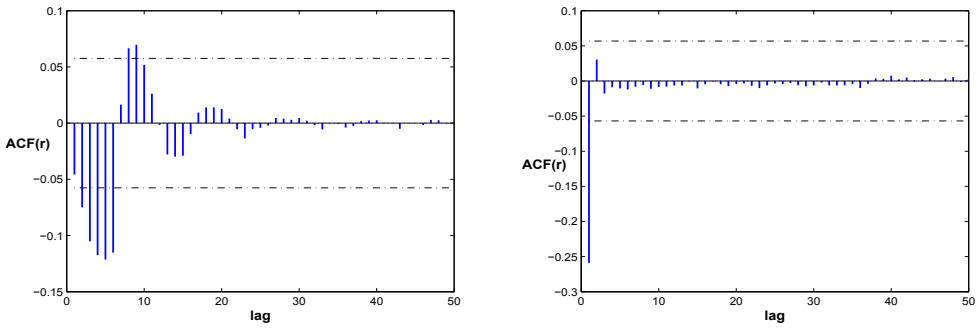

(a) $\tau = 0.5$ (b) $\tau = 3$

Figure 4.5: The average ACs of market return based on 1000 simulations for market state 1 with (a) $\tau = 0.5$ and (b) $\tau = 3$. Here $\gamma_f = 15$, $\gamma_m = 15$ and $\gamma_c = 3$.

4.5.1 State 1

In market state 1, the market is dominated jointly by the fundamental and contrarian traders (so that $\gamma_m < \gamma_c + \gamma_f/(1+a)$). In this case, the stability of the fundamental price of the underlying deterministic model is independent of the time horizon. Based on 1,000 simulations, Fig. 4.4 (a) reports the average spot profits of different strategies and Fig. 4.4 (b) illustrates the average accumulated profits based on a typical simulation. They show that the contrarian and fundamental strategies are profitable, but not the momentum strategy and the market maker. Note that the amounts of profit/loss are small, which is underlined by the stable market price.

To understand the mechanism of the profitability, we present the average return autocorrelations (ACs) based on 1000 simulations in Fig. 4.5 for $\tau = 0.5$ in (a) and $\tau = 3$ in (b). It shows some significant and negative ACs for small lags and insignificant ACs for large lags. This indicates market overreaction in short-run and hence the fundamental and contrarian trading can generate significant profits. There is no significant and positive ACs, indicating no market underreaction, and hence the momentum trading is not profitable.

4.5.2 State 2

In market state 2, the momentum traders are active, but their activities are balanced by the fundamental and contrarian traders (so that $\gamma_c + \gamma_f/(1+a) \leq \gamma_m \leq \gamma_c + \gamma_f$). In this case, the stability of the underlying deterministic model is illustrated in Fig. 4.2, showing that the fundamental price is stable for either short or longer time horizons, but unstable for medium time horizons. With the same parameters used in Fig. 4.2, we

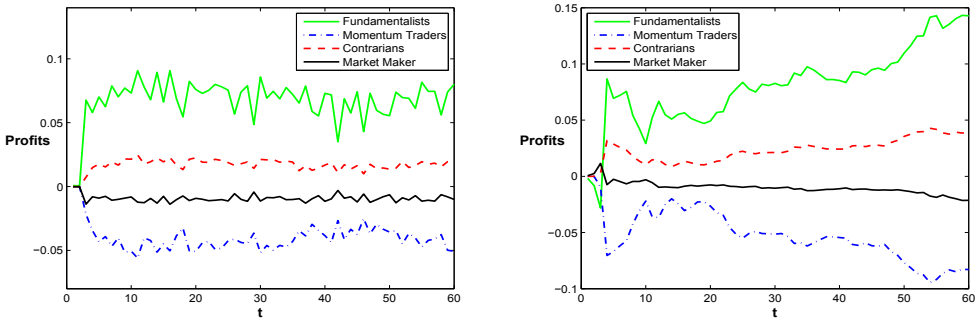

(a) Average spot profits (b) Average accumulated profits

Figure 4.6: (a) The average spot profits based on 1,000 simulations; (b) the average accumulated profits based on a typical simulation for market state 2. Here $\gamma_f = 20$, $\gamma_m = 22.6$, $\gamma_c = 5$ and $\tau = 0.5$.

illustrate the profitability of the different trading strategies in Fig. 4.6. It shows that the fundamental and contrarian trading strategies are profitable, but not the momentum traders and the market maker. Further simulations (not reported here) show the same result with different time horizons, although the losses/profits increase as time horizon increases.

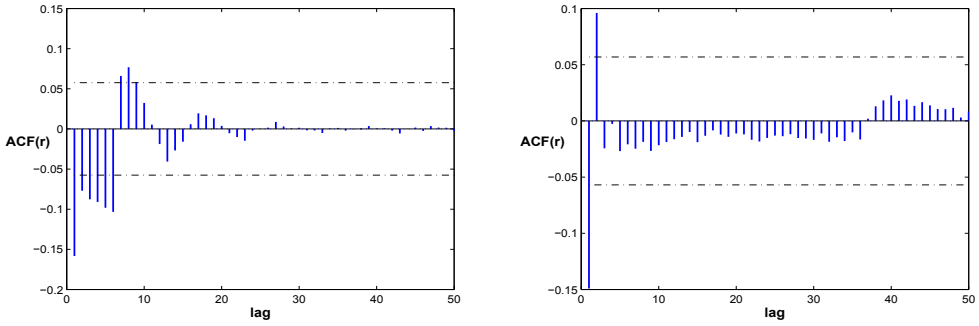

(a) $\tau = 0.5$ (b) $\tau = 3$

Figure 4.7: The average ACs of market return based on 1000 simulations for market state 2 with (a) $\tau = 0.5$ and (b) $\tau = 3$.

As in market state 1, we also calculate the return ACs with the same set of parameters as Fig. 4.2. Fig. 4.7 presents the average ACs based on 1000 simulations for time horizon $\tau = 0.5$ in (a) and $\tau = 3$ in (b), showing some significantly negative ACs, in particular for $\tau = 0.5$, over short lags. This indicates the profitability of the fundamental and contrarian trading due to market overreaction, but not for the momentum trading. Therefore, both states 1 and 2 lead to the same conclusion on the profitability, although the amount of profit/loss in state 2 is higher than in state 1.

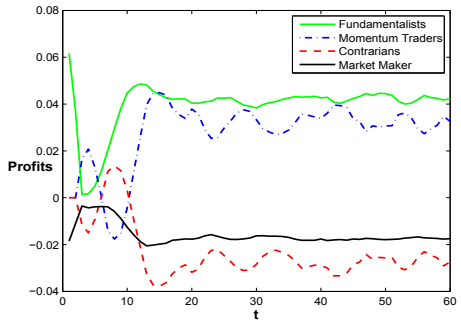

(a) Average spot profits for $\tau = 0.5$

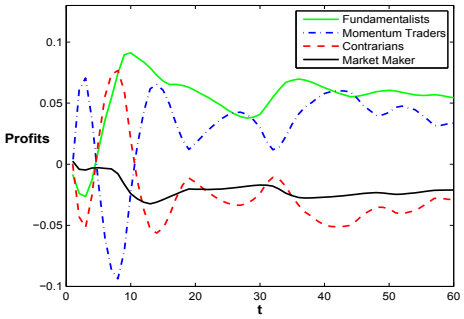

(b) Average accumulated profits for $\tau = 0.5$

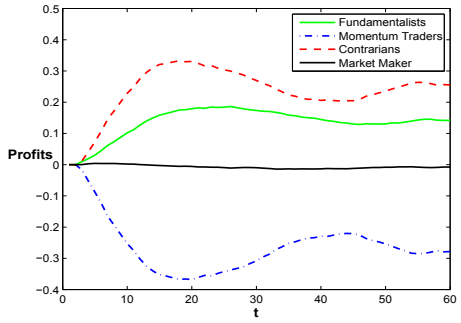

(c) Average spot profits for $\tau = 3$

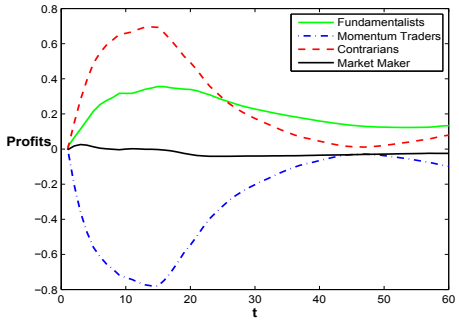

(d) Average accumulated profits for $\tau = 3$

Figure 4.8: The average spot profits based on 1000 simulations for (a) $\tau = 0.5$ and (c) $\tau = 3$ and the average accumulated profits based on a typical simulation for (b) $\tau = 0.5$ and (d) $\tau = 3$ for market state 3. Here $\gamma_f = 2$, $\gamma_m = 20$ and $\gamma_c = 10$.

4.5.3 State 3

In market state 3, the market is dominated by the momentum traders (so that $\gamma_m > \gamma_c + \gamma_f$). The stability of the underlying deterministic model is illustrated in Fig. 4.3, showing that the fundamental price is stable for short horizons, but unstable for longer horizons. With the same set of parameters in Fig. 4.3, we reports the profitability of the different trading in Fig. 4.8. It shows clearly that, for short horizon $\tau = 0.5$, the fundamental and momentum trading strategies are profitable, but not the contrarians, as illustrated in Figs. 4.8 (a) and (b). However, for longer horizon $\tau = 3$, the fundamental and contrarian strategies are profitable, but not the momentum traders, see Figs. 4.8 (c) and (d).

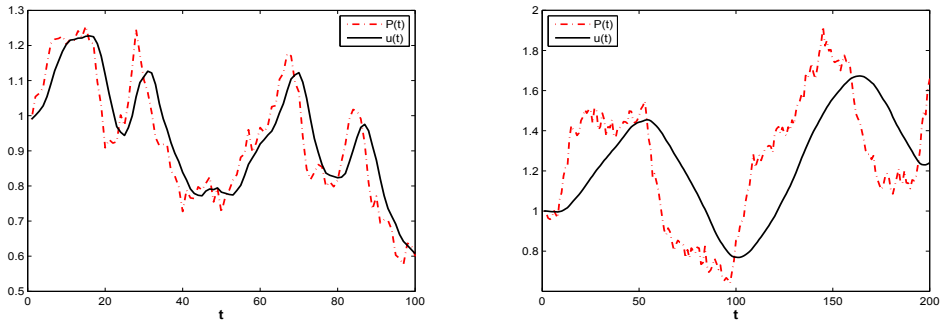

(a) Time series for $\tau = 0.5$ (b) Time series for $\tau = 3$

Figure 4.9: Time series of price $P(t)$ and price trend $u(t)$ for (a) $\tau = 0.5$ and (b) $\tau = 3$.

To explore the profit opportunity of the momentum trading with different time horizons, we plot the time series of the price and price trend in Fig. 4.9 (a) for $\tau = 0.5$ and Fig. 4.9 (b) for $\tau = 3$, based on the same simulation in Fig. 4.8 (b) and (d), respectively. There are two interesting observations. (i) For short horizon $\tau = 0.5$, the market price fluctuates due to the unstable steady state of the underlying deterministic system. When the market price increases, the price trend follows the market price closely and increases too, as illustrated in Fig. 4.9 (a). This implies that, with short holding period, the momentum trading strategy is profitable by taking long positions. Similarly, when the market price declines, the price trend follows. Hence the momentum trading is profitable by taking short positions. Therefore, the momentum trading is profitable (except for the starting periods of sudden changes in the price tendency). (ii) For longer horizon $\tau = 3$, the market price fluctuates widely due to the unstable fundamental value of the underlying deterministic system. The relation between market price and price trend is similar to the case for the short horizon, as illustrated in Fig. 4.9 (b). However, a longer horizon makes

the price trend less sensitive to the changes in price. Also, since the holding period is also longer, the momentum trading mis-matches the profitability opportunity. For example, when the market price reaches a peak at $t \approx 50$ (months), which is higher than the trend, the momentum traders buy the stocks. After holding the stocks for 3 years, they sell at a much lower price at $t \approx 86$, implying a loss from the momentum strategy. This illustrates that, with longer horizon, the momentum trading is not profitable.

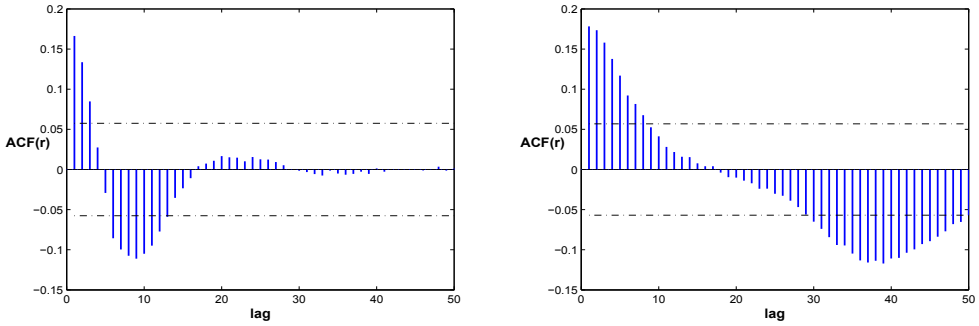

(a) $\tau = 0.5$ (b) $\tau = 3$

Figure 4.10: The average ACs of market return based on 1000 simulations for market state 3 with (a) $\tau = 0.5$ and (b) $\tau = 3$.

To provide further insight into the profitability mechanism, we calculate the return ACs and present the results in Fig. 4.10. It shows clearly the market underreaction in short run and overreaction in long run, characterized by significantly positive ACs for short lags and negative ACs for long lags for both short and longer horizons. With the short horizon and holding period, the momentum trading is profitable due to the underreaction in short-run (Fig. 4.10 (a)). However with the long time horizon, the momentum trading is no longer profitable for long holding period due to the overreaction in long-run (Fig. 4.10 (b)), although it can be profitable with short holding period due to the underreaction illustrated in Fig. 4.10 (b), which is verified in Fig. 4.11 with 3 years horizon and 6 month holding period. This result is consistent with Lou and Polk (2013).

It would be interesting to see if the model is able to replicate the time series momentum profit explored for the S&P 500 in Section 4.2 based on the momentum strategies (4.1) and (4.2). Table 4.3 reports the annual excess returns of various momentum trading strategies based on (4.1) investing in the model generated data in market state 3 for time horizon and holding period from 1 to 60 months. Fig. 4.12 reports the corresponding t-statistic of the average excess return of the momentum strategies for time horizon from 1 to 60 months periods and holding period equals to horizon, 1 month and 6 month periods. Similar results based on trading strategy (4.2) are reported in Table C.2 and Fig. C.2 in

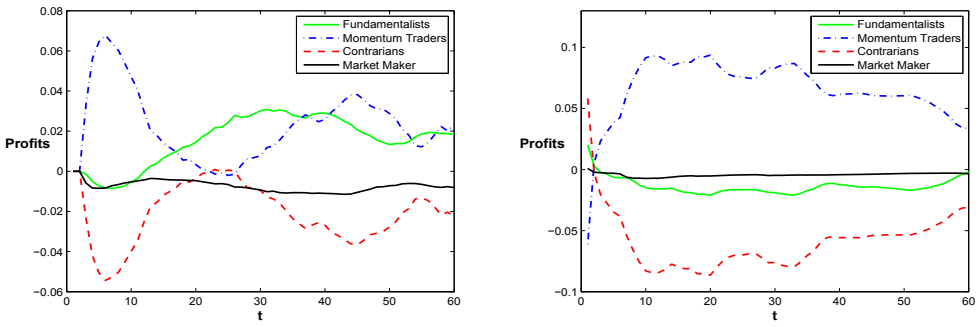

(a) Average spot profits (b) Average accumulated profits

Figure 4.11: (a) The average spot profits based on 1,000 simulations; (b) the average accumulated profits based on a typical simulation for market state 3 with 3 years horizon and 0.5 year holding period.

$(m \setminus n)$	1	3	6	12	24	36	48	60
1	1.23	3.30	3.05**	3.09***	1.71**	0.44	-0.17	-0.42
3	2.78	3.21	4.73**	4.16**	2.68**	0.25	-0.42	-0.55
6	2.48	3.85	5.74**	5.09**	2.29	-0.37	-1.41	-1.15
12	6.89**	7.87**	8.12***	5.91**	1.48	-1.78	-2.50*	-1.99
24	9.92***	9.89***	7.40**	2.89	-2.71	-4.82**	-3.82*	-2.14
36	8.84**	5.43	2.16	-1.79	-6.22**	-7.57***	-5.44**	-3.34*
48	5.00	2.41	-0.01	-3.66	-7.76***	-8.52***	-5.91***	-3.57*
60	2.50	-0.03	-2.01	-5.25	-9.00***	-9.19***	-6.15***	-3.63*

Table 4.3: The annualized percentage (log) excess returns of the momentum strategy (4.1) for the time series generated from the model in market state 3 with the horizon (m) and holding (n) from 1 to 60 months period. Note: *, **, *** denote the significance at 10%, 5% and 1% levels, respectively.

Appendix C.1. We see that both the profit and t-statistic patterns generated from the model are very similar to the S&P 500 reported in Section 4.2. The results are consistent with Moskowitz et al. (2012) who find that the time series momentum strategy with 12 months horizon and 1 month holding is the most profitable among others.

To complete this section, we add the following remarks. (i) The analysis of this chapter focuses on the same time horizon and holding period. An extension to different time horizon and holding period is presented in Appendix C.3. (ii) Simulations (not reported here) show that the level of profitability of momentum (contrarian) strategy is positively (negatively) related to β_m and negatively (positively) related to β_c. Also, the level of profitability of both momentum and contrarian strategies is positive related to the price adjustment speed μ. (iii) The time horizon τ can affect the profitability greatly. Recall that the stability of the system depends on $\gamma_i = \mu\alpha_i\beta_i$ $(i = f, m, c)$ and τ completely and the profitability is closely related to the market states. (iv) When investors switch their trading strategies based on some fitness functions, we extend the model in Appendices

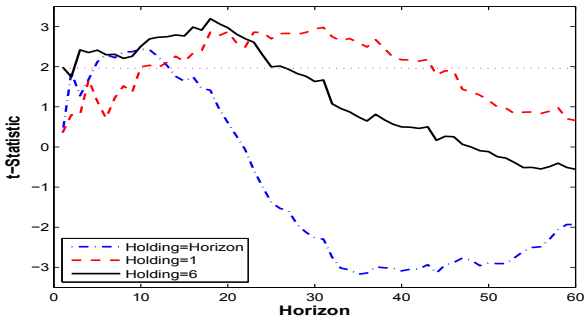

Figure 4.12: The t-Statistic of the average excess return of the momentum strategy (4.1) investing in the model generated data in market state 3 for time horizon from 1 to 60 months periods and holding equal to horizon ($n = m$), 1 month ($n = 1$) and 6 month periods ($n = 6$).

C.4 and C.5 and show that the profits/losses can be enhanced due to the switching among different trading strategies.

4.6 Conclusion

Based on market underreaction and overreaction hypotheses, momentum and contrarian strategies are widely used by financial market practitioners and their profitability has been extensively investigated by academics. However, most behavioral models do not specify the time horizon, which plays crucial a role in the performance of momentum and contrarian strategies. Following the recent development in the heterogeneous agent models literature, this chapter proposes a continuous-time heterogeneous agent model of investor behavior consisting of fundamental, contrarian, and momentum strategies. The underlying stochastic delay integro-differential equation of the model provides a unified approach to deal with different time horizons of momentum and contrarian strategies, which play an important role in the profitability empirically. By examining their impact on market stability explicitly and analyzing the profitability numerically, this chapter examines the profitability of the time series momentum trading strategies. We show that the profitability is closely related to the market states defined by the stability of the underlying deterministic model. In particular, we show that, in market state 3 where the momentum traders dominate the market, the momentum strategy is profitable when the time horizon is short and unprofitable when the time horizon is long. In other market states, the strategy is not profitable for any time horizon. We also provide some explanation to the profitability mechanism through autocorrelation patterns and the classical underreaction and overreaction hypotheses. In addition, we show that the momentum

strategy works in the stock index.

Although the model proposed in this chapter is very simple, it provides some insight into the time series momentum documented in recent empirical literature. As we discussed in the introduction, the time series momentum plays a very important role in explaining cross-sectional momentum, which had been widely researched in the literature. Motivated by the results obtained in this chapter, one can extend the market of one risky asset to one with many risky assets so that the profitability of portfolios constructed from momentum and contrarian strategies can be examined. We would expect the same mechanism can be used to explain cross-sectional momentum. In addition, it has been shown that volatility can affect the autocorrelations in returns and hence affect profitability and even trading volume. This could be examined by using the setup in this chapter. We leave these to future research.

Chapter 5

Optimality of Momentum and Reversal

5.1 Introduction

Chapter 4 shows the profitability of the momentum and contrarian strategies is conditional. In order to achieve an unconditional profitability, this chapter studies the optimality of trading strategies to reflect the short-run momentum and long-run reversal in financial markets. We extend the standard asset pricing model under geometric Brownian motion to incorporate a weighted average of mean reversion and moving average into the drift. When the preference is given by the log utility function, we obtain the optimal portfolio, which includes Merton's optimal portfolio as a special case. We show that a combined momentum and reversal strategy is optimal. To demonstrate the optimality of the strategy, we estimate the model to the S&P 500 index and show that neither pure momentum nor pure mean reversion strategies can outperform the market; however, the optimal strategy combining the momentum and mean reversion can outperform the market. In fact, different from the momentum strategy which is based on trend only, the optimal strategy takes not only the trend in return but also the market volatility into account. Through regression analysis, we further show that the optimal strategies are immune to market states, investor sentiment and market volatility.

The asset pricing model developed in this chapter takes not only the mean reversion but also the momentum effect into account directly. Therefore the historical prices underlying the momentum component affect the asset prices, resulting in a non-Markov process characterized by stochastic delay differential equations (SDDEs). This is very different from the Markov asset price process well documented in the literature (Merton 1969,

1971), where the dynamic programming method through HJB equation is most frequently used in solving the stochastic control problem. It becomes very challenging to solve the optimal control problem for DDEs because it involves infinite-dimensional PDEs. To overcome this challenge, we explore the latest development in the theory of maximum principle for control problem of SDDEs. By assuming the log utility preference, we derive the optimal strategies in closed form. This helps us to study the impact of historical information on the profitability of different strategies based on different time horizons.[1]

This chapter is closely related to the literature on momentum and reversal, two of the most prominent financial market anomalies; in particular, time series momentum. Momentum, on the one hand, is the tendency of assets with good (bad) recent performance to continue outperforming (underperforming) in short-run. Reversal, on the other hand, concerns predictability of assets that performed well (poorly) over a long period tend to subsequently underperform (outperform). Momentum and reversal have been documented extensively for a wide variety of assets. Jegadeesh and Titman (1993) document momentum for individual U.S. stocks, predicting returns over horizons of 3-12 months by returns over the past 3-12 months. De Bondt and Thaler (1985) document the reversal, predicting returns over horizons of up to five years by returns over the past 3-5 years. Fama and French (1992) document the value effect, which is closely related to reversal, whereby the ratio of an assets price relative to book value is negatively related to subsequent performance. Mean reversion in equity returns has been shown to induce significant market timing opportunities (Campbell and Viceira 1999, Wachter 2002 and Koijen et al. 2009). The evidence has been extended to stocks in other countries (Fama and French 1998), stocks within industries (Cohen and Lou 2012), across industries (Cohen and Frazzini 2008), and the global market with different asset classes (Asness, Moskowitz and Pedersen 2013). More recently, Moskowitz et al. (2012) investigate time series momentum that characterizes strong positive predictability of a security's own past returns.

This chapter is largely motivated by the empirical literature testing trading signals with combination of momentum and reversal. Balvers and Wu (2006) and Serban (2010) empirically show that a combination of momentum and mean-reversion strategies can outperform the pure momentum and pure mean reversion strategies for equity markets and foreign exchange markets respectively. Asness, Moskowitz and Pedersen (2013) highlight that studying value and momentum jointly is more powerful than examining each in isolation.[2] Koijen et al. (2009) proposes a theoretical model in which stock returns exhibit

[1] The impact of the time horizon on the profitability has been extensively investigated in the empirical literature, see, for example, De Bondt and Thaler (1985) and Jegadeesh and Titman (1993). However, due to the technical challenge, there are few theoretical results on it.

[2] They find that separate factors for value and momentum best explain the data for eight different markets and asset

momentum and mean reversion effects. They study the dynamic asset allocation problem with CRRA utility. However, the modelling of momentum in this chapter is very different from Koijen et al. (2009). In Koijen et al. (2009), the momentum is calculated by all the historical returns with geometrically decaying weights. This reduces the pricing dynamics to a Markovian system. In this chapter, the momentum is measured by the standard moving average over a moving window with a fixed "look-back period", which is consistent with the momentum literature. Also, Koijen et al. (2009) focuses on the performance of the hedging demand implied by the model, while the focus of this chapter is on the performance of the optimal strategies.

By estimating the model to the S&P 500, we are able to demonstrate that the optimal strategies based on the pure momentum and pure mean reversion models cannot outperform the market but a combination of them can outperform the market. The optimal strategies not only reflect the trading signal based on momentum and reversal effects, but also take the volatility into account. The robustness of the optimality of the optimal strategies are also tested in short run and long run, with different estimations, out of sample predictions, market states, investor sentiment and market volatility. Finally, we compare the performance of the optimal strategies with the time series momentum strategies used in Moskowitz et al. (2012). With different proxies, including the utility of wealth, Sharpe ratio and average return, we show that the profitability pattern reflected by the average return in most of the empirical literature underperform comparing to the optimal strategies.

This chapter is based on He, Li and Li (2014) and organized as follows. We first present the model and derive the optimal asset allocation in Section 5.2. We then estimate the model to the S&P500 in Section 5.3 and examine the performance of the optimal strategies in Section 5.4. Section 5.5 concludes. All the proofs and the robustness analysis are included in Appendix D.

5.2 Optimal Asset Allocation

In this section, we introduce an asset pricing model and study the optimal asset allocation problem.

classes. Furthermore, they show that momentum loads positively and value loads negatively on liquidity risk; however, an equal-weighted combination of value and momentum is immune to liquidity risk and generates substantial abnormal returns.

5.2.1 The Model

We consider a financial market with two tradable securities, a risky asset S and a riskless asset B satisfying

$$\frac{dB_t}{B_t} = rdt, \tag{5.1}$$

where the riskless interest rate r is a constant. The uncertainty is represented by a filtered probability space $(\Omega, \mathcal{F}, P, \{\mathcal{F}_t\}_{t\geq 0})$ on which a two-dimensional Brownian motion Z_t is defined. Let S_t be the price of the risky asset or the level of a market index at time t and the dividends are assumed to be reinvested. Following Koijen et al. (2009), we assume the instantaneous return of the risky asset is arrived at via a momentum term m_t and a long-run mean reversion term μ_t and the dynamics of stock returns is given by

$$\frac{dS_t}{S_t} = \big[\phi m_t + (1-\phi)\mu_t\big]dt + \sigma_S' dZ_t, \tag{5.2}$$

where ϕ is a constant, measuring the weight to the momentum component, σ_S is a two-dimensional volatility vector, and Z_t is a two-dimensional vector of independent Brownian motions. The mean reversion process μ_t is a stationary variable, defined by an Ornstein-Uhlenbeck process,

$$d\mu_t = \alpha(\bar{\mu} - \mu_t)dt + \sigma_\mu' dZ_t, \qquad \alpha > 0, \qquad \bar{\mu} > 0 \tag{5.3}$$

where $\bar{\mu}$ is the constant long-run expected rate of return, α is the rate at which μ_t converges to $\bar{\mu}$, and σ_μ' a two-dimensional vector of instantaneous volatilities. The momentum term m_t is defined by a stardard moving average (MA) of past returns over $[t-\tau, t]$,

$$m_t = \frac{1}{\tau}\int_{t-\tau}^{t} \frac{dS_u}{S_u}. \tag{5.4}$$

The modelling of momentum in this chapter is motivated by the time series momentum Moskowitz et al. (2012) who demonstrate that the average return over a past period (say, 12 months) is a positive predictor of its future returns, especially the return for the next month. This is different from Koijen et al. (2009). In Koijen et al. (2009), the momentum at time t is defined by

$$M_t = \int_0^t e^{-w(t-u)}\frac{dS_u}{S_u},$$

which is based on the past returns over $[0, t]$ with geometrically decaying weights. The advantage of M_t is that the process M_t can be treated as a Markovian process. Note that the weights over $[0, t]$ are not added up to one. Thus M_t cannot be treated as the standard

average of past returns. Also M_t is not rolling forward with a fixed time window. The momentum m_t introduced in this chapter is the standard moving average over a moving window $[t-\tau, t]$ with "look-back period" of $\tau > 0$ and the weights over the period are added up to one. This definition is consistent with the empirical momentum literature, which explores the price trends based on the returns over a fixed "look-back period".

The resulting asset price model (5.2)-(5.3) is characterized by a stochastic delay integro-differential system, which is non-Markovian. We show in Appendix D.1 that the process has a pathwisely unique solution and asset price is always positive for given initial values over $[-\tau, 0]$.

5.2.2 Optimal Asset Allocation

Consider a typical long-term investor who maximizes the expected utility of the terminal wealth. Assume that the preferences of the investor can be represented by a log utility function. Let W_t be the wealth of the investor at time t and π_t is the fraction of the wealth invested in the stock. Then the change in wealth follows

$$\frac{dW_t}{W_t} = \big\{\pi_t[\phi m_t + (1-\phi)\mu_t - r] + r\big\}dt + \pi_t \sigma_S' dZ_t. \tag{5.5}$$

The investment problem of the investor is given by

$$J(W, m, \mu, t, T) = \sup_{(\pi_u)_{u\in[t,T]}} \mathbb{E}_t[\ln W_T], \tag{5.6}$$

where T is the terminal time of the investment, and $J(W, m, \mu, t, T)$ is the value function corresponding to the optimal investment strategy. Then we show in Appendix D.2 that the optimal dynamic strategic allocation can be characterized by the following proposition.

Proposition 5.1 *For an investor with log utility, the optimal strategic allocation to stocks is given by*

$$\pi_t^* = \frac{\phi m_t + (1-\phi)\mu_t - r}{\sigma_S' \sigma_S}. \tag{5.7}$$

The optimal portfolio (5.7) reflects the myopic behavior of the investor with log utility. Two special cases are interesting. First, when $\phi = 0$, the asset price does not depend on the momentum and follows a standard geometric Brownian motion process

$$\frac{dS_t}{S_t} = \mu_t dt + \sigma_S' dZ_t.$$

In this case, the optimal portfolio reduces to (5.7) becomes

$$\pi_t^* = \frac{\mu_t - r}{\sigma_S' \sigma_S}, \tag{5.8}$$

which is the standard optimal strategy when the drift is mean-reverting. In particular, when $\mu_t = \mu$ is a constant, the optimal portfolio (5.8) collapses to $\pi_t^* = \frac{\mu - r}{\sigma_S' \sigma_S}$, which is the optimal portfolio in Merton (1971).

Secondly, when $\phi = 1$, the asset price depend only on the momentum. Correspondingly, the optimal portfolio (5.7) reduces to

$$\pi_t^* = \frac{m_t - r}{\sigma_S' \sigma_S}. \tag{5.9}$$

If we consider the trading signal indicated by the excess return $m_t - r$ only, with $\tau = 12$, the optimal portfolio (5.9) is consistent with the time series momentum strategy in Moskowitz et al. (2012) by constructing portfolios based on the monthly excess returns over the past 12 months and holds it for 1 month. Moskowitz et al. (2012) demonstrate that this strategy performs the best among all the momentum strategies with look-back period and holding period from 1 month to 48 months. If we take only the position and construct simple buy-and-hold momentum strategy over a large range of look-back period and holding period investigated in Moskowitz et al. (2012), (5.9) shows that the time series momentum strategies can be optimal when the mean-reverting is not significant in markets. This explains the dependence of the momentum profitability on market conditions and volatility. Note that the optimal portfolio (5.9) defines the optimal wealth fraction invested in the risky asset, depending on not only the excess return but also the volatility.

In general, the optimal portfolio (5.7) implies that a weighted average of momentum and mean-reverting strategies is optimal. Intuitively, it takes into account of both the short-run momentum and long-run reverting, which are well supported empirically. It is the simple form of the optimal portfolio (5.7) that facilitates the comparison of the performance with other trading strategies and the market. As demonstrated by the following analysis, its empirical implication can be very significant.

5.3 Model Estimation

To demonstrate the optimality of the optimal portfolio (5.7), we estimate the model to the S&P 500 in this section. In line with Campbell and Viceira (1999) and Koijen et al.

(2009), the mean-reversion variable is affine in the (log) dividend yield as follow,

$$\mu_t = \bar{\mu} + \nu(D_t - \mu_D) = \bar{\mu} + \nu X_t,$$

where ν is a constant, D_t indicates the (log) dividend yield with $\mathbb{E}(D_t) = \mu_D$, and $X_t = D_t - \mu_D$ denotes the de-meaned dividend yield. Thus the asset price model (5.2)-(5.3) become

$$\begin{cases} \dfrac{dS_t}{S_t} = \big[\phi m_t + (1-\phi)(\bar{\mu} + \nu X_t)\big]dt + \sigma_S' dZ_t, \\ dX_t = -\alpha X_t dt + \sigma_X' dZ_t, \end{cases} \tag{5.10}$$

where $\sigma_X = \sigma_\mu / \nu$.

The uncertainty in system (5.10) is driven by two independent Brownian motions. Without loss of generality, the volatility matrix of the dividend yield and return is parameterized to be lower triangular,

$$\Sigma = \begin{pmatrix} \sigma_S' \\ \sigma_X' \end{pmatrix} = \begin{pmatrix} \sigma_{S(1)} & 0 \\ \sigma_{X(1)} & \sigma_{X(2)} \end{pmatrix}.$$

That is, Σ is the Cholesky decomposition of the instantaneous variance matrix. Thus, the first element of Z_t is the shock to the return and the second element of Z_t is the dividend yield shock that is orthogonal to return shock. This setup follows Sangvinatsos and Wachter (2005) and Koijen et al. (2009).

By discretizing the continuous-time model at a monthly frequency to be consistent with the momentum and reversal literature, system (5.10) results in a bivariate Gaussian vector autoregression (VAR) model for the simple return and dividend yield, which are observable,

$$\begin{cases} R_{t+1} = \dfrac{\phi}{\tau}(R_t + R_{t-1} + \cdots + R_{t-\tau+1}) + (1-\phi)(\bar{\mu} + \nu X_t) + \sigma_S' \Delta Z_{t+1}, \\ X_{t+1} = (1-\alpha) X_t + \sigma_X' \Delta Z_{t+1}, \end{cases} \tag{5.11}$$

where $R_t = (S_t - S_{t-1})/S_{t-1}$ is the simple return of the stock at time t.[3]

We estimate the model (5.11) with maximum likelihood method by employing monthly S&P 500 data over the period January 1871–December 2012 obtained from the home page of Robert Shiller. We set the instantaneous short rate to $r = 4\%$ annually. As in Campbell and Shiller (1988*a*, 1988*b*), the dividend yield is defined as the log of the ratio between the last period dividend and the current index. We construct the total return index using

[3]Different from Koijen et al. (2009), we use the simple return to construct m_t and also discretize the stock price process into simple return rather than log return to be consistent with the momentum and reversal literature.

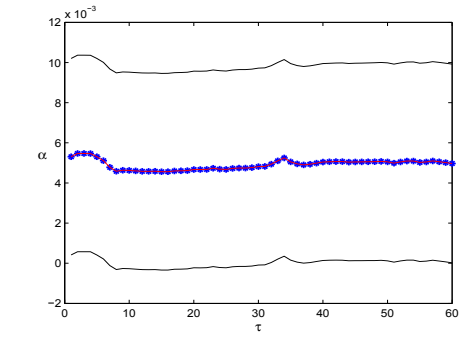

(a) Estimates of α

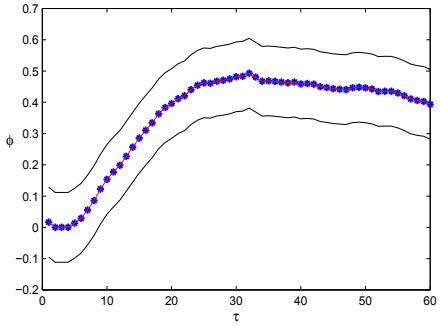

(b) Estimates of ϕ

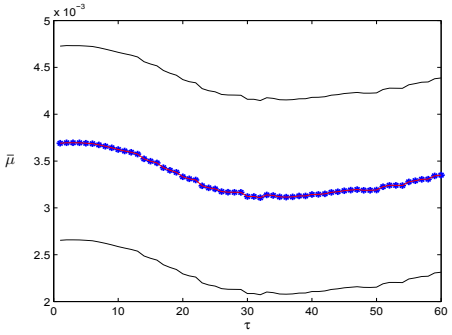

(c) Estimates of $\bar{\mu}$

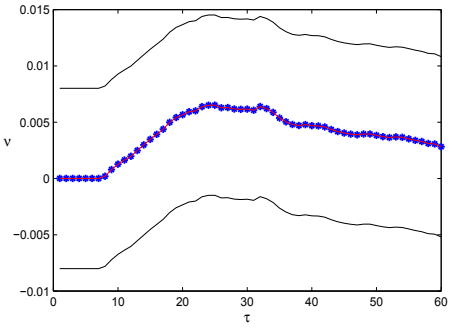

(d) Estimates of ν

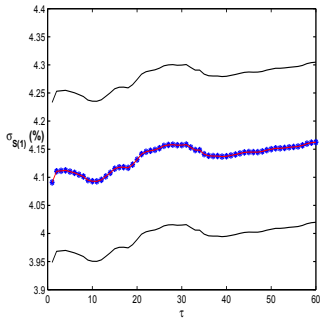

(e) Estimates of $\sigma_{S(1)}$

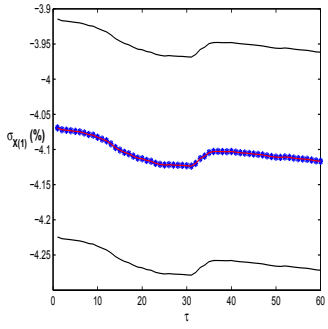

(f) Estimates of $\sigma_{X(1)}$

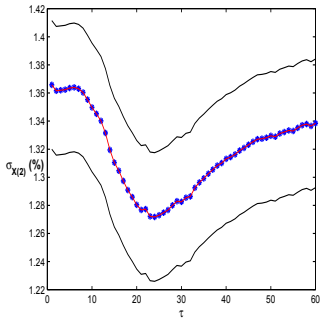

(g) Estimates of $\sigma_{X(2)}$

Figure 5.1: The estimates of (a) α; (b) ϕ; (c) $\bar{\mu}$; (d) ν; (e) $\sigma_{S(1)}$; (f) $\sigma_{X(1)}$ and (g) $\sigma_{X(2)}$ as functions of τ.

the price index series and the dividend series.

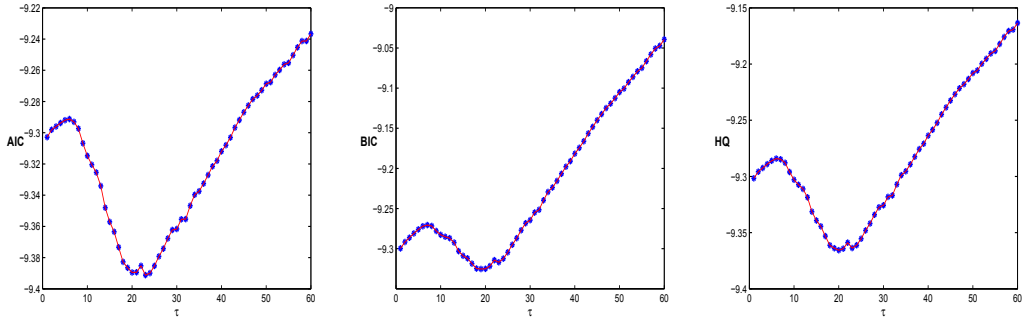

(a) AIC (b) BIC (c) HQ

Figure 5.2: (a) Akaike information criterion, (b) Bayesian information criterion and (c) Hannan–Quinn information criterion for $\tau \in [1, 60]$.

The estimated parameters in monthly terms are illustrated in Fig. 5.1 for τ ranging from 1 month to 5 years. As one of the key parameters of the model, Fig. 5.1 (b) shows that the momentum effect ϕ is statistically different from 0 for $\tau \geq 10$, indicating a significant momentum effect. Note that ϕ increases to 50% for $\tau \in [20, 30]$ and then decreases gradually when τ increases further. Other estimate results in terms of the level and significance in Fig. 5.1 are consistent with Koijen et al. (2009).

Obviously, the estimations depend on time horizon τ. To explore the optimal value for τ, we compare different information criteria for different τ, including AIC, BIC and HQ from 1 to 60 months in Fig. 5.2. AIC, BIC and HQ reach their minima at $\tau = 23, 19$ and 20 respectively, implying that the average returns over a past time period of 1.5—2 years can predict future return best. The increasing pattern of the criteria for longer τ indicates the return trend based on longer time horizon window has less explanatory power.

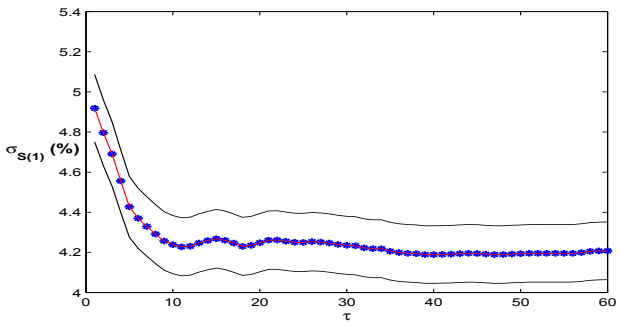

Figure 5.3: The estimates of $\sigma_{S(1)}$ for the pure momentum model ($\phi = 1$) for $\tau \in [1, 60]$.

To compare the performance of the optimal strategy, comparing with pure momentum

or mean-reverting strategies, we also estimate the index to the model with $\phi = 1$ and $\phi = 0$ respectively. For the pure momentum model ($\phi = 1$), Fig. 5.3 illustrates the estimates of $\sigma_{S(1)}$ for $\tau \in [1, 60]$. It shows that the volatility of the index decreases dramatically for small time horizons and becomes stable for large time horizons. It demonstrates that the past returns over up to one year can explain part of the return volatility but longer historical returns have less power in explaining return volatility. We also compare different information criteria for different τ. AIC, BIC and HQ all reach their minima at $\tau = 11$ (not reported here). It implies that the average returns over the past 11 months can predict future return best for the pure momentum model.

Parameters	α	$\bar{\mu}$	ν	$\sigma_{S(1)}$	$\sigma_{X(1)}$	$\sigma_{X(2)}$
Estimates (%)	0.55	0.37	$2.67 * 10^{-5}$	4.11	-4.07	1.36
Bounds (%)	(0.07, 1.03)	(0.31, 0.43)	(-0.46, 0.46)	(3.97, 4.25)	(-4.22, -3.92)	(1.32, 1.40)

Table 5.1: The estimates of the parameters for the pure mean reversion model.

Table 5.1 reports the estimated parameters for the pure mean reversion model ($\phi = 0$). The results are comparable to those for the full model illustrated in Fig. 5.1.

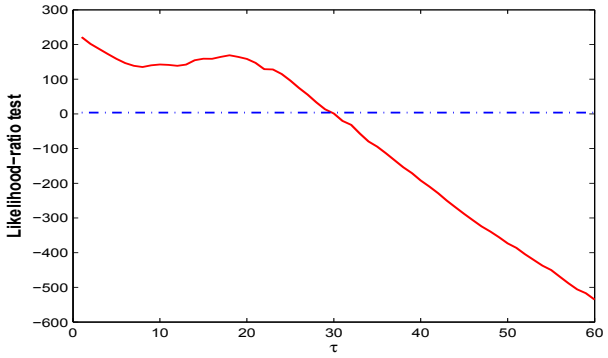

Figure 5.4: The log-likelihood ratio test for the pure mean-reversion model ($\phi = 0$) for $\tau \in [1, 60]$.

For comparison, we use a log-likelihood ratio test. We compare the full model (5.2)-(5.3) to the pure mean reversion model ($\phi = 0$) and Fig. 5.4 reports the log-likelihood ratio test with 95% confidence interval. It illustrates that the full model is significantly better than the pure mean reversion model for $\tau \leq 29$. This result is consistent with the literature that there is no momentum effect for large time horizon and the returns exhibit mean reversion in the long run. Therefore, we should not expect the full model with longer time horizons to fit the data better than the pure mean reversion model. We also compare the full model to the pure momentum model ($\phi = 1$) with respect to each τ and find that the full model is significantly better than the pure momentum model for

all τ (not reported here).

To avoid look ahead bias, we also estimate the models using rolling window data and report the results in Appendix D.3. In summary, we estimate the model to the index and show that the optimal strategy fits the data better with 1.5-2 year time horizons and also better than pure momentum and mean-reverting models. This observation is further supported by performance analysis in the following section.

5.4 Performance

Based on the estimation in the previous section, we examine the optimality of the optimal portfolio in this section. We first examine the performance of the optimal trading strategy (5.7) by using two proxies: the utility of portfolio wealth and the Sharpe ratio. Then we study the sensitivity of the performance of the optimal strategies to the market states, investor sentiment and market volatility. Finally, following the momentum and reversal literature, we implement some empirical analysis by focusing on the returns implied by the optimal strategy.

5.4.1 Performance of the Optimal Strategies

This subsection provides empirical evidence on the optimality of the trading strategy (5.7). We use two proxies to measure the performance of the optimal portfolio, the utility of the optimal portfolio wealth and the Sharpe ratio.

The Full Model

To measure the performance of the optimal strategy (5.7), we compare the realized utility of the optimal portfolio wealth invested in the S&P 500 index with different look-back period τ and 1-month holding period to the utility of a passive holding investment in the S&P 500 index with an initial wealth of \$1. We consider the look-back period τ from 1 month to 60 months and invest monthly. For comparison, all the portfolios start at the end of January 1876, (after 60 months of January 1871 to calculate the trading signals). As the benchmark, the log utility of an investment of \$1 to the index from January 1876 to December 2012 is equal to 5.7649. For a fixed look-back period $\tau \in \{1, 2, \cdots, 60\}$, say, $\tau = 12$, we calculate the moving average m_t at any point of time (in month) from January 1876 to December 2012 using the index levels over the time period. With the initial wealth of \$1 at January 1876 and the estimated parameters for $\tau = 12$ in Fig. 5.1, we calculate the monthly investment of the optimal portfolio wealth W_t based on (5.7).

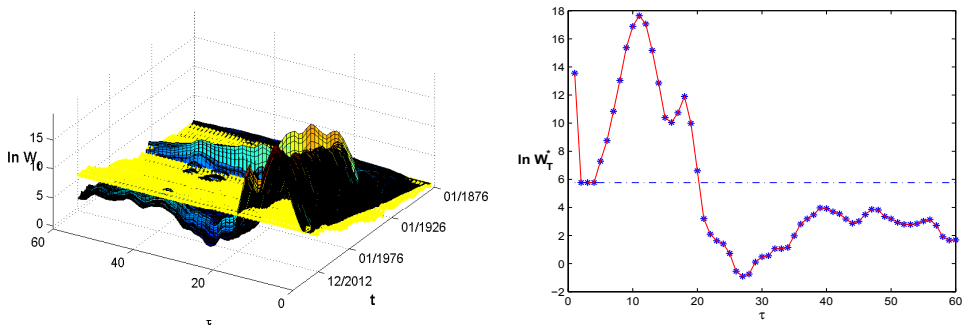

(a) Series of utility (b) Terminal utility

Figure 5.5: The utility of wealth from January 1876 until December 2012 for the optimal portfolio with $\tau \in [1, 60]$ and the passive holding portfolio.

For $\tau = 1, 2, \cdots, 60$, Fig. 5.5 (a) illustrates the utility of the portfolio wealth from January 1876 until December 2012 for the optimal portfolio with $\tau \in [1, 60]$ and the passive holding portfolio. For better visibility, we also plot the utility of terminal wealth in Fig. 5.5 (b). Both of them show that the optimal strategies outperform the market index at the end of investment period for $\tau \in [1, 20]$.

Moskowitz et al. (2012) document the momentum strategy based on 12-month horizon performs the best. So we examine the performance for $\tau = 12$ closely. Fig. 5.6 illustrates the time series of the optimal portfolio and the utility of wealth from January 1876 until December 2012 for $\tau = 12$. We also plot the corresponding index level and simple return of the total return index of S&P 500 in Fig. 5.6 (a) and (b) over the same time period. It shows that the index return and π_t^* are positively correlated, with a correlation of 0.3346. However, the correlations become 0.3498 and 0.1349 for $\tau = 11$ and $\tau = 27$, at which the terminal utility has its maximum and minimum respectively as illustrated in Fig. 5.5. From Fig. 5.6 (d), it seems that the profits are mainly contributed by the Great Depression in 1930s. Moskowitz et al. (2012) also find that the time series momentum strategy delivers its highest profits during the most extreme market episodes. We also study the performance using the data from January 1940 to December 2012 to avoid the Great Depression periods. Based on the new estimation (not reported here), we find that the optimal strategies still outperform the market and the performances of the strategies for the recent time period become even better for all time horizons. This indicates that the optimal strategy can outperform the market independent of market condition.

To provide further evidence, we conduct a Monte Carlo analysis. For $\tau = 12$, with the corresponding estimated parameters in Fig. 5.1, we simulate the model (5.10). Fig. 5.7 (a) illustrates the average portfolio utility based on 1,000 simulations, together with 95%

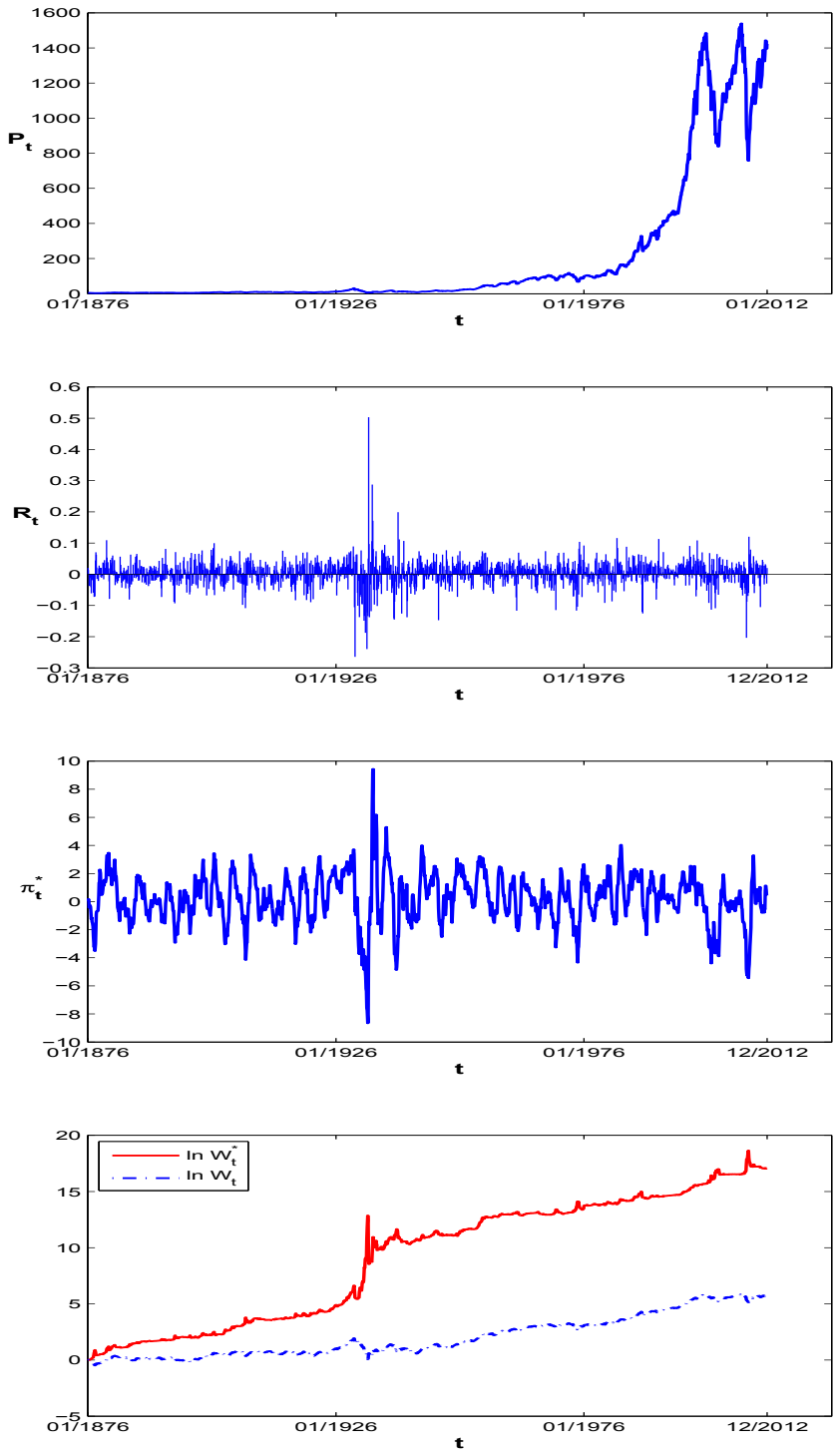

Figure 5.6: The time series of (a) the total return index level and (b) the simple return of the total return index of S&P 500; (c) the optimal portfolio and (d) the utility of wealth from January 1876 until December 2012 for $\tau = 12$.

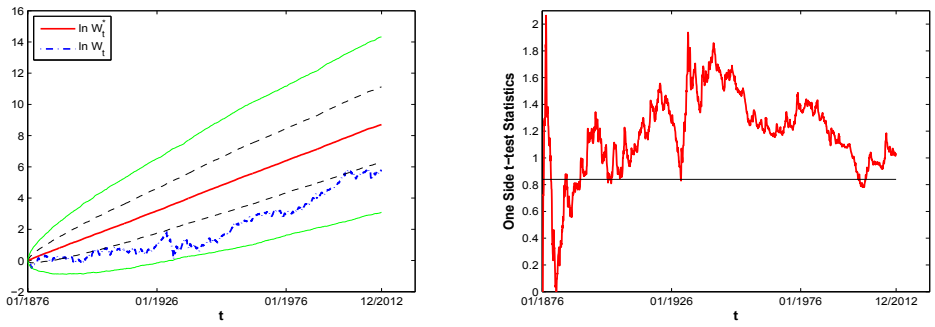

(a) Average utility (b) One sided t statistics

Figure 5.7: (a) average utility and (b) one sided t-test statistics based on 1000 simulations for $\tau = 12$.

confidence levels. It shows that first, the average performance of the optimal portfolio is better than S&P 500's. Secondly, the utility for the S&P 500 falls into the area and hence the average performance of the optimal strategy is indifferent from the market index. We also plot the two black dashed bounds for the 60% confidence level. It shows that, at 60% confidence level, the optimal strategy significantly outperforms the index. Fig. 5.7 (b) illustrates the one sided t-test statistics to test $\ln W_t^* > \ln W_t^{SP500}$. The t-statistics are above 0.84 in most of the time, which indicates a critical value at 80% confidence level Therefore, with 80% confidence, the optimal strategy significantly outperforms the index.

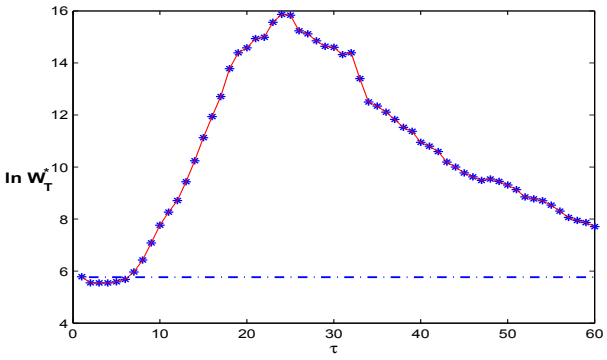

Figure 5.8: Average terminal utility based on 1000 simulations for $\tau \in [1, 60]$.

For $\tau \in [1, 60]$, Fig. 5.8 illustrates the average terminal utility based on 1,000 simulations, which displays a different terminal performance from Fig. 5.5. In fact, the terminal utility in Fig. 5.5 is based on only one specific trajectory (the real stock index), but Fig. 5.8 provides average performance based on 1,000 trajectories. We can see that the average terminal utility reaches its peak at $\tau = 24$, which is consistent with the result

based on the information criteria in Fig. 5.2, especially the AIC. Therefore, we show that the simulated average terminal utility is a better proxy characterizing the utility of the portfolio wealth. According to this proxy, the optimal strategies outperform the market for most of the time horizons τ.

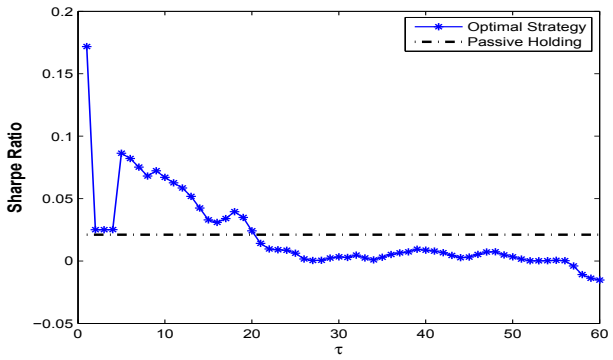

Figure 5.9: The Sharpe ratio for the optimal portfolio with $\tau \in [1, 60]$ and the passive holding portfolio from January 1881 until December 2012.

We also use Sharpe ratio to test the performance, which is defined as the ratio of the mean excess return on the (managed) portfolio and the standard deviation of the portfolio return. If a strategy's Sharpe ratio exceeds the market Sharpe ratio, the active portfolio dominates the market portfolio (in an unconditional mean-variance sense). For empirical applications, the (ex post) Sharpe ratio is usually estimated as the ratio of the sample mean of the excess return on the portfolio and the sample standard deviation of the portfolio return. The average monthly return on the total return index of the S&P 500 over the period January 1871–December 2012 is 0.42% with an estimated (unconditional) standard deviation of 4.11%. The Sharpe ratio of the market index is 0.021.

Next, we consider the optimal strategies (5.7). The return of the optimal portfolio wealth at time t is given by

$$R_t^* = (W_t^* - W_{t-1}^*)/W_{t-1}^* = \pi_{t-1}^* R_t + (1 - \pi_{t-1}^*)r. \tag{5.12}$$

Fig. 5.9 illustrates the Sharpe ratio for the optimal portfolio with $\tau \in [1, 60]$ and compares to the passive holding portfolio from January 1881 until December 2012. If we consider the optimal portfolio as a combination of the market portfolio and a risk free asset, then the optimal portfolio is on the capital market line and hence it should have equally good performance as the market according to the Sharpe criterion. However Fig. 5.9 demonstrates that the optimal portfolio (blue line) outperforms the market (black line) on average for small time horizon by taking the timing opportunity. Interestingly, the

results are perfectly consistent with the measure of terminal utility illustrated in Fig. 5.5.[4] In conclusion, we have shown that the optimal strategies outperform the market index.

The Pure Momentum Model

We now examine the performance of the pure momentum strategy and compare with the market index.

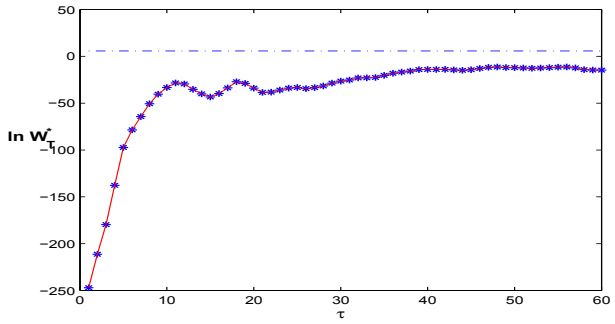

Figure 5.10: The utility of terminal wealth for $\tau \in [1, 60]$.

Based on the estimated parameters in Fig. 5.3, Fig. 5.10 illustrates the utilities of all the optimal portfolios for the pure momentum model ($\phi = 1$) at December 2012. It shows that the pure momentum strategies underperforms the index with all the time horizons from 1 to 60 months.

Fig. 5.11 illustrates the time series of the optimal portfolio and the utility of wealth from January 1876 until December 2012 for $\tau = 12$ for the pure momentum model. By comparing to Fig. 5.6 for the full model, the leverage of the pure momentum strategies is much higher indicated by the higher level of π_t^*. The optimal strategies for the pure momentum model suffer from high risk and hence perform worse than the optimal strategies for the full model. Therefore, the pure momentum strategy underperforms the market and the optimal strategy.

[4] This result is different from Marquering and Verbeek (2004) who argue that Sharpe ratio performance and the utility-based performance can be inconsistent because "*Sharpe ratio does not appropriately take into account time-varying volatility.*" However, if and when Sharpe ratio is a good measure is not the focus of this chapter.

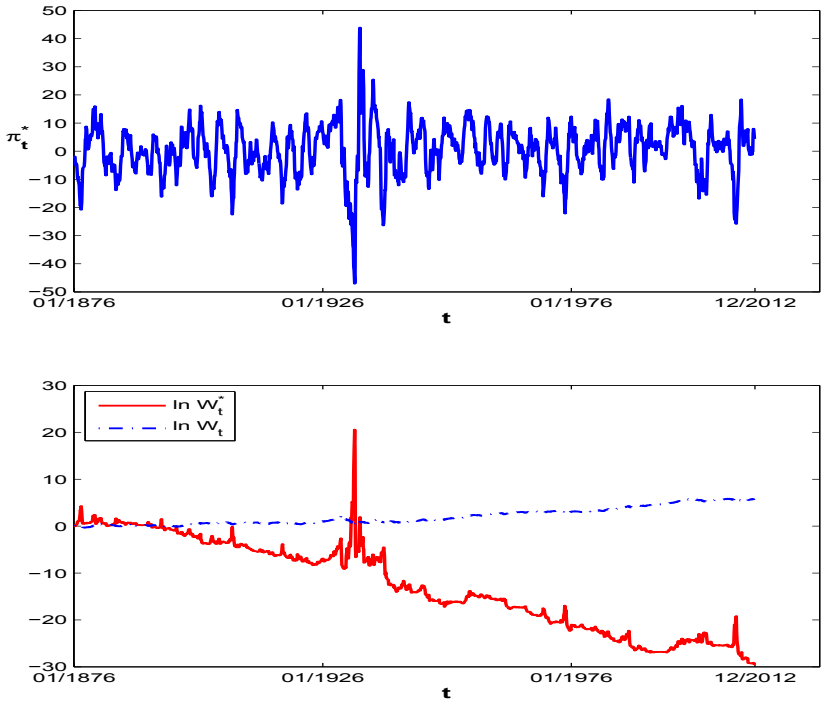

Figure 5.11: The time series of (a) the optimal portfolio and (b) the utility of wealth from January 1876 until December 2012 for $\tau = 12$ for the pure momentum model.

The Pure Mean Reversion Model

Similarly, we examine the performance of the pure mean reversion model and compare it with the market index.

Based on the estimates in Table 5.1, Fig. 5.12 illustrates the time series of the optimal portfolio and the utility of wealth from January 1876 until December 2012 for the pure mean reversion model. The performance of the strategy is about the same as the stock index, but worse than the optimal strategy (5.7) for the full model illustrated in Fig. 5.5.

Out of Sample Tests

In this subsection, we implement some out of sample tests to the optimal strategies by splitting the whole data set into two sub-sample periods. We use the first sample period to estimate the model and then apply the estimated parameters to the second part of the data to examine the performance of the strategies.

Many studies (see, for example, Jegadeesh and Titman 2011) show that (cross-sectional) momentum strategies perform poorly after the subprime crisis. We now fo-

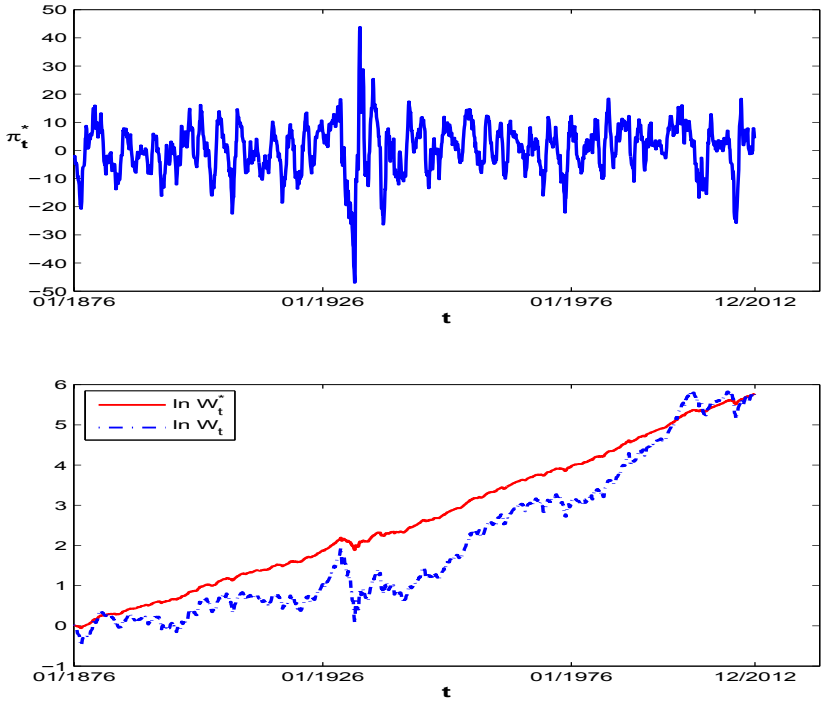

Figure 5.12: The time series of (a) the optimal portfolio and (b) the utility of wealth from January 1876 until December 2012 for the pure mean reversion model.

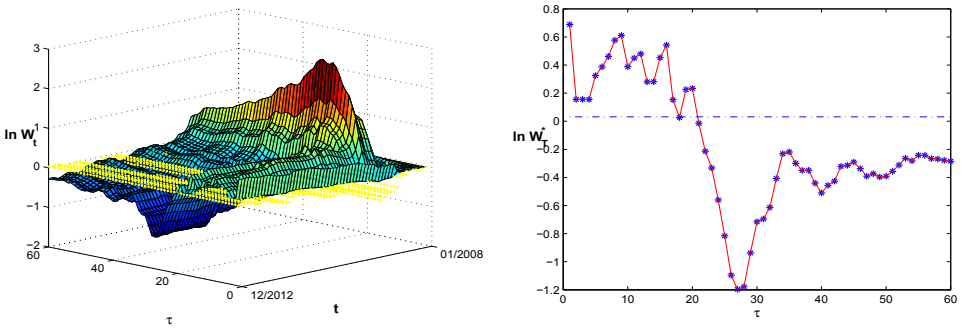

(a) Series of utility (b) Terminal utility

Figure 5.13: The utility of wealth from January 2008 until December 2012 for the optimal portfolio with $\tau \in [1, 60]$ and the passive holding portfolio with out of sample data of the last 5 years.

cus on the performance of the optimal strategies after the subprime crisis and use the last 5 years' data to test the performance. Fig. 5.13 illustrates the utility of wealth for $\tau \in [1, 60]$ for the out of sample tests based on the last 5 years. It clearly shows that the optimal strategies still outperform the market for time horizons up to 2 years.

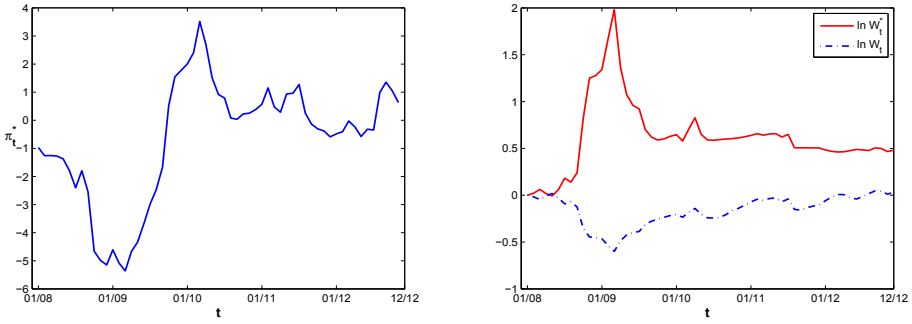

Figure 5.14: The time series of (a) the optimal portfolio and (b) the utility of wealth from January 2008 until December 2012 for $\tau = 12$ with out of sample data of last 5 years.

To better understand the performance of the out of sample tests, we fix the time horizon $\tau = 12$ and examine the time series of the optimal portfolio and the utility of the portfolio wealth from January 2008 until December 2012 in Fig. 5.14. It is clear that the optimal strategy outperforms the market over the who sub-sample period, in particular, during the financial crisis period around 2009.

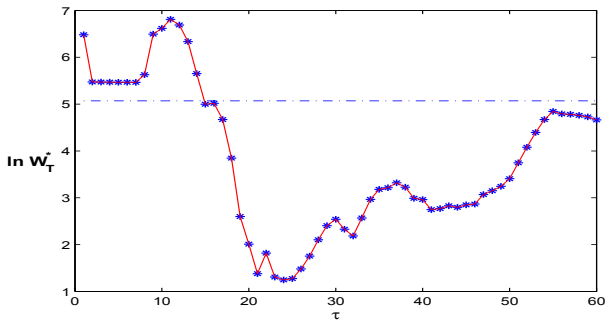

Figure 5.15: The utility of terminal wealth for $\tau \in [1, 60]$ based on the out of sample period of the last 71 years.

As another out of sample test, we split the whole data set into two equal periods: January 1871-December 1941 and January 1942-December 2012. We estimate the model to the first sub-sample period and do the out of sample test over the second sub-sample period. Notice the data in the two periods are quite different. The market index increases gradually in the first period but fluctuates widely in the second period as illustrated in

Fig. 5.6 (a). For the out of sample test, Fig. 5.15 illustrates the utility of terminal wealth for $\tau \in [1, 60]$ using sample data of the last 71 years. It becomes clear that the optimal strategy still outperforms the market for $\tau \in [1, 14]$.

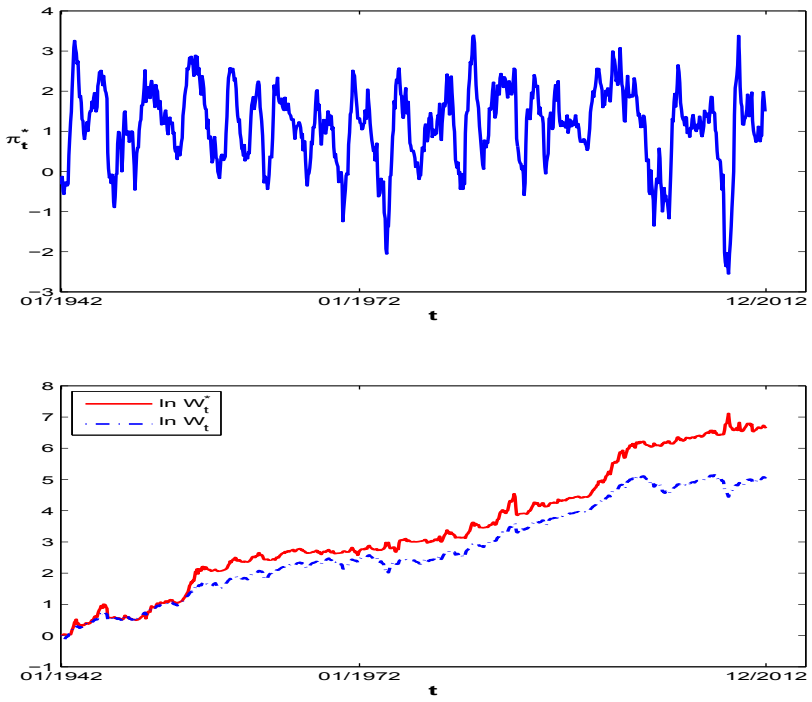

Figure 5.16: The time series of (a) the optimal portfolio and (b) the utility of wealth from January 1942 until December 2012 for $\tau = 12$ for the out of sample tests with out of sample data of last 71 years.

With fixed $\tau = 12$, Fig. 5.16 illustrates the corresponding time series of the optimal portfolio and the utility of the portfolio wealth by conducting the out of sample test from January 1942 until December 2012. It shows that the utility of the optimal strategy grows gradually and outperforms the market index. We also use the last 10 years and 20 years data as the out of sample data and find the results are robust.

We also conduct the performance analysis based upon rolling window estimation and report the results in Appendix D.3. The results are consistent with the main findings above. Overall, the analyses have demonstrated the optimality of the optimal trading strategy based on a large range of time horizons, in particular, we demonstrate the outperformance based on 12 month time horizon.

5.4.2 Market States, Sentiment and Volatility

In addition to the time horizon, the cross-sectional momentum literature has shown that the momentum profitability is also sensitive to market states, investor sentiment and market volatility. For example, Cooper et al. (2004) find that short-run (6 months) momentum strategies make profits in the up market and lose in the down market, but the up-market momentum profits reverse in the long-run (13-60 months). Hou et al. (2009) find momentum strategies with short time horizon (1 year) are not profitable in "down" market, but profitable in "up" market. Similar results of profitability are also reported in Chordia and Shivakumar (2002) that commonly using macroeconomic instruments related to the business cycle can generate positive returns to momentum strategies during expansionary periods and negative returns during recessions. Baker and Wurgler (2006, 2007) find that investment sentiment affects the cross-section stock returns and the aggregate stock market. Wang and Xu (2012) find that market volatility has significant power to forecast momentum profitability. For the time series momentum, however, Moskowitz et al. (2012) find that there is no significant relationship of the time series momentum profitability with either market volatility or investor sentiment.

We are interested in the dependence of the performance of the optimal strategy on market states, investor sentiment and market volatility. We regress the excess return of different strategies, including the optimal strategies for the full model, the pure momentum model and the pure mean reversion model and the time series momentum strategy, on different proxies for the market states, investor sentiment and market volatility. The regression results are reported in Appendix D.4. Overall, we find that the coefficients for all the regressions are insignificantly different from 0. In fact, the optimal strategies have optimally taken these factors into account and hence the returns of the optimal strategies have no significant relationship with these factors. Therefore, the optimal strategies are immune to the market states, investor sentiment and market volatility.

5.4.3 Comparison with Moskowitz, Ooi and Pedersen (2012)

The momentum strategies in the empirical studies are based on trading signals. In this section, we implement analysis following the empirical momentum literature, especially Moskowitz et al. (2012). First, to verify the profitability of the time series momentum strategy, we examine the excess return of buy-and-hold strategies when the position is determined by the sign of the optimal portfolio strategy (5.7) with different combinations of time horizons and holding periods (τ, h).

$(\tau \setminus h)$	1	3	6	9	12	24	36	48	60
1	0.1337	0.1387	0.1874*	0.1573*	0.0998	0.0222	0.0328	0.0479	0.0362
	(1.28)	(1.84)	(3.29)	(2.83)	(1.84)	(0.42)	(0.63)	(0.90)	(0.66)
3	0.0972	0.0972	0.0972	0.0972	0.0972	0.0972	0.0972	0.0972	0.0972
	(0.93)	(0.93)	(0.93)	(0.93)	(0.93)	(0.93)	(0.93)	(0.93)	(0.93)
6	0.2022	0.2173*	0.2315*	0.1462	0.0700	-0.0414	0.0199	0.0304	0.0014
	(1.93)	(2.28)	(2.60)	(1.75)	(0.88)	(-0.58)	(0.32)	(0.53)	(0.02)
9	0.3413*	0.3067*	0.2106*	0.1242	0.0333	-0.0777	-0.0095	0.0000	-0.0450
	(3.27)	(3.12)	(2.28)	(1.45)	(0.41)	(-1.16)	(-0.17)	(0.00)	(-1.11)
12	0.1941	0.1369	0.0756	-0.0041	-0.0647	-0.0931	-0.0234	-0.0137	-0.0587
	(1.85)	(1.40)	(0.80)	(-0.04)	(-0.76)	(-1.30)	(-0.41)	(-0.30)	(-1.46)
24	-0.0029	-0.0513	-0.0776	-0.0591	-0.0557	-0.0271	0.0261	-0.0020	-0.0082
	(-0.03)	(-0.51)	(-0.79)	(-0.62)	(-0.61)	(-0.34)	(0.40)	(-0.03)	(-0.15)
36	0.0369	0.0602	0.0517	0.0419	0.0416	0.0657	0.0351	0.0273	0.0406
	(0.35)	(0.59)	(0.52)	(0.43)	(0.44)	(0.81)	(0.49)	(0.42)	(0.64)
48	0.1819	0.1307	0.1035	0.0895	0.0407	-0.0172	0.0179	0.0500	0.0595
	(1.74)	(1.30)	(1.06)	(0.93)	(0.43)	(-0.21)	(0.24)	(0.70)	(0.86)
60	-0.0049	-0.0263	-0.0800	-0.1160	-0.1289	-0.0396	0.0424	0.0518	0.0680
	(-0.05)	(-0.26)	(-0.81)	(-1.20)	(-1.41)	(-0.49)	(0.55)	(0.69)	(0.92)

Table 5.2: The average excess return (%) of the optimal strategy for different look back period τ (different row) and different holding period h (different column).

Based on the index, for a given look-back period τ, we take long/short positions based on the sign of the optimal portfolio (5.7). Then for a given holding period h, we calculate the monthly excess return of the strategy (τ, h). Table 5.2 reports the average monthly excess return (in %) of the optimal strategy by skipping one month between the portfolio formation period and holding period to avoid the 1-month reversal in stock returns for different look back period (in the first column) and different holding period (in the first row). The average return is calculated using the same method as in Moskowitz et al. (2012). To calculate the momentum component and evaluate the profitability of holding period, we calculate the excess return of the optimal strategy over the period from January 1881 (10 years after January 1871 with 5 years for calculating the trading signals and 5 years for holding periods) to December 2012.

For comparison, Tables 5.3 reports the average return (%) for the optimal strategies for the pure momentum model.[5] Notice that Tables 5.2 and 5.3 indicate that the $(9, 1)$ strategy performs the best.[6] Note that the results are inconsistent with the results in the previous subsections using the processes of utility of wealth as a measure of performance. This is because the optimal strategy not only explores the return signal but also takes the

[5]Notice the position is completely determined by the sign of the optimal strategies. Therefore, the position used in Table 5.3 is the same as that of the time series momentum strategies in Moskowitz et al. (2012).

[6]This is consistent with the finding in Moskowitz et al. (2012), which documents $(9, 1)$ is the best strategy for equity market although 12-month horizon is the best for most asset classes.

$(\tau \setminus h)$	1	3	6	9	12	24	36	48	60
1	-0.0144	0.0652	0.0714	0.0689	0.0568	-0.0040	0.0006	0.0010	-0.0133
	(-0.14)	(0.89)	(1.34)	(1.52)	(1.37)	(-0.12)	(0.02)	(0.04)	(-0.57)
3	0.1683	0.1915*	0.1460	0.1536*	0.0764	-0.0360	-0.0290	-0.0143	-0.0395
	(1.61)	(2.16)	(1.91)	(2.20)	(1.17)	(-0.69)	(-0.72)	(-0.45)	(-1.38)
6	0.2906*	0.2633*	0.2635*	0.1884*	0.1031	-0.0484	-0.0130	0.0157	-0.0281
	(2.78)	(2.79)	(3.01)	(2.29)	(1.34)	(-0.75)	(-0.26)	(0.40)	(-0.77)
9	0.4075*	0.3779*	0.2422*	0.1538	0.0545	-0.0735	-0.0217	-0.0047	-0.0460
	(3.91)	(3.78)	(2.62)	(1.76)	(0.66)	(-1.05)	(-0.38)	(-0.10)	(-1.12)
12	0.2453*	0.1660	0.0904	0.0122	-0.0748	-0.1195	-0.0602	-0.0454	-0.0798
	(2.35)	(1.67)	(0.94)	(0.13)	(-0.86)	(-1.63)	(-1.02)	(-0.95)	(-1.88)
24	0.0092	-0.0242	-0.0800	-0.0962	-0.0955	-0.0682	-0.0081	-0.0140	-0.0211
	(0.09)	(-0.24)	(-0.81)	(-1.03)	(-1.06)	(-0.88)	(-0.13)	(-0.24)	(-0.39)
36	-0.0005	0.0194	0.0219	0.0212	0.0113	0.0030	0.0127	0.0241	0.0206
	(-0.01)	(0.19)	(0.23)	(0.22)	(0.12)	(0.04)	(0.18)	(0.37)	(0.33)
48	0.0779	0.0733	0.0231	0.0019	-0.0392	-0.0676	-0.0004	0.0435	0.0382
	(0.74)	(0.73)	(0.24)	(0.02)	(-0.42)	(-0.83)	(-0.01)	(0.61)	(0.55)
60	-0.0568	-0.0852	-0.1403	-0.1706	-0.1986	-0.1091	-0.0043	0.0157	0.0239
	(-0.54)	(-0.84)	(-1.41)	(-1.77)	(-2.15)	(-1.36)	(-0.06)	(0.22)	(0.34)

Table 5.3: The average excess return (%) of the optimal strategy for different look back period τ (different row) and different holding period h (different column) for the pure momentum model.

volatility into account.[7] Therefore, we argue that the profitability pattern characterized by the average returns (or excess returns) used by most of the empirical momentum literature may not be reflected at portfolio wealth level. This conclusion is also confirmed by comparing with Fig. 5.9. In fact, the Sharpe ratio in Fig. 5.9 characterizes both the return and risk. We can see that Fig. 5.9 has a similar profitability pattern to Table 5.2, especially the first column, but different from Fig. 5.8 for the average terminal utility of wealth.

We also study the average Sharpe ratio for the time series momentum strategy (green line) documented empirically for different time horizons and the strategy (momentum & mean reversion) (red dotted line) which is similar to the time series momentum strategy except that we use the sign of the optimal strategy $sign(\pi_t^*)$ as the trading signal instead of the average excess return over a past period for the time series momentum strategy. For comparison, we also plot the Sharpe ratio for the optimal portfolio and the passive holding portfolio illustrated in Fig. 5.9. Fig. 5.17 shows the average Sharpe ratio for the above four strategies with $\tau \in [1, 60]$ from January 1881 until December 2012. There are three observations from Fig. 5.17. First, the time series momentum strategy outperforms the market for short time horizons and the momentum and mean reversion strategy outperforms the market for both short and long time horizons. This is mainly

[7] In fact, Wang and Xu (2012) find that market volatility has significant power to forecast momentum profitability.

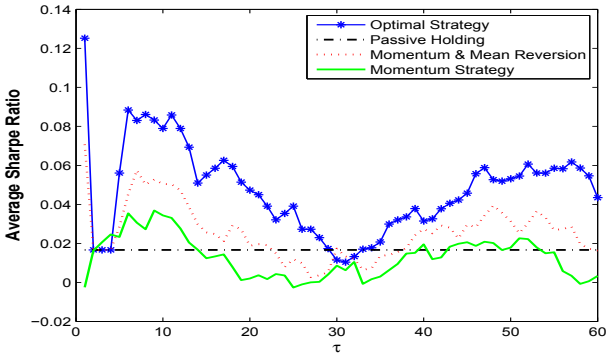

Figure 5.17: The average Sharpe ratio for the optimal portfolio, the momentum and mean reversion portfolio and the time series momentum portfolio with $\tau \in [1, 60]$ and the passive holding portfolio from January 1881 until December 2012.

due to the short run momentum and long run reversal effects. The second observation is that, by taking the mean reversion effect into account, the momentum and mean reversion strategy performs slightly better than the time series momentum strategy. Finally, the optimal strategy significantly outperforms both the momentum and mean reversion strategy and the time series momentum strategy. Notice the only difference between the optimal strategies and the momentum and mean reversion strategy is that the former considers the size of the portfolio position, while the latter only takes one unit position. This implies that, in addition to price trend, volatility is another very important factor for the timing opportunity.

Following Eq. (5) in Moskowitz et al. (2012), we study the performance of the cumulative excess return. That is, the return at time t is given by

$$\hat{R}_{t+1} = sign(\pi_t^*) \frac{0.1424}{\hat{\sigma}_{S,t}} R_{t+1}, \tag{5.13}$$

where 0.1424 is the sample standard deviation of the total return index. Following Moskowitz et al. (2012), the ex ante annualized variance $\hat{\sigma}_{S,t}^2$ for the total return index is calculated as the exponentially weighted lagged squared month returns as before

$$\hat{\sigma}_{S,t}^2 = 12 \sum_{i=0}^{\infty} (1-\delta)\delta^i (R_{t-1-i} - \bar{R}_t)^2. \tag{5.14}$$

To ensure no look ahead bias contaminates the results, we use the volatility estimates at time $t-1$ applied to time t returns throughout the analysis.

Fig. 5.18 illustrates the terminal values of the log cumulative excess return of the optimal strategy (5.7) and time series momentum strategy with $\tau \in [1, 60]$ and the passive

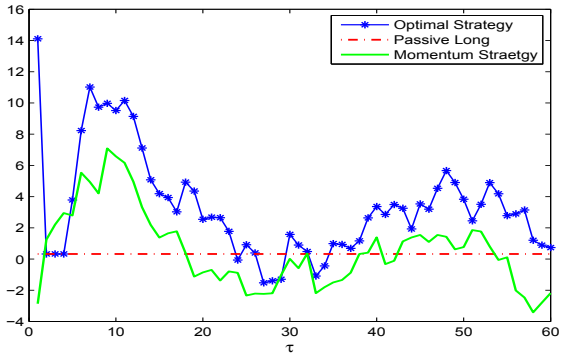

Figure 5.18: Terminal log cumulative excess return of the optimal strategy (5.7) and time series momentum strategy with $\tau \in [1, 60]$ and passive long strategy from January 1876 until December 2012.

long strategy from January 1876 until December 2012.[8] It illustrates that the optimal strategies outperform the time series momentum strategies. The time series momentum strategies outperform the market for small time horizons. The terminal values of the log cumulative excess return have similar patterns as the average Sharpe ratio in Fig. 5.17.

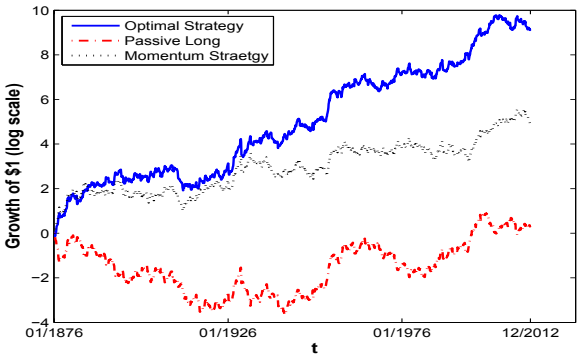

Figure 5.19: Log cumulative excess return of the optimal strategy (5.7) and momentum strategy with $\tau = 12$ and passive long strategy from January 1876 until December 2012.

With a 12 month time horizon, Fig. 5.19 illustrates the log cumulative excess return of the optimal strategy (5.7) and momentum strategy and the passive long strategy from January 1876 until December 2012. It shows that, first, the optimal strategy has the highest growth rate and the passive long strategy has the lowest growth rate. Secondly, we can replicate the pattern in Fig. 3 of Moskowitz et al. (2012), which documents that the time series momentum strategy outperforms the passive long strategy. Notice the time series momentum strategy documented in Fig. 5.19 should have the same performance

[8] Notice the passive long strategy introduced in Moskowitz et al. (2012) is different from the passive holding strategy studied in previous sections. Passive long means holding one share of the index each period, however, passive holding in this chapter means investing $1 in the index in the first period and holding it until the last period.

as the optimal strategy for the pure momentum model if we only consider the sign of the average excess return over the past period in (5.13). However, we have documented in the previous subsections that the optimal strategy for the pure momentum model performs badly if we also take the volatility into account. Therefore, we argue that the momentum strategies documented empirically may not work when the performance is measure at portfolio wealth level. In fact, the profits of the diversified TSMOM portfolio in Moskowitz et al. (2012) are mainly contributed by the bonds when scaling for the volatility in equation (5).

To conclude this section, by comparing the results for the optimal strategies and the time series momentum strategy in Moskowitz et al. (2012), we find that the trend is important. To explore it, the buy/sell signal (based on π_t^*) is more important than the size of the portfolio. Also, this chapter studies the S&P 500 index over 140 years of data, while Moskowitz et al. (2012) focus on the futures and forward contracts that include country equity indexes, currencies, commodities, and sovereign bonds. Despite a large difference between the data investigated, we find similar patterns for the time series momentum in the stock index and replicate their results with respect to the stock index.

5.5 Conclusion

To characterize the short-run momentum and long-run mean reversion in financial markets, we propose a continuous time model of asset price process with the drift as a weighted average of mean reversion and moving average components to explore the momentum and reversal effects. By applying the maximum principle for control problem of SDDE, we derive the optimal strategies analytically. We show the optimality of the optimal strategy comparing to pure momentum, pure mean reversion strategies, and market index. The optimality is immune to the market states, investor sentiment and market volatility. The profitability pattern reflected by the average return in most empirical literature may not be reflected at portfolio wealth level.

The model proposed in this chapter is simple and stylized. The weights to the momentum and mean reversion components are constant. When market conditions change, the weights can be different. Hence it would be interesting to model their dependence on market conditions. This can be modelled, for example, based on the replicator dynamics introduced in Chapter 2, or as a Markov switching process, or based on some rational learning process. The optimization problem is solved under log utility in this chapter, which avoids the intertemporal effect under general power utility functions which is con-

sidered in Koijen et al. (2009). Furthermore, we can consider stochastic volatilities of the index process. Finally, an extension to a multi-asset model to study the cross-sectional optimal strategies would be helpful to understand the cross sectional momentum.

Chapter 6

An Evolutionary CAPM under Heterogeneous Beliefs

6.1 Introduction

Most theoretical models on conditional CAPM are based on the representative agent economy by assuming perfect rationality and homogeneous beliefs. However, empirical evidence along with unconvincing justification of the assumption of unbounded rationality and investor psychology, have led to the incorporation of both heterogeneity in beliefs and bounded rationality into asset pricing and financial market modelling, see the surveys of the recent developments in the HAMs literature: Hommes (2006), LeBaron (2006), Lux (2009) and Chiarella et al. (2009). However, most of the HAMs analyzed in the literature involve a financial market with only one risky asset and are not in the context of the CAPM. Recently, some attempts have been made to develop HAMs with many assets.[1] Within a mean-variance framework, Chiarella et al. (2010, 2011) study a multi-asset CAPM through a consensus belief. In a dynamic setting, Chiarella et al. (2013) demonstrate the stochastic behavior of time-varying betas and show that there can be inconsistency between ex-ante and ex-post estimates of asset betas when agents are heterogeneous and boundedly rational.

The aim of this chapter is to extend the models described in the previous chapters with one risky asset to an evolutionary CAPM within the framework of HAMs to examine the

[1] We refer readers to Chiarella et al (2005), Westerhoff and Dieci (2006), Chen and Huang (2008) and Marsili, Raffaelli and Ponsot (2009) for developments in multi-asset market dynamics in the literature of HAMs. In particular, Westerhoff (2004) considers a multi-asset model with fundamentalists who concentrate on only one market and trend followers who invest in all markets; Dieci and Westerhoff (2010, 2012) explore deterministic models to study two stock markets denominated in different currencies, which are linked via the related foreign exchange market; Chen and Huang (2008) develop a computational multi-asset artificial stock market to examine the relevance of risk preferences and forcasting accuracy to the survival of investors; and Marsili et al. (2009) introduce a generic model of a multi-asset financial market to show that correlation feedback can lead to market instability when trading volumes are high.

impact of adaptive behavior of heterogeneous agents in a market with many risky assets. This chapter is closely related to Chiarella et al. (2013), but also differs from it in several respects. In Chiarella et al. (2013), the heterogeneous beliefs are modelled at the return level and agents do not change their strategies. A spill-over effect of market instability from one asset to others due to behavior change of agents is demonstrated through numerical simulations. In this chapter, the heterogeneous beliefs are modelled at the price level and agents are allowed to change their strategies based on a fitness function similar to that used by Brock and Hommes (1997 and 1998). The advantage of this setting is that we are able to examine the stability and spill-over effects analytically. We extend the single-period static model in Chiarella et al. (2010) to a dynamic equilibrium asset pricing model. As in Chiarella et al. (2013), we incorporate two types of investors, fundamentalists and trend followers, into the model. It is found that the instability of one asset, characterized by large fluctuations of market prices from the fundamental prices, can spill over to other assets when agents increasingly switch to better performing strategies. The spill-over effect is also associated with high trading volumes and persistent volatility, characterized by significantly positive and geometrically decaying autocorrelations in volume and volatility over long time horizons. Also the correlations between trading volume and volatility of risky assets are positive when asset payoffs are less correlated. These implications show that the evolutionary CAPM developed in this chapter can provide insight into market characteristics related to trading volume and volatility. Also consistent with Chiarella et al. (2013), we show that the commonly used rolling window estimates of time-varying betas may not be consistent with the ex-ante betas implied by the equilibrium model.

The chapter is based on Chiarella, Dieci, He and Li (2013) and organized as follows. Section 6.2 sets up a dynamical equilibrium asset pricing model in the context of the CAPM to incorporate heterogeneous beliefs and adaptive behavior of agents. Section 6.3 examines analytically the stability of the steady state equilibrium prices of the corresponding deterministic model. In Section 6.4, we conduct a numerical analysis of the stochastic model to explore the spill-over effects, together with the relation between trading volumes and volatility, and the consistency of time-varying betas between ex-ante and rolling window estimates. Section 6.5 concludes. All proofs are given in Appendix E.

6.2 The Model

We consider an economy with I agents, indexed by $i = 1, \cdots, I$, who invest in portfolios consisting of a riskless asset with risk free rate r_f and N risky assets, indexed by $j =$

$1, \cdots, N$ (with $N \geq 1$). Let $\mathbf{p}_t = (p_{1,t}, \cdots, p_{N,t})^\top$ be the prices, $\mathbf{d}_t = (d_{1,t}, \cdots, d_{N,t})^\top$ be the dividends and $\mathbf{x}_t := \mathbf{p}_t + \mathbf{d}_t$ be the payoffs of the risky assets in period t (from $t-1$ to t). Let $\mathbf{z}_{i,t}$ be the risky portfolio of agent i (in terms of the number of shares of each risky asset), then the end-of-period portfolio wealth of agent i is given by $W_{i,t+1} = \mathbf{z}_{i,t}^\top(\mathbf{x}_{t+1} - R_f\mathbf{p}_t) + R_f W_{i,t}$, where $R_f = 1 + r_f$.

Optimal Portfolio

Assume that agent i has a constant absolute risk aversion (CARA) utility $u_i(x) = -e^{-\theta_i x}$, where θ_i is the CARA coefficient. Assuming that the wealth of agent i is conditionally normally distributed, agent i's optimal investment portfolio is obtained by maximizing the certainty-equivalent utility of one-period-ahead wealth[2]

$$U_{i,t}(W_{i,t+1}) = E_{i,t}(W_{i,t+1}) - \frac{\theta_i}{2} Var_{i,t}(W_{i,t+1}). \tag{6.1}$$

Following Chiarella et al. (2010), the optimal portfolio of agent i at time t for time period $t+1$ is then given by

$$\mathbf{z}_{i,t} = \theta_i^{-1}\mathbf{\Omega}_{i,t}^{-1}[E_{i,t}(\mathbf{x}_{t+1}) - R_f\mathbf{p}_t], \tag{6.2}$$

where $E_{i,t}(\mathbf{x}_{t+1})$ and $\mathbf{\Omega}_{i,t} = [Cov_{i,t}(x_{j,t+1}, x_{k,t+1})]_{N\times N}$ are respectively the conditional expectation and variance-covariance matrix of agent i about the end-of-period payoffs of the risky assets, evaluated at time t.

Market Equilibrium

Assume that the I investors can be grouped into H agent-types, indexed by $h = 1, \cdots, H$, where the agents within the same group are homogeneous in their beliefs as well as risk aversion. The risk aversion of agents of type h is denoted by θ_h. We also denote by $I_{h,t}$ the number of investors in group h and by $n_{h,t} := I_{h,t}/I$ the market fraction of agents of type h in period t. Let $E_{h,t}(\mathbf{x}_{t+1})$ and $\mathbf{\Omega}_{h,t} = [Cov_{h,t}(x_{j,t+1}, x_{k,t+1})]_{N\times N}$ be respectively the conditional expectation and variance-covariance matrix of type-h agents at time t. Let $\mathbf{s} = (s_1, \cdots, s_N)^\top$ be the N-dimensional vector of average risky asset supply per agent. A supply shock to the market, denoted by a vector of random processes,[3] is assumed to follow $\boldsymbol{\xi}_{t+1} = \boldsymbol{\xi}_t + \boldsymbol{\sigma}_\kappa\boldsymbol{\kappa}_{t+1}$, where $\boldsymbol{\kappa}_{t+1}$ is a standard normal i.i.d. random variable with

[2] As is well known, the maximization of (6.1) is equivalent to maximizing the expected value of the above-defined CARA utility of wealth, $\max_{\mathbf{z}_{i,t}} E_{i,t}(u_i(W_{i,t+1}))$, provided that W_i is conditionally normally distributed in agent i's beliefs.

[3] The matrix $\boldsymbol{\sigma}_\kappa$ is not necessarily a diagonal matrix, that is, the supply noise processes of the N assets can be correlated. The same also holds for $\boldsymbol{\sigma}_\zeta$ in the dividend processes (6.5).

$E(\boldsymbol{\kappa}_t) = \mathbf{0}$ and $Cov(\boldsymbol{\kappa}_t) = \mathbf{I}$. Then the market clearing condition becomes

$$\sum_{h=1}^{H} n_{h,t}\theta_h^{-1}\boldsymbol{\Omega}_{h,t}^{-1}[E_{h,t}(\mathbf{x}_{t+1}) - R_f\mathbf{p}_t] = \mathbf{s} + \boldsymbol{\xi}_t. \tag{6.3}$$

Consensus Belief

We follow the construction in Chiarella et al. (2010 and 2013) to define an aggregate or consensus belief. Define the "average" risk aversion coefficient $\theta_{a,t} := (\sum_{h=1}^{H} n_{h,t}\theta_h^{-1})^{-1}$, which is a market population fraction weighted harmonic mean of the risk aversions of different types of heterogeneous agents. Specifically, if all agents have the same risk aversion coefficient $\theta_h = \theta$, then the "average" risk aversion coefficient $\theta_{a,t} = \theta$.[4] Then the aggregate beliefs at time t about variances/covariances and expected payoffs over the time interval $(t, t+1)$ are specified, respectively, as

$$\begin{aligned} \boldsymbol{\Omega}_{a,t} &= \theta_{a,t}^{-1}\Big(\sum_{h=1}^{H} n_{h,t}\theta_h^{-1}\boldsymbol{\Omega}_{h,t}^{-1}\Big)^{-1}, \\ E_{a,t}(\mathbf{x}_{t+1}) &= \theta_{a,t}\boldsymbol{\Omega}_{a,t}\sum_{h=1}^{H} n_{h,t}\theta_h^{-1}\boldsymbol{\Omega}_{h,t}^{-1}E_{h,t}(\mathbf{x}_{t+1}). \end{aligned} \tag{6.4}$$

The dividend process $\mathbf{d}_t$ is assumed to follow a martingale process

$$\mathbf{d}_{t+1} = \mathbf{d}_t + \boldsymbol{\sigma}_\zeta\boldsymbol{\zeta}_{t+1}, \tag{6.5}$$

where $\boldsymbol{\zeta}_{t+1}$ is a standard normal i.i.d. random variable with $E(\boldsymbol{\zeta}_t) = \mathbf{0}$ and $Cov(\boldsymbol{\zeta}_t) = \mathbf{I}$, independent of $\boldsymbol{\kappa}_{t+1}$. Moreover, agents are assumed to have homogeneous and correct conditional beliefs about the dividends (the unconditional expectation of which is assumed to be constant, $E(\mathbf{d}_t) = \overline{\mathbf{d}}$). Following Chiarella et al. (2010 and 2013), the market equilibrium prices (6.3) can therefore be rewritten as if they were determined by a homogeneous agent endowed with average risk aversion $\theta_{a,t}$ and the consensus beliefs $\{E_{a,t}, \boldsymbol{\Omega}_{a,t}\}$, namely

$$\mathbf{p}_t = \frac{1}{R_f}[E_{a,t}(\mathbf{p}_{t+1}) + \mathbf{d}_t - \theta_{a,t}\boldsymbol{\Omega}_{a,t}(\mathbf{s} + \boldsymbol{\xi}_t)]. \tag{6.6}$$

Note that at time t the dividends $\mathbf{d}_t$ are realized and agents formulate their beliefs about the next period payoff $\mathbf{x}_{t+1} = \mathbf{p}_{t+1} + \mathbf{d}_{t+1}$, based on the realized prices up to time $t-1$ and the dividends $\mathbf{d}_t$.

[4] This is the case that we use for the numerical analysis in Section 6.4.

Fitness

Following the discrete choice model (discussed for instance by Brock and Hommes (1997 and 1998)) the market fractions $n_{h,t}$ of agents of type h are determined by their fitness $v_{h,t-1}$, where the subscript $t-1$ indicates that fitness depends only on past observed prices and dividends. The fraction of agents using a strategy of type h is thus driven by "experience" through reinforcement learning. That is, given the fitness $v_{h,t-1}$, the fraction of agents using a strategy of type h is determined by the discrete choice model,

$$n_{h,t} = \frac{e^{\eta v_{h,t-1}}}{Z_t}, \qquad Z_t = \sum_h e^{\eta v_{h,t-1}}, \tag{6.7}$$

where $\eta > 0$ is the switching intensity of choice parameter measuring how sensitive agents are to selecting a better preforming strategy.[5] If $\eta = 0$, then agents are insensitive to past performance and pick a strategy at random with equal probability. In the other extreme case $\eta \to \infty$, all agents choose the forecast that performed best in the last period. An increase in the intensity of choice η can therefore represent an increase in the degree of rationality with respect to the evolutionary selection of strategies.

Given the utility maximization problem (6.1) of agents, we use a fitness measure that generalizes the 'risk-adjusted profit' introduced in Hommes (2001) (see Hommes and Wagener (2009) for a discussion about different choice of fitness functions and the relation between them), namely we set

$$v_{h,t} = \pi_{h,t} - \pi^B_{h,t} - C_h, \tag{6.8}$$

where $C_h \geq 0$ measures the cost of the strategy,

$$\pi_{h,t} := \mathbf{z}^\top_{h,t-1}(\mathbf{p}_t + \mathbf{d}_t - R_f \mathbf{p}_{t-1}) - \frac{\theta_h}{2}\mathbf{z}^\top_{h,t-1}\mathbf{\Omega}_{h,t-1}\mathbf{z}_{h,t-1} \tag{6.9}$$

and

$$\pi^B_{h,t} := \left(\frac{\theta_{a,t-1}}{\theta_h}\mathbf{s}\right)^\top (\mathbf{p}_t + \mathbf{d}_t - R_f \mathbf{p}_{t-1}) - \frac{\theta_h}{2}\left(\frac{\theta_{a,t-1}}{\theta_h}\mathbf{s}\right)^\top \mathbf{\Omega}_{h,t-1}\left(\frac{\theta_{a,t-1}}{\theta_h}\mathbf{s}\right). \tag{6.10}$$

Note that (6.9) can be naturally interpreted as the risk-adjusted profit of type h agent. It represents the realized profit adjusted by the subjective risk undertaken by investor h, which is consistent with investors' utility-maximizing portfolio choices. Expression (6.10) can be interpreted as the (risk-adjusted) profit on portfolio $\mathbf{z}^B_{h,t-1} := \frac{\theta_{a,t-1}}{\theta_h}\mathbf{s}$, which represents a 'benchmark' portfolio for agents of type h at time $t-1$. The portfolio

[5] In fact, η is inversely related to the variance of the noise in the observation of random utility.

$\mathbf{z}^B_{h,t-1}$ is proportional to the market portfolio. The proportionality coefficient $\frac{\theta_{a,t-1}}{\theta_h}$ takes into account the fact that the shares of the market portfolio of agents are positively correlated to their risk tolerance $(1/\theta_h)$. In the case that all agents have the same risk aversion (so that $\theta_{a,t-1} = \theta_h$), they all take the market portfolio. Put differently, the performance measure (6.8) views strategy h as a successful strategy only to the extent that it outperforms its market benchmark in terms of risk-adjusted profitability. More precisely, portfolio $z^B_{h,t}$ represents the portfolio that agents of type h would select at time t if all agents had *identical beliefs* (whichever they are) about the first and second moment of $\mathbf{x}_{t+1}$. In this case agents would (possibly) differ only in terms of their risk aversion and they would hold $z_{h,t} = z^B_{h,t}$ for all h. According to the fitness measure $v_{h,t} := \pi_{h,t} - \pi^B_{h,t} - C_h$, their portfolios would thus have identical performance (apart from the costs). In other words, the selected fitness measure $v_{h,t}$ is not affected by mere differences in risk aversion and accounts only of the profitability generated by the competing investment rules. Note that, in the case of zero supply of outside shares, the market clearing equation (6.3) leads to $E_{a,t}(\mathbf{x}_{t+1})/R_f = \mathbf{p}_t$. This is the case considered in Hommes (2001) for a single-risky-asset model. The market thus behaves as if it were 'risk-neutral' at the *aggregate* level[6] in this particular case and the performance measure reduces to the risk-adjusted profit considered in Hommes (2001).

Fundamentalists

Now we propose a model with classical heterogeneous agent-types and consider two types of agents, fundamentalists and trend followers, with $h = f$ and $h = c$, respectively. Following He and Li (2007), the fundamentalists realize the existence of non-fundamental traders, such as trend followers to be introduced in the following discussion. The fundamentalists believe that the stock price may be driven away from the fundamental value in the short-run, but it will eventually converge to the expected fundamental value in the long-run. Hence the conditional mean of the fundamental traders is assumed to follow

$$E_{f,t}(\mathbf{p}_{t+1}) = \mathbf{p}_{t-1} + \boldsymbol{\alpha}(E_{f,t}(\mathbf{p}^*_{t+1}) - \mathbf{p}_{t-1}), \tag{6.11}$$

where $\mathbf{p}^*_t = (p^*_{1,t}, \cdots, p^*_{N,t})$ is the vector of fundamental prices and the parameter $\boldsymbol{\alpha} = diag[\alpha_1, \cdots, \alpha_N]$ with $\alpha_j \in [0, 1]$ represents the speed of price adjustment of the fundamentalists toward their expected fundamental value or it reflects how confident they are in the fundamental value. The parameter α_j can be different for different risky assets. In particular, for $\alpha_j = 1$, the fundamental traders are fully confident about the

[6] Of course, risk aversion does affect decisions at the *agent-type* level.

fundamental value of risky asset j and adjust their expected price in the next period instantaneously to the expected fundamental value. For $\alpha_j = 0$, the fundamentalists become naive traders of asset j. We also assume that the fundamentalists have constant beliefs about the covariance matrix of the payoffs so that $\mathbf{\Omega}_{f,t} = \mathbf{\Omega}_0 := (\sigma_{jk})_{N\times N}$.

Fundamental Prices

To define the fundamental price $\mathbf{p}_t^*$, we consider a 'standard CAPM' with homogeneous beliefs where all agents have correct beliefs about the fundamental prices and are fully confident about their expected fundamental values (that is $\boldsymbol{\alpha} = diag[1, \cdots, 1]$). We also assume that their average risk aversion coefficient is constant over time, $\theta_{a,t} = \overline{\theta}$, and so are their common second-moment beliefs, $\mathbf{\Omega}_0$.[7] Correspondingly we define the fundamental price as

$$\mathbf{p}_t^* = \frac{1}{r_f}(\mathbf{d}_t - \overline{\theta}\mathbf{\Omega}_0(\mathbf{s} + \boldsymbol{\xi}_t)), \tag{6.12}$$

which is a martingale process under the assumptions about the exogenous dividend and market noise processes, so that

$$\mathbf{p}_{t+1}^* = \mathbf{p}_t^* + \boldsymbol{\epsilon}_{t+1}, \qquad \boldsymbol{\epsilon}_{t+1} = \frac{1}{r_f}(\boldsymbol{\sigma}_\zeta \boldsymbol{\zeta}_{t+1} - \overline{\theta}\mathbf{\Omega}_0 \boldsymbol{\sigma}_\kappa \boldsymbol{\kappa}_{t+1}) \sim \text{Normal i.i.d.} \tag{6.13}$$

In this case, it follows from Eq. (6.6) that the equilibrium price is given by $\mathbf{p}_t = \mathbf{p}_t^*$. Thus we can treat the benchmark CAPM case as the 'steady state' of the dynamics of the heterogeneous beliefs model.

Trend Followers

Unlike the fundamental traders, trend followers are technical traders who believe the future price change can be predicted from various patterns or trends generated from the historical prices. They are assumed to extrapolate the latest observed price change over a long-run sample mean price and to adjust their variance estimate accordingly. More precisely, their conditional mean and covariance matrices are assumed to satisfy

$$E_{c,t}(\mathbf{p}_{t+1}) = \mathbf{p}_{t-1} + \boldsymbol{\gamma}(\mathbf{p}_{t-1} - \mathbf{u}_{t-1}), \qquad \mathbf{\Omega}_{c,t} = \mathbf{\Omega}_0 + \lambda \mathbf{V}_{t-1}, \tag{6.14}$$

where $\mathbf{u}_{t-1}$ and $\mathbf{V}_{t-1}$ are sample means and covariance matrices of past market prices $\mathbf{p}_{t-1}, \mathbf{p}_{t-2}, \cdots$, the constant vector $\boldsymbol{\gamma} = diag[\gamma_1, \cdots, \gamma_N] > 0$ reflects the trend following

[7] Without switching, the average risk aversion $\overline{\theta}$ is constant and corresponds to the harmonic mean of the risk aversion coefficients of all agents. In our simulations, we will set $\overline{\theta} = \theta_a^*$, the average risk aversion coefficient at the steady state solution of the model.

strategy, and γ_j measures the extrapolation rate and high (low) values of γ_j correspond to strong (weak) extrapolation by trend followers, and λ measures the sensitivity of the second-moment estimate to the sample variance. This specification of the trend followers captures the extrapolative behavior of the trend followers, who expect price changes to occur in the same direction as the price trend observed over a past time window. Assume that $\mathbf{u}_{t-1}$ and $\mathbf{V}_{t-1}$ are computed recursively as

$$\begin{aligned}\mathbf{u}_{t-1} &= \delta\mathbf{u}_{t-2} + (1-\delta)\mathbf{p}_{t-1},\\ \mathbf{V}_{t-1} &= \delta\mathbf{V}_{t-2} + \delta(1-\delta)(\mathbf{p}_{t-1}-\mathbf{u}_{t-2})(\mathbf{p}_{t-1}-\mathbf{u}_{t-2})^{\top}.\end{aligned} \tag{6.15}$$

Effectively, the sample mean vector and variance-covariance matrix are calculated based on the all historical prices $\mathbf{p}_{t-1}, \mathbf{p}_{t-2}, \cdots$, spreading back to $-\infty$ with geometric decaying probability weights $(1-\delta)\{1, \delta, \delta^2, \cdots\}$. Therefore, as δ decreases, the weights on the latest prices increase but decay geometrically at a common rate of δ. For $\boldsymbol{\gamma} > \mathbf{0}$ and large δ, momentum traders calculate the trend based on a long time horizon. In particular, when $\delta = 0, E_{c,t}(\mathbf{p}_{t+1}) = \mathbf{p}_{t-1}$ and $\mathbf{V}_{t-1} = \mathbf{0}$, implying naive behavior by the trend followers. However, when $\delta = 1$, $\mathbf{u}_{t-1} = \mathbf{u}_0$ and $\mathbf{V}_{t-1} = \mathbf{V}_0$, and therefore $E_{c,t}(\mathbf{p}_{t+1}) = \mathbf{p}_{t-1} + \boldsymbol{\gamma}(\mathbf{p}_{t-1} - \mathbf{u}_0)$, so that trend followers are momentum traders.

The Complete Dynamic Model

Based on the analysis above, the optimal demands of the fundamentalists and trend followers are given, respectively, by

$$\mathbf{z}_{f,t} = \theta_f^{-1}\boldsymbol{\Omega}_o^{-1}[\mathbf{p}_{t-1} + \mathbf{d}_t + \boldsymbol{\alpha}(\mathbf{p}_t^* - \mathbf{p}_{t-1}) - R_f\mathbf{p}_t] \tag{6.16}$$

and

$$\mathbf{z}_{c,t} = \theta_c^{-1}[\boldsymbol{\Omega}_0 + \lambda\mathbf{V}_{t-1}]^{-1}[\mathbf{p}_{t-1} + \mathbf{d}_t + \boldsymbol{\gamma}(\mathbf{p}_{t-1} - \mathbf{u}_{t-1}) - R_f\mathbf{p}_t]. \tag{6.17}$$

Finally, the general dynamic model (6.6) reduces to the random nonlinear dynamical system

$$\begin{cases} \mathbf{p}_t = \dfrac{\theta_{a,t}}{R_f}\boldsymbol{\Omega}_{a,t}\Big[\dfrac{n_{f,t}}{\theta_f}\boldsymbol{\Omega}_0^{-1}\big(\mathbf{p}_{t-1}+\boldsymbol{\alpha}(\mathbf{p}_t^*-\mathbf{p}_{t-1})\big) \\ \qquad + \dfrac{n_{c,t}}{\theta_c}(\boldsymbol{\Omega}_0+\lambda\mathbf{V}_{t-1})^{-1}\big(\mathbf{p}_{t-1}+\boldsymbol{\gamma}(\mathbf{p}_{t-1}-\mathbf{u}_{t-1})\big)-\mathbf{s}-\boldsymbol{\xi}_t\Big]+\dfrac{1}{R_f}\mathbf{d}_t, \\ \mathbf{p}_t^* = \dfrac{1}{r_f}(\mathbf{d}_t-\theta_a^*\boldsymbol{\Omega}_0(\mathbf{s}+\boldsymbol{\xi}_t)), \\ \mathbf{u}_t = \delta\mathbf{u}_{t-1}+(1-\delta)\mathbf{p}_t, \\ \mathbf{V}_t = \delta\mathbf{V}_{t-1}+\delta(1-\delta)(\mathbf{p}_t-\mathbf{u}_{t-1})(\mathbf{p}_t-\mathbf{u}_{t-1})^\top, \\ n_{f,t} = \dfrac{1}{1+e^{-\eta v_{\Delta,t-1}}}, \\ \boldsymbol{\xi}_t = \boldsymbol{\xi}_{t-1}+\boldsymbol{\sigma}_\kappa\boldsymbol{\kappa}_t, \\ \mathbf{d}_t = \mathbf{d}_{t-1}+\boldsymbol{\sigma}_\zeta\boldsymbol{\zeta}_t, \end{cases} \tag{6.18}$$

where

$$\theta_{a,t} = \Big(\frac{n_{f,t}}{\theta_f}+\frac{n_{c,t}}{\theta_c}\Big)^{-1}, \qquad \boldsymbol{\Omega}_{a,t} = \frac{1}{\theta_{a,t}}\Big(\frac{n_{f,t}}{\theta_f}\boldsymbol{\Omega}_0^{-1}+\frac{n_{c,t}}{\theta_c}(\boldsymbol{\Omega}_0+\lambda\mathbf{V}_{t-1})^{-1}\Big)^{-1},$$

$$\begin{aligned} v_{\Delta,t} := v_{f,t}-v_{c,t} &= \left(\mathbf{z}_{f,t-1}-\frac{\theta_{a,t-1}\mathbf{s}}{\theta_f}\right)^\top\left(\mathbf{p}_t+\mathbf{d}_t-R_f\mathbf{p}_{t-1}-\frac{\theta_f}{2}\boldsymbol{\Omega}_0(\mathbf{z}_{f,t-1}+\frac{\theta_{a,t-1}\mathbf{s}}{\theta_f})\right) \\ &\quad -\left(\mathbf{z}_{c,t-1}-\frac{\theta_{a,t-1}\mathbf{s}}{\theta_c}\right)^\top\left(\mathbf{p}_t+\mathbf{d}_t-R_f\mathbf{p}_{t-1}-\frac{\theta_c}{2}(\boldsymbol{\Omega}_0+\lambda\mathbf{V}_{t-2})(\mathbf{z}_{c,t-1}+\frac{\theta_{a,t-1}\mathbf{s}}{\theta_c})\right)-C_\Delta, \end{aligned}$$

$$n_{c,t} = 1-n_{f,t}, \qquad C_\Delta = C_f-C_c \geq 0.$$

In summary, we have established an adaptively heterogeneous beliefs model of asset prices under the CAPM framework. The resulting model is characterized by a stochastic difference system with seven variables, which is difficult to analyze directly. To understand the interaction of the deterministic dynamics and noise processes, we first study the dynamics of the corresponding deterministic model in Section 6.3. The stochastic model (6.18) is then analyzed in Section 6.4.

6.3 Dynamics of the Deterministic Model

By assuming that the fundamental price and the dividend are constants $\mathbf{p}_t^* = \mathbf{p}^*$, $\mathbf{d}_t = \bar{\mathbf{d}}$, and there is no supply shock $\boldsymbol{\xi}_t = 0$, the system (6.18) becomes the deterministic

dynamical system[8]

$$\begin{cases} \mathbf{p}_t = \dfrac{\theta_{a,t}}{R_f}\boldsymbol{\Omega}_{a,t}\Big[\dfrac{n_{f,t}}{\theta_f}\boldsymbol{\Omega}_0^{-1}\big(\mathbf{p}_{t-1} + \boldsymbol{\alpha}(\mathbf{p}^* - \mathbf{p}_{t-1})\big) \\ \qquad\qquad + \dfrac{n_{c,t}}{\theta_c}(\boldsymbol{\Omega}_0 + \lambda\mathbf{V}_{t-1})^{-1}\big(\mathbf{p}_{t-1} + \boldsymbol{\gamma}(\mathbf{p}_{t-1} - \mathbf{u}_{t-1})\big) - \mathbf{s}\Big] + \dfrac{1}{R_f}\bar{\mathbf{d}}, \\ \mathbf{u}_t = \delta\mathbf{u}_{t-1} + (1-\delta)\mathbf{p}_t, \\ \mathbf{V}_t = \delta\mathbf{V}_{t-1} + \delta(1-\delta)(\mathbf{p}_t - \mathbf{u}_{t-1})(\mathbf{p}_t - \mathbf{u}_{t-1})^\top, \\ n_{f,t} = \dfrac{1}{1 + e^{-\eta v_{\Delta,t-1}}}. \end{cases} \tag{6.19}$$

The dynamical system (6.19) should not be interpreted as a deterministic approximation of stochastic system (6.18), based on some type of asymptotic convergence, but rather just as a system obtained by setting the dividend, the supply and the fundamental price at their unconditional mean levels. The analysis of this 'deterministic skeleton' is a common practice in the heterogeneous-agent literature, and it is aimed at gaining some initial insights into the impact of the parameters on the underlying dynamics. Although the properties of the deterministic skeleton do not carry over to the stochastic model in general, important connections between the dynamical structure of the stochastic model and that of the underlying deterministic model exist and have been highlighted in recent literature on stochastic heterogeneous-agent models (see, e.g. Chiarella et al. 2011 and Zhu et al. 2011).

The system (6.19) has a unique steady state $(\mathbf{p}_t, \mathbf{u}_t, \mathbf{V}_t, n_{f,t}) = (\mathbf{p}^*, \mathbf{p}^*, \mathbf{0}, n_f^*)$, where, following Eq. (6.12), the fundamental steady state price, $\mathbf{p}^*$, is given by

$$\mathbf{p}^* = \frac{1}{r_f}(\bar{\mathbf{d}} - \theta_a^*\boldsymbol{\Omega}_0\mathbf{s}) \tag{6.20}$$

and $n_f^* = 1/(1 + e^{\eta C_\Delta})$. Hence, at the steady state, $n_c^* = 1 - n_f^*$ and $\theta_{a,t} = \theta_a^* = 1/(n_f^*/\theta_f + n_c^*/\theta_c)$. Let $\theta_0 := \theta_f/\theta_c$. Note that if $\theta_f = \theta_c = \theta$, then $\theta_{a,t} = \theta$ and $\theta_0 = 1$.

For the $N^2 + 5N + 2$ dimensional system (6.19), we are able to obtain the following proposition on the local stability of the steady state. The proof is given in the Appendix E.2.

Proposition 6.1 *For the system* (6.19)*,*

(i) if $R_f \geq \delta(1+\gamma_j)$ for all $j \in \{1, \cdots, N\}$, then the steady state $(\boldsymbol{p}^*, \boldsymbol{p}^*, \boldsymbol{0}, n_f^*)$ is locally asymptotically stable;

[8]The state variables $\mathbf{p}_t$, $\mathbf{u}_t$, $\mathbf{V}_t$ and $n_{f,t}$ in Eq. (6.19) can be expressed in terms of $\mathbf{p}_{t-1}$, $\mathbf{u}_{t-1}$, $\mathbf{V}_{t-1}$, $n_{f,t-1}$, $\mathbf{p}_{t-2}$, $\mathbf{u}_{t-2}$, $\mathbf{V}_{t-2}$ and $n_{f,t-2}$, which have N, N, $N(N+1)/2$, 1, N, N, $N(N+1)/2$ and 1 dimensions respectively. So the dimension of the system (6.19) is $N^2 + 5N + 2$. For instance, when $N = 1$, it is an 8-dimensional system.

(ii) if $R_f < \delta(1+\gamma_j)$ *for all* $j \in \{1, \cdots, N\}$*, then the steady state is locally asymptotically stable when* $C_\Delta \neq 0$ *and* $\eta < \widehat{\eta}_j := \frac{1}{C_\Delta} \ln \frac{R_f - \delta(1-\alpha_j)}{\theta_0[\delta(1+\gamma_j)-R_f]}$ *for all* $j \in \{1, \cdots, N\}$ *and undergoes a Hopf bifurcation when* $\eta = \widehat{\eta}_j$ *for some* $j \in \{1, \cdots, N\}$*. If* $C_\Delta = 0$*, then the steady state is locally asymptotically stable when* $\theta_0\gamma_j < \alpha_j + (1+\theta_0)(\frac{R_f}{\delta} - 1)$ *for all* j*;*

(iii) if $R_f < \delta(1+\gamma_j)$ *for some* $j \in J_o \subseteq \{1, \cdots, N\}$*, then the steady state is locally asymptotically stable when* $\eta < \widehat{\eta}_m := \min_{j \in J_o} \widehat{\eta}_j$ *and undergoes a Hopf bifurcation when* $\eta = \widehat{\eta}_m$*.*

The results in Proposition 6.1 are significant with respect to the intuitive and simple conditions on the stability of the steady state for such a high dimensional system. First, when the trend followers are not very active (so that $\gamma_j \leq R_f/\delta - 1$), the steady state of the system is stable. Second, the stability condition (ii) is equivalent to

$$\frac{R_f}{\delta} - 1 < \gamma_j < \frac{(\frac{R_f}{\delta} - 1)(1 + \theta_0 e^{\eta C_\Delta}) + \alpha_j}{\theta_0 e^{\eta C_\Delta}}, \qquad j = 1, \cdots, N.$$

Hence, even when the trend followers are active (so that $\gamma_j > R_f/\delta - 1$), the system can still be stable when the fundamentalists dominate the market at the steady state or, equivalently, the switching intensity is sufficiently small. In short, Proposition 6.1 shows clearly that increases in C_c, α_j and θ_c stabilize the system, while increases in C_f, δ, γ and θ_f destabilize the system. Intuitively, the fundamentalists play a stabilizing role in the market. The activity of fundamentalists is enhanced with an increase in α_j or decreases in C_f (since a decrease in C_f increases the market fraction of fundamentalists) and θ_f (since a decrease in θ_f increases fundamentalists' long/short position when the fundamental price moves away from the market price).

To understand how the impact of switching in a market with many risky assets is different from a market with a single risky asset, we consider a special case where agents invest in a market with one risk-free asset and one risky asset, say asset j. In this case,

system (6.19) reduces to

$$\begin{cases} p_{j,t} = \dfrac{\bar{d}_j}{R_f} + \dfrac{1}{R_f\left(\frac{n_{f,t}}{\theta_f\sigma_j^2} + \frac{n_{c,t}}{\theta_c(\sigma_j^2+\lambda V_{j,t-1})}\right)}\left[\dfrac{n_{f,t}\big(p_{j,t-1}+\alpha_j(p_j^*-p_{j,t-1})\big)}{\theta_f\sigma_j^2}\right. \\ \qquad\qquad \left. + \dfrac{n_{c,t}\big(p_{j,t-1}+\gamma_j(p_{j,t-1}-u_{j,t-1})\big)}{\theta_c(\sigma_j^2+\lambda V_{j,t-1})} - s_j\right], \\ u_{j,t} = \delta u_{j,t-1} + (1-\delta)p_{j,t}, \\ V_{j,t} = \delta V_{j.t-1} + \delta(1-\delta)(p_{j,t}-u_{j,t-1})^2, \\ n_{f,t} = \dfrac{1}{1+e^{-\eta v_{\Delta,t-1}}}. \end{cases} \tag{6.21}$$

The dynamics of the system (6.21) can be characterized by the following proposition (the proof is given in the Appendix E.1).

Proposition 6.2 *For the system* (6.21)*,*

(i) if $R_f \geq \delta(1+\gamma_j)$, then the steady state $(p_j^*, p_j^*, 0, n_f^*)$ of the system is always locally asymptotically stable;

(ii) if $R_f < \delta(1+\gamma_j)$, then the steady state is locally asymptotically stable when $\eta < \widehat{\eta}_j$ and $C_\Delta \neq 0$ and undergoes a Hopf bifurcation when $\eta = \widehat{\eta}_j$. When $C_\Delta = 0$, the steady state is locally asymptotically stable if $\theta_0\gamma_j < \alpha_j + (1+\theta_0)(\frac{R_f}{\delta} - 1)$.

By comparing the local stability conditions in Propositions 6.1 and 6.2, one can see that the stability conditions of each risky asset due to the increasing switching intensity are independent of the parameters specific to any other asset and, surprisingly, the correlations among risky assets have no impact on the local stability properties.[9] This result is due to the peculiar properties of the Jacobian matrix and the adaptive behavior considered (this becomes clear from the proofs in the appendices E.1 and E.2). Hence the local stability properties of asset j in the multi-asset model are exactly the same as if asset j was considered in isolation (that is, in the model with only risky asset j and the risk-free asset).

Propositions 6.1 and 6.2 provide an initial insight into the mechanisms governing the joint price dynamics of multiple risky assets, showing that locally instability plays a very small role in the spill-over phenomena that we will discuss in what follows, but globally the instability of one asset can spill over to the other assets due to its correlations with other assets.

[9] Mathematically, this is due to the fact that the fitness measure and the variance-covariance matrices are in higher order terms. Certainly they can affect the nonlinear dynamics, but not the dynamics of the linearized system.

To better understand the implications of Propositions 6.1 and 6.2 and the price dynamics of the model, we consider an example of two risky assets and a riskless asset with

$$\mathbf{\Omega}_0 = \begin{pmatrix} \sigma_1^2 & \rho_{12}\sigma_1\sigma_2 \\ \rho_{12}\sigma_1\sigma_2 & \sigma_2^2 \end{pmatrix}$$

and set[10] $\mathbf{s} = (0.1, 0.1)^\top$, $\theta_f = 1$, $\theta_c = 1$, $\lambda = 1.5$, $C_f = 4$, $C_c = 1$, $\rho_{12} = 0.5$, $\delta = 0.98$, $\boldsymbol{\gamma} = diag[0.3, 0.3]$ and $\boldsymbol{\alpha} = diag[0.4, 0.5]$. We choose the annual values[11] of the following parameters: $r_f = 0.025$, $\sigma_1 = 0.6$, $\sigma_2 = 0.4$ and $\bar{\mathbf{d}} = (0.08, 0.05)^\top$. In this chapter, we consider monthly time steps (i.e. $K = 12$).

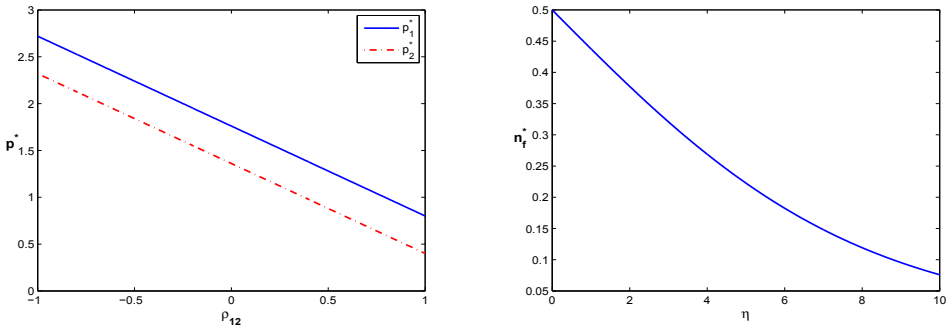

(a) Steady-state prices (b) Steady-state market fraction

Figure 6.1: (a) The fundamental steady state price $\mathbf{p}^* = (p_1^*, p_2^*)$ as a function of the correlation ρ_{12} with $\eta = 1$; (b) The equilibrium market fractions of fundamentalists n_f^* as a function of the switching intensity η.

Based on this set of parameters, the model has the following implications. First, the equilibrium steady state fundamental price decreases when the correlation coefficient increases and, when the fundamental strategy costs more than the trend follower strategy, the steady state market fraction of the fundamentalists reduces as the switching intensity increases. These results are illustrated in Figs. 6.1 (a) and (b) respectively for the two-asset system (6.19). In fact, Eq. (6.20) determines the dependence of the steady state fundamental price on the parameters. Fig. 6.1 (a) illustrates a negative linear relationship between the fundamental steady state price $\mathbf{p}^* = (p_1^*, p_2^*)$ and the correlation ρ_{12}.

Secondly, as implied by Propositions 6.1 and 6.2, asset prices become unstable as the switching intensity η increases. This is illustrated in Fig. 6.2. With the chosen parameters, one can verify that $R_f < \delta(1 + \gamma_j)$ for $j = 1, 2$, and the bifurcation values for

[10] The set of parameters is fixed in all numerical analysis unless specified otherwise.

[11] The annualised parameters are converted to monthly, weekly and daily parameters in the standard way, by rescaling r_f, $\mathbf{\Omega}_0$, $\boldsymbol{\alpha}$, $\bar{\mathbf{d}}$, $\boldsymbol{\gamma}$, C_f and C_c via the factor $1/K$, where the frequency K is set to 12 (monthly), 50 (weekly), 250 (daily). As shown in Chiarella et al. (2013), the parameter δ is converted to $K\delta/[1 + (K-1)\delta]$ to preserve the average memory length of the time average of past returns.

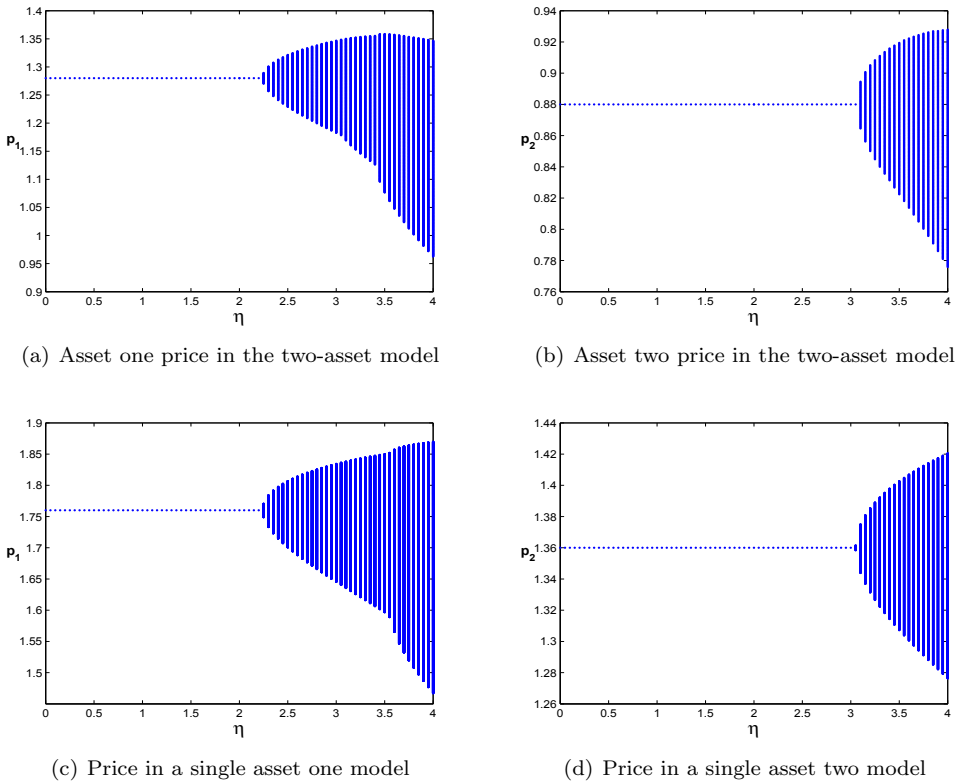

(a) Asset one price in the two-asset model

(b) Asset two price in the two-asset model

(c) Price in a single asset one model

(d) Price in a single asset two model

Figure 6.2: The bifurcations of the two risky asset prices with respect to η (a) and (b), the two-asset model (6.19); and (c) and (d) the single risky asset model (6.21).

asset one and two are $\widehat{\eta}_1 \approx 2.2384$ and $\widehat{\eta}_2 \approx 3.0485$ respectively. According to Proposition 6.1, when $\eta < \widehat{\eta}_1$ the two prices are stable; when $\widehat{\eta}_1 < \eta < \widehat{\eta}_2$, the price of asset two is still stable, however the price of asset one becomes unstable; when $\eta > \widehat{\eta}_2$, the prices of both assets become unstable.[12] Fig. 6.2 plots the price bifurcation diagrams with respect to the switching intensity parameter η for both system (6.19) with two risky assets and system (6.21) with one risky asset. For the single risky asset model, Figs. 6.2 (c) and (d) show that an increase in the switching intensity η makes the steady state price unstable, leading to the complicated price dynamics documented in Brock and Hommes (1998). With two risky assets, Figs. 6.2 (a) and (b) show that the steady state is stable when the switching intensity η is low, but becomes unstable as the switching intensity increases. The time series of prices and the market fraction of the fundamentalist in Figs. 6.3 (a)-(c) provide further evidence on the analysis above. At first, both assets and the market fraction are stable and constant when $\eta = 1.5$ is small (Fig. 6.3 (a)). As η increases to 2.5, asset

[12]Note that here we use the words 'stable' and 'unstable' in a loose, yet intuitive, sense. Strictly speaking, the local asymptotic stability of the steady state of the multi-asset model is lost when $\eta = \min_j \widehat{\eta}_j$, as stated in Proposition 6.1.

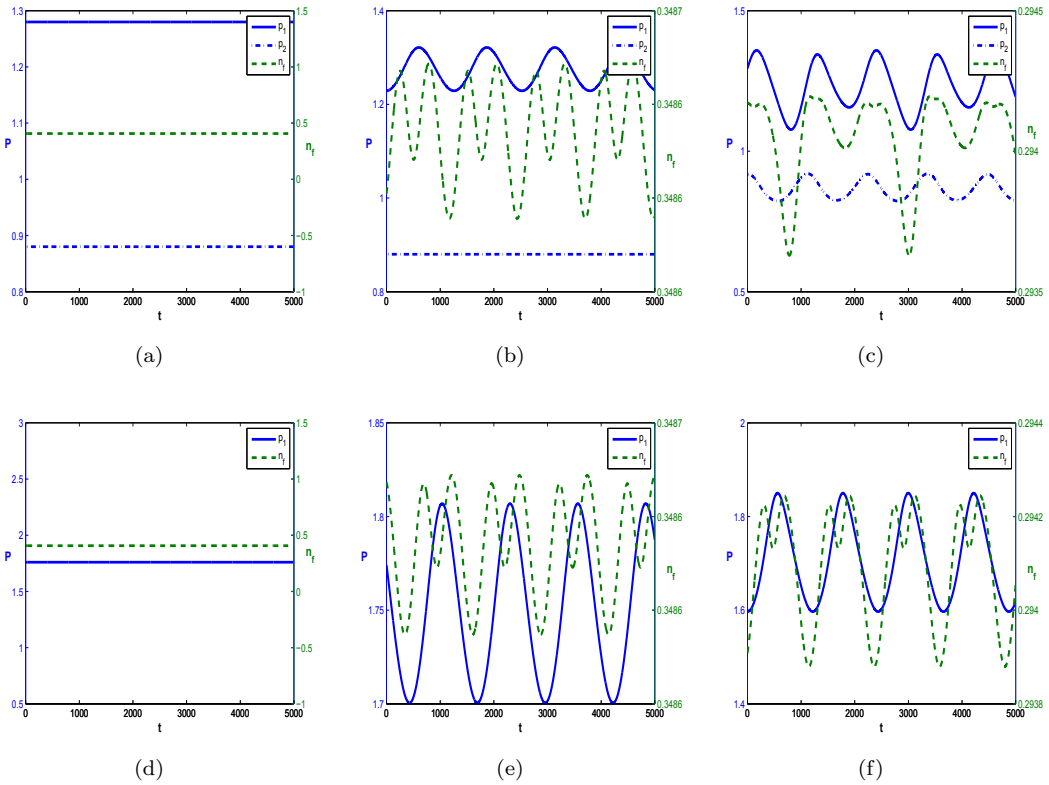

Figure 6.3: Time series plots of $p_{1,t}$, $p_{2,t}$ and $n_{f,t}$ in the two-asset model ((a)-(c)) and of $p_{1,t}$ in the single-asset one model ((d)-(f)) with $\eta = 1.5$ in (a) and (d); $\eta = 2.5$ in (b) and (e); and $\eta = 3.5$ in (c) and (f).

one and then asset two become unstable as illustrated in Fig. 6.3 (b). As η increases to 3.5, both asset prices become unstable (see Fig. 6.3 (c)). Also the price of risky asset one of the two-asset model is more irregular compared to the regular fluctuations in Fig. 6.3 (f) of the one asset model. Also, as the switching intensity η increases, even small fluctuations in the market fractions of agents can cause large fluctuations in asset prices.

Thirdly, the model displays a very interesting spill-over effect, which can be very different from portfolio effect. As we discussed earlier, the stability is a local result and the stability conditions of the risky assets are independent among the risky assets. When one asset becomes unstable, one would expect the spill-over of instability of the asset to spread to the other assets due to the portfolio effect. However, this may not always be the case, as demonstrated in Fig. 6.4. For $\eta = 2.5$, Fig. 6.4 (a) shows that the price is unstable for asset one, but stable for asset two. Intuitively, the price fluctuations in asset one would be caused by changing portfolio positions taken by the two types of agents for asset one, which is confirmed by Fig. 6.4 (c). However, this intuition does not carry over

to asset two for which the price is constant but the portfolio positions taken by agents for the asset are also varying, as illustrated in Fig. 6.4 (d). The portfolio variations due

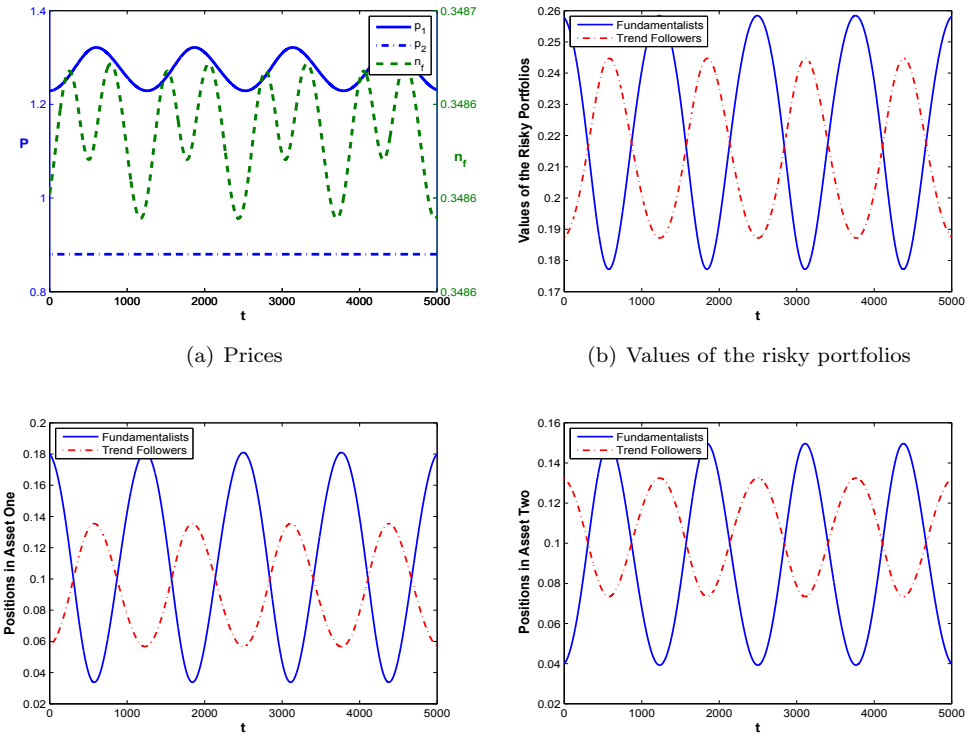

(a) Prices

(b) Values of the risky portfolios

(c) Positions in Asset One

(d) Positions in Asset Two

Figure 6.4: The time series of (a) the prices and market fraction; (b) portfolio values of the fundamentalists and trend followers; and portfolio positions of two types of agents in asset one (c) and asset two (d). Here $\eta = 2.5$.

to the portfolio effect lead to the fluctuations of the portfolio values of the agents that are illustrated in Fig. 6.4 (b). How can this happen? As a matter of fact, there are two reasons behind this interesting phenomenon. First, the variations of the risky assets in the portfolios are caused by the correlation between risky assets (reflected in both $\mathbf{\Omega}_0$ and $\mathbf{V}_t$) and the time-varying population fractions. Hence, even when the price of asset two is constant, the portfolio positions of agents in asset two may not be constant. Secondly, the spill-over effect is a nonlinear rather than a linear effect, meaning that the stability of asset two in the nonlinear system is observed when the initial values are near the steady state values; otherwise, stability may not be maintained. Fig. 6.5 shows how the instability of asset one spill over to asset two for $\eta \in (\hat{\eta}_1, \hat{\eta}_2)$ increases from 2.24 in (a) to 2.5 in (b) and then to 3.04 in (c) when the initial prices are far away from the steady state price levels. Note that asset two is locally stable for $\eta \in (\hat{\eta}_1, \hat{\eta}_2)$. Hence the spill-over

effect reflects the dynamics of the nonlinear system. In fact, we do observe such spill-over effects in the bifurcation plots in Fig. 6.2. Note that the first small price jump of asset one in Fig. 6.2 (a) after the initial bifurcation (at $\eta = \hat{\eta}_1$) occurs at $\eta = \hat{\eta}_2$, which is the bifurcation of the second asset in the single asset model (in Fig. 6.2 (d)). This implies that, when asset two becomes unstable, there is a spill-over effect from asset two to asset one characterized by the price jump of asset one near $\hat{\eta}_2$. Interestingly, as the intensity increases further, say $\eta \approx 3.4$, the fluctuations of asset one increases significantly, which is demonstrated by the large price jump of asset one for $\eta > 3.4$.

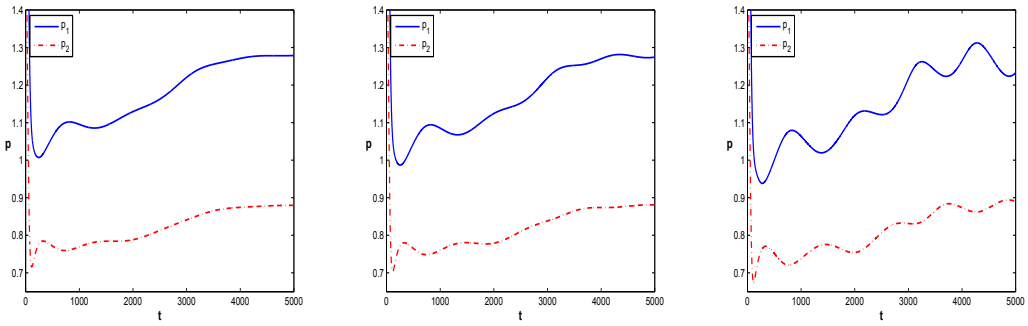

(a) $\eta = 2.24$ (b) $\eta = 2.5$ (c) $\eta = 3.04$

Figure 6.5: The market prices for $\eta = 2.24$ (a), 2.5 (b) and 3.04 (c) when initial values are far away from the steady state.

In addition, numerical simulations (not reported here) show that an increase in ρ_{12} leads to increases in the fluctuations of the prices when the system (6.19) becomes unstable. Intuitively, as the correlation of the two risky assets increases, diversification becomes less effective, hence assets become more risky, and consequently the fundamental equilibrium prices decrease (in order to have a high expected return). Also, simulations show (not reported here) that market prices become more volatile when the trend followers are less concerned about the sample variance; that is when λ becomes small, even though λ does not affect the local stability of the system (6.19). In fact, when λ becomes small, the demand of the trend followers increases so that they become more active in the market, leading to a more volatile market.

In summary, we have shown that the rational behavior of agents in switching to better performing strategies can lead to market instability and a non-linear spill-over of price fluctuations from one asset to other assets. The nonlinear dynamics due to the spill-over effect can lead to high trading volume and high volatility. This becomes clearer in the discussion of the stochastic model in the next section.

6.4 Price Behavior of the Stochastic Model

In this section, through numerical simulations, we first focus on the spill-over effect by examining the interaction between the dynamics of the deterministic model and the noise processes and explore the potential power of the model to explain price deviations from the fundamental prices and also high volatility. We then provide an evolutionary capital asset pricing model (ECAPM) and compare the ex-ante betas with the rolling window estimates of the betas used in the literature. Finally we study the relationship between the price volatility and trading volumes. We choose $\boldsymbol{\sigma}_\kappa = diag[0.001, 0.001]$ and $\boldsymbol{\sigma}_\zeta = diag[0.002, 0.002]$, representing 0.1% and 0.2% standard deviations of the noisy supply and dividend processes respectively in this section.

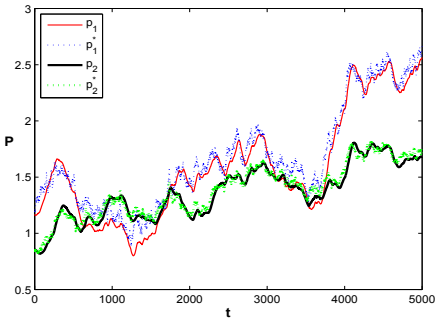

(a) Prices with $\eta = 1.5$

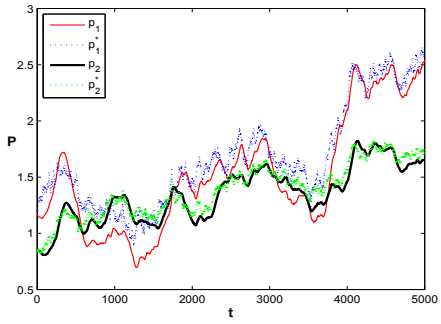

(b) Prices with $\eta = 3.5$

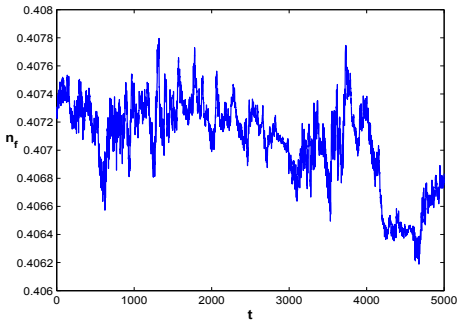

(c) Market fraction with $\eta = 1.5$

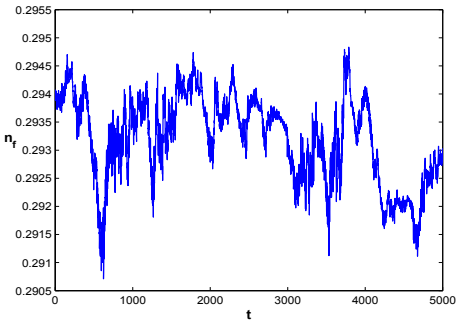

(d) Market fraction with $\eta = 3.5$

Figure 6.6: The time series of the fundamental price (the dotted line) and the market prices (the solid line) of the two-asset model with (a) $\eta = 1.5$ and (b) $\eta = 3.5$, and the corresponding market fractions of the fundamentalists in (c) and (d).

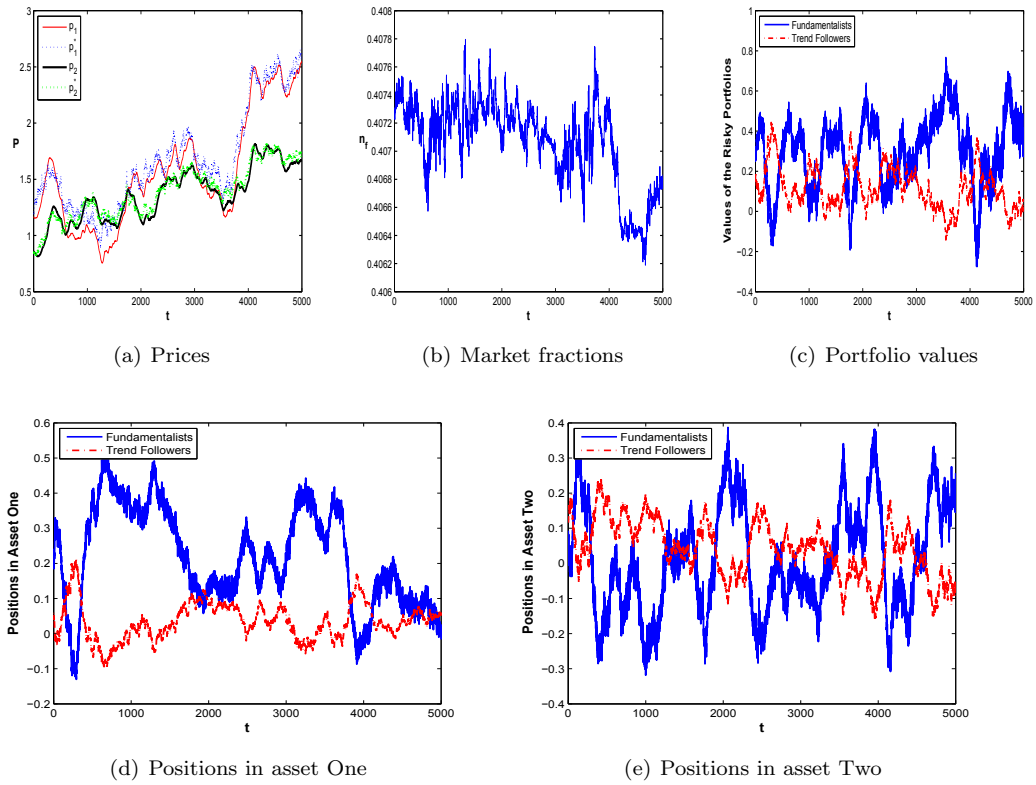

(a) Prices (b) Market fractions (c) Portfolio values

(d) Positions in asset One (e) Positions in asset Two

Figure 6.7: The time series of prices (a), market fractions of the fundamentalists (b), the portfolio values of two types of agents (c), the portfolio positions in asset one (d) and asset two (e) of the stochastic model with $\eta = 2.5$.

6.4.1 The Spill-over Effect

First, we examine the spill-over effect by exploring the joint impact of the switching intensity η and the two noise processes on the market price dynamics. To examine the impact of stability of the deterministic model on the price dynamics, in particular, the time-varying betas, for the stochastic model, with the same random draws of the dividend and supply noise processes, Fig. 6.6 plots the fundamental price (the blue and green dotted lines) and the market prices (the red and black solid lines) in (a) and (b) and the corresponding market fractions of the fundamentalists of the two-asset model for two different switching intensities η. For $\eta = 1.5$, Figs. 6.6 (a) and (c) demonstrate that the market price follows the fundamental price closely with about 40% of the fundamentalists. This is underlined by the stable fundamental steady state of the deterministic model (6.19) illustrated in Fig. 6.3 (a). For $\eta = 3.5$, Figs. 6.6 (b) and (d) indicate that the market price fluctuates around the fundamental price in a cyclical fashion with about 29% of the fundamentalists, which is underlined by the bifurcation of periodic oscillations of the

corresponding deterministic model (see Fig. 6.3 (c)). Corresponding to Fig. 6.4 for the deterministic model, Fig. 6.7 plots the time series of the prices in (a), the market fraction of the fundamentalists in (b), the portfolio values of the two agents in (c), the portfolio positions in asset one (d) and asset two (e) of the stochastic model. The large fluctuations of the stochastic model, in particular in the portfolio values and the portfolio positions, compared to the deterministic model reflect the impact of the nonlinear interaction of the spill-over effects and the noise processes.

6.4.2 Time-varying Betas

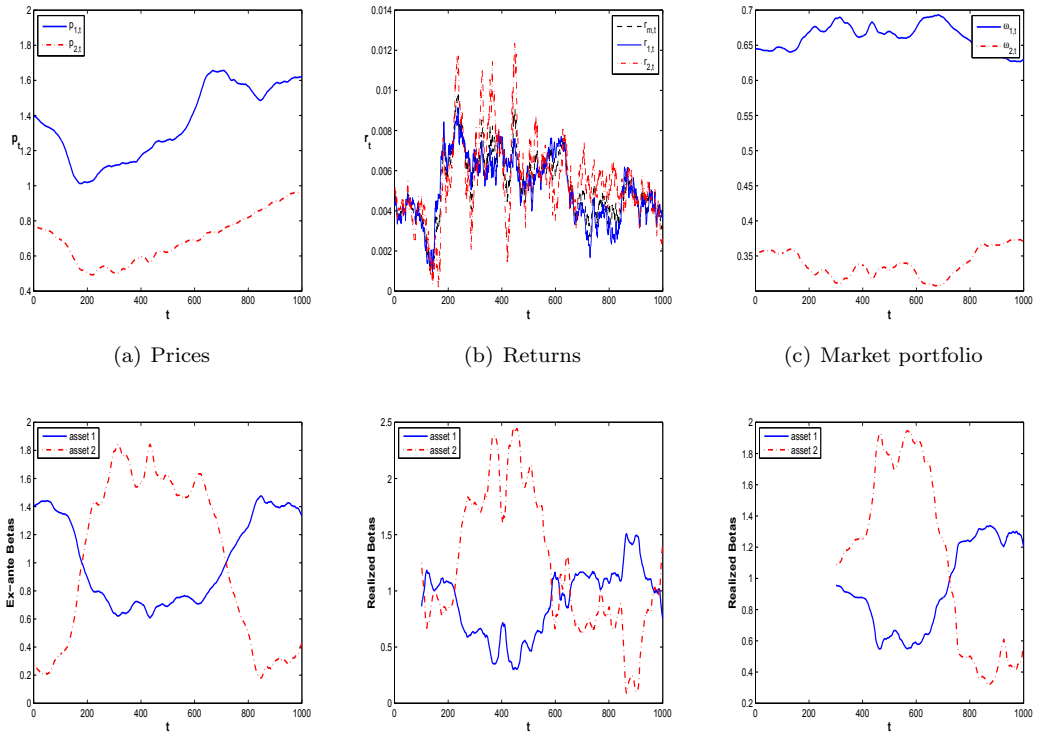

(a) Prices (b) Returns (c) Market portfolio

(d) Ex-ante betas (e) Rolling estimates of betas with rolling window of 100 (f) Rolling estimates of betas with rolling window of 300

Figure 6.8: Time series of (a) the market prices; (b) the returns; (c) the proportions of the total market wealth invested in risky assets; (d) the ex-ante betas of the risky assets; and the estimates of the betas using rolling windows of (e) 100 and (f) 300 with $\eta = 1.5$.

Next, we examine the stochastic nature of the time-varying beta coefficients of the evolutionary CAPM. The value of the market portfolio $\mathbf{s}$ at time t in the market equilibrium is given by $W_{m,t} = \mathbf{p}_t^\top \mathbf{s}$ and the payoff is $W_{m,t+1} = \mathbf{x}_{t+1}^\top \mathbf{s}$. Hence, under the consensus

belief

$$E_{a,t}(W_{m,t+1}) = E_{a,t}(\mathbf{x}_{t+1})^\top \mathbf{s}, \qquad Var_{a,t}(W_{m,t+1}) = \mathbf{s}^\top \mathbf{\Omega}_{a,t} \mathbf{s}. \tag{6.22}$$

Define the returns of risky asset j and the market portfolio m, respectively, by

$$r_{j,t+1} = \frac{x_{j,t+1}}{p_{j,t}} - 1, \qquad r_{m,t+1} = \frac{W_{m,t+1}}{W_{m,t}} - 1, \tag{6.23}$$

from which

$$E_{a,t}(r_{j,t+1}) = \frac{E_{a,t}(x_{j,t+1})}{p_{j,t}} - 1, \qquad E_{a,t}(r_{m,t+1}) = \frac{E_{a,t}(W_{m,t+1})}{W_{m,t}} - 1.$$

Following Chiarella, Dieci and He (2011), we obtain the standard CAPM-like return

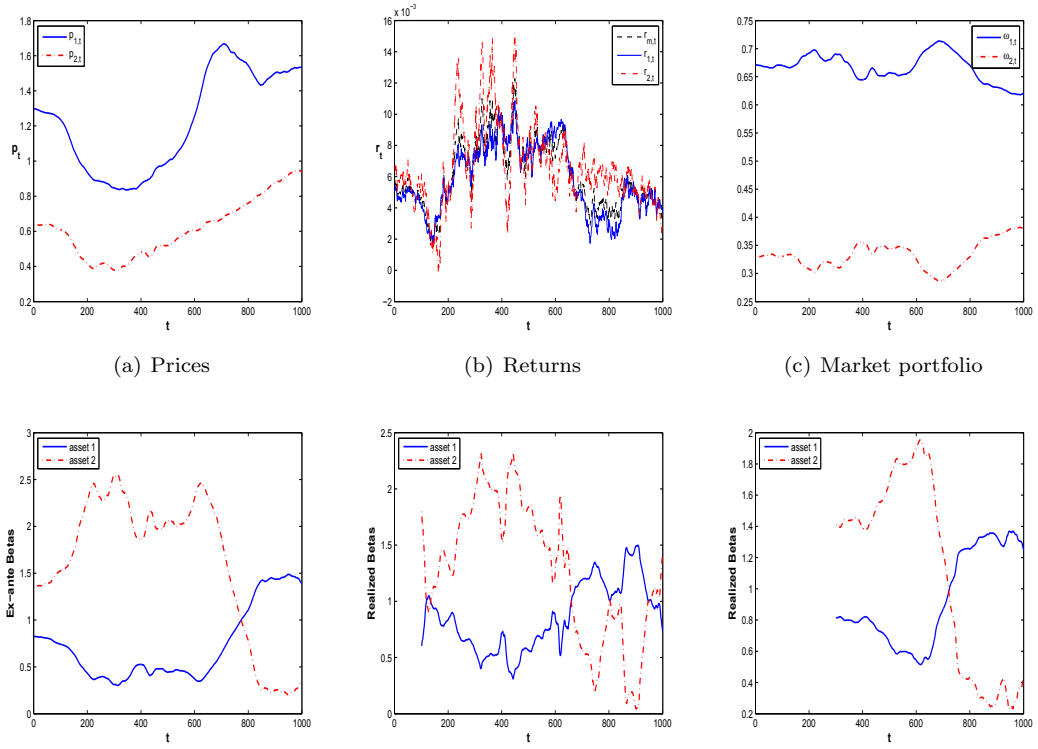

(a) Prices (b) Returns (c) Market portfolio

(d) Ex-ante betas (e) Rolling estimates of betas with rolling window of 100 (f) Rolling estimates of betas with rolling window of 300

Figure 6.9: Time series of (a) the market prices; (b) the returns; (c) the proportions of the total market wealth invested in risky assets; (d) the ex-ante betas of the risky assets; and the estimates of the betas using rolling windows of (e) 100 and (f) 300 with $\eta = 3.5$.

relation

$$E_{a,t}(\mathbf{r}_{t+1}) - r_f \mathbf{1} = \boldsymbol{\beta}_{a,t}[E_{a,t}(r_{m,t+1}) - r_f], \tag{6.24}$$

where

$$\boldsymbol{\beta}_{a,t} = (\beta_{1,t}, \cdots, \beta_{N,t})^\top, \qquad \beta_{j,t} = \frac{Cov_{a,t}(r_{m,t+1}, r_{j,t+1})}{Var_{a,t}(r_{m,t+1})} \tag{6.25}$$

are the beta coefficients in market equilibrium. Notice that the betas in Eq. (6.25) are ex-ante in the sense that they reflect the market equilibrium condition under the consensus belief $E_{a,t}$ and $\boldsymbol{\Omega}_{a,t}$. In addition, Eq. (6.23) also implies $r_{m,t+1} = \boldsymbol{\omega}_t^\top \mathbf{r}_{t+1}$, leading to $\boldsymbol{\omega}_t^\top \boldsymbol{\beta}_{a,t} = 1$, where $\boldsymbol{\omega}_t = \mathbf{P}_t \mathbf{s}/(\mathbf{p}_t^\top \mathbf{s})$ with $\mathbf{P}_t = diag[p_{1,t}, \cdots, p_{N,t}]$ are the proportions of the total wealth (ex dividend) in the economy invested in the risky assets at time t.

To examine the time-varying betas of the stochastic model, we choose two switching intensities $\eta = 1.5$ and 3.5 as before. The time series of the market prices, fractions of the fundamentalists, the proportions of the market portfolio invested in the two risky assets, the ex-ante betas of the risky assets, and the estimates of the betas using rolling windows of 100 and 300 are illustrated in Fig. 6.8 for $\eta = 1.5$ and in Fig. 6.9 for $\eta = 3.5$. For $\eta = 1.5$, the fundamental price of the deterministic model is stable, the variation of the beta coefficients in Fig. 6.8 (d) is large but less significant compared to the beta coefficients in Fig. 6.9 (d) for $\eta = 3.5$ (where the fundamental price of the deterministic model is unstable). Both the pattern and the level of the beta coefficients for $\eta = 1.5$ are very different from those for $\eta = 3.5$. More importantly, both Figs. 6.8 and 6.9 show that the rolling estimates of the betas do not necessarily reflect the nature of the ex-ante betas implied by the CAPM, which is consistent with the results in Chiarella et al. (2013). Interestingly, the estimated betas for window of 100 are more volatile compared to the ex-ante betas. However, an increase in the rolling window from 100 to 300 in (e) and (f) of Figs. 6.8 and 6.9 smooths the variations of the beta estimates significantly, leading to a similar pattern to the ex-ante betas.

6.4.3 Trading Volume and Volatility

Finally, we examine the dynamic relation between price volatility and trading volume. As in Banerjee and Kremer (2010), the price volatility is measured by the price difference $|p_{j,t} - p_{j,t-1}|$ and the trading volume at time t is defined by

$$\begin{aligned}\mathbf{X}_t = &\min\{n_{f,t-1}, n_{f,t}\}|\mathbf{z}_{f,t} - \mathbf{z}_{f,t-1}| + \min\{n_{c,t-1}, n_{c,t}\}|\mathbf{z}_{c,t} - \mathbf{z}_{c,t-1}| \\ &+ |n_{f,t} - n_{f,t-1}|\hat{\mathbf{X}}_t,\end{aligned} \tag{6.26}$$

where

$$\hat{\mathbf{X}}_t = \begin{cases} |\mathbf{z}_{f,t} - \mathbf{z}_{c,t-1}|, & n_{f,t} \geq n_{f,t-1}, \\ |\mathbf{z}_{c,t} - \mathbf{z}_{f,t-1}|, & n_{f,t} < n_{f,t-1}. \end{cases}$$

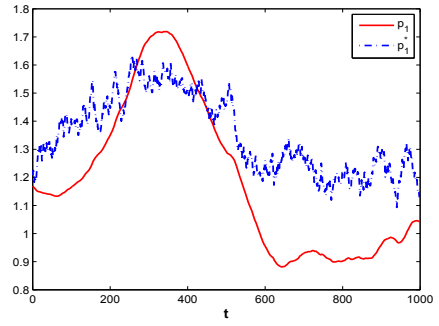

(a) Prices of asset one

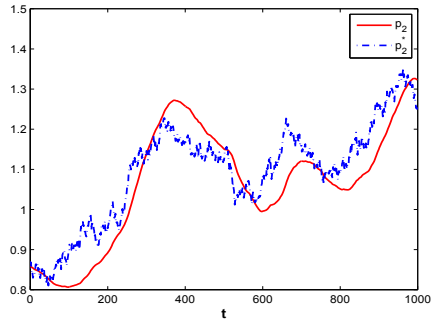

(b) Prices of asset two

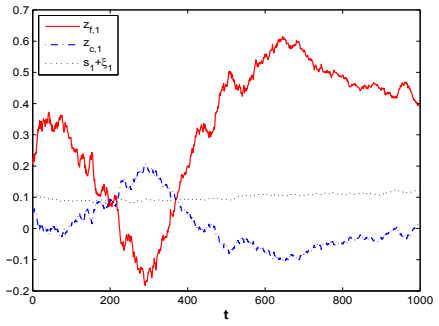

(c) The positions in asset one

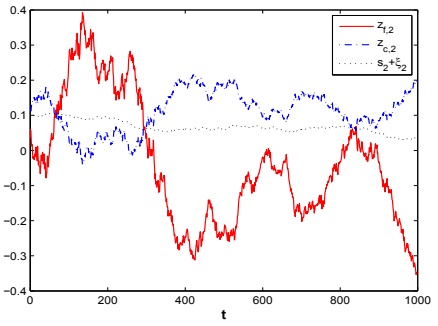

(d) The positions in asset two

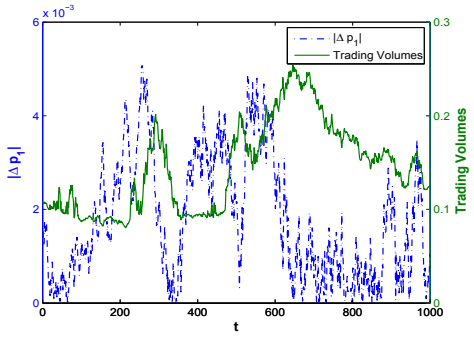

(e) Volatility and volumes of asset one

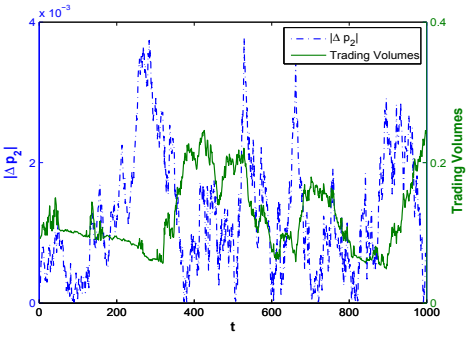

(f) Volatility and volumes of asset two

Figure 6.10: The time series of market prices and fundamental price of asset one (a) and asset two (b); the portfolio positions in asset one (c) and asset two (d); the price volatility and trading volume of asset one (e) and asset two (f). Here $\rho_{12} = 0.5$ and $\eta = 1.5$.

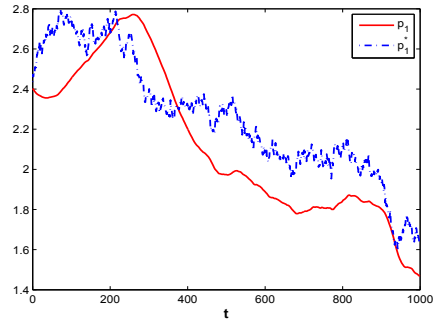

(a) Prices of asset one

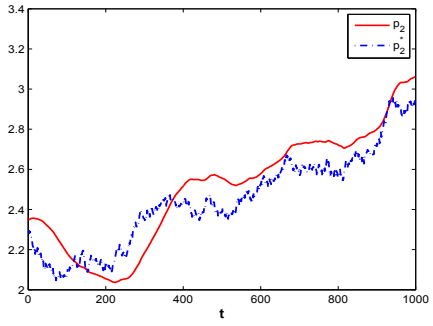

(b) Prices of asset two

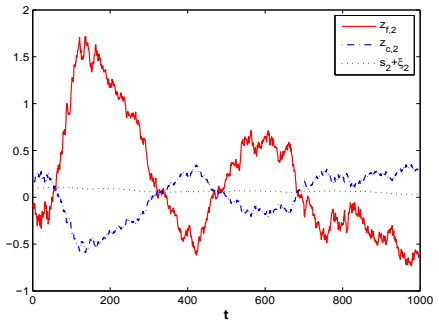

(c) The positions in asset one

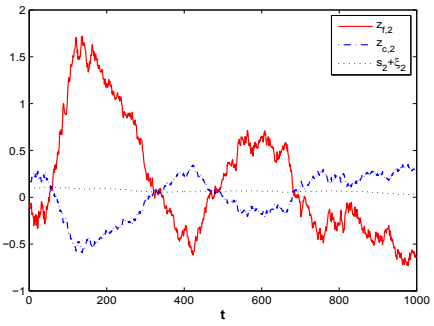

(d) The positions in asset two

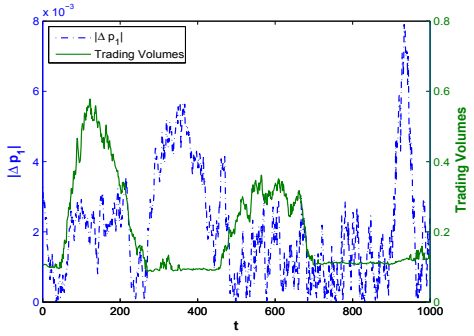

(e) Volatility and volumes of asset one

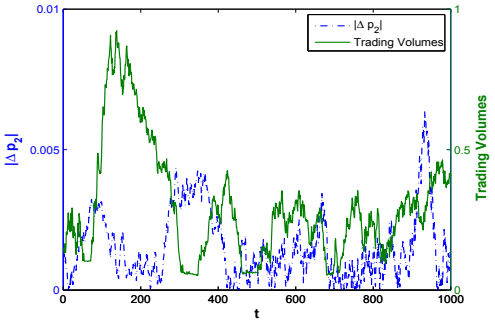

(f) Volatility and volumes of asset two

Figure 6.11: The time series of market prices and fundamental price of asset one (a) and asset two (b); the portfolio positions in asset one (c) and asset two (d); the price volatility and trading volume of asset one (e) and asset two (f). Here $\rho_{12} = -0.9$ and $\eta = 1.5$.

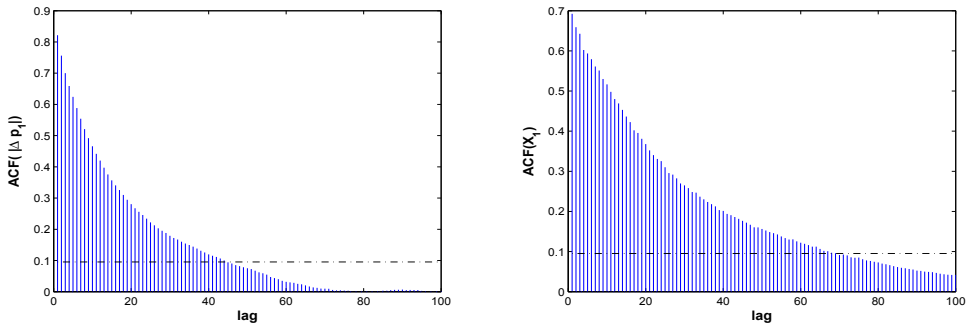

(a) The ACs of the price volatility (b) The ACs of the trading volume

Figure 6.12: The ACs of the price volatility and the trading volume of asset one with $\eta = 1.5$.

Due to the switching mechanism, the total trading volume $\mathbf{X}_t$ in (6.26) can be decomposed into three components. The first and second components correspond to the trading volume of the agents who use, respectively, the fundamental and trend following trading strategies at both time $t-1$ and t. The third component corresponds to the trading volume of those agents who change their strategies from $t-1$ to t. In particular, when $n_{f,t} > n_{f,t-1}$, a fraction of $n_{f,t} - n_{f,t-1}$ agents change their strategies from the trend following strategy at time $t-1$ (with a demand of $z_{c,t-1}$) to the fundamental strategy at time t (with a demand of $z_{f,t}$).

To explore the dynamics of the volatility and trading volume, we set $\eta = 1.5$ and choose two values of $\rho_{12} = 0.5$ and -0.9 to examine the impact of the correlation. The time series of prices, demands, price volatility and trading volumes are illustrated in Fig. 6.10 with $\rho_{12} = 0.5$ and Fig. 6.11 with $\rho_{12} = -0.9$ for a typical simulation. With the same random seeds, Figs. 6.10 and 6.11 illustrate the significant impact of the portfolio effect due to the different choices of the correlation coefficient $\rho_{12} = 0.5$ and -0.9. Figs. 6.10 and 6.11 (a) and (b) show that the market prices can deviate from the fundamental prices from time to time, though they follow each other in the long-run. Figs. 6.10 and 6.11 (c) and (d) show that the fundamentalists and trend followers take opposite positions in risky assets in general, as expected in market equilibrium with two types of agents trading against each other. Figs. 6.10 and 6.11 (e) and (f) indicate that both volatility and trading volume are persistent, which is further verified by the autocorrelations (ACs) of the price volatility and trading volume of risky asset one in Figs. 6.12 (a) and (b) respectively. The results are based on 100 numerical simulations with the same parameters but different random processes. They demonstrate that the ACs for both the volatility and trading volume are highly significant and decaying over long lags.

Intuitively, the correlation should play an important role in the relation between volatil-

ity and trading volume. With the two different values of $\rho_{12} = 0.5$ and -0.9, Figs. 6.10 and 6.11 (e) and (f) depict the relationship between the price volatility and the trading volume of the two-asset model. The observation is summarized statistically by the plot in Fig. 6.13 of the relation between the correlation coefficient ρ_{12} and the average correlation between price volatility and trading volume of the two assets (asset one in (a) and asset two in (b)) and correlation in volatility (c) and trading volumes among the two assets based on 100 simulations. We observe that the correlation between the volatility and trading volume is positive (negative) when assets are less (more) correlated, but the correlations in both volatilities and trading volumes of the two assets are high when both assets are highly correlated. The result is very intuitive; when the payoffs are less correlated in agents' beliefs, both price volatility and trading volume of the two assets are also less correlated. In summary, the persistence in price volatility and trading volume and the autocorrelation patterns in volatility and trading volume illustrated by the model are closely related to the characteristics of financial markets.

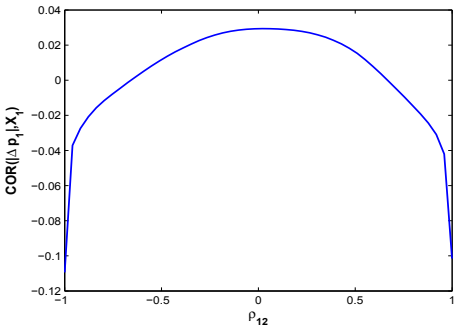

(a) Correlation between trading volume and volatility for asset one

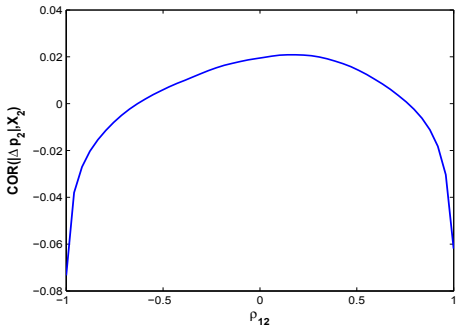

(b) Correlation between trading volume and volatility for asset two

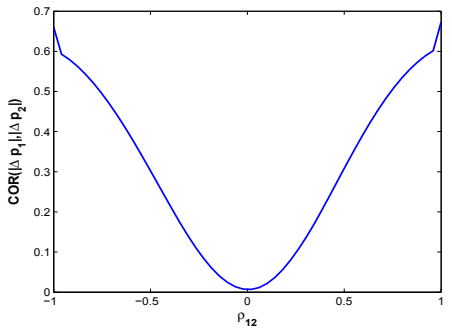

(c) The volatility correlation

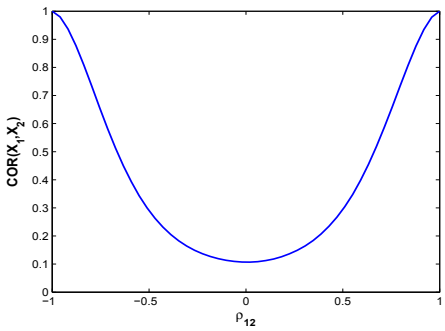

(d) The trading volume correlation

Figure 6.13: The correlation between trading volumes and volatilities for asset one (a) and asset two (b) and the correlations of price volatilities (c) and trading volumes (d) of the two risky assets. The results are based on 100 simulations with $\eta = 1.5$.

6.5 Conclusion

This chapter extends the single-period equilibrium CAPM of Chiarella et al. (2010) to a dynamic equilibrium evolutionary CAPM to incorporate adaptive switching behavior of heterogeneous agents. By analyzing the stability of the underlying deterministic model, we show that the evolutionary CAPM is capable of characterizing spill-over effects, persistence in price volatility and trading volume, and realistic correlations between price volatility and trading volume. Also, the stochastic nature of time-varying betas implied by the equilibrium model may not be consistent with the rolling window estimate of betas used in the empirical literature. The model provides further explanatory power of the recently developed HAMs.

In this chapter, the numerical analysis is focused on the case of two risky assets, though the stability analysis is conducted for any number of risky assets. It would be interesting to see how an increase in the number of risky assets could have different effects. We expect the main results obtained in this chapter to hold. The statistical analysis is mainly based on some Monte Carlo simulations and a systematical study of the empirical relevance using econometric methods would be interesting. We leave these issues to the future research.

Chapter 7

Conclusion and Future Research

The representative agent paradigm with homogeneous expectation has been the dominant framework for the development of theories in portfolio analysis, equilibrium asset pricing and no arbitrage pricing. However, despite its simplicity and analytical tractability, the assumption of homogeneous expectation is unrealistic. Empirical evidence, unconvincing justification of the assumption of unbounded rationality and investor psychology have led to the incorporation of heterogeneity in beliefs and bounded rationality into financial modelling. When agents' expectations are formulated based on historical information, the economic systems exhibit an expectation feedback mechanism and hence lagged information plays a very important role in the new paradigm. A large part of literature also shows the predictable powers of historical returns empirically. However, the impact of the historical information and especially the time horizons have not been well understood in extant literature. This thesis contributes to the development of financial market modelling and asset price dynamics with heterogeneous beliefs and time delays to tackle the above two important issues. The thesis consists of three parts. Firstly, we provide a unified approach to characterize trend chasing, adaptive switching and herding behavior in a continuous-time HAMs framework and extensively investigate the impacts of different bounded behavior on various market behavior, the stylized facts and the long range dependence in return volatility. Secondly, we extend the models in the first part to study the mechanism of momentum profitability. We provide market conditions on the momentum profitability, which underlies the time series and cross-sectional momentum effect well documented in empirical literature, and further provide an optimal investment strategy to explore the momentum and reversal effects. Thirdly, the thesis develops an evolutionary capital asset pricing model with heterogeneous beliefs. The main contributions of the three parts and related future research are summarized as follows.

7.1 Continuous-time Heterogeneous Agent Models

Most of the heterogeneous agent models developed in the literature are in discrete-time setup. Among various issues in the literature, the impact of adaptive behavior on market stability has been well studied, while the impact of lagged prices (used by chartists to form their expectations) on market stability has not been well understood due to the problem of high dimensional systems. This thesis develops a continuous-time framework to study the joint impact of lagged prices and adaptive behavior of heterogeneous agents. By using either the replicator dynamics in Chapter 2 or the master equations in Chapter 3 in population evolution literature, we extend the discrete-time HAMs to continuous-time models. The delay differential equations provide a uniform approach to study the impact of the lagged prices through a time delay parameter.

The analysis of the models provides not only some consistent results to discrete-time HAMs, such as stabilizing effect of fundamentalists, destabilizing effect of chartists, and rational routes to market instability, but also a double edged effect of an increase in lagged prices on market stability. An increase in the using of lagged prices can not only destabilize, but also stabilize the market price. More importantly, the adaptive switching and herding behavior of agents can increase market price fluctuations. By introducing market noise and fundamental noise and imposing a stochastic process on population fractions, we extensively examine how market volatility can be affected by trend chasing, adaptive switching, and herding, the most important factors as well documented and studied in the empirical literature on market volatility. We show that, both the herding and trend chasing based on long time horizon increase the fluctuations of market price deviation from the fundamental price and volatility of market return. With respect to the switching, it reduces the volatility in returns but leads to an "U"-shaped price volatility as the switching intensity increases. Therefore herding and switching have opposite effect on return volatility. We also show that, although the trend chasing, switching and herding all contribute to the power-law behavior, the significant levels for the ACs increase in the time horizon and herding, but an initial increase and then decrease when the switching intensity increases. In addition, with the herding, the market noise plays an essential role in generating the power-law behavior.

The results provide some further insights into different mechanism of generating bubbles and crashes, excess volatility, and power-law behavior in volatility. Whether a particular market is dominated by herding or switching is an empirical question which is left for future research.

7.2 The Momentum and Reversal Effects

Two of the most studied phenomena in financial market are the short run momentum and long run reversal, which have become central to the market efficiency debate. However, most behavioral models do not specify the time horizon, which plays crucial role in the performance of momentum and contrarian strategies. Based on the models in the first part, we propose a continuous-time heterogeneous agent model of investor behavior consisting of fundamental, contrarian, and momentum strategies in Chapter 4. By examining their impact on market stability explicitly and analyzing the profitability numerically, we show that the profitability of time series momentum is closely related to the market states defined by the stability of the underlying deterministic model. In particular, we show that when the momentum traders dominate the market, the momentum strategy is profitable when the time horizon is short and unprofitable when the time horizon is long. Otherwise, the momentum strategy is not profitable for any time horizon. We also provide some explanation to the profitability mechanism through autocorrelation patterns and the classical underreaction and overreaction hypotheses.

By taking advantage of the continuous-time framework in characterizing the time horizons, Chapter 5 models the drift in the standard geometric Brownian motion asset pricing model as a weighted average of mean reversion and moving average. By applying the maximum principle for control problem of SDDE, we derive the optimal strategies analytically. We show the optimality of the optimal strategy comparing to pure momentum, pure mean reversion strategies, and market index. The optimality is immune to market states, investor sentiment and market volatility. The profitability pattern reflected by the average return in most empirical literature may not reflect at portfolio wealth level.

Although the model proposed in Chapter 4 is very simple, it provides some insight into the time series momentum documented in the recent empirical literature. Motivated by the results obtained in this chapter, one can extend the market of one risky asset to the one with many risky assets so that the profitability of portfolios constructed from momentum and contrarian strategies can be examined. We expect that the same mechanism can be used to explain cross-sectional momentum. In addition, it has been shown that volatility can affect the autocorrelations in returns and hence affect profitability and even trading volume. This could be examined by using the setup in Chapter 4. The model proposed in Chapter 5 is simple and stylized. The weights to the momentum and mean reversion components are constant. When market condition changes, the weights can be different. Hence it would be interesting to model their dependence on market conditions. This can be modelled, for example, based on a replicator dynamics introduced in Chapter

2, or as a Markov switching process, or based on some rational learning process. The optimization problem is solved under log utility in this chapter, which eliminates the intertemporal effect under general power utility functions considered by Koijen et al. (2009). Furthermore, we can consider stochastic volatility models for the stock index. Finally, an extension to a multi-asset model to study the cross-sectional optimal strategies would be helpful to understand the cross sectional momentum. We leave these for future research.

7.3 The Evolutionary CAPM under Heterogeneous Beliefs

At last, the thesis extends the above single risky asset models to a multi-asset model of a dynamic equilibrium evolutionary CAPM to incorporate the adaptively switching behavior of heterogeneous agents in Chapter 6. By analyzing the stability of the underlying deterministic model, we show that the evolutionary CAPM is capable of characterizing spill-over effects, persistence in price volatility and trading volume, and realistic correlations between price volatility and trading volume. Also, the stochastic nature of time-varying betas implied by the equilibrium model may not be consistent with the rolling window estimate of betas used in the empirical literature. The model provides further explanatory power of the recently developed HAMs.

In this chapter, the numerical analysis is focused on the case of two risky assets though the stability analysis is conducted for any number of risky assets. It would be interesting to see how an increase in the number of risky assets could have different effects. We expect the main results obtained in this chapter to hold. The statistical analysis is mainly based on some Monte Carlo simulations and a systematical study of the empirical relevance using econometric methods would be interesting. We leave these issues for future research.

Appendix A

Proofs of Chapter 2

A.1 Market Fraction Dynamics

In this section, we show the consistence of (2.11) and (2.12).

On the one hand, notice that $U_i(t)$ is deterministic in (2.9), and hence it follows from (2.12) that

$$dn_f(t) = \frac{\beta e^{\beta U_f(t)} dU_f(t)[e^{\beta U_f(t)} + e^{\beta U_c(t)}] - \beta e^{\beta U_f(t)}[e^{\beta U_f(t)} dU_f(t) + e^{\beta U_f(t)} dU_c(t)]}{[e^{\beta U_f(t)} + e^{\beta U_c(t)}]^2}, \quad \text{(A.1)}$$

that is,

$$dn_f(t) = \frac{\beta e^{\beta U_f(t)} e^{\beta U_c(t)}[dU_f(t) - dU_c(t)]}{[e^{\beta U_f(t)} + e^{\beta U_c(t)}]^2}. \quad \text{(A.2)}$$

By applying (2.12) again, we have (2.11).

On the other hand, it follows from (2.11) that

$$\frac{dn_f(t)}{n_f(t)[1 - n_f(t)]} = d\beta[U_f(t) - U_c(t)], \quad \text{(A.3)}$$

that is,

$$d\Big[\ln \frac{n_f(t)}{1 - n_f(t)}\Big] = d\beta[U_f(t) - U_c(t)]. \quad \text{(A.4)}$$

Taking the integral of (A.4) yields

$$\ln \frac{n_f(t)}{1 - n_f(t)} = \beta[U_f(t) - U_c(t)] + c, \quad \text{(A.5)}$$

$$\frac{n_f(t)}{1 - n_f(t)} = e^{\beta[U_f(t) - U_c(t)] + c}, \quad \text{(A.6)}$$

$$n_f(t) = \frac{e^{\beta U_f(t)}}{e^{\beta U_f(t)} + e^{\beta U_c(t) - c}}, \tag{A.7}$$

where the constant c can be determined by the initial values.

In the rest of the chapter, we use (2.12) as the dynamics of the population fraction by choosing $c = 0$.

Alternatively, we can also choose (2.11) instead of (2.12) to characterize the dynamics of the population fraction. In this case, we may introduce new variables $\pi(t) := \pi_f(t) - \pi_c(t)$ and $U(t) := U_f(t) - U_c(t)$. Then the new system is still 4-dimensional with the state variables $\big(P(t), u(t), U(t), n_f(t)\big)$. Notice that (2.12) always has two constant solutions $n_f(t) = 0$ and $n_f(t) = 1$, so the new system has two equilibrium lines in addition to the fundamental steady state.

Appendix B

Proofs and Discussions of Chapter 3

B.1 Analytical Solution for the Master Equation

We solve the master equation using the approximation method introduced by Aoki (2002). Assume the fraction of fundamentalists in a given moment is determined by its expected mean (m), the drift, and, an additive fluctuation component s of order $1/N^{1/2}$ around this value. Thus we can write

$$\frac{N^f}{N} = m + \frac{1}{\sqrt{N}}s, \tag{B.1}$$

where s is a standard white noise. The asymptotically approximate solution of the master equation is given by the system of coupled differential equations

$$\begin{aligned} \frac{dm}{dt} &= \zeta(t)m - [\zeta(t) + \xi(t)]m^2, \\ \frac{\partial Q}{\partial t} &= [2(\zeta(t) + \xi(t))m - \zeta(t)]\frac{\partial}{\partial s}(sQ(s,t)) \\ &\quad + \frac{m[\zeta(t) + m(\xi(t) - 1)]}{2}\frac{\partial^2}{\partial s^2}Q(s,t), \end{aligned} \tag{B.2}$$

where $Q(s,t)$ is the transition density function of the spread s at time t. The first equation of (B.2) is a deterministic ordinary differential equation which displays logistic dynamics for the trend. The second equation is a second order stochastic partial differential equation, known as the *Fokker-Planck* equation that drives the spread component (i.e. the fluctuations around the trend) of the probability flow. By letting m equal to its steady state $m^* = \frac{\zeta}{\zeta+\xi}$, we have the distribution function θ for the spread s is given by

$$\theta(s) = Ce^{-\frac{s^2}{2\sigma^2}} \qquad \text{with} \qquad \sigma^2 = \frac{\zeta\xi}{(\zeta+\xi)^2}, \tag{B.3}$$

which is a Gaussian density. Therefore, the two components of the dynamics of the proportion of fundamentalists as represented by (B.1) are quantified. Accordingly the evolution of the proportion of fundamentalists is given by the trend, described by (B.2), plus a stochastic noise distributed according to (B.3). So we have (3.5). For more details, we refer to Chiarella and Di Guilmi (2011*a*).

B.2 Comparison to Chapter 2 and Nonlinear Effect of Herding

To examine the effect of herding, we present the corresponding results of no-herding model in Chapter 2. Unless specified otherwise, we choose the parameter values $k = 0.05$, $\mu = 1$, $\beta_f = 1.4$, $\beta_c = 1.4$, $C_f = 0.05$, $C_c = 0.03$, $\eta_f = 0.5$, $\eta_c = 0.6$, $\tau_f = 10$, $\tau_c = 5$, and $\bar{F} = 1$.

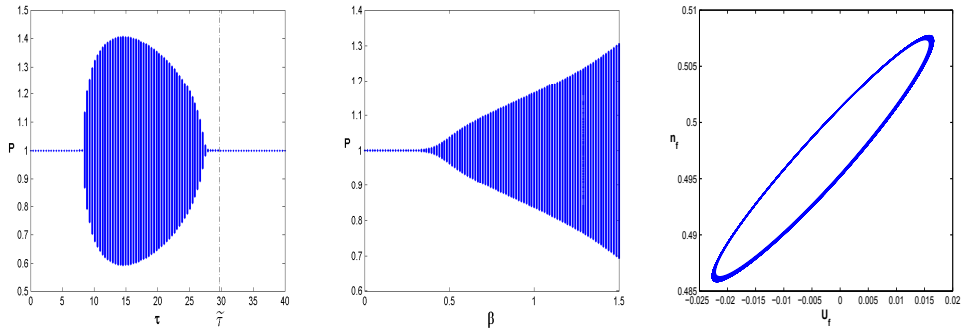

(a) Price bifurcation in τ (b) Price bifurcation in β (c) Phase plot of U_f and n_f

Figure B.1: (a) The bifurcation of the market prices with respect to τ with $\beta = 1$; (b) The bifurcation of market price with respect to β with $\tau = 8$; (c) The phase plot of the relationship between the fitness U_f and the market fraction n_f with $\tau = 16$ and $\beta = 1$ for the model in Chapter 2.

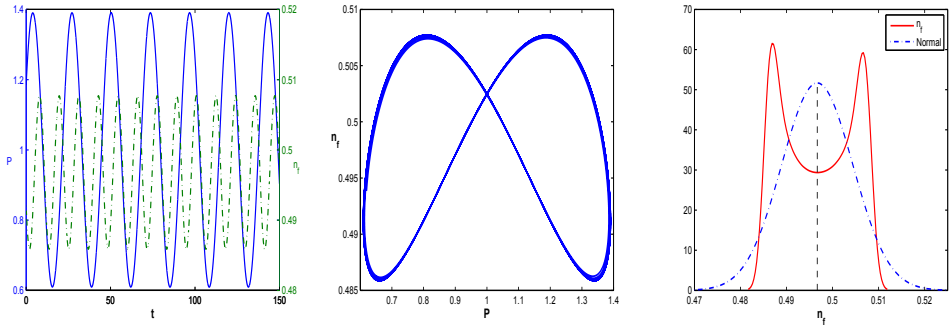

(a) Time series of P and n_f (b) Phase plot of (P, n_f) (c) The density of n_f

Figure B.2: (a) The time series of the market prices $P(t)$ (the blue solid line) and the market fraction $n_f(t)$ of fundamentalists (the green dash dot line); (b) the phase plot of $(P(t), n_f(t))$; and (c) the density distribution of the market fraction $n_f(t)$.

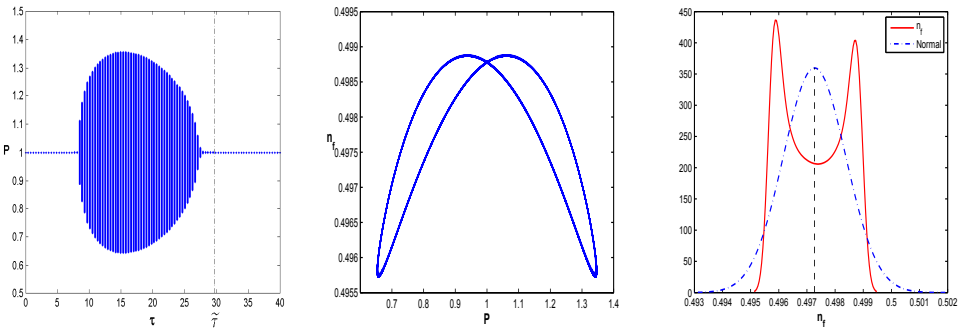

(a) Price bifurcation (b) Phase plot of (P, n_f) (c) The density of n_f

Figure B.3: (a) The bifurcation diagram of the market prices with respect to τ for model (3.8); (b) the corresponding phase plot of $(P(t), n_f(t))$ and (c) the density distribution of the market fraction $n_f(t)$ of the fundamentalists. Here $v = 0.1$ and $\tau = 16$.

B.3 Price Volatility Comparison to Chapter 2

This appendix presents some results from Chapter 2 and price volatility of the herding model.

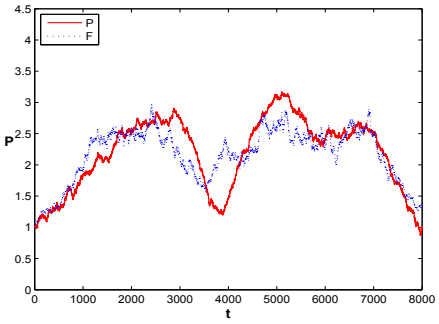

(a) Prices for $\tau = 3$

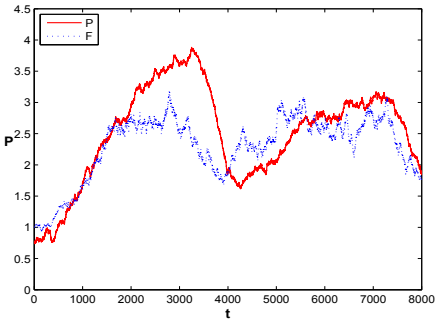

(b) Prices for $\tau = 16$

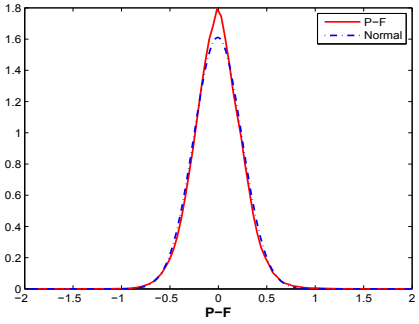

(c) Price deviation density for $\tau = 3$

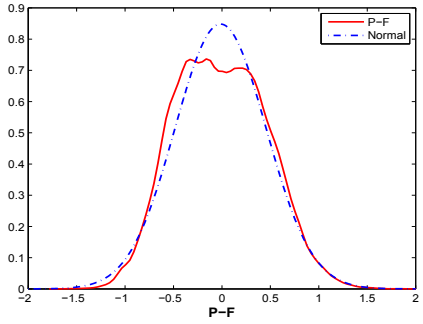

(d) Price deviation density for $\tau = 16$

Figure B.4: The time series of the fundamental price $F(t)$ (the blue dotted line) and the market prices $P(t)$ (the red solid line) with (a) $\tau = 3$ and (b) $\tau = 16$, and the distributions of the deviations of the market prices from the fundamental prices $P(t) - F(t)$ with (c) $\tau = 3$ and (d) $\tau = 16$ for the model in Chapter 2. Here $\sigma_F = 0.12$ and $\sigma_M = 0.15$.

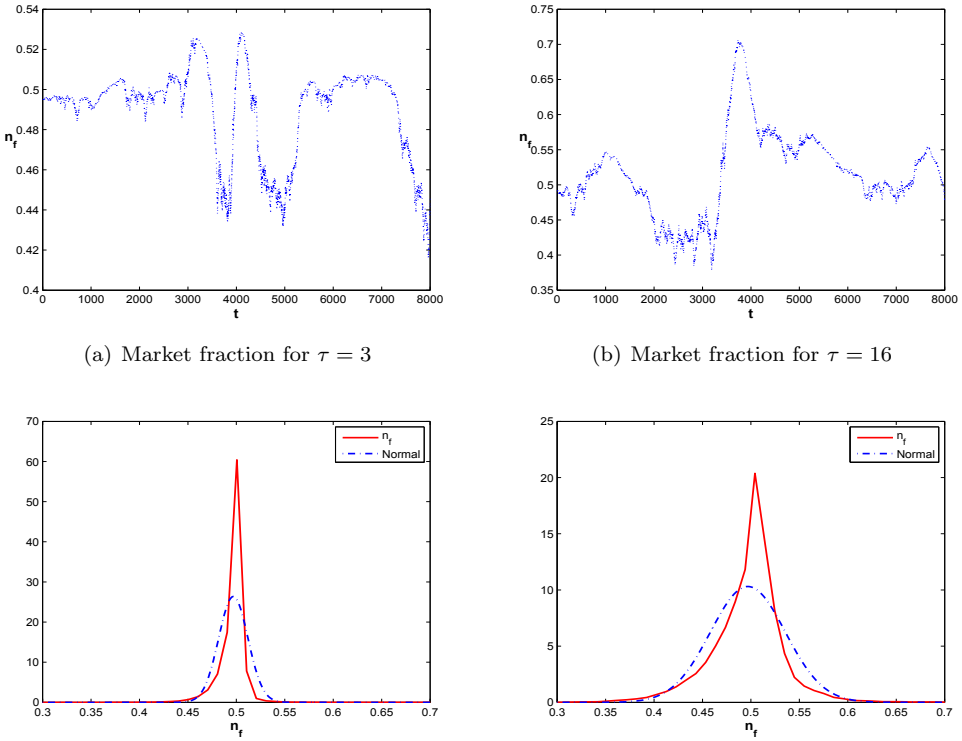

(a) Market fraction for $\tau = 3$

(b) Market fraction for $\tau = 16$

(c) Market fraction density for $\tau = 3$

(d) Market fraction density for $\tau = 16$

Figure B.5: The time series of the fractions of the fundamentalists with (a) $\tau = 3$ and (b) $\tau = 16$ and the corresponding distributions with (c) $\tau = 3$ and (d) $\tau = 16$ for the model in Chapter 2. Here $\sigma_F = 0.12$ and $\sigma_M = 0.15$.

Appendix C

Proofs and Model Extensions of Chapter 4

C.1 Time Series Momentum Profit

$(m \setminus n)$	1	3	6	12	24	36	48	60
1	1.64	3.61**	1.61	3.00***	2.01**	2.01**	1.55*	1.12
3	1.15	2.15	2.88	3.34**	2.67*	1.88	1.57	1.25
6	4.21	4.39*	5.47**	4.67**	2.74	1.77	1.67	1.37
12	9.24***	7.81***	6.72**	5.22**	2.83	1.82	1.70	1.82
24	7.20**	6.92**	5.47*	3.81	2.28	1.68	8 1.83	2.68
36	3.98	4.50	2.80	1.58	0.72	0.93	1.55	2.97
48	1.76	0.14	-1.19	-1.94	-1.59	-0.43	1.30	2.51
60	-2.55	-4.24	-4.84	-3.86	-2.11	0.07	1.80	2.74

Table C.1: The annualized percentage (log) excess returns of momentum strategies (4.2) for the S&P 500 with the horizon (m) and holding (n) from 1 to 60 months period. Note: *, **, *** denote the significance at 10%, 5% and 1% levels, respectively.

C.2 Proofs and Remarks for the Deterministic Model

The characteristic equation of the system (4.11) at the fundamental steady state $P = \bar{F}$ is given by[1]

$$\lambda + \gamma_f - \gamma_m + \gamma_c + \frac{\gamma_m}{\lambda \tau_m}(1 - e^{-\lambda \tau_m}) - \frac{\gamma_c}{\lambda \tau_c}(1 - e^{-\lambda \tau_c}) = 0. \tag{C.1}$$

For delay integro-differential equation, the eigenvalue analysis can be complicated.

[1]It is known (see Hale 1997) that the stability is characterized by the eigenvalues of the characteristic equation of the system at the steady state.

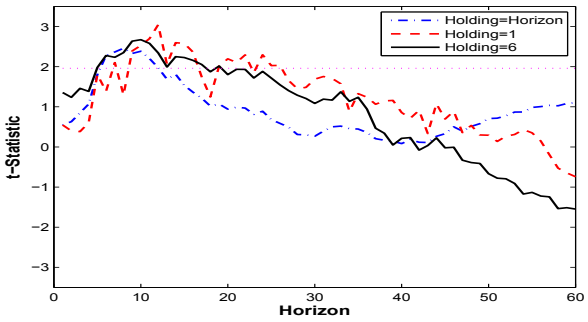

Figure C.1: The t-Statistic of the average excess return of the momentum strategies (4.2) investing the S&P 500 for time horizon from 1 to 60 months periods and holding equal to horizon ($n = m$), 1 month ($n = 1$) and 6 month periods ($n = 6$).

$(m \setminus n)$	1	3	6	12	24	36	48	60
1	1.81	3.53	3.28**	3.20***	1.78**	0.44	-0.17	-0.42
3	3.38	3.28	4.93**	4.56***	2.46*	0.33	-0.28	-0.32
6	6.35*	6.57**	6.02**	5.46**	1.75	-0.72	-1.63	-1.20
12	6.86**	7.29**	7.09**	4.74*	0.58	-2.50	-2.95**	-2.64**
24	5.22	5.28	3.94	0.82	-3.02	-4.85**	-3.97*	-2.46
36	1.32	0.24	-1.61	-4.91	-7.96***	-7.81***	-5.39**	-3.23
48	-1.46	-2.69	-4.30	-6.57**	-8.66***	-7.61***	-4.99**	-3.28
60	-2.42	-5.80	-6.47*	-6.31*	-6.97**	-5.83*	-4.14	-2.71

Table C.2: The annualized percentage (log) excess returns of momentum strategies (4.2) for the time series generated from the model in market state 3 with the horizon (m) and holding (n) from 1 to 60 months period. Note: *, **, *** denote the significance at 10%, 5% and 1% levels, respectively.

Proof of Proposition 4.1

The characteristic equation (C.1) reduces to

$$\lambda + \gamma_f + \gamma_c - \frac{\gamma_c}{\lambda\tau_c}(1 - e^{-\lambda\tau_c}) = 0, \tag{C.2}$$

which has no zero eigenvalue. The root of (C.2) has negative real part $-\gamma_f$ when $\tau_c \to 0$. Let $\lambda = i\omega(\omega > 0)$ be a root of Eq. (C.2). Substituting it into Eq. (C.2) and separating the real and imaginary parts yield

$$\omega^2\tau_c - \gamma_c(\cos\omega\tau_c - 1) = 0, \qquad \omega\tau_c(\gamma_f + \gamma_c) - \gamma_c \sin\omega\tau_c = 0,$$

which lead to

$$\omega^2\tau_c^2 + 2\tau_c\gamma_c + \tau_c^2(\gamma_f + \gamma_c)^2 = 0, \tag{C.3}$$

However equation (C.3) cannot be true for $\tau_c > 0$, hence $\lambda \neq i\omega$.

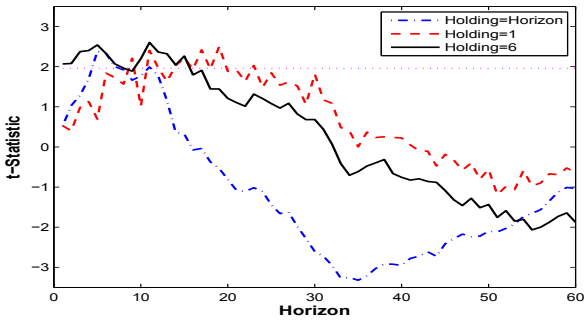

Figure C.2: The t-Statistic of the average excess return of the momentum strategy (4.2) investing in the model generated data in market state 3 for time horizon from 1 to 60 months periods and holding equal to horizon ($n = m$), 1 month ($n = 1$) and 6 month periods ($n = 6$).

It is known that, as τ_c varies, the sum of the multiplicities of roots of Eq. (C.2) in the open right half-plane can change only if a root appears on or crosses the imaginary axis (see Ruan and Wei 2003 and Li and Wei 2009). Therefore, all roots of Eq. (C.2) have negative real parts for all $\tau_c \geq 0$. This implies the local stability of the system (4.12).

Proof of Proposition 4.2

The characteristic equation (C.1) collapses to

$$\lambda + \gamma_f - \gamma_m + \frac{\gamma_m}{\lambda \tau_m}(1 - e^{-\lambda \tau_m}) = 0, \tag{C.4}$$

which has no zero eigenvalue. Substituting $\lambda = i\omega(\omega > 0)$ into Eq. (C.4) and separating the real and imaginary parts yield

$$\omega^2 \tau_m + \gamma_m(\cos \omega \tau_m - 1) = 0, \qquad \omega \tau_m(\gamma_f - \gamma_m) + \gamma_m \sin \omega \tau_m = 0. \tag{C.5}$$

Let $a = \max\{-\sin x/x; x > 0\}(\approx 0.2172)$. When $\gamma_m < \gamma_f/(1 + a)$, the two functions $y_1 := \frac{\gamma_m - \gamma_f}{\gamma_m} x$ and $y_2 := \sin x$ have no intersection for $x > 0$, hence the second equation in (C.5) cannot hold and Eq. (C.4) has no pure imaginary root. Correspondingly, Eq. (C.4) has no root appearing on the imaginary axis. In addition, Eq. (C.4) has only one negative eigenvalue when $\tau_m \to 0$. Therefore, all roots of Eq. (C.4) have negative real parts for all $\tau_m \geq 0$ when $\gamma_m < \gamma_f/(1+a)$, which leads to the local stability of the system (4.13).

Next, we consider the case of $\gamma_m \geq \gamma_f/(1 + a)$. If follows from Eq. (C.5) that

$$\omega^2 + (\gamma_f - \gamma_m)^2 - \frac{2\gamma_m}{\tau_m} = 0. \tag{C.6}$$

When $\tau_m > \tau^*_{m,1} := \frac{2\gamma_m}{(\gamma_f-\gamma_m)^2}$, Eq. (C.6) has no solution, implying that $\lambda = i\omega$ is not an eigenvalue. Hence there is no stability switching for $\tau_m > \tau^*_{m,1}$. Substituting $\lambda = \Re\{\lambda\} + i\Im\{\lambda\}$ into Eq. (C.4) and separating the real and imaginary parts yield

$$\begin{aligned} &\Re^2\{\lambda\} + \Im^2\{\lambda\} + (\gamma_f - \gamma_m)\Re\{\lambda\} + \frac{\gamma_m}{\tau_m}(1 - e^{-\Re\{\lambda\}\tau_m}\cos\Im\{\lambda\}) = 0, \\ &2\Re\{\lambda\}\Im\{\lambda\} + (\gamma_f - \gamma_m)\Im\{\lambda\} + \frac{\gamma_m}{\tau_m}e^{-\Re\{\lambda\}\tau_m}\sin\Im\{\lambda\}\tau_m = 0. \end{aligned} \tag{C.7}$$

When $\tau_m \to \infty$, if there exists a root λ with $\Re\{\lambda\} > 0$, then (C.7) reduces to

$$\begin{aligned} &\Re^2\{\lambda\} + \Im^2\{\lambda\} + (\gamma_f - \gamma_m)\Re\{\lambda\} = 0, \\ &2\Re\{\lambda\}\Im\{\lambda\} + (\gamma_f - \gamma_m)\Im\{\lambda\} = 0, \end{aligned} \tag{C.8}$$

which hold only when $\gamma_m > \gamma_f$. Note that (C.8) cannot hold with $\Re\{\lambda\} = 0$ since (C.4) has no zero eigenvalue. Therefore, (C.4) has at least one root with positive real part for $\gamma_m > \gamma_f$ and all roots with negative real parts for $\gamma_m \le \gamma_f$ when $\tau_m \to \infty$. So the fundamental steady state of system (4.13) is asymptotically stable for $\gamma_m \le \gamma_f$ and unstable for $\gamma_m > \gamma_f$ when $\tau_m > \tau^*_{m,1}$. However, if $\tau_m < \tau^*_{m,1}$, by substituting Eq. (C.6) into the first equation of (C.5) we have

$$\frac{\tau_m}{\gamma_m}(\gamma_f - \gamma_m)^2 - \cos\left[\sqrt{2\gamma_m\tau_m - (\gamma_f - \gamma_m)^2\tau_m^2}\right] - 1 = 0. \tag{C.9}$$

Let $\tau^*_{m,l}$ be the minimum positive root of (C.9). Then all the eigenvalues of Eq. (C.4) have negative real parts when $0 \le \tau_m < \tau^*_{m,l}$ and Eq. (C.4) has a pair of pure imaginary roots when $\tau_m = \tau^*_{m,l}$. In addition, it can be verified that $\Delta(\tau^*_{m,l}) := \frac{d\Re\{\lambda(\tau_m)\}}{d\tau_m}\,|_{\tau_m=\tau^*_{m,l}} \neq 0$. So $P = \bar{F}$ undergoes a Hopf bifurcation at $\tau_m = \tau^*_{m,l}$.

Furthermore, the stability switching happens only once when $\gamma_m > \gamma_f$ and only twice when $\gamma_f/(1+a) \le \gamma_m \le \gamma_f$. In fact, the stability switching[2] at a bifurcation value τ^*_m depends on the sign of $\Delta(\tau^*_m) := \frac{d\Re\{\lambda(\tau_m)\}}{d\tau_m}\,|_{\tau_m=\tau^*_m}$. An increase in τ_m near the bifurcation value τ^*_m may result in a switching of the steady state from stable to unstable when $\Delta(\tau^*_m) > 0$ and from unstable to stable when $\Delta(\tau^*_m) < 0$. For a Hopf bifurcation value τ^*_m, we have $\Delta(\tau^*_m) := \frac{d\Re\{\lambda\}}{d\tau_m}\,|_{\tau_m=\tau^*_m} = \frac{\Im^2\{\lambda\}\left(2\gamma_m-\gamma_f-\tau^*_m(\gamma_f-\gamma_m)^2\right)}{\tau^*_m\left(\left(\gamma_f-\gamma_m+\gamma_m\cos\Im\{\lambda\}\tau^*_m\right)^2+\left(2\Im\{\lambda\}-\gamma_m\sin\Im\{\lambda\}\tau^*_m\right)^2\right)}$. Let $\tau^*_{m,2} := \frac{2\gamma_m-\gamma_f}{(\gamma_f-\gamma_m)^2}$ $(< \tau^*_{m,1})$. Then $sign(\Delta(\tau^*_m)) > 0$ for $\tau^*_m < \tau^*_{m,2}$ and $sign(\Delta(\tau^*_m)) < 0$ for $\tau^*_m > \tau^*_{m,2}$, implying that an unstable fundamental steady state cannot become stable

[2]For simplicity, we arbitrarily assume that the bifurcating periodic solutions are stable and can be globally extended, which can be observed in the numerical simulations. We refer to He et al. (2009) for the computation of stability and the proof of global existence for the periodic solutions.

as τ_m varies within $(\tau^*_{m,l}, \tau^*_{m,2})$ and a stable fundamental steady state cannot become unstable as τ_m varies within $(\tau^*_{m,2}, \infty)$. When $\gamma_m > \gamma_f$, it has been proved that $P = \bar{F}$ is stable for $\tau_m < \tau^*_{m,l}$ and unstable for either τ_m in some right neighborhood of $\tau^*_{m,l}$ or $\tau_m > \tau^*_{m,1}$. Hence the stability switches only once at $\tau^*_{m,l}$, implying that $P = \bar{F}$ is unstable for $\tau_m > \tau^*_{m,l}$. Let $\tau^*_{m,h}$ be the largest of the roots of Eq. (C.9) that are less than $\tau^*_{m,1}$. When $\gamma_f/(1+a) \leq \gamma_m \leq \gamma_f$, $P = \bar{F}$ is stable for either $\tau_m < \tau^*_{m,l}$ or $\tau_m > \tau^*_{m,1}$. Due to $\tau^*_{m,h}$ is a Hopf bifurcation and $\Delta(\tau^*_{m,h}) < 0$, $P = \bar{F}$ is unstable for τ in some left neighborhood of $\tau^*_{m,h}$. Hence the stability switches only twice at $\tau^*_{m,l}$ and $\tau^*_{m,h}$, implying that $P = \bar{F}$ is unstable for $\tau^*_{m,l} < \tau_m < \tau^*_{m,h}$ and stable for either $\tau_m < \tau^*_{m,l}$ or $\tau_m > \tau^*_{m,h}$. This completes the proof.

Proof of Proposition 4.3

The characteristic equation (C.1) becomes

$$\lambda + \gamma_f - \gamma_m + \gamma_c + \frac{\gamma_m - \gamma_c}{\lambda\tau}(1 - e^{-\lambda\tau}) = 0. \tag{C.10}$$

Substituting $\lambda = i\omega(\omega > 0)$ into Eq. (C.10) and separating the real and imaginary parts yield

$$\begin{aligned} &\omega^2\tau + (\gamma_m - \gamma_c)(\cos\omega\tau - 1) = 0, \\ &\omega\tau(\gamma_f - \gamma_m + \gamma_c) + (\gamma_m - \gamma_c)\sin\omega\tau = 0. \end{aligned} \tag{C.11}$$

We first consider the case of $\gamma_m \leq \gamma_c$. In this case, the first equation of (C.11) cannot hold, meaning that equation (C.10) has no pure imaginary root. Note that (C.10) has no zero eigenvalue and the root of (C.10) is negative when $\tau \to 0$. Hence all the roots of (C.10) have negative real parts for $\tau \geq 0$, leading to the local stability of the steady state.

Second, we consider the case of $\gamma_m > \gamma_c$. In this case, if $\gamma_c < \gamma_m < \gamma_c + \gamma_f/(1+a)$ then the second equation of (C.11) cannot hold, implying that $\lambda \neq i\omega$. However, if $\gamma_m \geq \gamma_c + \gamma_f/(1+a)$, similar discussion to the Appendix C.2, we have the local stability for $\gamma_m \leq \gamma_f + \gamma_c$ and instability for $\gamma_m > \gamma_f + \gamma_c$ when $\tau > \tau_1^* := \frac{2(\gamma_m - \gamma_c)}{(\gamma_f - \gamma_m + \gamma_c)^2}$. When $\tau < \tau_l^*$, where τ_l^* is the minimum positive roof of the following equation $\frac{\tau}{\gamma_m - \gamma_c}(\gamma_f - \gamma_m + \gamma_c)^2 - \cos\left[\sqrt{2(\gamma_m - \gamma_c)\tau - (\gamma_f - \gamma_m + \gamma_c)^2\tau^2}\right] - 1 = 0$, all the eigenvalues of Eq. (C.10) have negative real parts. When $\tau = \tau_l^*$, Eq. (C.10) has a pair of purely imaginary roots.

Therefore, the stability switching happens only once when $\gamma_m > \gamma_c + \gamma_f$ and only twice when $\gamma_c + \gamma_f/(1+a) \leq \gamma_m < \gamma_c + \gamma_f$, and consequently completes the proof.

Some Remarks on Proposition 4.3

These remarks provide some properties on the nature of bifurcations related to Proposition 4.3, including the number of bifurcations, stability switching and the dependence of the bifurcation values on the parameters of the model.

First, it follows from the proof of Proposition 4.3 that all the roots of $h(\tau)$ except $\tau = \tau_1^*$ are Hopf bifurcation values. Note that $h(\tau_1^*) = 0$. However, we know that $\omega = 0$ if and only if $\tau = \tau_1^*$. Hence τ_1^* is not a bifurcation value.

Second, when $\gamma_c + \gamma_f/(1+a) \leq \gamma_m < \gamma_c + \gamma_f$, the number of bifurcations defined by $h(\tau^*) = 0$ is odd. Indeed, it follows from $h'(\tau_1^*) = \frac{-\gamma_f[2(\gamma_m-\gamma_c)-\gamma_f]}{\gamma_m-\gamma_c} < 0$ that $h(\tau_1^* - 0) > 0$. Note that $h(0) < 0$, $h(\tau)$ is continuous and $y = h(\tau)$ is not tangent to $y = 0$ when $| \frac{\gamma_f}{\gamma_m-\gamma_c} - 1 | \neq \frac{2}{(1+2k)\pi}$, $k = 0, 1, 2, \cdots$. Therefore if $| \frac{\gamma_f}{\gamma_m-\gamma_c} - 1 | \neq \frac{2}{(1+2k)\pi}$, then $h(\tau)$ has odd roots when $\tau \in (0, \tau_1^*)$, that is, the number of the Hopf bifurcation that the fundamental steady state price $P = \bar{F}$ undergoes in the interval $(0, \tau_1^*)$ must be odd. Furthermore, the number of the Hopf bifurcation that the fundamental steady state price $P = \bar{F}$ can undergo in the interval $(0, \tau_1^*)$ increases when $\gamma_f + \gamma_c \to \gamma_m$. In fact, we have $h'(\tau) = \frac{\gamma_m-\gamma_c-(\gamma_f-\gamma_m+\gamma_c)^2\tau}{\sqrt{2(\gamma_m-\gamma_c)\tau-(\gamma_f-\gamma_m+\gamma_c)^2\tau^2}} \sin\sqrt{2(\gamma_m-\gamma_c)\tau-(\gamma_f-\gamma_m+\gamma_c)^2\tau^2}$. When $\gamma_f + \gamma_c \to \gamma_m$, $\max_\tau \left\{\sqrt{2(\gamma_m-\gamma_c)\tau-(\gamma_f-\gamma_m+\gamma_c)^2\tau^2}\right\} \to \infty$, hence the sign of $h'(\tau)$ can change many times. This implies that the number of roots of $h(\tau)$ increases in this case. Despite the facts that the number of bifurcations defined by $h(\tau^*) = 0$ is odd and the number of the Hopf bifurcation increases when $\gamma_f + \gamma_c \to \gamma_m$, Proposition 4.3 shows that the stability switches only twice. This is verified numerically in Fig. 4.2 and Fig. C.3. In Fig. 4.2 (a), there are three Hopf bifurcation values, while in Fig. C.3 (a), there are five bifurcation values. However, the stability switches only twice in Fig. 4.2 (b) and Fig. C.3 (b).

Finally, the first bifurcation value τ_l^* depends on the population fractions, the extrapolation rates and the speed of the price adjustment. It increases as γ_f or γ_c increase, or γ_m decreases, however it is always bounded away from zero and infinity. In fact, when $\gamma_m \geq \gamma_c + \gamma_f/(1+a)$, let $x = \sqrt{2(\gamma_m-\gamma_c)\tau-(\gamma_f-\gamma_m+\gamma_c)^2\tau^2}$. Solving τ then leads to $\tau(x) = \frac{\gamma_m-\gamma_c}{(\gamma_f-\gamma_m+\gamma_c)^2} - \sqrt{\frac{(\gamma_m-\gamma_c)^2}{(\gamma_f-\gamma_m+\gamma_c)^4} - \frac{x^2}{(\gamma_f-\gamma_m+\gamma_c)^2}}$. Note that $\tau = 0$ implies $x = 0$ and $x(\tau)$ is an increasing function of τ. Hence the first bifurcation value τ_l^* corresponds the minimum positive root x_l^* of the following function $h(x) = -\sqrt{1 - \frac{(\gamma_f-\gamma_m+\gamma_c)^2x^2}{(\gamma_m-\gamma_c)^2}} - \cos x = 0$. It can be shown that $\frac{\pi}{2} < x_l^* < \pi$ and while $| \frac{\gamma_f-\gamma_m+\gamma_c}{\gamma_m-\gamma_c} |$ decreases, x_l^* increases, implying that τ_l^* increases. Therefore, when $\gamma_c + \gamma_f/(1+a) \leq \gamma_m \leq \gamma_c + \gamma_f$, the first bifurcation value τ_l^* increases as either γ_f or γ_c decrease, or γ_m increases. When $\gamma_m > \gamma_c + \gamma_f$, the first bifurcation value τ_l^* increases as either γ_f or γ_c increase, or γ_m decreases. Furthermore, let $x_{min} = \{\sqrt{1-ax^2} + \cos x = 0 \mid \frac{\pi}{2} < x < \pi\} (\approx 2.5536)$. Because of $\frac{\gamma_f-\gamma_m+\gamma_c}{\gamma_m-\gamma_c} < a$, we

have $x_{min} < x_l^* < \pi$, implying $\tau(x_{min}) < \tau_l^* < \tau(\pi)$, where

$$\tau(x_{min}) = \frac{\gamma_m - \gamma_c}{(\gamma_f - \gamma_m + \gamma_c)^2} - \sqrt{\frac{(\gamma_m - \gamma_c)^2}{(\gamma_f - \gamma_m + \gamma_c)^4} - \frac{x_{min}^2}{(\gamma_f - \gamma_m + \gamma_c)^2}},$$

$$\tau(\pi) = \frac{\gamma_m - \gamma_c}{(\gamma_f - \gamma_m + \gamma_c)^2} - \sqrt{\frac{(\gamma_m - \gamma_c)^2}{(\gamma_f - \gamma_m + \gamma_c)^4} - \frac{\pi^2}{(\gamma_f - \gamma_m + \gamma_c)^2}}.$$

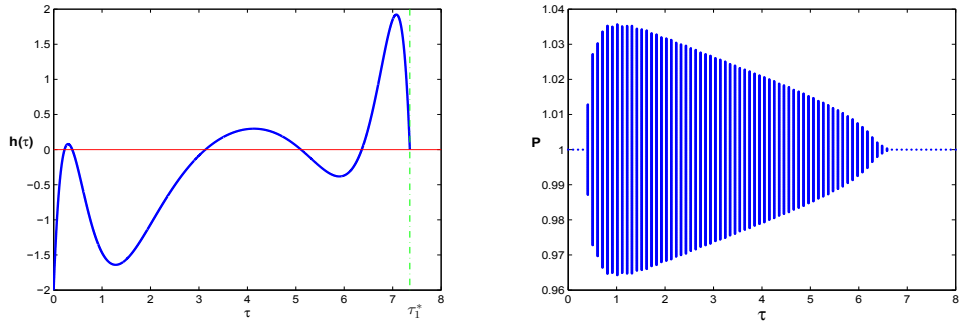

(a) The function $h(\tau)$ (b) Price bifurcation

Figure C.3: (a) The function $h(\tau)$; (b) the bifurcation diagram of the market price. Here $\gamma_f = 20$, $\gamma_m = 22.8$ and $\gamma_c = 5$.

C.3 The General Case with Any Positive τ_m and τ_c

In the general case, the market stability of the system (4.11) can be characterized by the following proposition.

Proposition C.1 *The fundamental steady state price of the system* (4.11) *is*

(i) asymptotically stable for all $\tau_m, \tau_c \geq 0$ *when* $\gamma_m < \gamma_c + \frac{\gamma_f}{1+a}$;

(ii) asymptotically stable for either $0 \leq \tau_m, \tau_c < \tau_l^*$ *or* $\tau_m, \tau_c > \tau_h^*$ *when* $\gamma_c + \frac{\gamma_f}{1+a} \leq \gamma_m \leq \gamma_c + \gamma_f$; *and*

(iii) asymptotically stable for $\tau_m, \tau_c < \tau_l^*$ *when* $\gamma_m > \gamma_c + \gamma_f$.

Proof 1 *We first consider the case of* $\gamma_m \leq \gamma_c + \gamma_f/(1+a)$.[3] *Suppose there exist* $\tau_m^{(1)} \geq 0$ *and* $\tau_c^{(1)} \geq 0$ *such that the fundamental steady state* $P = \bar{F}$ *of system* (4.11) *is unstable for the delay pair* $(\tau_m, \tau_c) = \left(\tau_m^{(1)}, \tau_c^{(1)}\right)$. *Without loss of generality, assume* $\tau_m^{(1)} > \tau_c^{(1)}$.

[3]Assume arbitrarily again that the stable periodic solutions bifurcating from the Hopf bifurcation can be extended with respect to the time horizons.

Proposition 4.3 implies $P = \bar{F}$ is stable when $(\tau_m, \tau_c) = \left(\tau_c^{(1)}, \tau_c^{(1)}\right)$. If $P = \bar{F}$ is stable when $(\tau_m, \tau_c) = \left(\frac{\tau_m^{(1)}+\tau_c^{(1)}}{2}, \tau_c^{(1)}\right)$, then let $(\tau_m^{(2)}, \tau_c^{(2)}) = \left(\tau_m^{(1)}, \frac{\tau_m^{(1)}+\tau_c^{(1)}}{2}\right)$. Otherwise, let $(\tau_m^{(2)}, \tau_c^{(2)}) = \left(\frac{\tau_m^{(1)}+\tau_c^{(1)}}{2}, \tau_c^{(1)}\right)$. So $P = \bar{F}$ is stable when $(\tau_m, \tau_c) = \left(\tau_c^{(2)}, \tau_c^{(2)}\right)$ and unstable when $(\tau_m, \tau_c) = \left(\tau_m^{(2)}, \tau_c^{(2)}\right)$. Repeating the above process, we have a sequence of nested closed intervals $[\tau_c^{(1)}, \tau_m^{(1)}] \supset [\tau_c^{(2)}, \tau_m^{(2)}] \supset [\tau_c^{(3)}, \tau_m^{(3)}] \supset \cdots$ and $\lim_{n\to\infty}(\tau_m^{(n)} - \tau_c^{(n)}) = 0$.[4] By the nested interval theorem, there exists a $\tau^{(\infty)} \in [\tau_c^{(n)}, \tau_m^{(n)}]$ such that $\tau_m^{(n)} \to \tau^{(\infty)}$ as $n \to \infty$. So $P = \bar{F}$ is unstable when $(\tau_m, \tau_c) = \left(\tau^{(\infty)}, \tau^{(\infty)}\right)$, which contradicts Proposition 4.3. Therefore, $P = \bar{F}$ is stable for all $\tau_m, \tau_c \geq 0$ when $\gamma_m \leq \gamma_c + \gamma_f/(1+a)$.

Similarly, items (ii) and (iii) can be proved.

Simulations (not reported here) show that if momentum traders do not dominate the market ($\gamma_m \leq \gamma_c + \gamma_f$), then momentum traders always lose no matter how long time horizons are used, and contrarians can make profits when τ_m and τ_c are large, and lose when τ_c is small and τ_m is large. If momentum traders dominate the market ($\gamma_m > \gamma_c + \gamma_f$), then, for any given $\tau_c > 0$, momentum strategy is profitable when τ_m is small and unprofitable when τ_m is big; and the profitabilities for contrarians are opposite for any given $\tau_m > 0$. These results are consistent with the analysis in Section 4.5.

C.4 Population Evolution between Momentum and Contrarian Traders

To focus on the impact of time horizons, we consider a special case of fixed market fractions in previous sections, which have shown that the time horizons and the joint impact of different traders play very important roles in the stability of market price and profitability. In this section we investigate the impact of population evolution on the market price and profitability. The switching mechanism follows the modelling in Chapter 2.

Let $q_f(t)$, $q_m(t)$ and $q_c(t)$ be the market fractions of fundamentalists, momentum traders and contrarians respectively. We first suppose there is no switching between fundamentalists and chartists and choose constant market fraction of fundamentalists $q_f(t) = \alpha_f$. Assume the market fractions of the two kinds of chartists have a fixed component and a time varying component. Let m_m and m_c be the fixed proportions of momentum and contrarian traders who stay with their strategy over time, respectively. Then $1-\alpha_f-m_m-m_c$ is the proportion of chartists who may switch from one strategy to the other: we denote them as *switching or adaptively rational* chartists. Among switching

[4] If $\frac{\tau_m^{(n)}+\tau_c^{(n)}}{2}$ is a bifurcation value, then by the definition of bifurcation, we can choose a proper value close to it as $\tau_m^{(n+1)}$ (or $\tau_c^{(n+1)}$) such that $P = \bar{F}$ is stable when $(\tau_c, \tau_m) = (\tau_c^{(n+1)}, \tau_c^{(n+1)})$ and unstable when $(\tau_c, \tau_m) = (\tau_c^{(n+1)}, \tau_m^{(n+1)})$.

chartists, denote by $n_m(t)$ and $n_c(t) = 1 - n_m(t)$ the proportions of momentum and contrarian traders at time t, respectively. Therefore, $q_m(t) = m_m + (1 - \alpha_f - m_m - m_c)n_m(t)$ and $q_c(t) = m_c + (1 - \alpha_f - m_m - m_c)n_c(t)$. The net profits of the momentum and contrarian strategies over a short time interval $[t - dt, t]$ can be measured respectively by $\pi_m(t)dt = D_m(t)dP(t) - C_m dt$ and $\pi_c(t)dt = D_c(t)dP(t) - C_c dt$, where $C_m,\ C_c \geq 0$ are constant costs of the strategies per unit time. To measure performance of the strategies, we introduce a cumulated profits by $U_i(t) = \eta \int_{-\infty}^{t} e^{-\eta(t-s)}\pi_i(s)ds$, $i = m, c$, where $\eta > 0$ represents a decay parameter of the historical profits. That is the performance is defined by a cumulated net profit of the strategy decaying exponentially over all past time. Consequently, $dU_i(t) = \eta\big[\pi_i(t) - U_i(t)\big]dt$, $i = m, c$. Following Hofbauer and Sigmund (1998) (Chapter 7), the evolution dynamics of the market populations are governed by $dn_i(t) = \beta n_i(t)[dU_i(t) - d\bar{U}(t)]$, $i = m, c$, where $d\bar{U}(t) = n_m(t)dU_m(t) + n_c(t)dU_c(t)$ is the average performance of the two strategies and the switching intensity $\beta > 0$ is a constant, measuring the intensity of choice. In particular, if $\beta = 0$, there is no switching between strategies, while for $\beta \to \infty$ all agents switch immediately to the better strategy.

To sum up, by letting $U(t) = U_m(t) - U_c(t)$, $\pi(t) = \pi_m(t) - \pi_c(t)$ and $C = C_m - C_c$, the market price of the risky asset is determined according to the following stochastic delay integro-differential system

$$\begin{cases} dP(t) = \mu\Big[q_f(t)D_f(t) + q_m(t)D_m(t) + q_c(t)D_c(t)\Big]dt + \sigma_M dW_M(t), \\ dU(t) = \eta\Big[\pi(t) - U(t)\Big]dt, \end{cases} \tag{C.12}$$

where

$$\begin{aligned} &q_f(t) = \alpha_f, \qquad q_m(t) = m_m + (1 - \alpha_f - m_m - m_c)n_m(t), \\ &q_c(t) = m_c + (1 - \alpha_f - m_m - m_c)\big(1 - n_m(t)\big), \qquad n_m(t) = \frac{1}{1 + e^{-\beta U(t)}}, \\ &D_f(t) = \beta_f\big(F(t) - P(t)\big), \qquad D_m(t) = \tanh\Big(\beta_m\big(P(t) - \frac{1}{\tau_m}\int_{t-\tau_m}^{t} P(s)ds\big)\Big), \\ &D_c(t) = \tanh\Big(-\beta_c\big(P(t) - \frac{1}{\tau_c}\int_{t-\tau_c}^{t} P(s)ds\big)\Big), \\ &\pi(t) = \mu\big[q_f(t)D_f(t) + q_m(t)D_m(t) + q_c(t)D_c(t)\big]\big[D_m(t) - D_c(t)\big] - C. \end{aligned}$$

Dynamics of the Deterministic Model

The deterministic skeleton of (C.12) is given by

$$\begin{cases} \dfrac{dP}{dt} = \mu\Big[q_f(t)D_f(t) + q_m(t)D_m(t) + q_c(t)D_c(t)\Big]dt, \\ \dfrac{dU}{dt} = \eta\Big[\pi(t) - U(t)\Big], \end{cases} \tag{C.13}$$

whose steady state is $(P, U) = (\bar{F}, -C)$, consisting of the constant fundamental price and the strategy cost disparity.

If there is no intensity of choice, that is $\beta = 0$, then the system (C.13) reduces to the constant population model (4.11) with the constant market population fractions of the three kinds of agents $(\alpha_f, \alpha_m, \alpha_c) = (\alpha_f, \frac{1-\alpha_f+m_m-m_c}{2}, \frac{1-\alpha_f-m_m+m_c}{2})$. For the case of $\beta > 0$, at the fundamental steady state, the proportions of the switching momentum and contrarian traders are $\frac{1}{1+e^{\beta C}} := n_m^*$ and $\frac{1}{1+e^{-\beta C}} := n_c^*$ respectively, and hence the market fractions of momentum and contrarian traders become $q_m(t) = m_m + \frac{1-\alpha_f-m_m-m_c}{1+e^{\beta C}} := \alpha_m^*$ and $q_c(t) = m_c + \frac{1-\alpha_f-m_m-m_c}{1+e^{-\beta C}} := \alpha_c^*$ respectively. Obviously, when $C = 0$, $n_m^* = n_c^* = \frac{1}{2}$ for any β. This makes sense because the difference in profits is zero at the fundamental steady state. However, if $C > 0$, that is costs for momentum strategy exceed the costs for contrarian trading rules, then there are more contrarians than momentum traders among the switching chartists at the fundamental steady state, i.e., $n_c^* \geq n_m^*$. (If $C < 0$, then $n_c^* \leq n_m^*$.) Furthermore, when $C > 0$, an increase in β leads to a decrease in n_m^*, the fraction using the expensive momentum strategy. This makes economic sense. There is no point in paying any cost at a fundamental steady state for a trading strategy that yields no extra profit at that fundamental steady state. As intensity of choice β increases, the mass on the most profitable strategy in net terms increases.

We still use $\gamma_i,\ i = f, m, c$ to characterize the activity of type-i agent, where $\gamma_f = \mu\alpha_f\beta_f$, $\gamma_m = \mu\alpha_m^*\beta_m$ and $\gamma_c = \mu\alpha_c^*\beta_c$. Then the characteristic equation of the system (C.13) at the fundamental steady state $(P, U) = (\bar{F}, -C)$ is given by

$$(\lambda + \eta)\Big(\lambda + \gamma_f - \gamma_m + \gamma_c + \frac{\gamma_m}{\lambda\tau_m}(1 - e^{-\lambda\tau_m}) - \frac{\gamma_c}{\lambda\tau_c}(1 - e^{-\lambda\tau_c})\Big) = 0. \tag{C.14}$$

Notice $\eta > 0$ and the second multiplication factor of Eq. (C.14) shares the same form as the characteristic equation (C.1) except for the expression of γ_m and γ_c. So the price dynamics of the system (C.13) can be characterized by Proposition C.1.

Simulations show that the population evolution can enlarge the period and oscillation amplitude of the market price (not reported here). We choose $\alpha_f = 0.3$, $m_m = 0.3$,

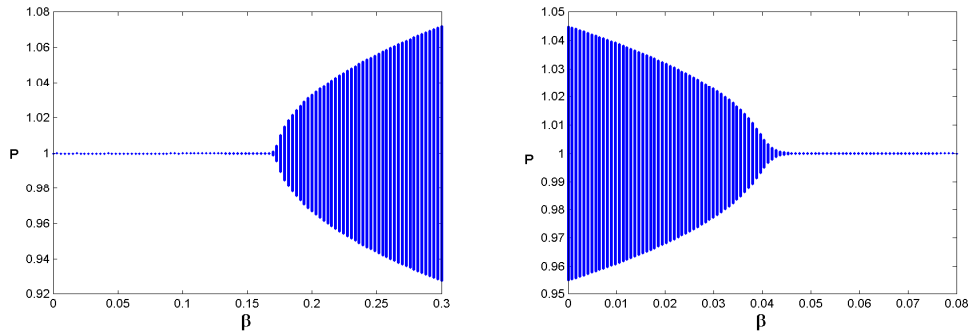

(a) $\beta_f = 4.7$, $\beta_m = 7.5$, $\beta_c = 6.7$ and $C = -2$ (b) $\beta_f = 3.33$, $\beta_m = 7.5$, $\beta_c = 6.67$ and $C = 2$

Figure C.4: Price bifurcation with respect to β for (a) $C < 0$ and (b) $C > 0$.

$m_c = 0.2$, $\mu = 10$, $\eta = 0.5$, $\tau_m = 1.2$, $\tau_c = 1.2$ and $\bar{F} = 1$. When $\beta = 0$, we have $\gamma_m < \gamma_c + \gamma_f/(1+a)$ and Proposition C.1 (i) shows that the steady state of the system (C.13) is stable for all $\tau_m, \tau_c \geq 0$. However, one can verify that $\gamma_m > \gamma_c + \gamma_f/(1+a)$ when the intensity of choice β is greater than 0.11. Proposition C.1 (ii) and (iii) demonstrate that the steady state is unstable when $\tau_m, \tau_c \in (\tau_l^*, \tau_h^*)$. The results are illustrated in Fig. C.4 (a). On the other hand, when $C > 0$, an increase in the intensity of choice β may stabilize the unstable market price as shown in Fig. C.4 (b). When the intensity of choice is small ($\beta < 0.12$), the market price is unstable. With the increase in β, the market price becomes stable. Therefore, the population evolution has a conditional impact on the market stability.

Profitability

The results of profitability are similar to those for the no switching model (4.10) when the switching intensity β is not too large, and hence we do not report them. In addition, we find that the switching can enlarge the profits and losses by choosing the same parameters (the market fraction parameters being chosen to satisfy $\alpha_j = \alpha_j^*$, $j = m, c$) for the no switching model (4.10) and switching model (C.12).

C.5 Population Evolution among Fundamentalist, Momentum and Contrarian Traders

Let $q_f(t) = m_f + (1 - m_f - m_m - m_c) n_f(t)$ where m_f is the fixed proportion of fundamentalists who stay with their strategy over time and $n_f(t)$ is the proportion of fundamentalists among the switching traders. The technique of modelling population evolution among

fundamentalist, momentum and contrarian traders in this section is the same as previous section. Then the market price of the risky asset is determined according to the following stochastic delay integro-differential system

$$\begin{cases} dP(t) = \mu\Big[q_f(t)D_f(t) + q_m(t)D_m(t) + q_c(t)D_c(t)\Big]dt + \sigma_M dW_M(t), \\ dU_1(t) = \eta\Big[\pi_1(t) - U_1(t)\Big]dt, \\ dU_2(t) = \eta\Big[\pi_2(t) - U_2(t)\Big]dt, \end{cases} \tag{C.15}$$

where

$$\begin{aligned} &q_f(t) = 1 - q_m(t) - q_c(t), \qquad q_m(t) = m_m + (1 - m_f - m_m - m_c)n_m(t), \\ &q_c(t) = m_c + (1 - m_f - m_m - m_c)n_c(t), \qquad n_m(t) = \frac{1}{1 + e^{\beta U_1(t)} + e^{\beta(U_1(t) - U_2(t))}}, \\ &n_c(t) = \frac{1}{1 + e^{\beta U_2(t)} + e^{\beta(U_2(t) - U_1(t))}}, \\ &\pi_1(t) = \mu\big[q_f(t)D_f(t) + q_m(t)D_m(t) + q_c(t)D_c(t)\big]\big[D_f(t) - D_m(t)\big] - C_1, \\ &\pi_2(t) = \mu\big[q_f(t)D_f(t) + q_m(t)D_m(t) + q_c(t)D_c(t)\big]\big[D_f(t) - D_c(t)\big] - C_2. \end{aligned}$$

The steady state of the deterministic part of the system (C.15) is $(P, U_1, U_2) = (\bar{F}, -C_1, -C_2)$ and the dynamics can be also characterized by Proposition C.1.

The profitability property is consistent with that in Appendix C.4.

Appendix D

Proofs and Discussions of Chapter 5

D.1 Properties of the Solutions to the System (5.2)-(5.3)

Let $C([-\tau,0],R)$ be the space of all continuous functions $\varphi:[-\tau,0]\to R$. For a given initial condition $S_t=\varphi_t$, $t\in[-\tau,0]$ and $\mu_0=\hat{\mu}$, the following proposition shows that the system (5.2)-(5.3) admits pathwise unique solutions such that $S_t>0$ almost surely for all $t\geq 0$ whenever $\varphi_0>0$ almost surely.

Proposition D.1 *The system* (5.2)-(5.3) *has a pathwise unique solution* (S,μ) *for a given* $\mathcal{F}_0$*-measurable initial process* $\varphi:\Omega\to C([-\tau,0],R)$. *Furthermore, if* $\varphi_0>0$ *a.s., then* $S_t>0$ *for all* $t\geq 0$ *a.s..*

Proof 2 *Let* $t\in[0,\tau]$. *Then the system* (5.2)-(5.3) *becomes*

$$\begin{cases} dS_t = S_t dN_t, & t\in[0,\tau],\\ d\mu_t = \alpha(\bar{\mu}-\mu_t)dt+\sigma_\mu' dZ_t, & t\in[0,\tau],\\ S_0=\varphi_0 \quad \textit{and} \quad \mu_0=\hat{\mu}. \end{cases} \tag{D.1}$$

where $N_t=\int_0^t\left[\frac{\phi}{\tau}\int_{s-\tau}^s\frac{d\varphi_u}{\varphi_u}+(1-\phi)\mu_s\right]ds+\int_0^t\sigma_S' dZ_s$ *is a semimartingale. Denote by* $[N,N]_t=\int_0^t\sigma_S'\sigma_S ds$, $t\in[0,\tau]$, *its quadratic variation. Then the system* (D.1) *has a unique solution*

$$\begin{cases} S_t=\varphi_0\exp\left\{N_t-\frac{1}{2}[N,N]_t\right\},\\ \mu_t=\bar{\mu}+(\hat{\mu}-\bar{\mu})\exp\{-\alpha t\}+\sigma_\mu'\exp\{-\alpha t\}\int_0^t\exp\{\alpha u\}dZ_u \end{cases}$$

for $t\in[0,\tau]$. *This clearly implies that* $S_t>0$ *for all* $t\in[0,\tau]$ *almost surely, when* $\varphi_0>0$ *a.s.. By a similar argument, it follows that* $S_t>0$ *for all* $t\in[\tau,2\tau]$ *a.s.. Therefore* $S_t>0$

for all $t \geq 0$ a.s., by induction. Note that the above argument also gives existence and pathwise-uniqueness of the solution to the system (5.2)-(5.3).

D.2 Proof of Proposition 5.1

To solve the stochastic control problems, there are two approaches: the dynamic programming method (HJB equation) and the maximum principle. The SDDE is not Markovian so we cannot use the dynamic programming method. Recently, Chen and Wu (2010) introduce a maximum principle for the optimal control problem of SDDEs, and this method is further extended by Øksendal, Sulem and Zhang (2011) to consider a one dimensional system allowing both delays of moving average type and jumps. Because the optimal control problem of SDDEs is relative new to the field of economics and finance, we first introduce the maximum principle in Chen and Wu (2010) briefly and refer the reader to the original for details.

Brief Introduction to the Maximum Principle for an Optimal Control Problem of SDDE

Consider a past-dependent state X_t of a control system

$$\begin{cases} dX_t = b(t, X_t, X_{t-\tau}, v_t, v_{t-\tau})dt + \sigma(t, X_t, X_{t-\tau}, v_t, v_{t-\tau})dZ_t, & t \in [0, T], \\ X_t = \xi_t, \qquad v_t = \eta_t, & t \in [-\tau, 0], \end{cases} \tag{D.2}$$

where Z_t is a d-dimensional Brownian motion on $(\Omega, \mathcal{F}, P, \{\mathcal{F}_t\}_{t\geq 0})$, and $b : [0, T] \times \mathbb{R}^n \times \mathbb{R}^n \times \mathbb{R}^k \times \mathbb{R}^k \to \mathbb{R}^n$ and $\sigma : [0, T] \times \mathbb{R}^n \times \mathbb{R}^n \times \mathbb{R}^k \times \mathbb{R}^k \to \mathbb{R}^{n\times d}$ are given functions. In addition, v_t is an $\mathcal{F}_t(t \geq 0)$-measurable stochastic control with values in U, where $U \subset \mathbb{R}^k$ is a nonempty convex set, $\tau > 0$ is a given finite time delay, $\xi \in C[-\tau, 0]$ is the initial path of X, and η, the initial path of $v(\cdot)$, is a given deterministic continuous function from $[-\tau, 0]$ into U such that $\int_{-\tau}^{0} \eta_s^2 ds < +\infty$. The problem is to find the optimal control $u(\cdot) \in \mathcal{A}$, such that

$$J(u(\cdot)) = \sup\{J(v(\cdot)); v(\cdot) \in \mathcal{A}\}, \tag{D.3}$$

where $\mathcal{A}$ denotes the set of all admissible controls and the associated performance function J is given by

$$J(v(\cdot)) = \mathbb{E}\Big[\int_0^T L(t, X_t, v_t, v_{t-\tau})dt + \Phi(X_T)\Big],$$

where $L : [0,T]\times\mathbb{R}^n\times\mathbb{R}^k\times\mathbb{R}^k \to \mathbb{R}$ and $\Phi : \mathbb{R}^n \to \mathbb{R}$ are given functions. Assume **(H1)** the functions b, σ, L and Φ are continuously differentiable with respect to $(X_t, X_{t-\tau}, v_t, v_{t-\tau})$ and their derivatives are bounded.

In order to derive the maximum principle, we introduce the following adjoint equation,

$$\begin{cases} -dp_t = \big\{(b_X^u)^\top p_t + (\sigma_X^u)^\top z_t + \mathbb{E}_t[(b_{X_\tau}^u|_{t+\tau})^\top p_{t+\tau} + (\sigma_{X_\tau}^u|_{t+\tau})^\top z_{t+\tau}] \\ \qquad + L_X(t, X_t, u_t, u_{t-\tau})\big\}dt - z_t dZ_t, \quad t \in [0,T], \\ p_T = \Phi_X(X_T), \qquad p_t = 0, \qquad t \in (T, T+\tau], \\ z_t = 0, \qquad t \in [T, T+\tau]. \end{cases} \tag{D.4}$$

We refer readers to the Theorem 2.2 and Theorem 2.1 in Chen and Wu (2010) for the existence and uniqueness of the solutions of the systems (D.2) and (D.4) respectively.

Next, define a Hamiltonian function H from $[0,T] \times \mathbb{R}^n \times \mathbb{R}^n \times \mathbb{R}^k \times \mathbb{R}^k \times L^2_{\mathcal{F}}(0, T+\tau; \mathbb{R}^n) \times L^2_{\mathcal{F}}(0, T+\tau; \mathbb{R}^{n\times d})$ to $\mathbb{R}$ as follows,

$$\begin{aligned} &H(t, X_t, X_{t-\tau}, v_t, v_{t-\tau}, p_t, z_t) = \\ &\langle b(t, X_t, X_{t-\tau}, v_t, v_{t-\tau}), p_t\rangle + \langle \sigma(t, X_t, X_{t-\tau}, v_t, v_{t-\tau}), z_t\rangle + L(t, X_t, v_t, v_{t-\tau}). \end{aligned}$$

Assume **(H2)** the functions $H(t, \cdot, \cdot, \cdot, \cdot, p_t, z_t)$ and $\Phi(\cdot)$ are concave with respect to the corresponding variables respectively for $t \in [0,T]$ and given p_t and z_t. Then we have the following proposition on the maximum principle of the stochastic control system with delay by summarizing the Theorem 3.1, Remark 3.4 and Theorem 3.2 in Chen and Wu (2010).

Proposition D.2 *(i) Let $u(\cdot)$ be an optimal control of the optimal stochastic control problem with delay subject to* (D.2) *and* (D.3)*, and $X(\cdot)$ be the corresponding optimal trajectory. Then we have*

$$\max_{v\in U}\langle H_v^u + \mathbb{E}_t[H_{v_\tau}^u|_{t+\tau}], v\rangle = \langle H_v^u + \mathbb{E}_t[H_{v_\tau}^u|_{t+\tau}], u_t\rangle, \qquad a.e.,\ a.s.; \tag{D.5}$$

(ii) Suppose $u(\cdot) \in \mathcal{A}$ and let $X(\cdot)$ be the corresponding trajectory, p_t and z_t be the solution of the adjoint equation (D.2)*. If **(H1)**, **(H2)** and* (D.5) *hold for $u(\cdot)$, then $u(\cdot)$ is an optimal control for the stochastic delayed optimal problem* (D.2) *and* (D.3)*.*

Proof of Proposition 5.1

Next, we apply the theory in Chen and Wu (2010) summarized in previous subsection to our stochastic control problem.

Let $P_u := \ln S_u$ and $V_u := \ln W_u$. Then the stochastic delayed optimal problem in Section 5.2 becomes to maximize $\mathbb{E}_u[\Phi(X_T)] := \mathbb{E}_u[\ln W_T] = \mathbb{E}_u[V_T]$, subject to

$$\begin{cases} dX_u = b(u, X_u, X_{u-\tau}, \pi_u)du + \sigma(u, X_u, \pi_u)dZ_u, & u \in [t, T], \\ X_u = \xi_u, \qquad v_u = \eta_u, & u \in [t-\tau, t], \end{cases} \tag{D.6}$$

where

$$X_u = \begin{pmatrix} P_u \\ \mu_u \\ V_u \end{pmatrix}, \qquad \sigma = \begin{pmatrix} \sigma_S' \\ \sigma_\mu' \\ \pi_u \sigma_S' \end{pmatrix},$$

$$b = \begin{pmatrix} \frac{\phi}{\tau}(P_u - P_{u-\tau}) + (1-\phi)\mu_u - (1-\phi)\frac{\sigma_S'\sigma_S}{2} \\ \alpha(\bar{\mu} - \mu_u) \\ -\frac{\pi_u^2 \sigma_S'\sigma_S}{2} + \pi_u\Big[\frac{\phi}{\tau}(P_u - P_{u-\tau}) + \frac{\sigma_S'\sigma_S}{2}\phi + (1-\phi)\mu_u - r\Big] + r \end{pmatrix}.$$

Then we have the following adjoint equation

$$\begin{cases} -dp_u = \big\{(b_X^{\pi^*})^\top p_u + (\sigma_X^{\pi^*})^\top z_u + \mathbb{E}_u[(b_{X_\tau}^{\pi^*}|_{u+\tau})^\top p_{u+\tau} + (\sigma_{X_\tau}^{\pi^*}|_{u+\tau})^\top z_{u+\tau}] \\ \qquad + L_X\big\}du - z_u dZ_u, \quad u \in [t, T], \\ p_T = \Phi_X(X_T), \qquad p_u = 0, \qquad u \in (T, T+\tau], \\ z_u = 0, \qquad u \in [T, T+\tau], \end{cases}$$

where

$$p_u = (p_u^i)_{3\times 1}, \qquad z_u = (z_u^{ij})_{3\times 2}, \qquad (b_X^{\pi^*})^\top = \begin{pmatrix} \frac{\phi}{\tau} & 0 & \frac{\phi}{\tau}\pi_u^* \\ 1-\phi & -\alpha & (1-\phi)\pi_u^* \\ 0 & 0 & 0 \end{pmatrix},$$

$$(b_{X_\tau}^{\pi^*}|_{u+\tau})^\top = \begin{pmatrix} -\frac{\phi}{\tau} & 0 & -\frac{\phi}{\tau}\pi_{u+\tau}^* \\ 0 & 0 & 0 \\ 0 & 0 & 0 \end{pmatrix}, \qquad \Phi_X(X_T) = \begin{pmatrix} 0 \\ 0 \\ 1 \end{pmatrix}, \qquad L_X = 0,$$

$$(\sigma_X^{\pi^*})^\top = (\sigma_{X_\tau}^{\pi^*}|_{u+\tau})^\top = \mathbf{0}_{2\times 3\times 3}.$$

Since the parameters and terminal values for dp_u^3 are deterministic, we can assert $z_u^{31} = z_u^{32} = 0$ for $u \in [t, T]$, which leads to $p_u^3 = 1$ for $u \in [t, T]$. Then the Hamiltonian function

H is given by

$$\begin{aligned} H = &\big[\frac{\phi}{\tau}(P_u - P_{u-\tau}) + (1-\phi)\mu_u - (1-\phi)\frac{\sigma_S'\sigma_S}{2}\big]p_u^1 + \alpha(\bar{\mu} - \mu_u)p_u^2 \\ &+ \Big\{ -\frac{\pi_u^2\sigma_S'\sigma_S}{2} + \pi_u\big[\frac{\phi}{\tau}(P_u - P_{u-\tau}) + \frac{\sigma_S'\sigma_S}{2}\phi + (1-\phi)\mu_u - r\big] + r\Big\}p_u^3 \\ &+ \sigma_S' \begin{pmatrix} z_u^{11} \\ z_u^{12} \end{pmatrix} + \sigma_\mu' \begin{pmatrix} z_u^{21} \\ z_u^{22} \end{pmatrix}, \end{aligned}$$

so that

$$H_\pi^{\pi^*} = -\pi_u^*\sigma_S'\sigma_S + \frac{\phi}{\tau}(P_u - P_{u-\tau}) + \frac{\sigma_S'\sigma_S}{2}\phi + (1-\phi)\mu_u - r.$$

It can be also obtained that $\mathbb{E}_u[H_{\pi_\tau}^{\pi^*}|_{u+\tau}] = 0$. Therefore,

$$\langle H_\pi^{\pi^*} + \mathbb{E}_u[H_{\pi_\tau}^{\pi^*}|_{u+\tau}], \pi\rangle = \pi_u\big[-\pi_u^*\sigma_S'\sigma_S + \frac{\phi}{\tau}(P_u - P_{u-\tau}) + \frac{\sigma_S'\sigma_S}{2}\phi + (1-\phi)\mu_u - r\big].$$

Taking the derivative with respect to π_u and letting it equal zero yield

$$\begin{aligned} \pi_u^* &= \frac{\frac{\phi}{\tau}(P_u - P_{u-\tau}) + \frac{\sigma_S'\sigma_S}{2}\phi + (1-\phi)\mu_u - r}{\sigma_S'\sigma_S} \\ &= \frac{\phi M_u + (1-\phi)\mu_u - r}{\sigma_S'\sigma_S}. \end{aligned}$$

D.3 Rolling Window Estimations

In this section we implement rolling window estimation. We first fix $\tau = 12$ and estimate parameters of (5.11) at each month by using past 20 years' data to avoid look ahead bias. Fig. D.1 illustrates the estimated parameters. The big jump in estimated $\sigma_{S(1)}$ during 1930-1950 is consistent with the big volatility of market return illustrated in Fig. D.2 (b).

Fig. D.2 illustrates the time series of (a) the index level and (b) the simple return of the total return index of S&P 500; (c) the optimal portfolio and (d) the utility of wealth from December 1890 until December 2012 for $\tau = 12$ with 20 years rolling window estimated parameters. The index return and π_t^* are positively correlated with correlation 0.0620. In addition, we find that the profits are higher after 1930s.

Fig. D.1 also illustrates an interesting phenomenon that the estimated ϕ is very close to zero for three periods of time, implying insignificant momentum but significant mean reversion effect. By comparing Figs. D.1 (b) and (e), the insignificant ϕ is accompanied by high volatility $\sigma_{S(1)}$. Fig. D.3 illustrates the correlations of the estimated $\sigma_{S(1)}$ with

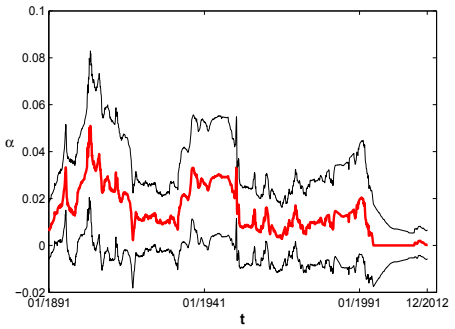

(a) Estimates of α

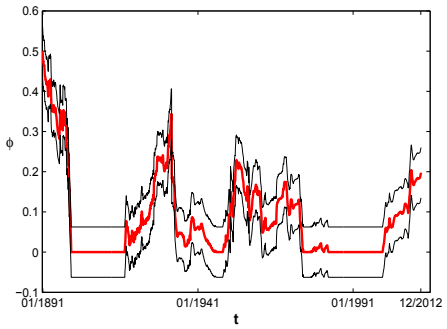

(b) Estimates of ϕ

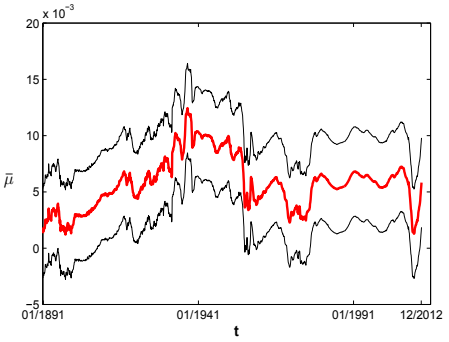

(c) Estimates of $\bar{\mu}$

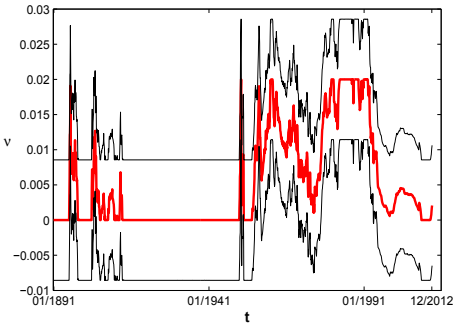

(d) Estimates of ν

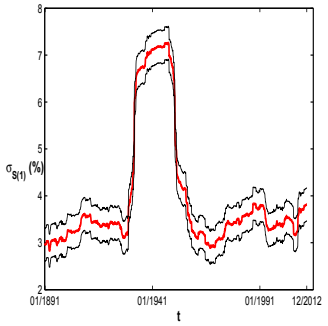

(e) Estimates of $\sigma_{S(1)}$

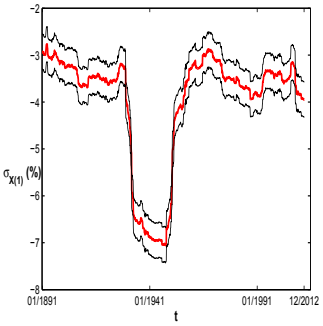

(f) Estimates of $\sigma_{X(1)}$

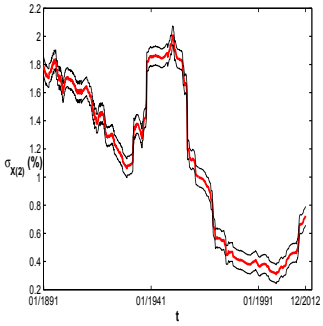

(g) Estimates of $\sigma_{X(2)}$

Figure D.1: The estimates of (a) α; (b) ϕ; (c) $\bar{\mu}$; (d) ν; (e) $\sigma_{S(1)}$; (f) $\sigma_{X(1)}$ and (g) $\sigma_{X(2)}$ for $\tau = 12$ based on the data of past 20 years.

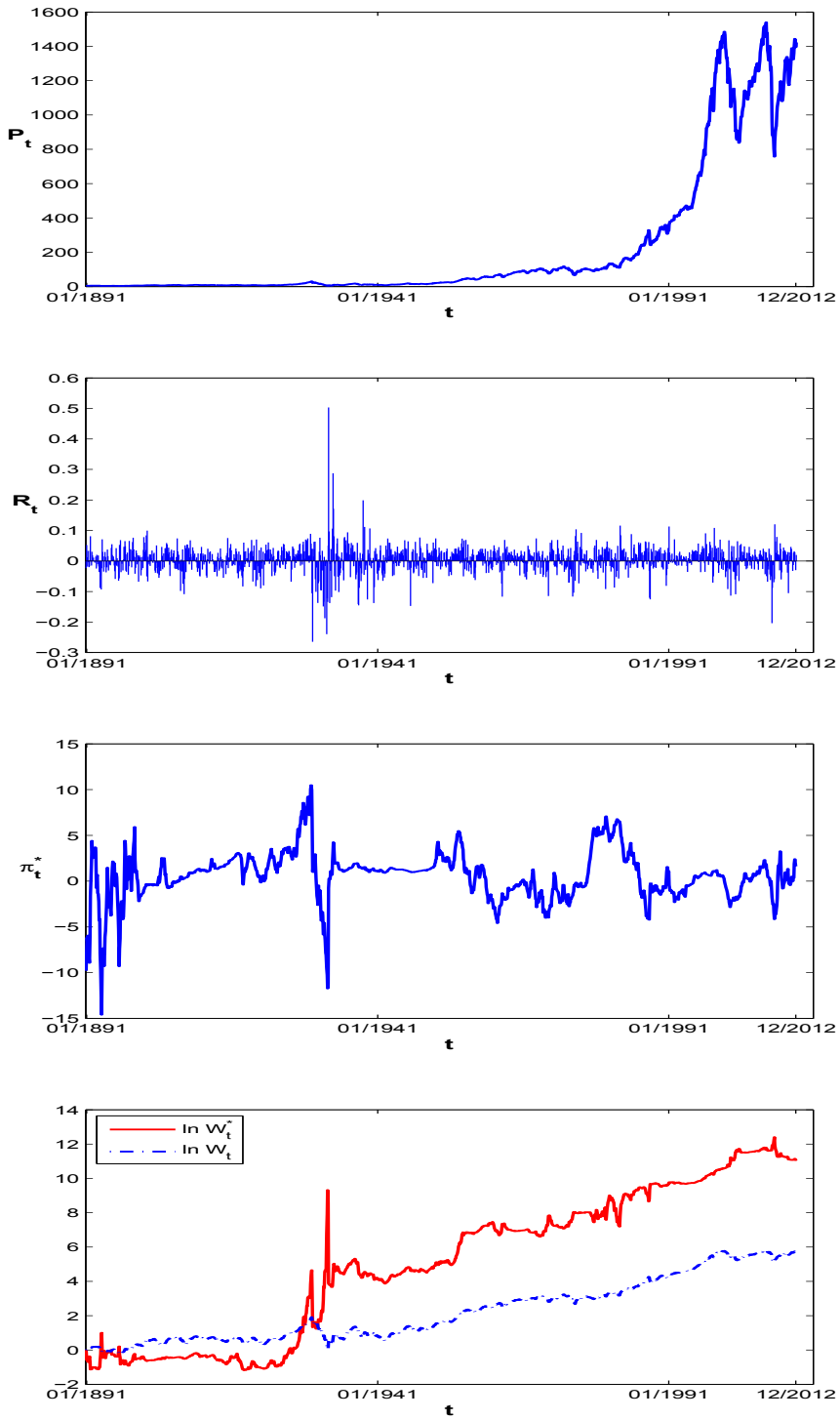

Figure D.2: The time series of (a) the index level and (b) the simple return of the total return index of S&P 500; (c) the optimal portfolio and (d) the utility of wealth from December 1890 until December 2012 for $\tau = 12$ with 20 years rolling window estimated parameters.

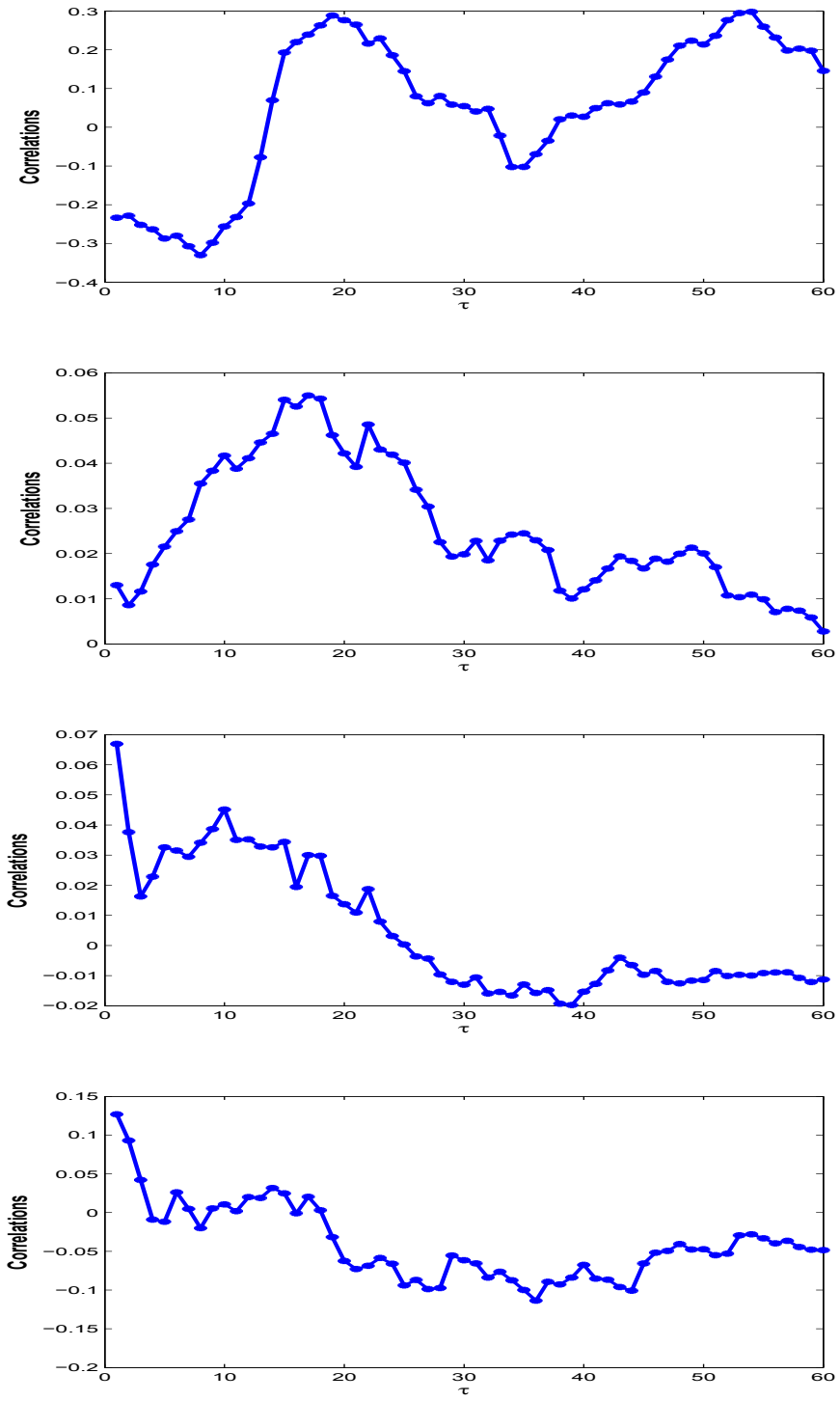

Figure D.3: The correlations of the estimated $\sigma_{S(1)}$ with (a) the estimated ϕ and the return of the optimal strategies for (b) the full model, (c) the pure momentum model and (d) the TSM return.

(a) the estimated ϕ and the return of the optimal strategies for (b) the full model, (c) the pure momentum model and the time series momentum return for $\tau \in [1, 60]$. Interestingly, bigger volatility is accompanied by less significant momentum effect with small time horizons ($\tau \leq 13$). But ϕ and $\sigma_{S(1)}$ are positive correlated when the time horizon becomes large. One possible reason is that big time horizon makes the trading signal less sensitive to the changes in price and hence the trading signal is significant only when the market price changes dramatically in high volatility period. Fig. D.3 (c) and (d) show that the profitability of the optimal strategies for the pure momentum model and the TSM strategies are sensitive to market volatility. The return is positively (negatively) related to market volatility for short (long) time horizons. But Fig. D.3 (b) shows that the optimal strategies for the full model perform well even in high volatility market.

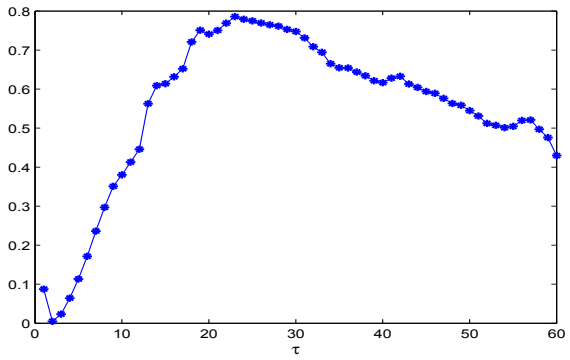

Figure D.4: The fraction of ϕ significantly different from zero for $\tau \in [1, 60]$.

We also study other time horizons. We find that the estimates of $\sigma_{S(1)}$, $\sigma_{X(1)}$ and $\sigma_{X(2)}$ are insensitive to τ but the estimates of ϕ are sensitive to τ. Specifically, the smaller τ is, the less significantly ϕ is different from zero. Fig. D.4 illustrates the corresponding fraction of ϕ which is significantly different from zero. It shows that the momentums with 20-30 months horizons occur the most frequently during the period of December 1890 until December 2012.

Fig. D.5 (a) illustrates the utility of wealth from December 1890 until December 2012 for the optimal portfolio with $\tau \in [1, 60]$ and the passive holding portfolio. Especially, the utility of terminal wealth illustrated in Fig. D.5 (b) shows that the optimal strategy works well for short horizons $\tau \leq 20$ and the terminal utility reaches its peak at $\tau = 12$.

Fig. D.6 illustrates the estimates of $\sigma_{S(1)}$ for the pure momentum model ($\phi = 1$) based on the data of past 20 years and the big jump in volatility is due to the Great Depression in 1930s.

Fig. D.7 illustrates the time series of (a) the optimal portfolio and (b) the utility of

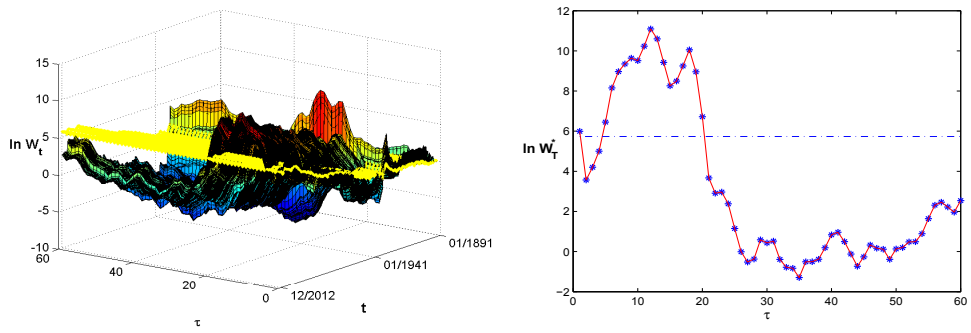

Figure D.5: The utility of wealth from December 1890 until December 2012 for the optimal portfolio with $\tau \in [1, 60]$ and the passive holding portfolio with 20 years rolling window estimated parameters.

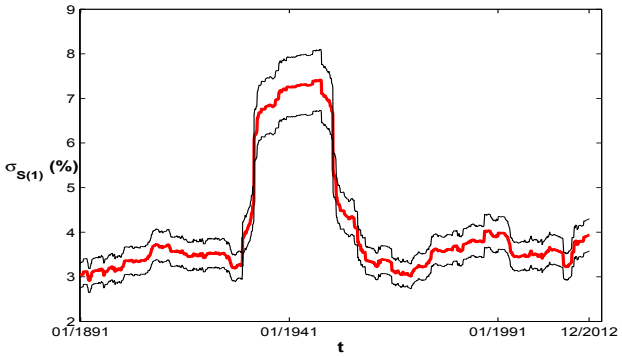

Figure D.6: Estimates of $\sigma_{S(1)}$ for the pure momentum model ($\phi = 1$) based on the data of past 20 years.

wealth from December 1890 until December 2012 for $\tau = 12$ for the pure momentum model with 20 years rolling window estimated parameters. By comparing Fig. D.6 and Fig. D.7 (b), the optimal strategy implied by the pure momentum model suffers huge losses during the big market volatility period. But Fig D.2 illustrates that the optimal strategy implied by the full model makes big profits during the big market volatility period.

Fig. D.8 illustrates the estimates of (a) α; (b) ϕ; (c) $\bar{\mu}$; (d) ν; (e) $\sigma_{S(1)}$; (f) $\sigma_{X(1)}$ and (g) $\sigma_{X(2)}$ for the pure mean-reversion model based on the data of past 20 years.

Fig. D.9 illustrates the time series of the optimal portfolio and the utility of wealth from December 1890 until December 2012 for the pure mean-reversion model with 20 years rolling window estimated parameters. After eliminating the look-ahead bias, the pure mean-reversion strategy cannot outperform the stock index anymore.

We also implement the estimations for different window sizes of 25, 30 and 50 years and we find that the estimated parameters are insensitive to the size of rolling window

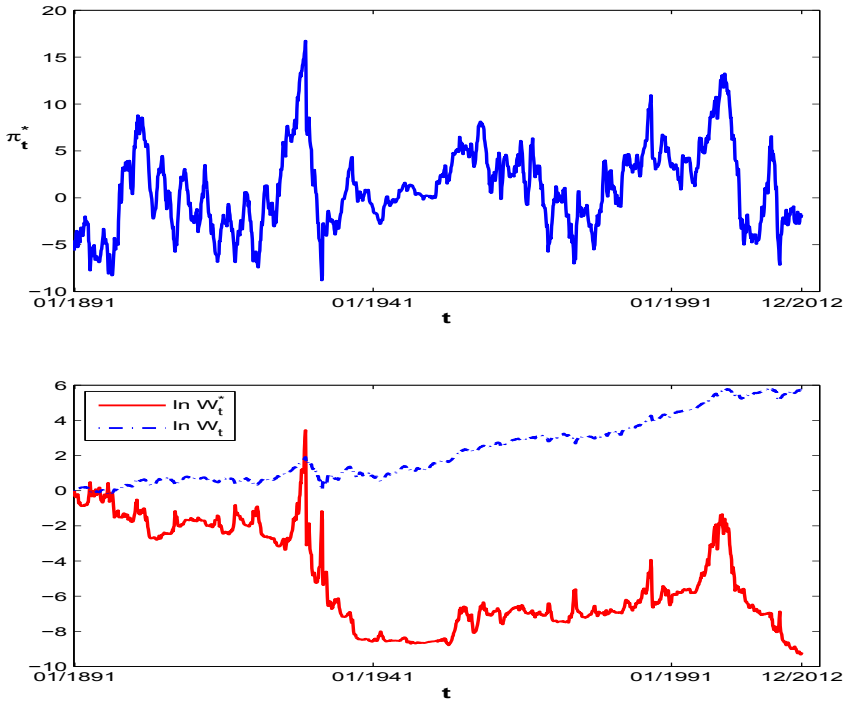

Figure D.7: The time series of (a) the optimal portfolio and (b) the utility of wealth from December 1890 until December 2012 for $\tau = 12$ for the pure momentum model with 20 years rolling window estimated parameters.

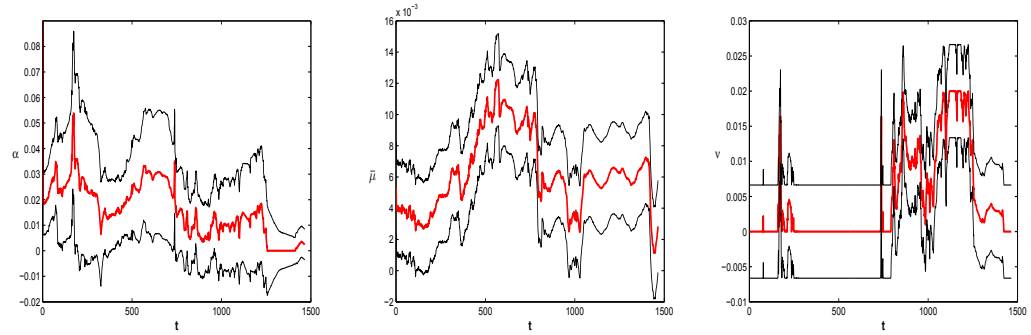

(a) Estimates of α (b) Estimates of $\bar{\mu}$ (c) Estimates of ν

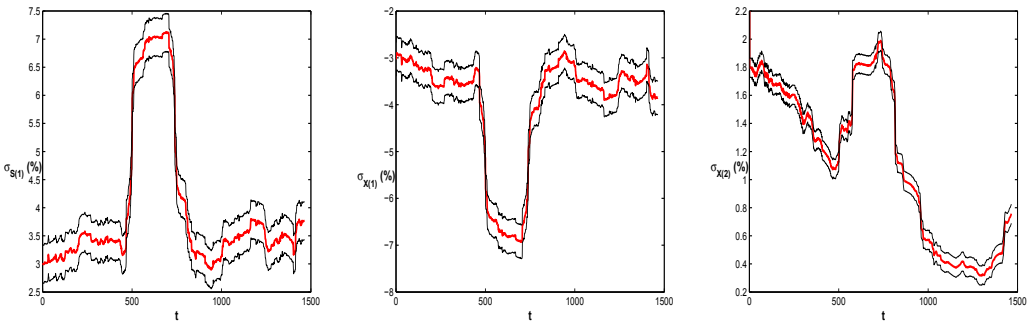

(d) Estimates of $\sigma_{S(1)}$ (e) Estimates of $\sigma_{X(1)}$ (f) Estimates of $\sigma_{X(2)}$

Figure D.8: The estimates of (a) α; (b) ϕ; (c) $\bar{\mu}$; (d) ν; (e) $\sigma_{S(1)}$; (f) $\sigma_{X(1)}$ and (g) $\sigma_{X(2)}$ for the pure mean-reversion model based on the data of past 20 years.

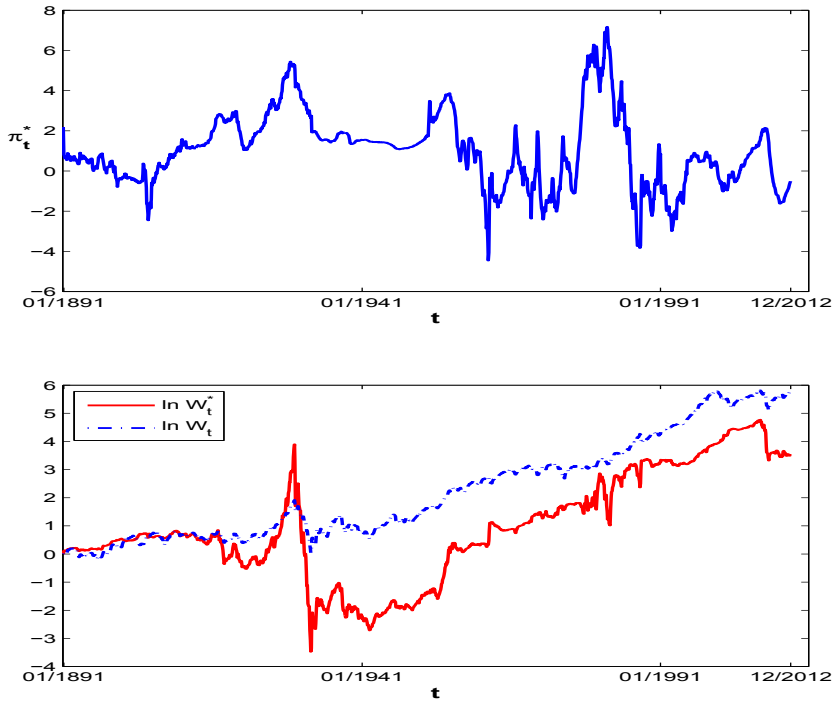

Figure D.9: The time series of (a) the optimal portfolio and (b) the utility of wealth from December 1890 until December 2012 for the pure mean-reversion model with 20 years rolling window estimated parameters.

(not reported here).

D.4 Regressions on the Market States, Sentiment and Volatility

Market States

First, we follow Cooper et al. (2004) and Hou et al. (2009) and define market state using the cumulative return of the stock index (including dividends) over the most recent 36 months.[1] We label a month as an up (down) market month if the market's three-year return is non-negative (negative). There are 1165 up months and 478 down months from February 1876[2] to December 2012.

	Observations (N)	Average Excess Return
Unconditional Return	1643	0.0087
		(2.37)
Up Market	1165	0.0081
		(4.09)
Down Market	478	0.0101
		(0.87)

Table D.1: The average excess return of the optimal strategy for $\tau = 12$.

We compute the average return of the optimal strategy and compare the average returns between up and down market months. Table D.1 presents the average unconditional excess returns and the average excess returns for up and down market months. The excess return of the optimal strategy (5.7) is significant positive in up market but insignificant in down market.

We use the following regression model to test for the difference in returns:

$$R_t^* - r = \alpha + \kappa I_t(UP) + \beta(R_t - r) + \epsilon_t, \tag{D.7}$$

where $R_t^* = (W_t^* - W_{t-1}^*)/W_{t-1}^*$ in (5.12) is the month t return of the optimal strategy, $R_t - r$ is the excess return of the stock index, and $I_t(UP)$ is a dummy variable that takes the value of one if month t is in an up month, and zero otherwise. The regression intercept α measures the average return of the optimal strategy in down market months, and the coefficient κ captures the incremental average return in up market months relative to down months. We also replace the market state dummy in (D.7) with the lagged market return over the previous 36 months (nor reported here), and the results are robust.

[1] The results are similar if we use the alternative 6, 12 or 24 month market state definition, even though they are more sensitive to sudden changes in market sentiment.

[2] We escape January 1876 in which there is no return to the optimal strategy.

	Full Model	Pure Momentum	Pure Mean Reversion	TSM
α	0.0094	0.0476	-0.0000	0.0060
	(1.46)	(1.34)	(-0.01)	(3.23)
κ	0.0005	0.0041	-0.0005	-0.0014
	(0.06)	(0.10)	(-0.32)	(-0.63)
β	-1.0523	-6.7491	0.3587	-0.1548
	(-12.48)	(-14.60)	(22.97)	(-6.39)

Table D.2: The coefficients for the regression (D.7).

Tables D.2 reports the regression coefficients for the full model, the pure momentum model, pure mean reversion model and the time series momentum strategy in Moskowitz et al. (2012) for $\tau = 12$ respectively. κs are insignificant for all strategies.

	Full Model	Pure Momentum	Pure Mean Reversion	TSM
α	0.0086	0.0423	0.0002	0.0058
	(1.44)	(1.32)	(0.18)	(3.29)
κ	-0.0008	-0.0034	-0.0002	-0.0017
	(-0.11)	(-0.09)	(-0.14)	(-0.81)
β_1	0.1994	0.7189	0.0708	0.1341
	(1.90)	(1.27)	(3.84)	(4.30)
β_2	-2.5326	-15.5802	0.6991	-0.4964
	(-22.16)	(-25.31)	(34.88)	(-14.63)

Table D.3: The coefficients for the regression (D.8).

Now we run the following regression:

$$R_t^* - r = \alpha + \kappa I_t(UP) + \beta_1(R_t - r)I_t(UP) + \beta_2(R_t - r)I_t(DOWN) + \epsilon_t, \tag{D.8}$$

the regression coefficients are reported in Table D.3.

	Full Model	Pure Momentum	Pure Mean Reversion	TSM
α	0.0083	0.0409	0.0002	0.0057
	(1.22)	(1.08)	(0.14)	(3.03)
κ	0.0006	0.0037	-0.0002	-0.0012
	(0.07)	(0.08)	(-0.14)	(-0.53)

Table D.4: The coefficients for the regression (D.9).

We run the following regression:

$$R_t^* - r = \alpha + \kappa I_{t-1}(UP) + \epsilon_t, \tag{D.9}$$

and Table D.4 reports the coefficients.

	Full Model	Pure Momentum	Pure Mean Reversion	TSM
κ	0.0005	0.0041	-0.0005	-0.0014
	(0.06)	(0.10)	(-0.32)	(-0.63)

Table D.5: The coefficients for the regression (D.10).

We also study the beta adjusted momentum returns:

$$\begin{aligned} R_t^* - r &= \alpha^{CAPM} + \beta^{CAPM}(R_t - r) + \varepsilon_t, \\ R_t^* - r - \beta^{CAPM}(R_t - r) &= \alpha + \kappa I_t(UP) + \epsilon_t, \end{aligned} \tag{D.10}$$

and Table D.5 reports the coefficients.

Investor Sentiment

	Full Model	Pure Momentum	Pure Mean Reversion	TSM
a	0.0059	0.0267	0.0005	0.0040
	(1.77)	(1.74)	(1.49)	(2.57)
b	0.0040	0.0134	-0.0003	0.0023
	(1.20)	(0.87)	(-1.01)	(1.48)

Table D.6: The coefficients for the regression (D.11).

In this subsection, we examine the relationship between the excess return of the optimal strategies and investor sentiment by running the following regression:

$$R_t^* - r = a + bT_{t-1} + \epsilon, \tag{D.11}$$

where T_t is the sentiment index measures used by Baker and Wurgler (2006). The data on the Baker-Wurger sentiment index from 07/1965 to 12/2010 is obtained from the Jeffrey Wurglers web site. Table D.6 reports the coefficients. We also examine monthly changes of the level of sentiment by replacing T_t with its monthly changes and their orthogonalized indexes. The coefficients are also insignificant.

Market Volatility

Finally, we examine the predictability of market volatility to the profitability. First, we run the following regression:

$$R_t^* - r = \alpha + \kappa\hat{\sigma}_{S,t-1} + \epsilon_t, \tag{D.12}$$

	Full Model	Pure Momentum	Pure Mean Reversion	TSM
α	0.0089	0.0457	-0.0002	0.0047
	(2.27)	(2.09)	(-0.24)	(4.32)
κ	-0.0155	-0.1392	0.0151	0.0105
	(-0.16)	(-0.26)	(0.77)	(0.39)

Table D.7: The coefficients for the regression (D.12).

where the ex ante annualized volatility $\hat{\sigma}_{S,t}$ is given by (5.14). Table D.7 reports the coefficients.

	Full Model	Pure Momentum	Pure Mean Reversion	TSM
α	0.0058	0.0264	0.0007	0.0045
	(1.35)	(1.10)	(0.82)	(3.78)
κ_1	0.1937	1.1647	-0.0469	-0.0317
	(0.69)	(0.75)	(-0.83)	(-0.41)
κ_2	0.1894	1.1368	-0.0452	0.0783
	(1.92)	(2.07)	(-2.25)	(2.86)

Table D.8: The coefficients for the regression (D.13).

Second, we run the regression by following Wang and Xu (2012):

$$R_t^* - r = \alpha + \kappa_1 \hat{\sigma}_{S,t-1}^+ + \kappa_2 \hat{\sigma}_{S,t-1}^- + \epsilon_t, \tag{D.13}$$

where $\hat{\sigma}_{S,t}^+$ ($\hat{\sigma}_{S,t}^-$) is equal to $\hat{\sigma}_{S,t}$ if the market state is up (down) and otherwise equal to 0. Table D.8 reports the coefficients.

Appendix E

Proofs of Chapter 6

E.1 Proof of Proposition 6.2

To provide some insights into the proof of the model with many risky assets, we first start with the case of one risky asset.

In order to prove the local stability properties of the deterministic model (6.19), we start from the simplified one-risky-asset case (6.21). We omit the index j of the unique risky asset for simplicity.

Note that p_t depends only on p_{t-1}, u_{t-1}, V_{t-1}, and on $n_{f,t}$. The same holds for the state variables u_t and V_t. The differential of the fitness function at time t, $v_{\Delta,t}$, depends on p_{t-2}, u_{t-2}, V_{t-2} and p_{t-1} through the demand functions $z_{f,t-1}$ and $z_{c,t-1}$, on $n_{f,t-1}$ through $\theta_{a,t-1}$, as well as on p_t, p_{t-1}, p_{t-2} directly. Formally, suitable changes of variables allow us to express the dynamical system (6.21) as an 8-dimensional map, by which the state of the system at time t is expressed as a function of the state of the system at time $t-1$. We set

$$q_{f,t} := n_{f,t+1} = (1+\exp(-\eta v_{\Delta,t}))^{-1}, \qquad p_t^L := p_{t-1}, \quad u_t^L := u_{t-1}, \quad V_t^L := V_{t-1},$$

so that we can write the map driving dynamical system (6.21) as

$$\begin{aligned}
p_t &= F(p_{t-1}, u_{t-1}, V_{t-1}, q_{f,t-1}),\\
u_t &= \delta u_{t-1} + (1-\delta) F(p_{t-1}, u_{t-1}, V_{t-1}, q_{f,t-1}),\\
V_t &= \delta V_{t-1} + \delta(1-\delta)\left[F(p_{t-1}, u_{t-1}, V_{t-1}, q_{f,t-1}) - u_{t-1}\right]^2,\\
q_{f,t} &= \left\{1+\exp\left[-\eta Q(p_{t-1}, u_{t-1}, V_{t-1}, q_{f,t-1}, p_{t-1}^L, u_{t-1}^L, V_{t-1}^L, q_{f,t-1}^L)\right]\right\}^{-1}.
\end{aligned}$$

In particular, the function Q in the fourth equation above corresponds to $v_{\Delta,t}$, and has

the structure

$$Q = v_{\Delta,t} = \hat{\zeta}_{f,t-1}\hat{\pi}_{f,t} - \hat{\zeta}_{c,t-1}\hat{\pi}_{c,t} - C_\Delta,$$

where, for $h \in \{f, c\}$,

$$\hat{\zeta}_{h,t-1} := z_{h,t-1} - \frac{\theta_{a,t-1}}{\theta_h}s, \quad \hat{\pi}_{h,t} := p_t + \overline{d} - R_f p_{t-1} - \frac{\theta_h}{2}\sigma^2_{h,t-1}\left(z_{h,t-1} + \frac{\theta_{a,t-1}}{\theta_h}s\right)$$

and $\sigma^2_{h,t-1} = \sigma^2$ for $h = f$, $\sigma^2_{h,t-1} = \sigma^2 + \lambda V_{t-2}$ for $h = c$. One can check that both $\hat{\zeta}_{h,t-1}$ and $\hat{\pi}_{h,t}$ vanish at the fundamental steady state. It follows that all the partial derivatives of Q with respect to any of the state variables also vanish at the steady state, and the same holds for the derivatives of $q_{f,t}$. Also, all the partial derivatives of V_t (except $\partial V_t/\partial V_{t-1}$) are zero at the steady state due to the higher-order term $(p_t - u_{t-1})^2$ and the fact that $p = u$ at the steady state. By ordering the variables as $p, u, V, q_f, p^L, u^L, V^L, q^L_f$, the Jacobian matrix evaluated at the fundamental steady state has the left block triangular structure

$$\mathbf{J} = \begin{pmatrix} \mathbf{A} & \mathbf{0} \\ \mathbf{I} & \mathbf{0} \end{pmatrix}, \tag{E.1}$$

where $\mathbf{0}$ and $\mathbf{I}$ are the 4-dimensional null and identity matrices, respectively, and

$$\mathbf{A} = \begin{pmatrix} \dfrac{\partial F}{\partial p} & \dfrac{\partial F}{\partial u} & \dfrac{\partial F}{\partial V} & \dfrac{\partial F}{\partial q_f} \\ (1-\delta)\dfrac{\partial F}{\partial p} & \delta + (1-\delta)\dfrac{\partial F}{\partial u} & (1-\delta)\dfrac{\partial F}{\partial V} & (1-\delta)\dfrac{\partial F}{\partial q_f} \\ 0 & 0 & \delta & 0 \\ 0 & 0 & 0 & 0 \end{pmatrix}.$$

It follows that the characteristic equation for $\mathbf{J}$ is given by

$$\chi^5(\chi - \delta)(\chi^2 + m_1\chi + m_2) = 0,$$

where[1]

$$m_1 = \frac{\alpha + \delta\gamma}{R_f(1 + \theta_0 e^{\eta C_\Delta})} - \frac{\delta\gamma + 1}{R_f} - \delta, \quad m_2 = \delta\left[\frac{1+\gamma}{R_f} - \frac{\alpha + \gamma}{R_f(1 + \theta_0 e^{\eta C_\Delta})}\right].$$

As $0 < \delta < 1$, it follows that stability depends only on the roots of the 2nd-degree polynomial $\chi^2 + m_1\chi + m_2$. The latter represents the characteristic polynomial of the two-dimensional upper-left block of matrix $\mathbf{A}$ (that we denote as $\mathbf{B}$). A well-known

[1] See later for the N-asset case with the computational details regarding $\frac{\partial F}{\partial p}$ and $\frac{\partial F}{\partial u}$.

necessary and sufficient condition for both characteristic roots of $\mathbf{B}$, say χ_1 and χ_2, to have modulus smaller than one (implying that the steady state is locally asymptotically stable in our case) is the set of inequalities,

$$1 + m_1 + m_2 > 0, \quad 1 - m_1 + m_2 > 0, \quad m_2 < 1. \tag{E.2}$$

The first and second inequalities of (E.2) always hold for any $\eta \geq 0$. The third condition is equivalent to

$$\delta(1+\gamma) - R_f < \frac{\delta(\alpha+\gamma)}{1+\theta_0 e^{\eta C_\Delta}}. \tag{E.3}$$

If $R_f \geq \delta(1+\gamma)$, then condition (E.3) always holds for any $\eta \geq 0$. If $R_f < \delta(1+\gamma)$, then (E.3) holds when $\eta < \widehat{\eta} := \frac{1}{C_\Delta} \ln \frac{R_f - \delta(1-\alpha)}{\theta_0[\delta(1+\gamma)-R_f]}$. If $C_\Delta = 0$, then Eq. (E.3) holds when $\frac{R_f-\delta(1-\alpha)}{\theta_0[\delta(1+\gamma)-R_f]} > 1$, which is equivalent to $\theta_0\gamma < \alpha + (1+\theta_0)(\frac{R_f}{\delta} - 1)$. This proves Proposition 6.2.

E.2 Proof of Proposition 6.1

Consider the general case (6.19) of N risky assets. The structure of the map is the same as in the simplified one-risky-asset case, except that the variables $\mathbf{p}_t$, $\mathbf{u}_t$, $\mathbf{p}_t^L$, $\mathbf{u}_t^L$ have dimension N, whereas $\mathbf{V}_t$ and $\mathbf{V}_t^L$ have dimension $M := N(N+1)/2$ (e.g. $M = 3$ for the two-asset case). Again, $\mathbf{p} = \mathbf{u}$ at the steady state, and the derivatives of each component of $\mathbf{V}_t$ in system (6.19) with respect to any of the state variables (with the exception of $\mathbf{V}_{t-1}$) vanish at the steady state. Turning to the derivatives of $q_{f,t} := n_{f,t+1}$, note that function Q has the structure

$$Q = v_{\Delta,t} = \hat{\boldsymbol{\zeta}}_{f,t-1}^\top \hat{\boldsymbol{\pi}}_{f,t} - \hat{\boldsymbol{\zeta}}_{c,t-1}^\top \hat{\boldsymbol{\pi}}_{c,t} - C_\Delta$$

where, for $h = f, c$,

$$\hat{\boldsymbol{\zeta}}_{h,t-1} := \mathbf{z}_{h,t-1} - \frac{\theta_{a,t-1}}{\theta_h}\mathbf{s}, \quad \hat{\boldsymbol{\pi}}_{h,t} := \mathbf{p}_t + \overline{\mathbf{d}} - R_f \mathbf{p}_{t-1} - \frac{\theta_h}{2}\boldsymbol{\Omega}_{h,t-1}\left(\mathbf{z}_{h,t-1} + \frac{\theta_{a,t-1}}{\theta_h}\mathbf{s}\right),$$

with $\boldsymbol{\Omega}_{h,t-1} = \boldsymbol{\Omega}_0$ for $h = f$ and $\boldsymbol{\Omega}_{h,t-1} = \boldsymbol{\Omega}_0 + \lambda \mathbf{V}_{t-2}$ for $h = c$. Similar to the one-asset case, both $\hat{\boldsymbol{\zeta}}_{h,t-1}$ and $\hat{\boldsymbol{\pi}}_{h,t}$ vanish at the fundamental steady state, and the same holds for any of the partial derivatives of $q_{f,t}$. The Jacobian matrix of the system of dimension $N^2 + 5N + 2$ at the fundamental steady state is thus again characterized by the structure (E.1), where the variables are ordered as $\mathbf{p}, \mathbf{u}, \mathbf{V}, q_f, \mathbf{p}^L, \mathbf{u}^L, \mathbf{V}^L, q_f^L$. In particular, in this case, $\mathbf{0}$ and $\mathbf{I}$ represent the null matrix and the identity matrix of order $2N+N(N+1)/2+1$

(e.g. dimension 8 in the case of two assets) respectively, and[2]

$$\mathbf{A} = \begin{pmatrix} D_{\mathbf{p}}\mathbf{F} & D_{\mathbf{u}}\mathbf{F} & D_{\mathbf{V}}\mathbf{F} & D_{q_f}\mathbf{F} \\ (1-\delta)D_{\mathbf{p}}\mathbf{F} & \delta\mathbf{I} + (1-\delta)D_{\mathbf{u}}\mathbf{F} & (1-\delta)D_{\mathbf{V}}\mathbf{F} & (1-\delta)D_{q_f}\mathbf{F} \\ \mathbf{0} & \mathbf{0} & \delta\mathbf{I} & \mathbf{0} \\ 0 & 0 & 0 & 0 \end{pmatrix},$$

where $D_{\mathbf{x}}\mathbf{F}$ denotes the partial Jacobian matrix with respect to the variable $\mathbf{x}$. Again, what matters for stability are the eigenvalues of the upper left block (of dimension $2N \times 2N$), given by

$$\mathbf{B} = \begin{pmatrix} D_{\mathbf{p}}\mathbf{F} & D_{\mathbf{u}}\mathbf{F} \\ (1-\delta)D_{\mathbf{p}}\mathbf{F} & \delta\mathbf{I} + (1-\delta)D_{\mathbf{u}}\mathbf{F} \end{pmatrix}.$$

Consider now the difference equation for the price vector

$$\mathbf{p}_t = \mathbf{F}(\mathbf{p}_{t-1}, \mathbf{u}_{t-1}, \mathbf{V}_{t-1}, q_{f,t-1}).$$

The partial Jacobian with respect to $\mathbf{p}$ is given by

$$D_{\mathbf{p}}\mathbf{F} = \frac{\theta_{a,t}}{R_f}\mathbf{\Omega}_{a,t}\left[\frac{q_{f,t-1}}{\theta_f}\mathbf{\Omega}_0^{-1}(\mathbf{I}-\boldsymbol{\alpha}) + \frac{1-q_{f,t-1}}{\theta_c}(\mathbf{\Omega}_0 + \lambda\mathbf{V}_{t-1})^{-1}(\mathbf{I}+\boldsymbol{\gamma})\right]$$

where $\mathbf{I}$ is the N-dimensional identity matrix, $\boldsymbol{\alpha} := diag(\alpha_1, \alpha_2, ..., \alpha_N)$ and $\boldsymbol{\gamma}$:=$diag(\gamma_1, \gamma_2, ..., \gamma_N)$. At the steady state (where $\mathbf{\Omega}_{a,t} = \mathbf{\Omega}_0$) we obtain

$$D_{\mathbf{p}}\mathbf{F}(\mathbf{p}^*, \mathbf{p}^*, \mathbf{0}, q_f^*) = \frac{\theta_a^*}{R_f}\left[\frac{n_f^*}{\theta_f}(\mathbf{I}-\boldsymbol{\alpha}) + \frac{1-n_f^*}{\theta_c}(\mathbf{I}+\boldsymbol{\gamma})\right],$$

where

$$\frac{\theta_a^*}{\theta_f}n_f^* = \frac{1}{1+\theta_0 e^{\eta C_\Delta}}, \quad \frac{\theta_a^*}{\theta_c}(1-n_f^*) = \frac{\theta_0 e^{\eta C_\Delta}}{1+\theta_0 e^{\eta C_\Delta}}.$$

Note that $D_{\mathbf{p}}\mathbf{F}(\mathbf{p}^*, \mathbf{p}^*, \mathbf{0}, q_f^*)$ is a diagonal matrix. This implies that the fixed component $\mathbf{\Omega}_0$ of variance/covariance beliefs, in particular the correlations, has no effect on the dynamics of the linearized system around the steady state. Similarly, one obtains for $D_{\mathbf{u}}\mathbf{F}$ the expression

$$D_{\mathbf{u}}\mathbf{F}(\mathbf{p}^*, \mathbf{p}^*, \mathbf{0}, q_f^*) = -\frac{\theta_a^*}{R_f}\frac{1-n_f^*}{\theta_c}\boldsymbol{\gamma},$$

[2]The null matrices in the third row of $\mathbf{A}$ now have dimension $M \times N$ (first and second entry) and $M \times 1$ (fourth entry). The identity matrix in the third entry has dimension M. The identity matrix in the second row has dimension N.

which is also a diagonal matrix. Every submatrix of block **B** is therefore an N-dimensional diagonal matrix. It follows that the characteristic equation of **J** is given by

$$\chi^{\frac{(N+1)(N+4)}{2}}(\chi-\delta)^{\frac{N(N+1)}{2}}\prod_{j=1}^{N}(\chi^2+m_{1,j}\chi+m_{2,j})=0,$$

where in particular the characteristic equation of **B** is represented by the product of the N 2nd-degree polynomials, and the coefficients $m_{1,j}$ and $m_{2,j}$ have the same structure as those of the one-asset case, namely

$$m_{1,j}=\frac{\alpha_j+\delta\gamma_j}{R_f(1+\theta_0 e^{\eta C_\Delta})}-\frac{\delta\gamma_j+1}{R_f}-\delta,\quad m_{2,j}=\delta\left[\frac{1+\gamma_j}{R_f}-\frac{\alpha_j+\gamma_j}{R_f(1+\theta_0 e^{\eta C_\Delta})}\right].$$

Each of the above second-order polynomials is naturally associated with one of the risky assets. The steady state $(\mathbf{p}^*,\mathbf{p}^*,\mathbf{0},q_f^*)$ is thus locally asymptotically stable if and only if, for *all* $j\in\{1,2,...,n\}$,

$$1+m_{1,j}+m_{2,j}>0,\quad 1-m_{1,j}+m_{2,j}>0,\quad m_{2,j}<1. \tag{E.4}$$

Similar to the one-asset case, the first two inequalities hold for any $\eta\geq 0$. The above set of inequalities is thus satisfied for any $\eta\geq 0$ if $R_f\geq\delta(1+\gamma_j)$. If $R_f<\delta(1+\gamma_j)$, it is satisfied only if $\eta<\widehat{\eta}_j:=\frac{1}{C_\Delta}\ln\frac{R_f-\delta(1-\alpha_j)}{\theta_0[\delta(1+\gamma_j)-R_f]}$ or, in the particular case $C_\Delta=0$, if $\theta_0\gamma_j<\alpha_j+(1+\theta_0)(\frac{R_f}{\delta}-1)$. Since stability requires that condition (E.4) holds for all $j\in\{1,2,...,n\}$, the statement of Proposition 6.1 follows.

Bibliography

Akgiray, V. (1989), 'Conditional heteroscedasticity in time series of stock returns: Evidence and forecasts', *Journal of Business* **62**, 55–80.

Alfarano, S., Lux, T. and Wagner, F. (2005), 'Estimation of agent-based models: The case of an asymmetric herding model', *Computational Economics* **26**, 19–49.

Alfarano, S., Lux, T. and Wagner, F. (2008), 'Time variation of higher moments in a financial market with heterogeneous agents: An analytical approach', *Journal of Economic Dynamics and Control* **32**, 101–136.

Allen, H. and Taylor, M. (1990), 'Charts, noise and fundamentals in the London foreign exchange market', *Economic Journal* **100**, 49–59.

Amilon, H. (2008), 'Estimation of an adaptive stock market model with heterogeneous agents', *Journal of Empirical Finance* **15**, 342–362.

Ang, A. and Chen, J. (2007), 'CAPM over the long run: 1926–2001', *Journal of Empirical Finance* **14**, 1–40.

Aoki, M. (2002), *Modeling Aggregate Behaviour and Fluctuations in Economics*, Cambridge University Press.

Asness, C., Moskowitz, T. and Pedersen, L. (2013), 'Value and momentum everywhere', *Journal of Finance* **68**, 929–985.

Baker, M. and Wurgler, J. (2006), 'Investor sentiment and the cross-section of stock returns', *Journal of Finance* **57**, 1645–1679.

Baker, M. and Wurgler, J. (2007), 'Investor sentiment in the stock makret', *Journal of Economic Perspectives* **21**, 129–151.

Balvers, R. and Wu, Y. (2006), 'Momentum and mean reversion across national equity markets', *Journal of Empirical Finance* **13**, 24–48.

Banerjee, A. (1992), 'A simple model of herd behavior', *Quarterly Journal of Economics* **107**, 797–817.

Banerjee, S. and Kremer, I. (2010), 'Disagreement and learning: Dynamic patterns of trade', *Journal of Finance* **65**, 1269–1302.

Barberis, N. and Shleifer, A. (2003), 'Style investing', *Journal of Financial Economics* **68**, 161–199.

Barberis, N., Shleifer, A. and Vishny, R. (1998), 'A model of investor sentiment', *Journal of Financial Economics* **49**, 307–343.

Beja, A. and Goldman, M. (1980), 'On the dynamic behavior of prices in disequilibrium', *Journal of Finance* **35**, 235–247.

Bollerslev, T. (1986), 'Generalized autoregressive conditional heteroskedasticity', *Journal of Econometrics* **31**, 307–327.

Bollerslev, T., Engle, R. and Wooldridge, J. (1988), 'A capital asset pricing model with time varying covariances', *Journal of Political Economy* **96**, 116–131.

Boswijk, H., Hommes, C. and Manzan, S. (2007), 'Behavioral heterogeneity in stock prices', *Journal of Economic Dynamics and Control* **31**, 1938–1970.

Braun, P., Nelson, D. and Sunier, A. (1990), 'Good news, bad news, volatility and betas', *Journal of Finance* **50**, 1575–1603.

Brock, W. and Hommes, C. (1997), 'A rational route to randomness', *Econometrica* **65**, 1059–1095.

Brock, W. and Hommes, C. (1998), 'Heterogeneous beliefs and routes to chaos in a simple asset pricing model', *Journal of Economic Dynamics and Control* **22**, 1235–1274.

Brock, W., Hommes, C. and Wagener, F. (2009), 'More hedging instruments may destabilize markets', *Journal of Economic Dynamics and Control* **33**, 1912–1928.

Brock, W., Lakonishok, J. and LeBaron, B. (1992), 'Simple technical trading volatility and the stochastic properties of stock returns', *Journal of Finance* **47**, 1731–1764.

Campbell, J. and Shiller, R. (1988*a*), 'The dividend-price ratio and expectations of future dividends and discount factors', *Review of Financial Studies* **1**, 195–228.

Campbell, J. and Shiller, R. (1988*b*), 'Stock prices, earnings, and expected dividends', *Journal of Finance* **43**, 661–676.

Campbell, J. and Viceira, L. (1999), 'Consumption and portfolio decisions when expected returns are time varying', *Quarterly Journal of Economics* **114**, 433–495.

Campbell, J. and Vuolteenaho, T. (2004), 'Bad beta, good beta', *American Economic Review* **94(5)**, 1249–1275.

Chen, L. and Wu, Z. (2010), 'Maximum principle for the stochastic optimal control problem with delay and application', *Automatica* **46**, 1074–1080.

Chen, S.-H., Chang, C. and Du, Y. R. (2012), 'Agent-based economic models and econometrics', *Knowledge Engineering Review* **27**, 187–219.

Chen, S.-H. and Huang, Y. (2008), 'Risk preference, forecasting accuracy and survival dynamics: Simulations based on a multi-asset agent-based artifical stock market', *Journal of Economic Behavior and Organization* **67**, 702–717.

Chiarella, C. (1992), 'The dynamics of speculative behaviour', *Annals of Operations Research* **37**, 101–123.

Chiarella, C., Dieci, R. and Gardini, L. (2005), 'The dynamic interaction of speculation and diversification', *Applied Mathematical Finance* **12(1)**, 17–52.

Chiarella, C., Dieci, R. and He, X. (2007), 'Heterogeneous expectations and speculative behaviour in a dynamic multi-asset framework', *Journal of Economic Behavior and Organization* **62**, 402–427.

Chiarella, C., Dieci, R. and He, X. (2009), *Heterogeneity, Market Mechanisms and Asset Price Dynamics*, Elsevier, pp. 277–344. in *Handbook of Financial Markets: Dynamics and Evolution*, Eds. Hens, T. and K.R. Schenk-Hoppe.

Chiarella, C., Dieci, R. and He, X. (2010), *A framework for CAPM with heterogeneous beliefs*, Springer, pp. 353–369. in *Nonlinear Dynamics in Economics, Finance and Social Sciences: Essays in Honour of John Barkley Rosser Jr.*, Eds. Bischi, G.-I., C. Chiarella and L. Gardini.

Chiarella, C., Dieci, R. and He, X. (2011), 'Do heterogeneous beliefs diversify market risk?', *European Journal of Finance* **17**, 214–258.

Chiarella, C., Dieci, R. and He, X. (2013), 'Time-varying beta: a boundedly rational equilibrium approach', *Journal of Evolutionary Economics* **23**, 609–639.

Chiarella, C., Dieci, R., He, X. and Li, K. (2013), 'An evolutionary CAPM under heterogeneous beliefs', *Annals of Finance* **9**, 185–215.

Chiarella, C. and Di Guilmi, C. (2011*a*), 'The financial instability hypothesis: A stochastic microfoundation framework', *Journal of Economic Dynamics and Control* **35**, 1151–1171.

Chiarella, C. and Di Guilmi, C. (2011*b*), Limit distribution of evolving strategies in financial markets, working paper 294, Quantitative Finance Research Centre, University of Technology, Sydney.

Chiarella, C. and He, X. (2002), 'Heterogeneous beliefs, risk and learning in a simple asset pricing model', *Computational Economics* **19**, 95–132.

Chiarella, C. and He, X. (2003*a*), 'Dynamics of beliefs and learning under a_l-processes – The Heterogeneous case', *Journal of Economic Dynamics and Control* **27**, 503–531.

Chiarella, C. and He, X. (2003*b*), 'Heterogeneous beliefs, risk and learning in a simple asset pricing model with a market maker', *Macroeconomic Dynamics* **7**, 503–536.

Chiarella, C., He, X. and Hommes, C. (2006), 'A dynamic analysis of moving average rules', *Journal of Economic Dynamics and Control* **30**, 1729–1753.

Chiarella, C., He, X., Wang, D. and Zheng, M. (2008), 'The stochastic bifurcation behaviour of speculative financial markets', *Physica A* **387**, 3837–3846.

Chiarella, C., He, X. and Zheng, M. (2011), 'An analysis of the effect of noise in a heterogeneous agent financial market model', *Journal of Economic Dynamics and Control* **35**. 148-162.

Chordia, T. and Shivakumar, L. (2002), 'Momentum, business cycle, and time-varying expected returns', *Journal of Finance* **57**, 985–1019.

Cohen, L. and Frazzini, A. (2008), 'Economic links and predictable returns', *Journal of Finance* **63**, 1977–2011.

Cohen, L. and Lou, D. (2012), 'Complicated firms', *Journal of Financial Economics* **104**, 383–400.

Cooper, M., Gutierrez, R. and Hameed, A. (2004), 'Market states and momentum', *Journal of Finance* **59**, 1345–1365.

Daniel, K., Hirshleifer, D. and Subrahmanyam, A. (1998), 'Investor psychology and investor security market under-and overreactions', *Journal of Finance* **53**, 1839–1886.

Day, R. and Huang, W. (1990), 'Bulls, bears and market sheep', *Journal of Economic Behavior and Organization* **14**, 299–329.

De Bondt, W. and Thaler, R. (1985), 'Does the stock market overreact?', *Journal of Finance* **40**, 793–808.

De Bondt, W. and Thaler, R. (1989), 'Anomalies: A mean-reverting walk down wall street', *Economic Perspectives* **3**, 189–202.

Di Guilmi, C., He, X. and Li, K. (2013), Herding, trend chasing, and market volatility, working paper 337, Quantitative Finance Research Centre, University of Technology, Sydney.

Dieci, R. and Westerhoff, F. (2010), 'Heterogeneous speculators, endogenous fluctuations and interacting markets: A model of stock prices and exchange rates', *Journal of Economic Dynamics and Control* **34**, 743–764.

Dieci, R. and Westerhoff, F. (2012), On the inherent instability of international financial markets: Natural nonlinear interactions between stock and foreign exchange markets, working paper, University of Bologna.

Diks, C. and van der Weide, R. (2003), Heterogeneity as a natural source of randomness, CeNDEF, working paper 03-05, University of Amsterdam.

Diks, C. and van der Weide, R. (2005), 'Herding, a-synchronous updating and heterogeneity in memory in a CBS', *Journal of Economic Dynamics and Control* **29**, 741–763.

Dybvig, P. and Ross, S. (1985), 'Differential information and performance measurement using a security market line', *Journal of Finance* **40**, 383–400.

Engle, R. (1982), 'Autoregressive conditional heteroscedasticity with estimates of the variance of UK inflation', *Econometrica* **50**, 987–1008.

Fama, E. (1970), 'Efficient capital markets: A review of theory and empirical eork', *Journal of Finance* **25**, 383–423.

Fama, E. and French, K. (1992), 'The cross section of expected stock returns', *Journal of Finance* **47**, 427–465.

Fama, E. and French, K. (1996), 'Multifactor explanations of asset pricing anomalies', *Journal of Finance* **51**, 55–84.

Fama, E. and French, K. (1998), 'Value versus growth: The international evidence', *Journal of Finance* **53**, 1975–1999.

Fama, E. and French, K. (2006), 'The value premium and the CAPM', *Journal of Finance* **61**(5), 2163–2185.

Farmer, J. and Joshi, S. (2002), 'The price dynamics of common trading strategies', *Journal of Economic Behavior and Organization* **49**, 149–171.

Franke, R. (2010), 'On the specification of noise in two agent-based asset pricing models', *Journal of Economic Dynamics and Control* **34**, 1140–1152.

Franke, R. and Westerhoff, F. (2011), 'Estimation of a structural stochastic volatility model of asset pricing', *Computational Economics* **38**, 53–83.

Franke, R. and Westerhoff, F. (2012), 'Structural stochastic volatility in asset pricing dynamics: Estimation and model contest', *Journal of Economic Dynamics and Control* **36**, 1193–1211.

Frankel, J. and Froot, K. (1986), 'Understanding the US dollars in the eighties: The expectations of chartists and fundamentalists', *Economic Record, Supplementary Issue* **62**, 24–38.

George, T. and Hwang, C. (2004), 'The 52-week high and momentum investing', *Journal of Finance* **59**, 2145–2176.

Goodwin, R. (1951), 'The nonlinear accelerator and the persistence of business cycles', *Econometrica* **19**, 1–17.

Gopalsamy, K. (1992), *Stability and oscillations in delay differential equation of population dynamics*, Kluwer Academic Publisher, London.

Griffin, J., Ji, X. and Martin, J. (2003), 'Momentum investing and business cycle risk: Evidence from pole to pole', *Journal of Finance* **58**, 2515–2547.

Haldane, J. (1932), 'A contribution to the theory of price fluctuations', *Review of Economic Studies* **1**, 186–195.

Hale, J. (1997), *Theory of Functional Differential Equations*, Springer, New York.

Hamilton, J. (1989), 'A new approach to the economic analysis of nonstationary time series and the business cycle', *Econometrica* **57**(2), 357–384.

Hamilton, J. (1990), 'Analysis of time series subject to changes in regime', *Journal of Econometrics* **45**, 39–70.

Hansen, L. and Richard, S. (1987), 'The role of conditioning information in deducing testable restrictions implied by dynamic asset pricing models', *Econometrica* **55**, 587–613.

He, X. and Li, K. (2012), 'Heterogeneous beliefs and adaptive behaviour in a continuous-time asset price model', *Journal of Economic Dynamics and Control* **36**, 973–987.

He, X. and Li, K. (2014), Time series momentum and market stability, working paper 341, Quantitative Finance Research Centre, University of Technology, Sydney.

He, X., Li, K. and Li, Y. (2014), 'Optimality of momentum and reversal', *SSRN Working Paper* .

He, X., Li, K., Wei, J. and Zheng, M. (2009), 'Market stability switches in a continuous-time financial market with heterogeneous beliefs', *Economic Modelling* **26**, 1432–1442.

He, X. and Li, Y. (2007), 'Power law behaviour, heterogeneity, and trend chasing', *Journal of Economic Dynamics and Control* **31**, 3396–3426.

He, X. and Zheng, M. (2010), 'Dynamics of moving average rules in a continuous-time financial market model', *Journal of Economic Behavior and Organization* **76**, 615–634.

Hofbauer, J. and Sigmund, K. (1998), *Evolutionary Games and Population Dynamics*, Cambridge University Press.

Hohnisch, M. and Westerhoff, F. (2008), 'Business cycle synchronization in a simple Keynesian macro-model with socially transmitted economic sentiment and international sentiment spill-over', *Structural Change and Economic Dynamics* **19**, 249–259.

Hommes, C. (2001), 'Financial markets as nonlinear adaptive evolutionary systems', *Quantitative Finance* **1**, 149–167.

Hommes, C. (2006), *Heterogeneous Agent Models in Economics and Finance*, Vol. 2 of *Handbook of Computational Economics*, North-Holland, pp. 1109–1186. in *Agent-based Computational Economics*, Eds. Tesfatsion, L. and K.L. Judd.

Hommes, C., Huang, H. and Wang, D. (2005), 'A robust rational route to randomness in a simple asset pricing model', *Journal of Economic Dynamics and Control* **29**, 1043–1072.

Hommes, C. and Wagener, F. (2009), *Complex Evolutionary Systems in Behavioral Finance*, number Chapter 4 *in* 'Handbooks in Finance', North-Holland, pp. 217–276. in *Handboof of Financial Markets: Dynamics and Evolution*, Eds. Hens, T. and K.R. Schenk-Hoppé.

Hong, H. and Stein, J. (1999), 'A unified theory of underreaction, momentum trading, and overreaction in asset markets', *Journal of Finance* **54**, 2143–2184.

Hou, K., Peng, L. and Xiong, W. (2009), A tale of two anomalies: The implications of investor attention for price and earnings momentum, working paper, Ohio State University.

Howroyd, T. and Russell, A. (1984), 'Cournol oligopoly models with time delays', *Journal of Mathematical Economics* **13**, 97–103.

Jagannathan, R. and Wang, Z. (1996), 'The conditional CAPM and cross-section of expected returns', *Journal of Finance* **51**, 3–53.

Jegadeesh, N. and Titman, S. (1993), 'Returns to buying winners and selling losers: Implications for stock market efficiency', *Journal of Finance* **48**, 65–91.

Jegadeesh, N. and Titman, S. (2001), 'Profitability of momentum strategies: An evaluation of alternative explanations', *Journal of Finance* **56**, 699–720.

Jegadeesh, N. and Titman, S. (2011), 'Momentum', *Annual Review of Financial Economics* **3**, 493–509.

Kalecki, M. (1935), 'A macroeconomic theory of the business cycle', *Econometrica* **3**, 327–344.

Keim, D. (1988), *Stock Market Regularities: A Synthesis of the Evidence and Explanations, in Elroy Dimson, ed.: Stock Market Anomalies*, Cambridge University Press, Cambridge.

Keynes, J. (1936), *The general theory of employment, interest and money*, Harcourt, Brace and World, New York.

Kirman, A. (1993), 'Ants, rationality, and recruitment', *Quarterly Journal of Economics* **108**, 137–156.

Koijen, R., Rodríguez, J. and Sbuelz, A. (2009), 'Momentum and mean reversion in strategic asset allocation', *Management Science* **55**, 1199–1213.

Lakonishok, J., Shleifer, A. and Vishny, R. (1994), 'Contrarian investment, extrapolation and risk', *Journal of Finance* **49**, 1541–1578.

Larson, A. (1964), 'The hog cycle as harmonic motion', *Journal of Farm Economics* **46**, 375–386.

LeBaron, B. (2006), *Agent-based Computational Finance*, Vol. 2 of *Handbook of Computational Economics*, North-Holland, pp. 1187–1233. in *Agent-based Computational Economics*, Eds. Tesfatsion, L. and K.L. Judd.

Lewellen, J. and Nagel, S. (2006), 'The conditional CAPM does not explain asset-pricing anomalies', *Journal of Financial Economics* **82**(3), 289–314.

Li, K. and Wei, J. (2009), 'Stability and Hopf bifurcation analysis of a prey-predator system with two delays', *Chaos, Solitons and Fractals* **42**, 2606–2613.

Lintner, J. (1965), 'The valuation of risk assets and the selection of risky investments in stock portfolios and capital budgets', *Review of Economic Studies* **47**, 13–37.

Lou, D. and Polk, C. (2013), Comomentum: Inferring arbitrage activity from return correlations, working paper, LSE.

Lux, T. (1995), 'Herd behaviour, bubbles and crashes', *Economic Journal* **105**, 881–896.

Lux, T. (2009), *Stochastic Behavioural Asset Pricing and Stylized Facts*, Elsevier, pp. 161–215. in *Handbook of Financial Markets: Dynamics and Evolution*, Eds. Hens, T. and K.R. Schenk-Hoppé.

Mackey, M. (1989), 'Commodity price fluctuations: Price dependent delays and nonlinearities as explanatory factors', *Journal of Economic Theory* **48**, 495–509.

Marquering, W. and Verbeek, M. (2004), 'The economic value of predicting stock index returns and volatility', *Journal of Financial and Quantitative Analysis* **39**, 407–429.

Marsili, M., Raffaelli, G. and Ponsot, B. (2009), 'Dynamic instability in generic model of multi-assets markets', *Journal of Economic Dynamics and Control* **33**, 1170–1181.

Matsumoto, A. and Szidarovszky, F. (2011), 'Delay differential neoclassical growth model', *Journal of Economic Behavior and Organization* **78**, 272–289.

Merton, R. (1969), 'Lifetime portfolio selection under uncertainty: The continuous-time case', *Review of Economics and Statistics* **51**, 247–257.

Merton, R. (1971), 'Optimum consumption and portfolio rules in a continuous time model', *Journal of Economic Theory* **3**, 373–413.

Moskowitz, T. and Grinblatt, M. (1999), 'Do industries explain momentum?', *Journal of Finance* **54**, 1249–1290.

Moskowitz, T., Ooi, Y. H. and Pedersen, L. H. (2012), 'Time series momentum', *Journal of Financial Economics* **104**, 228–250.

Mossin, J. (1966), 'Equilibrium in a capital asset market', *Econometrica* **35**, 768–783.

Novy-Marx, R. (2012), 'Is momentum really momentum?', *Journal of Financial Economics* **103**, 429–453.

Øksendal, B., Sulem, A. and Zhang, T. (2011), 'Optimal control of stochastic delay equations and time-advanced backward stochastic differential equations', *Advances in Applied Probability* **43**, 572–596.

Pagan, A. (1996), 'The econometrics of financial markets', *Journal of Empirical Finance* **3**, 15–102.

Pesaran, M. and Timmermann, A. (1994), 'Forecasting stock returns, an examination of stock market trading in the presence of transaction costs', *Journal of Forecasting* **13**, 335–367.

Pesaran, M. and Timmermann, A. (1995), 'Predictability of stock returns: Robustness and economic significance', *Journal of Finance* **50**, 1201–1228.

Phillips, A. (1954), 'Stabilisation policy in a closed economy', *Economic Journal* **64**, 290–321.

Phillips, A. (1957), 'Stabilisation policy and the time-forms of lagged responses', *Economic Journal* **67**, 265–277.

Ruan, S. and Wei, J. (2003), 'On the zeros of transcendental functions with applications to stability of delay differential equations with two delays', *Dynamics of Continuous Discrete and Impulsive Systems Series A: Mathematical Analysis* **10**, 863–874.

Sagi, J. and Seasholes, M. (2007), 'Firm-specific attributes and the cross-section of momentum', *Journal of Financial Economics* **84**, 389–434.

Sangvinatsos, A. and Wachter, J. A. (2005), 'Does the failure of the expectations hypothesis matter for long-term investors?', *Journal of Finance* **60**, 179–230.

Scharfstein, D. and Stein, J. (1990), 'Herd behavior and investment', *American Economic Review* **80**, 465–479.

Serban, A. (2010), 'Combining mean reversion and momentum trading strategies in foreign exchange markets', *Journal of Banking and Finance* **34**, 2720–2727.

Sharpe, W. (1964), 'Capital asset prices: A theory of market equilibrium under conditions of risk', *Journal of Finance* **19**, 425–442.

Simon, H. (1956), *Models of Man: Social and Rational; Mathematical Essays on Rational Human Behavior in Society Settings*, John Wiley, New York.

Thaler, R. (1987*a*), 'Anomalies: Seasonal movements in security prices ii: weekend, holiday turn of the month, and intraday effects', *Journal of Economic Perspectives* **1**, 169–177.

Thaler, R. (1987*b*), 'Anomalies: The January effect', *Journal of Economic Perspectives* **1**, 197–201.

Vayanos, D. and Woolley, P. (2013), 'An institutional theory of momentum and reversal', *Review of Financial Studies* **26**, 1087–1145.

Wachter, J. (2002), 'Portfolio and consumption decisions under mean-reverting returns: An exact solution for complete markets', *Journal of Financial and Quantitative Analysis* **37**, 63–91.

Wang, K. and Xu, J. (2012), Market volatility and momentum, working paper, University of Toronto.

Westerhoff, F. (2004), 'Multiasset market dynamics', *Macroeconomic Dynamics* **8**, 591–616.

Westerhoff, F. and Dieci, R. (2006), 'The effectiveness of Keynes-Tobin transaction taxes when heterogeneous agents can trade in different markets: A behavioral finance approach', *Journal of Economic Dynamics and Control* **30**, 293–322.

Yoshida, H. and Asada, T. (2007), 'Dynamic analysis of policy lag in a Keynes-Goodwin model: Stability, instability, cycles and chaos', *Journal of Economic Behavior and Organization* **62**, 441–469.

Zeeman, E. (1974), 'On the unstable behavior of stock exchange', *Journal of Mathematical Economics* **1**, 39–49.

Zhu, M., Wang, D. and Guo, M. (2011), 'Stochastic equilibria of an asset pricing model with heterogeneous beliefs and random dividends', *Journal of Economic Dynamics and Control* **35**, 131–147.